**UNIVERSIDAD COMPLUTENSE DE MADRID**

FACULTAD DE CIENCIAS QUÍMICAS

**TESIS DOCTORAL**

**Caucho nitrilo autorreparable y reciclable: un camino hacia la sostenibilidad**

**Self-healing and recyclable nitrile rubber: a pathway to sustainability**

MEMORIA PARA OPTAR AL GRADO DE DOCTOR

PRESENTADA POR

**Saul Ismael Utrera Barrios**

Directores

Marianella Hernández Santana

Miguel Ángel López Manchado

Madrid, 2023

# UNIVERSIDAD COMPLUTENSE DE MADRID

## FACULTAD DE CIENCIAS QUÍMICAS



## TESIS DOCTORAL

## CAUCHO NITRILO AUTORREPARABLE Y RECICLABLE: UN CAMINO HACIA LA SOSTENIBILIDAD

MEMORIA PARA OPTAR AL GRADO DE DOCTOR

PRESENTADA POR

**Saul Ismael Utrera Barrios**

Directores

Marianella Hernández Santana

Miguel Ángel López Manchado

Madrid, 2023

## INSTITUTO DE CIENCIA Y TECNOLOGÍA DE POLÍMEROS

CONSEJO SUPERIOR DE INVESTIGACIONES CIENTÍFICAS

# COMPLUTENSE UNIVERSITY OF MADRID

## FACULTY OF CHEMICAL SCIENCES

**DOCTORAL THESIS**

## SELF-HEALING AND RECYCLABLE NITRILE RUBBER: A PATHWAY TO SUSTAINABILITY

A DISSERTATION FOR THE DEGREE OF DOCTOR OF PHILOSOPHY

SUBMITTED BY

**Saul Ismael Utrera Barrios**

Supervisors

Marianella Hernández Santana

Miguel Ángel López Manchado

Madrid, 2023

**INSTITUTE OF POLYMER SCIENCE AND TECHNOLOGY**

SPANISH NATIONAL RESEARCH COUNCIL

**DECLARACIÓN DE AUTORÍA Y ORIGINALIDAD DE LA TESIS PRESENTADA PARA OBTENER EL TÍTULO DE DOCTOR**

D. Saul Ismael Utrera Barrios, estudiante en el Programa de Doctorado en Química Avanzada de la Facultad de Ciencias Químicas de la Universidad Complutense de Madrid, como autor de la tesis presentada para la obtención del título de Doctor y titulada:

CAUCHO NITRILO AUTORREPARABLE Y RECICLABLE: UN CAMINO HACIA LA SOSTENIBILIDAD
SELF-HEALING AND RECYCLABLE NITRILE RUBBER: A PATHWAY TO SUSTAINABILITY

y dirigida por Marianella Hernández Santana y Miguel Ángel López Manchado.

**DECLARO QUE:**

La tesis es una obra original que no infringe los derechos de propiedad intelectual ni los derechos de propiedad industrial u otros, de acuerdo con el ordenamiento jurídico vigente, en particular, la Ley de Propiedad Intelectual (R.D. legislativo 1/1996, de 12 de abril, por el que se aprueba el texto refundido de la Ley de Propiedad Intelectual, modificado por la Ley 2/2019, de 1 de marzo, regularizando, aclarando y armonizando las disposiciones legales vigentes sobre la materia), en particular, las disposiciones referidas al derecho de cita.

Del mismo modo, asumo frente a la Universidad cualquier responsabilidad que pudiera derivarse de la autoría o falta de originalidad del contenido de la tesis presentada de conformidad con el ordenamiento jurídico vigente.

En Madrid, a 18 de diciembre de 2023

Fdo. Saul Ismael Utrera Barrios

La presente tesis doctoral se ha realizado en el Grupo de Compuestos Poliméricos (PCG) perteneciente al Departamento de Nanomateriales Poliméricos y Biomateriales del Instituto de Ciencia y Tecnología de Polímeros (ICTP) del Consejo Superior de Investigaciones Científicas (CSIC) bajo la dirección de la doctora Marianella Hernández Santana y el profesor Miguel Ángel López Manchado.

'*Tell me one last thing,*' said Harry. '*Is this real? Or has this been happening inside my head?*'

Dumbledore beamed at him, and his voice sounded loud and strong in Harry's ears even though the bright mist was descending again, obscuring his figure.

'*Of course it is happening inside your head, Harry, but why on earth should that mean that it is no real?*'

King's Cross, Harry Potter and the Deathly Hallows

(Bloomsbury, 2007)

by **J. K. Rowling**

*A aquellos que tuvieron que dejar su hogar*

*en busca de una vida mejor.*


*To those who had to leave their home,*

*looking for a better life.*

## Agradecimientos

Quiero empezar dando mi más sincero agradecimiento a *España*. Hace más de 5 años llegué a un país totalmente desconocido para mí, pero que supo abrazarme y hacerme parte de su dinámica en poco tiempo. Gracias España (y gracias, Madrid) por convertirte en algo más que el lugar donde me vi obligado a vivir. Eres mi casa, y estoy muy orgulloso de que ahora también seas **mi país**. Sin las oportunidades que tú y tu gente me dieron, nada de esto habría sido posible. *The only pain that I want in my life is* **Spain** ❤️💛.

En segundo lugar quiero agradecer a mis directores de tesis: *Marianella Hernández Santana* y *Miguel Ángel López Manchado*. El éxito de mi experiencia en España, en parte, se debe a haberme encontrado con ustedes. *Marianella*, gracias por tanto. Gracias por tu confianza. Gracias por tu cariño. Gracias por tu enorme calidad humana. Gracias por nunca decirle que no a mis ideas más locas. Espero que mi trabajo y mi esfuerzo hayan podido recompensar, aunque sea un poco, lo mucho que me diste en este tiempo. Más allá de cualquier aspecto académico y profesional, no tengo dudas de que lo más valioso que me llevo de esta experiencia es haberte conocido. *Miguel Ángel*, gracias por inspirarme a hacerlo mejor siempre. Gracias por poner a prueba mis ideas y conocimientos. Aunque no siempre lo entendí a la primera, al ver el resultado final de mis contribuciones me ha quedado claro que no habrían podido alcanzar ese nivel sin tus sugerencias.

A mi directora honorífica, *Raquel Verdejo*, que aunque no aparezca en la portada de este trabajo, he aprendido tanto de ella que sería una injusticia enorme no reconocerlo. *Raquel*, gracias por tu disposición. Gracias por tu apoyo. Gracias por motivarme y también exigirme.

Equipos, Infraestructura e Informática: *Manuel Rus* y *Alberto Hernando*. Tuve la suerte de contar con todos ustedes.

A aquellos que como yo llegaron al ICTP desde lugares muy lejanos (y otros no tan lejanos) pero formaron parte de un intercambio de culturas que solo enriqueció mi experiencia predoctoral. Gracias *Albanelly Soto*, *Francisco González*, *Łukasz Zedler*, *Lorenzo Mirizzi*, *Edward Centeno* y *Sofía Faina*. Espero que volvamos a coincidir pronto, preferiblemente fuera de España.

I would also like to thank the *Vrije Universiteit Brussels* (VUB) and the *Physical Chemistry and Polymer Science* (FYSC) and *Brubotics* groups for welcoming me with open arms and making my experience in Brussels unforgettable. Thanks to *Joost Brancart*, *Seppe Terryn*, and *Niklas Steenackers*, because I owe the academic success of my research stay to your support. **Dankjulliewel!** To my VUB friends, especially *Aleix Costa-Cornellá* and *Francesca Furia* and the spanish team, *Valentina Lozano*, *Manuel Fontenla* and *Danna Centellas*, it was my pleasure to meet all of you along this way. As I said when I said goodbye, thank you all for making me feel like one of the group since the day I arrived. See you soon in Madrid!

A mis amigos de la vida, porque ¿qué sería de esta vida sin amigos? *Paolo Tanasi, Christian Laya, Oriana Medina, Eduardo Evaristo, Javier Stavola* y *Adriana Silva*. Me complace saber que aunque nuestras múltiples obligaciones nos impidan vernos con la frecuencia que quisiéramos, siempre estaremos los unos para los otros cuando más lo necesitemos. ¡Los quiero mucho!

Al amor de mi vida, *Dario Del Cuore*. Amorino, haber contado con tu compañía en esta etapa tan crítica ha sido clave para mi salud mental. Gracias por creer en mí.

Gracias por motivarme. Gracias por tu inmensa paciencia para con este insoportable malhumorado. Gracias porque a pesar de la distancia siempre te sentí conmigo. Gracias por abrirme las puertas a tu vida, a tu familia y a tus amigos. Gracias por Lisboa y por Palermo. Eres lo mejor que me ha pasado en mucho tiempo. Y aunque no soportes a mi grupo italiano favorito, debo usar una de sus canciones para recordarte que *tu sei il mio unico grande amore.*

A mi familia, porque detrás de toda gran tesis, siempre hay una gran familia. A mi papá, *Saul Utrera*, y mi segunda madre, *Ymperio Zapata*, por su apoyo verdaderamente incondicional. Gracias por entenderme. Gracias por amarme como sé que lo hacen. He tenido la mayor de las suertes al tenerlos durante mi vida. ¡Los amo!

A mi abuela, *Alexis Cabello*, por ser el motor de mi existencia. Eres el mayor ejemplo de superación porque como ninguna otra has sabido salir adelante a pesar de todas las adversidades que nos han tocado vivir. Sigue inspirándome con tu fortaleza, pero sobre todo, sigue llenándome con tu amor. ¡Te amo!

A mis ángeles de la guarda, mi madre, *Silene Barrios*, y mi hermana, *Nicold Alejandra*, por protegerme día a día. Las siento a mi lado siempre.

Y, finalmente, quiero agradecer al Saul del pasado. Gracias por no haberte rendido. Gracias por haber encontrado una razón para seguir las múltiples veces que pensaste en dejarlo. Gracias por traerme hasta aquí.

A todos, mi eterno agradecimiento.

# Table of Contents

# List of Tables

# List of Figures

viii

# Abbreviations and Symbols

| | **A** |
|---|---|
| $a$ | Weight fraction of the filler in the compound |
| A | Ampere |
| ACN | Acrylonitrile |
| AP | 2-aminopyridine |
| AR | Abrasion resistance |
| ARI$_A$ | Abrasion resistance index (method A) |
| ATR | Attenuated Total Reflectance mode |

| | **B** |
|---|---|
| bar | Bar |
| BDS | Broadband dielectric spectroscopy |
| BP | Tert-butyl pyridine |
| bPEI | Poly(ethyleneimine) |
| BIIR | Brominated butyl rubber |

| | **C** |
|---|---|
| $C_1$ | Crosslinking units contribution |
| $C_2$ | Mooney-Rivlin elastic constant |
| Ca-A | Calcium alginate |

| | |
|---|---|
| CaO | Calcium oxide |
| CB | Carbon black |
| $C_B$ | Compression set |
| CBS | $n$-cyclohexyl-$2$-benzothiazole sulfenamide |
| CE | Circular Economy |
| CF | Cellulose fibers |
| cm | Centimeters |
| CNT | Carbon nanotubes |
| CRI | Cure rate index |
| CSIC | Spanish National Research Council |

## D

| | |
|---|---|
| $D$ | Fragility strength |
| $d$ | Distance between structures (Bragg's law) |
| $d_1$ | Density of Standard Rubber #1 |
| DAP | 2,6-diaminopyridine |
| DCP | Dicumyl peroxide |
| DCPD | Dicyclopentadiene |
| DMA | Dynamic mechanical analysis |
| dNm | Decinewtons per meter |
| DSC | Differential scanning calorimetry |
| $d_t$ | Density of the test rubber |

## E

| | |
|---|---|
| $E'$ | Storage modulus |
| $E''$ | Loss modulus |
| $E_a$ | Activation energy |

xii

| | |
|---|---|
| EB | Elongation at break |
| EC | Economía Circular |
| ELT | End-of-life tires |
| EP | Electrode polarization |
| EPA | United States Environmental Protection Agency |
| ETRMA | European Tyre & Rubber Manufacturers' Association |
| EU | European Union |

**F**

| | |
|---|---|
| FTIR | Fourier-transform infrared spectroscopy |

**G**

| | |
|---|---|
| g | Grams |
| G-PPD | p-phenylenediamine-modified Graphene oxide |
| GTR | Ground tire rubber |
| GO | Graphene oxide |

**H**

| | |
|---|---|
| h | Hour |
| $H_2SO_4$ | Sulfuric acid |
| HIPS | High-impact polystyrene |
| HN | Havriliak-Negami function |
| HTPB | Hydroxy-terminated polybutadiene |
| Hz | Hertz |

**I**

| | |
|---|---|
| ICTP | Institute of Polymer Science and Technology |

| | |
|---|---|
| IIR | Butyl rubber |
| ION | Iodine number |
| IPN | Interpenetrated polymeric networks |

| **J** | |
|---|---|
| J | Joule |

| **K** | |
|---|---|
| $k$ | Boltzmann's constant |
| K | Kelvin |
| kg | Kilograms |
| kV | Kilovolts |

| **L** | |
|---|---|
| LCA | Life cycle assessment |

| **M** | |
|---|---|
| $m$ | Fragility index |
| $m_1$ | Mass before immersion in solvent (crosslink density) |
| $m_2$ | Mass after 72 h immersion in solvent (crosslink density) |
| $m_3$ | Mass after evaporation of the absorbed solvent (crosslink density) |
| $M^*$ | Complex dielectric modulus |
| M100 | Stress at 100 % strain |
| M300 | Stress at 300 % strain |
| M500 | Stress at 500 % strain |
| MAH | Maleic anhydride |
| $M_c$ | Average molecular weight between crosslinks |

| | |
|---|---|
| $m_f$ | Mass after immersion in solvent (chemical resistance) |
| mg | Milligrams |
| MgO | Magnesium oxide |
| MgSO$_4$ | Magnesium sulfate |
| MH | Maximum torque |
| $m_i$ | Mass before immersion in solvent (chemical resistance) |
| min | Minutes |
| mL | Milliliters |
| ML | Minimun torque |
| mm | Millimeters |
| MO | Metal oxide |
| mol | Mole |
| MPa | Megapascals |
| ms | Milliseconds |
| MU | Mooney units |
| MWS | Maxwell-Wagner-Sillars relaxation |

### N

| | |
|---|---|
| $N_A$ | Avogadro's number |
| NBR | Nitrile rubber |
| nm | Nanometers |

### O

| | |
|---|---|
| ODS | Objetivos de Desarrollo Sostenible |
| OAN | Oil absorption number |

|         |                                  |
|---------|----------------------------------|
| **P**   |                                  |
| PAA     | Poly(acrylic acid)               |
| PAN     | Polyacrylonitrile                |
| PCL     | Polycaprolactone                 |
| PCR     | Peak cure rate                   |
| $P_{damaged}$ | Mechanical property after damage |
| PDMS    | Poly(dimethylsiloxane)           |
| PEO     | Poly(ethylene oxide)             |
| $P_{healed}$ | Mechanical property after healing |
| phr     | Parts per hundred rubber         |
| PLA     | Poly(lactic acid)                |
| PMMA    | Poly(methyl methacrylate)        |
| $P_{pristine}$ | Mechanical property before healing |
| PS      | Polystyrene                      |
| PU      | Polyurethanes                    |
| PVAc    | Poly(vinyl acetate)              |

|         |                                  |
|---------|----------------------------------|
| **Q**   |                                  |
| q       | Distance in reciprocal space     |

|         |                                  |
|---------|----------------------------------|
| **R**   |                                  |
| R       | Universal gas constant           |
| R1      | Recycled 1                       |
| R2      | Recycled 2                       |
| R3      | Recycled 3                       |
| RI      | Reinforcement index (mechanical) |
| RT      | Room temperature                 |

|  | **S** |
| --- | --- |
| *s* | Seconds |
| S | Sulfur |
| SA | Stearic acid |
| SDG | Sustainable Development Goals |
| SEM | Scanning electron microscopy |
| $SiO_2$ | Silica |
| SM | Shape memory effect |
| STSA | Statistical Thickness External Surface Area |

|  | **T** |
| --- | --- |
| *T* | Temperature |
| t90 | Optimal curing time |
| $\tan(\delta)$ | Tangent of the phase angle |
| TESPT | Bis[3-(triethoxysilyl)propyl]tetrasulfide |
| Tg | Glass transition temperature |
| TGA | Thermogravimetric analysis |
| Ti | Ionic transition temperature |
| TP | Toner powder |
| TPE | Thermoplastic elastomer |
| TPV | Thermoplastic vulcanizate |
| ts1 | Scorch time |
| TS | Tensile strength |

|  | **U** |
| --- | --- |
| UN | United Nations |

## V

| | |
|---|---|
| V | Volt |
| $V_f$ | Volume fraction of the filler in the recipe |
| VFTH | Vogel-Fulcher-Tammann-Hesse function |
| $V_r$ | Volume fraction of rubber in the recipe |
| $V_s$ | Molar volume of toluene |
| VUB | Vrije Universiteit Brussels |

## W

| | |
|---|---|
| WAXS | Wide Angle X-ray Scattering |
| WEEE | Waste from electrical and electronic equipment |
| WSTP | Waste synthetic running tracks |
| wt.% | Weight percentage |

## X

| | |
|---|---|
| XCNF | Carboxylated cellulose nanofibers |
| XNBR | Carboxylated nitrile rubber |
| XRD | X-Ray diffraction |
| XSBR | Carboxylated styrene-butadiene rubber |

## Z

| | |
|---|---|
| ZnAc | Zinc acetate |
| ZDMA | Zinc dimethacrylate |
| ZnSt | Zinc stearate |
| ZnO | Zinc oxide |
| $ZnO_2$ | Zinc peroxide |
| ZT | Zinc thiolate |

## Others (in alphabetical order)

| | |
|---|---|
| $\omega$ | Angular frequency |
| Å | Angstrom |
| β | Asymmetric broadening of the complex dielectric function |
| $\varepsilon^*$ | Complex dielectric function |
| $\sigma_c$ | Compressive stress |
| $\nu$ | Crosslink density |
| °C | Degrees Celsius |
| $\sigma_0$ | Dc-conductivity |
| $\Delta\varepsilon$ | Dielectric strength |
| χ | Flory-Huggins interaction parameter |
| $\eta$ | Healing efficiency |
| $\varepsilon''$ | Imaginary part of the dielectric function |
| $\Delta m$ | Mass change |
| $\Delta m_t$ | Mass loss of the test rubber piece |
| $\Delta m_1$ | Mass loss of Standard Rubber #1 test piece |
| μm | Micrometers |
| $\Delta E'$ | Payne Effect |
| $\Delta M$ | Torque difference |
| $\varepsilon'$ | Real part of the dielectric function |
| $\sigma_{red}$ | Reduced stress |
| $\tau_{HN}$ | Relaxation time |
| $\varepsilon_0$ | Relaxed dielectric constant |
| $\rho_r$ | Rubber density |
| $\varepsilon$ | Strain |
| λ | Strain ratio |

| $\sigma$ | Stress |
| $\alpha$ | Symmetric broadening of the complex dielectric function |
| $\varepsilon_\infty$ | Unrelaxed dielectric constant |

| $\sigma$ | Stress |
| $\varepsilon_\infty$ | Unrelaxed dielectric constant |

**Resumen**

# Resumen

## CAUCHO NITRILO AUTORREPARABLE Y RECICLABLE: UN CAMINO HACIA LA SOSTENIBILIDAD

Los Objetivos de Desarrollo Sostenible (ODS) exigen un uso más eficiente de nuestros recursos y la construcción de un futuro ecológicamente viable. Para responder a estas demandas, la Economía Circular (EC) contempla varios principios orientados a asegurar que los materiales y productos permanezcan en un ciclo de uso continuo el mayor tiempo posible. En este contexto, el diseño de nuevos materiales que consideren los principios de **Reparar** y **Reciclar** para extender su vida en servicio es de elevada importancia científica, ambiental y económica.

En los últimos 20 años, e inspirada por la naturaleza, la Ciencia ha buscado conferir a los materiales la capacidad de reparar sus propios daños. Esto se denomina autorreparación. La posibilidad de autorrepararse puede encontrarse en diversos animales como las estrellas de mar, moluscos, insectos, e incluso en los seres humanos, visiblemente en la piel. La siguiente figura muestra algunos ejemplos de autorreparación en la naturaleza. Esta capacidad natural ha sido biomimetizada en casi todas las familias de materiales, siendo particularmente relevante en los polímeros, porque sirve como una estrategia para reducir el impacto de sus desechos.

Por su parte, el reciclaje, tal y como lo pensamos actualmente, tuvo su origen en Japón en el siglo XI, donde se registró la primera reutilización de papel desechado;

pero el símbolo que hoy nos permite identificarlo no vio luz hasta 1970. Aunque ambas estrategias no nacieron ayer, la necesidad de desarrollar hábitos de consumo responsables indica que es hoy cuando se muestran más útiles e imperativas que en cualquier otro momento en la historia.



Dentro de los polímeros, los elastómeros son materiales termoestables que se caracterizan por estar constituidos molecularmente por una red tridimensional entrecruzada covalentemente e irreversible que no les permite reprocesarse y moldearse como un termoplástico. Esto se deriva en un modelo de consumo lineal basado en el principio de *fabricar, consumir y desechar*, que sin el manejo adecuado, no es compatible con los principios de la Economía circular. Pero avanzar sin los elastómeros no es una opción. Estos materiales se utilizan en diversos sectores industriales que van desde la industria automotriz hasta la aeroespacial.

Bajo esta perspectiva, el objetivo principal de esta tesis doctoral ha sido el desarrollo de nuevos elastómeros autorreparables y reciclables, con un desempeño mecánico robusto, incluso después de múltiples ciclos de reciclaje. Para ello se ha seleccionado un terpolímero conocido como caucho nitrilo carboxilado (XNBR). La capacidad de autorreparación y la reciclabilidad se logró mediante la construcción de una red entrecruzada iónicamente a través de la incorporación de óxidos metálicos (concretamente, óxido de zinc, ZnO y óxido de magnesio, MgO) capaces de formar una sal metálica de coordinación con los grupos carboxílicos en la estructura molecular del XNBR. Esta unidad funcional, denominada par iónico, tiene la capacidad de agregarse en estructuras de orden superior, conocidas como clústeres, que responden a la temperatura, convirtiendo el material termoestable en uno moldeable, venciendo así las restricciones impuestas por los entrecruzamientos covalentes tradicionales.

Inicialmente, como parte de una revisión bibliográfica que fue más allá de comprender el estado-del-arte, se propuso una nueva clasificación de los elastómeros autorreparables basada en el mecanismo involucrado y su desarrollo histórico. Esta clasificación se condensó en cuatro generaciones que presentan de forma exhaustiva la naturaleza de los enlaces e interacciones dinámicas implicadas (no covalentes, covalentes y combinaciones entre ellos), aportando además los últimos avances en el campo de los cauchos autorreparables.

Como primer resultado experimental, se estudió la dinámica molecular de diferentes compuestos basados en redes covalentes e iónicas y combinaciones entre ellas mediante espectroscopía dieléctrica de banda ancha. Se comprobó que la red entrecruzada influye notablemente en la resistencia y la calidad de las interacciones entre las cadenas poliméricas afectando dos propiedades claves del XNBR: la resistencia a la abrasión y la resistencia química.

Posteriormente se proporcionó una visión global de la reciclabilidad de un XNBR entrecruzado iónicamente. Se destacaron cambios en la dinámica molecular a través

Resumen

de múltiples ciclos de reciclado, que impactan de forma directa sobre diferentes propiedades, más allá de los ensayos de tracción típicamente empleados para caracterizar esta habilidad. Se encontraron pruebas de un delicado equilibrio entre la densidad de entrecruzamiento y los enredos moleculares entre las cadenas poliméricas que afectan a la dinámica del material reciclado. El reciclado también restringe la dinámica molecular cerca de los dominios iónicos, debido a un aumento en la densidad de entrecruzamiento, causada por una disminución del tamaño de los agregados iónicos. Se observaron diferencias insignificantes en el comportamiento a la fatiga por compresión y una mayor resistencia química en diferentes disolventes, lo que garantiza un rendimiento adecuado en condiciones más cercanas al servicio, al menos hasta tres ciclos de reciclaje.

Luego se realizó un análisis exhaustivo de la influencia del ZnO y el MgO en las propiedades físicas del caucho, abordando al mismo tiempo aspectos de sostenibilidad como la autorreparación y la reciclabilidad. Un análisis comparativo a densidades de entrecruzamiento iguales reveló que el exceso de ZnO imparte rigidez debido a su función como carga semireforzante. En cambio, contenidos iguales de óxido indujeron propiedades mecánicas superiores en el compuesto de MgO en comparación con el ZnO debido a la mayor atracción electrostática de sus cationes más pequeños. Una innovación significativa en esta parte del estudio fue el uso de la espectroscopía dieléctrica para determinar la temperatura óptima del protocolo de autorreparación, apartándose de los enfoques tradicionales de ensayo y error empleados habitualmente. Se alcanzaron eficiencias de autorreparación de la resistencia a la tracción de hasta un 79 % y de la elongación máxima de hasta el 95 %, después de aplicar un tratamiento térmico de 110 °C durante 3 h. El material también mantuvo una reciclabilidad total (recuperación del 100 % de las propiedades mecánicas máximas después del reprocesado y moldeo) a lo largo de los tres ciclos de reciclado. Los materiales exhibieron una excelente resistencia a la tracción de 19 MPa, y una alta deformación, superior al 700 %, valores sobresalientes en el campo de los materiales elastoméricos. Estos resultados permitieron ensamblar con éxito una

mano robótica, lo que demuestra la aplicación práctica de estos hallazgos y desvela el potencial de este tipo de elastómeros en aplicaciones avanzadas, como la robótica, donde el uso de elastómeros iónicos ya no es sólo una posibilidad, sino una realidad tangible.

Como última fase de esta investigación, se estudiaron y compararon los efectos de la incorporación de diferentes cargas reforzantes sobre la reciclabilidad, la capacidad de autorreparación y el rendimiento mecánico del XNBR entrecruzado iónicamente. Se analizaron varias cargas de refuerzo convencionales, como el negro de carbono y la sílice, así como cargas sostenibles no convencionales, como la celulosa, el polvo de neumáticos fuera de uso, y desechos de tóner. La adición de un polvo de desechos de neumáticos modificado químicamente mostró el mejor equilibrio entre prestaciones mecánicas, reciclabilidad y autorreparación, proporcionando un uso alternativo de los desechos de neumáticos, generando valor añadido y contribuyendo a la consolidación de la circularidad de los elastómeros iónicos.

Esta tesis doctoral servirá como punto de partida para el desarrollo de más y mejores sistemas elastoméricos que sean ambiental y económicamente viables, capaces de ser empleados en diversas industrias tan avanzadas como el campo de la robótica blanda. De esta manera, se continúa allanando el camino hacia soluciones que alinean el avance tecnológico con las prácticas sostenibles.

# Resumen

**Abstract**

# Abstract

---

SELF-HEALING AND RECYCLABLE NITRILE RUBBER:

A PATHWAY TO SUSTAINABILITY

---

The United Nations (UN) Sustainable Development Goals (SDGs) call for more efficient use of resources and the forging of an ecologically viable future. To meet these demands, the Circular Economy (CE) considers several principles aimed at ensuring that materials and products remain in a continuous use cycle for as long as possible. In this context, the design of new materials that incorporate the principles of **Repair** and **Recycle** to prolong their lifetime is of paramount scientific, environmental, and economic significance.

Over the past two decades, inspired by nature, Science has sought to endow materials with the capability of self-repair. Self-repair or self-healing ability, observed in diverse animals such as starfish, mollusks, insects, and human skin, has been biomimetically integrated into almost all material families. The following figure shows some examples of self-healing in nature. This is particularly pivotal in polymers, where it serves as a strategic approach to reduce the environmental impact of their waste.

Recycling, as conceptualized today, traces its roots back to 11th-century in Japan, with the first documented reuse of discarded paper. The easily recognizable symbol that we associate with recycling did not emerge until 1970. While these strategies

are not new, the current need for responsible consumption habits underscores their increased relevance more than ever before in history.
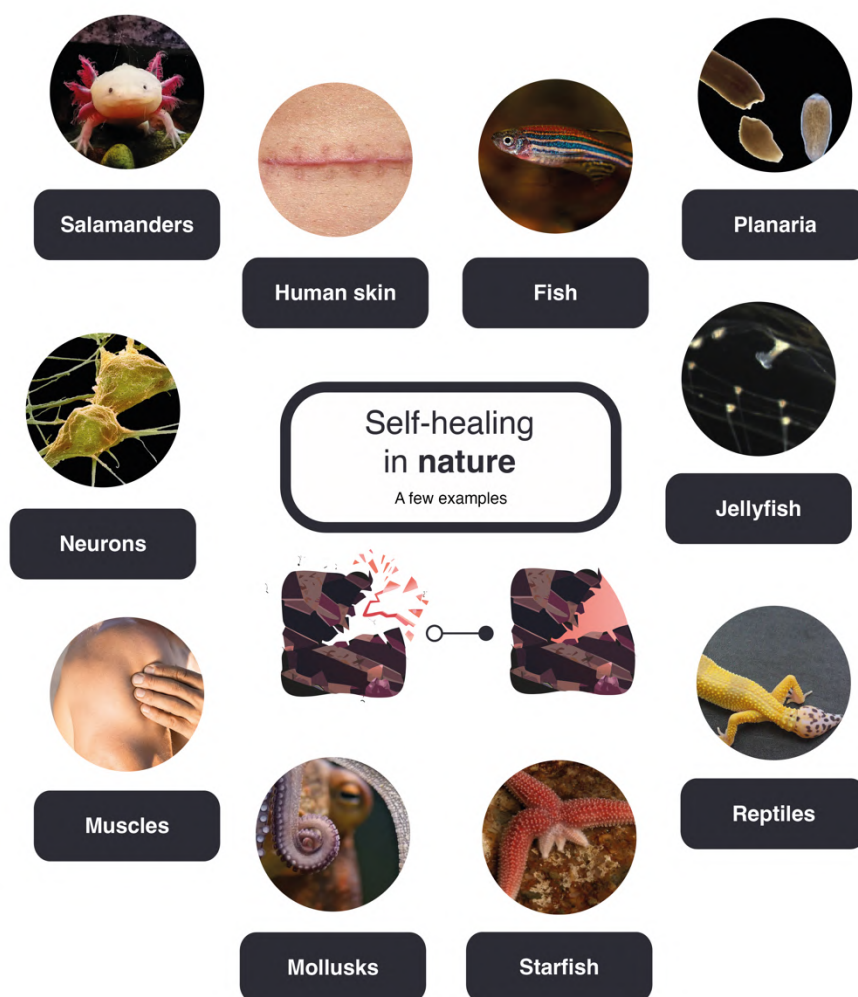


Among the polymers, elastomers are thermoset materials that are molecularly characterized by an irreversible, covalently crosslinked three-dimensional network. This structure hinders their reprocessing and molding like thermoplastics, leading to a linear consumption model of *make, use, and dispose* incompatible with CE principles, without proper management. Yet, advancing without elastomers is not feasible because of their use in diverse industries, from automotive to aerospace.

In this sense, the main objective of this doctoral thesis has been the development of new self-healing and recyclable elastomers with robust mechanical performance, even after multiple recycling cycles. For that, a terpolymer known as carboxylated nitrile rubber (XNBR) was selected. Self-healing capability and recyclability were achieved

by the formation of an ionically crosslinked network via the incorporation of metal oxides (specifically, zinc oxide, ZnO, and magnesium oxide, MgO). These oxides form metal salts coordination with the carboxylic groups in the molecular structure of XNBR. These functional units, known as ionic pairs, can aggregate into higher-order thermally-responsive structures, transforming the thermoset material into a moldable one, thereby overcoming the constraints of traditional covalent crosslinking.

Initially, beyond a mere state-of-the-art review, a novel classification of self-healing elastomers was proposed based on the mechanisms involved and their historical evolution. This classification was condensed into four generations, exhaustively presenting the nature of the dynamic bonds and interactions involved (non-covalent, covalent, and combinations thereof) while also highlighting the latest advancements in self-healing rubbers.

In the initial experimental phase, the molecular dynamics of compounds based on covalent and ionic networks and their combinations were explored using broadband dielectric spectroscopy (BDS). The findings revealed that the crosslinked network profoundly influenced the strength and interactions of the polymer chains, impacting two critical properties of XNBR: abrasion resistance and chemical resistance.

Subsequently, a comprehensive perspective on the recyclability of ionically crosslinked XNBR was offered for the first time, emphasizing the changes in molecular dynamics across multiple recycling cycles beyond standard tensile tests. This study revealed a delicate equilibrium between the crosslink density and molecular entanglements, significantly influencing the dynamics of the recycled material. Recycling was found to restrict molecular dynamics near ionic domains due to an increase in crosslink density, resulting from a reduction in the size of the ionic aggregates. Notably, minimal differences in compressive fatigue behavior and improved chemical resistance in different solvents were observed, ensuring adequate performance under near-service conditions, at least for up to three recycling cycles.

Abstract

An in-depth analysis was then conducted on the impact of ZnO and MgO on the physical properties of rubber, simultaneously addressing sustainability aspects such as self-healing and recyclability. A comparative study at equal crosslink densities showed that excess ZnO imparts stiffness because of its role as a semi-reinforcing filler. Conversely, equal oxide contents led to enhanced mechanical properties in MgO compounds compared with ZnO, which was attributed to the stronger electrostatic attraction of its smaller cations. A significant innovation in this segment of the study was the employment of BDS to pinpoint the optimal self-healing protocol temperature, deviating from typical trial-and-error methodologies. Self-healing efficiencies of tensile strength (TS) up to 79 % and elongation at break (EB) up to 95 % were achieved after 3 h of thermal treatment at 110 °C. Additionally, the selected ionic rubber maintained complete recyclability (100 % recovery of the maximum mechanical properties) through three recycling cycles. The developed materials demonstrated a remarkable TS of 19 MPa and EB exceeding 700 %, which is exceptional for soft materials. These results enabled the successful assembly of a soft robotic hand, showcasing the practical application of these findings and revealing the potential of such elastomers in advanced applications such as robotics, where their use is now a tangible reality beyond mere possibility.

In the final phase of this study, the effects of incorporating various reinforcing fillers on the overall recyclability, self-healing capacity, and mechanical performance of ionically crosslinked XNBR were examined and compared. Several reinforcing fillers, both conventional (carbon black and silica) and unconventional sustainable (such as cellulose; ground tire rubber, GTR, from end-of-life tires, ELT; and toner cartridge waste), were analyzed. The addition of modified GTR demonstrated the best balance between mechanical performance, recyclability, and self-healing, offering an alternative application for tire waste, adding value and contributing to the consolidation of circularity in ionic elastomers.

This doctoral thesis serves as a foundation for the development of more environmentally and economically viable elastomeric systems suitable for use in

industries as advanced as the field of soft robotics. By pushing the boundaries of what is possible in elastomers, this research paves the way for transformative solutions that align technological advancements with sustainable practices.

## Abstract

**Preface**

# Preface

## Motivation

The Circular Economy (CE) envisions a world in which the continuous reuse of products and materials reduces the demand for finite resources and curbs environmental pollution. Therefore, the development of self-healing and recyclable materials has emerged as a key innovation. Self-healing materials possess the ability to autonomously (and sometimes automatically) repair their own damage, which can range from small cracks to catastrophic failure. Because of this ability, their lifetimes are extended. Moreover, at the end of their service life, recyclable materials can be recovered and diverted from the waste stream to be reprocessed and transformed into new products.

The introduction of **_Repair_** and **_Recycle_** is of paramount interest for the production of new polymeric materials, particularly thermoset polymers. Properly managed thermoplastics can be reprocessed and reused because of their ability to mold at high temperatures. Thermosets, on the other hand, are known for their thermal stability and covalent, non-dynamic crosslinked structures, which pose significant challenges for reprocessing and contribute to the increase in polymeric waste.

Within thermosets, elastomers, characterized by their elasticity, are a group of polymers that are essential to modern life. They are amorphous and highly deformable materials with high molecular weights and low glass transition temperatures (Tg) but are slightly crosslinked and thus elastic. Crosslinked elastomers, i.e. rubbers, are able to retract within 1 min to less than 1.5 times its

original length after being stretched at room temperature to twice its length (ASTM D1566, Standard Terminology Related to Rubber). For this reason, they are used in several applications, including tires as the most characteristic, but also in shoe soles, hoses, gaskets, seals, conveyor belts, gloves, catheters, sporting goods, bridge expansion joints, insulation, cases and flexible cables, damping components, toys, etc., intended for many sectors such as automotive, medical and healthcare, construction, clothing and footwear, chemical, petrochemical, mining, aerospace, military, and more. The following image summarizes the most important rubber applications.



All these applications and sectors involve high production and consumption of elastomers, which have rapidly increased over the years and have led to significant waste generation. According to the European Tyre & Rubber Manufacturers'

Association (ETRMA) in its most recent report available (2021), more than 4.2 million tons of tires and 2.3 million tons of general rubber goods were produced in 2020. Thanks to the efforts of the tire value chain during the last 25 years and European regulations, the logistical issue of the collection of End-of-Life Tires (ELT) has been solved through the setup of Extended Producer Responsibility schemes. As a result, valuable materials contained in tires have become available for recycling. Of the approximately 3 million tonnes of tires reaching the end-of-life stage, just 1.6 million tonnes (approximately 53 % of the total collected) are recycled into rubber, steel, and textile fibers. It is important to note that the reutilization strategies for these recycled materials often involve the creation of lower value-added products. Examples of such applications include the use of recycled rubber in playground surfaces or as infill for football fields. No data are available for other rubber products where recycling efforts are lower.

In other countries with more lax environmental legislation, the picture is even bleaker. According to the United States Environmental Protection Agency (EPA), in its latest report on municipal solid waste (2018), 9.6 million tonnes of rubber and leather waste were generated in the United States of America, of which less than 19 % has been recycled and almost 55 % has ended up in landfills, while the rest goes to energy recovery or co-incineration in the cement industry. Available data from other populous and rapidly developing economies, like China and India, where both production and consumption rates are significantly high, do not suggest more promising scenarios. This underscores the pressing need to improve the circularity of the elastomeric products. Thus, the development of new self-healing and recyclable materials is of great scientific, environmental, and economic relevance, impacting multiple sectors and contributing to several Sustainable Development Goals (SDG) of the United Nations (UN).

For example, the use of self-repairing and recyclable materials ensures reduced maintenance costs and the need for frequent replacements that translate into not only advanced but also sustainable infrastructure. This helps build robust industries

and motivates other innovations that prioritize longevity and sustainability over short-term gains (SDG 9: Industry, Innovation, and Infrastructure). However, the applications of self-healing and recyclable materials are not limited to industrial environments. Their integration into urban planning and construction could be transformative. Imagine flexible hoses or pipes in buildings that repair their own cracks or more durable roof waterproofing membranes, leading to cities requiring less resource-intensive maintenance. Such cities would not only be more sustainable but also more cost-effective in the long term, ensuring that urban life remains sustainable as the world's population continues to grow (SDG 11: Sustainable Cities and Communities).

However, the essence of these materials in extending product lifetime and minimizing waste directly encourages responsible consumption (SDG 12: Responsible Consumption and Production). Fewer frequent replacements and reuses of materials at the end of their first service life means that fewer resources are extracted, processed, and transported, resulting in a smaller overall environmental footprint (SDG 13: Climate action). When considering SDGs 14 and 15, the connections may seem less direct, but they are profound. While these materials themselves may not directly mitigate climate change, reducing waste from more durable products means less ocean (SDG 14: Life under water) and land (SDG 15: Life on land) pollution, thus preserving our ecosystems. Therefore, the development of materials that are self-healing and recyclable is indispensable for achieving the 2030 Agenda and the UN SDGs.

This sounds like part of the plot of a futuristic movie, but the truth is that scientists have made substantial progress in creating self-healing and recyclable materials from metals and concrete to rubbers and composites. But how does a material become self-healing and recyclable?

For elastomers, the repair process can be driven by extrinsic or intrinsic mechanisms. Extrinsic mechanisms are extrinsic to the molecular structure of the matrix and are

based on the incorporation of external agents normally dispersed within rubber into microcapsules or vascular networks. When damage occurs, these capsules or networks break, releasing the repair agent and sealing the cracks. Intrinsic mechanisms include the mobility and diffusion of polymeric chains, or the use of dynamic bonds or supramolecular interactions that are reversible when an external stimulus is applied. Some of the dynamic bonds and supramolecular interactions widely used in self-healing rubbers are disulfide bonds, ionic interactions, metal-ligand coordination bonds, hydrogen bonds, and Host-Guest and Diels-Alder chemistry, among others. If crosslinked networks can be constructed from these bonds and interactions, upon application of a stimulus, such as temperature or electrical current, these networks are deconstructed, releasing the polymeric chains and converting the originally thermostable material into a moldable one. The advantage of the intrinsic mechanisms in rubbers is that, owing to these principles, the material gains self-healing capacity and recyclability.

The potential of self-healing and recyclable materials is evident; however, they still face persistent challenges. One of these is the chemical stability of many commercial elastomers, which hinders the reactions necessary for the construction of dynamic crosslinked networks. Therefore, the choice of matrix must be made carefully to avoid the need for successive modifications and raw materials that only perpetuate the contamination spiral. On the other hand, developing a self-healing mechanism that is efficient and effective for a wide range of damage is not a simple task. This includes ensuring that the material can fully repair cracks or breaks without compromising its mechanical properties. The actual conditions of the healing protocol are challenging because of the large number of variables that must be optimized (post-damage time, healing time, contact conditions, temperature, pressure, etc.). The ability of a material to maintain its self-healing capability and recyclability over time and after multiple cycles is essential for its long-term viability. The development and manufacture of these materials often involve expensive processes and a large number of ingredients. Elastomers are subjected to a

compounding process that involves a large number of additives with diverse functions, such as reinforcing agents, anti-aging agents (essentially antioxidants and antiozonants), plasticizers, colorants, odorants, and process aids, each with a specific function. Reducing the number of ingredients involved, their costs, and ensuring scalability for mass production in specific applications are significant challenges. Finally, from a research point of view, establishing standards and regulations to ensure reproducibility and comparability between materials, as well as safety, efficacy, and quality, is essential, especially in critical industries such as the automotive, aerospace, and medical industries. In summary, although self-healing and recyclable elastomers offer many exciting possibilities, their development and practical applications require overcoming technical, economic, and regulatory challenges.

This doctoral thesis proposes fundamental research to overcome some of these challenges and thereby develop self-healing and recyclable materials. It is also sought that the materials developed are scalable towards advanced applications, such as the manufacture of soft robotic grippers. For this purpose, carboxylated nitrile rubber (XNBR) was used. XNBR is a variant of nitrile rubber (NBR), a random terpolymer of acrylonitrile, butadiene and acrylic or methacrylic acid, which contains carboxyl groups as active functional groups. Nitrile rubbers and their derivatives are commonly considered the workhorses of the automotive rubber industry because of its outstanding mechanical properties, resistance to oils, fuels, lubricants, and greases, heat resistance, and relatively low cost. The next figure summarizes the most important properties of XNBR. Because of the presence of carboxyl groups in its molecular structure, XNBR can form a crosslinked network based on ionic interactions in the presence of a metal cation. This results in an ionic elastomer.

Ionic elastomers consist of a crosslinked network formed by ionic-rich domains owing to metal salt coordination. According to the Eisenberg model, these ionic domains gather in higher structures known as multiplets, which in turn form clusters that can dissociate and associate with temperature, thereby demonstrating their

reversible nature. The latter are characterized by a high proportion of trapped chains, which restrict mobility and lead to the appearance of a new transition (i.e., ionic transition) above Tg. This dynamic characteristic enables them to be considered healing moieties and favors recycling.
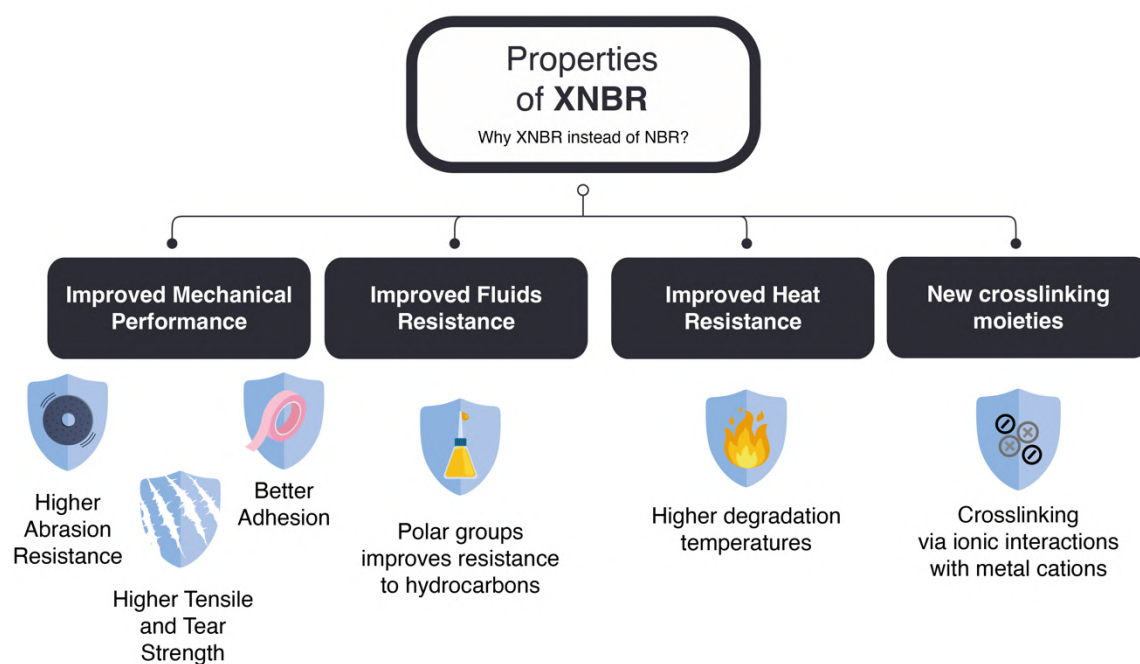


Thus, this research is designed to follow CE principles and serve as a starting point for the development of new economically and environmentally friendly rubbers with potential use in several industries and as an alternative strategy for the management of polymeric waste.

## Objectives

The main objective of this doctoral thesis is to develop self-healing and recyclable ionic elastomers using commercially available and cost-effective raw materials while minimizing the number of additives required. The focus is on maintaining the mechanical performance of the material even after multiple recycling cycles. Sustainability is also supported by the reduction in the number of additives required for compounding. The technical feasibility of these materials in the manufacturing

of soft robotic grippers will be evaluated. The incorporation of sustainable reinforcing fillers, such as cellulose fibers (CF), ground tire rubber (GTR) from ELT, and waste parts from toner cartridges, will also be evaluated. The combination of **Repair** and **Recycle**, with optimized recipes and processes, as well as sustainable fillers intended for advanced applications, will improve the quality of the rubber products developed. These materials will contribute decisively to the UN SDG. The following scheme represents the main objective of this doctoral thesis.



To fulfill this main goal, this research focused on five specific objectives:

**Design of methodology:** *Develop* a methodology based on intrinsic healing mechanisms for the self-healing and recyclability of XNBR, focusing on the creation of ionic elastomers. This approach should leverage the unique properties of XNBR to enhance both the self-healing efficiency and the sustainability of the material.

**Optimization of self-healing conditions:** *Optimize* the self-healing conditions of the developed ionic elastomers by minimizing the required time and temperature. Utilize advanced characterization techniques, such as broadband dielectric

spectroscopy (BDS), to fine-tune the healing process to maximize efficiency and effectiveness.

**Evaluation of recyclability:** *Assess* the recyclability of the prepared ionic elastomers over multiple recycling cycles. This evaluation should involve monitoring a range of properties beyond uniaxial tensile tests to gain a comprehensive understanding of the behavior and endurance of the material through repeated recycling.

**Exploration of advanced applications:** *Investigate* the potential applications of the prepared self-healing and recyclable ionic elastomers in advanced fields such as soft robotics. The focus should be on reducing maintenance needs, minimizing environmental impacts, and extending the operational lifecycle of the products.

**Preparation of reinforced elastomers:** *Develop* reinforced ionic elastomers based on XNBR by incorporating both conventional and non-conventional fillers. Study the impact of these fillers on the self-healing capability, recyclability, and mechanical performance.

## Structure

This doctoral thesis has been divided into seven chapters:

**Chapter 1** introduces state-of-the-art self-healing and recyclable elastomers. It presents a new classification for self-healing elastomers composed of generations, based on their historical development and healing mechanisms. The potential of these advanced materials for commercial applications, including high-performance sectors, has been explored.

**Chapter 2** details the materials, general experimental techniques, and methods used throughout the preparation and characterization of the developed rubber compounds.

**Chapter 3** discusses the development of an ionically crosslinked network in XNBR. It presents an in-depth study of molecular dynamics using BDS. The prepared network described in this chapter served as the basis for the rest of the developments in this doctoral thesis.

**Chapter 4** offers a comprehensive evaluation of recyclability, focusing on the changes in molecular dynamics through multiple recycling cycles. It details the development of a rubber recipe and scalable recycling process, analyzing the behavior of the material, especially in terms of crosslink density and molecular entanglements.

**Chapter 5** deals with an exhaustive analysis of the impact of different oxides on the construction of crosslinking points in ionic elastomers and their influence on the mechanical performance, repairability, and recyclability. BDS was used for the first time to ascertain the optimal temperature for the healing protocol, which differs from the conventional trial-and-error methods. Using an optimized compound, the feasibility of manufacturing tendon-driven soft robotic grippers was demonstrated, thereby addressing the challenges in soft robotics related to load capacity, durability, and sustainability.

**Chapter 6** provides a comparative analysis of various conventional and sustainable reinforcing fillers for XNBR-based ionic elastomers. It revisits the balance between mechanical strength, self-healing capacity, and recyclability, contributing to the development of sustainable materials that combine robust mechanical properties with ecological viability.

**Chapter 7** presents the conclusions of the thesis and offers a future outlook, summarizing the key findings and suggesting directions for further work in the field of sustainable, self-healing, and recyclable ionic elastomers.

Finally, the **Appendices** include indexed publications, dissemination articles, participation, and contributions to national and international conferences as well as the research stay carried out at the *Vrije Universiteit Brussels* (VUB) in Belgium. The following figure summarizes the structure of this doctoral thesis.

**1** **Introduction**
- Comprehensive state-of-the-art review
- New classification of self-healing materials

**2** **Experimental**
- Summary of the materials, compounding, vulcanization and characterization techniques used

XNBR

ZnO

MgO

Crosslinking

Molecular dynamics

Abrasion resistance

**3** **Rubber networks**
- Development and characterization of ionically crosslinked networks

Physico-chemical properties

Thermal properties

Chemical resistance

**4** **Recyclable rubber**
- In-depth analysis of recyclability through multiple properties and recycling cycles

**5** **Self-healing rubber**
- Optimized self-repairing and recyclability conditions
- Feasibility of their use in soft robotic grippers

**6** **Reinforced rubber**
- First comparative analysis of conventional and sustainable fillers in repairability and recyclability

Molecular dynamics

Mechanical properties

Morphology

Dynamic properties

Metal oxide comparison

Optimization of healing conditions by BDS

Soft robotic gripper assembly

Soft robotic gripper actuation

Carbon black and Silica

Cellulose

GTR

Toner cartridges

**7** **Final remarks**
- General conclusions, prospects and recommended future work

# 1 Introduction

# Chapter 1.  Introduction

According to the World Bank [1] by 2050, an increase in global waste generation is anticipated, reaching 3.4 billion tons annually, a drastic increase from the current 2.01 billion tons. Asia, Europe, and North America are collectively responsible for over 70 % of this total waste production (Figure 1.1).
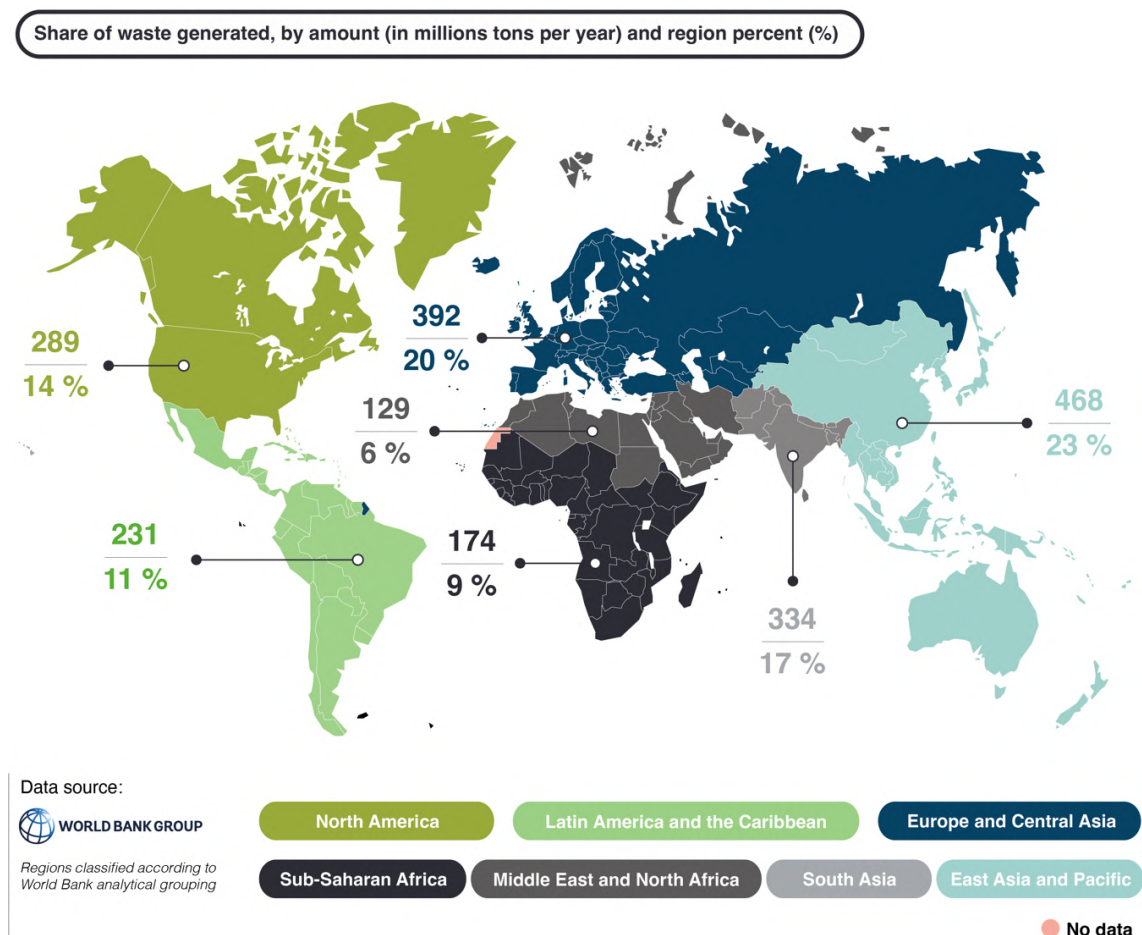


**Figure 1.1.** Share of waste generated worldwide. Adapted from the data in [1].

Of the current total waste output, 2 % is categorized as rubber and leather waste. This represents over 40 million tons per year worldwide. Rubber waste is particularly problematic due to its challenging reprocessing. Unlike plastics, the inherent structure of rubbers, characterized by an irreversible crosslinked network, makes them thermosetting materials and, therefore, not amenable to conventional temperature-driven reshaping or reprocessing techniques. Moreover, rubber products often incorporate numerous additives, each serving a distinct purpose in product performance. The manufacturing of those additives also carries its own environmental burdens, potentially exacerbating the ecological impact of rubber materials beyond current estimations. Despite all these challenges, progress without rubbers, and polymers in general, is inconceivable, given their critical role in different applications.

Our world, significantly shaped by the myriad applications of polymers, is also moving towards the ideals of a Circular Economy (CE) and striving to achieve the United Nations Sustainable Development Goals (SDG). In this context, the dilemma surrounding rubbers demands immediate actions. Scientific endeavors are increasingly focused on meeting the needs for continuous reuse of materials, aiming to lessen reliance on finite resources and mitigate environmental pollution. A notable development in this area are self-healing and recyclable materials. These innovative materials possess the capability to repair themselves, either autonomously or automatically, thereby prolonging their lifetime. Furthermore, their recyclability ensures that, upon reaching the end of their extended lifetime, they can be reused, diverting them from the waste stream and transforming them into new products.

The implementation of **Repair** and **Recycle** strategies is critical in the development of new polymeric materials, especially thermoset polymers like rubbers. **Chapter 1** of this doctoral thesis will delve into fundamental definitions related to elastomers and rubbers, alongside exploring the essential concepts of recyclability and self-repair as key strategies in fostering a more sustainable society.

## 1.1. Elastomers

Elastomers, a distinct category within the broad family of polymers, are characterized by their remarkable ability to withstand high deformations, and then return to their original dimensions once the applied stress is removed [2]. This attribute, known as elasticity, is their defining characteristic. ASTM D1566-21a [3] about Standard Terminology Relating to Rubber, provides a simple but precise definition as follows:

> **Elastomer**, *noun*—an elastic polymer.

Elastomeric materials find their use in a myriad of applications, with tires being the most notable example. However, as highlighted in the **Preface**, their utility extends far beyond, encompassing shoe soles, hoses, gaskets, seals, conveyor belts, gloves, catheters, and a range of sporting goods. They are also crucial in the construction of bridge expansion joints, as well as in the manufacture of insulation materials, flexible cables, and casings. Additionally, elastomers are key components in shock absorbers, an array of toys, and many other products.

This wide range of applications makes it an essential player in multiple industries, including automotive, medical and healthcare, construction, clothing and footwear, chemical, petrochemical, mining, aerospace, and military. Each of these industries relies on the unique properties of elastomeric materials for different applications [4].

Elastomers can be either non-crosslinked or crosslinked, each category possessing distinct properties and implications. Non-crosslinked elastomers retain a simpler molecular structure, offering greater flexibility. However, they lack the enhanced durability and thermal stability of their crosslinked counterparts. This distinction makes non-crosslinked elastomers suitable for applications like medical tubing and certain types of adhesives, where flexibility and conformability are more critical than long-term durability. On the other hand, crosslinked elastomers are characterized by their interconnected molecular structure. This crosslinking imparts more resistant to

swelling by organic liquids, enhanced mechanical strength, and thermal stability, making these elastomers ideal for applications requiring durability and resilience, such as automotive tires and industrial seals. Crosslinked elastomers are also called rubbers [2,5,6]. ASTM D1566-21a [3] about Standard Terminology Relating to Rubber, provides a precise definition as follows:

> **Rubber**, *noun*—crosslinked elastic material compounded from an elastomer, susceptible to large deformations by a small force and capable of rapid, forceful recovery to approximately its original dimensions and shape upon removal of the deforming force.

In the available scientific literature and within the industry, the term *elastomer* is often used synonymously with *rubber*. In this doctoral thesis, these terms will be treated as interchangeable, because all elastomers developed will be crosslinked. However, *rubber* is a term with broader applications. It not only denotes crosslinked rubber products but is also employed to describe raw rubber, rubber adhesives, and rubber glues. More significantly, the term *rubber* is used in technical definitions describing states and properties of matter, such as *rubber elasticity*, *rubbery state*, and *rubbery matrix*. [2]

The process by which rubbers undergo crosslinking of their polymer chains is known as vulcanization [7,8]. This reaction allows them to transform from a more plastic state to one formed by a three-dimensional crosslinked network (Figure 1.2), thereby acquiring, improving or extending the characteristic property of elasticity. To induce this reaction, it is necessary to blend the elastomer with the additives comprising the vulcanization system [5,9]. The crucial additive in this system is the crosslinking agent, which determines the nature of the bonds between rubber chains [5].

Sulfur (S) is the most widespread vulcanization agent used in diene rubber, forming S-based covalent crosslinks. Vulcanization with S allows precise control over material processing, but requires the combination of other ingredients to achieve optimum cure times. These ingredients include: (1) accelerator, to increase the reaction rate; (2) activators, to initiate the action of the accelerator, and in specific manufacturing

processes and environmental conditions, such as hot environments, (3) retarders, to slow down the initiation of the reaction [7].
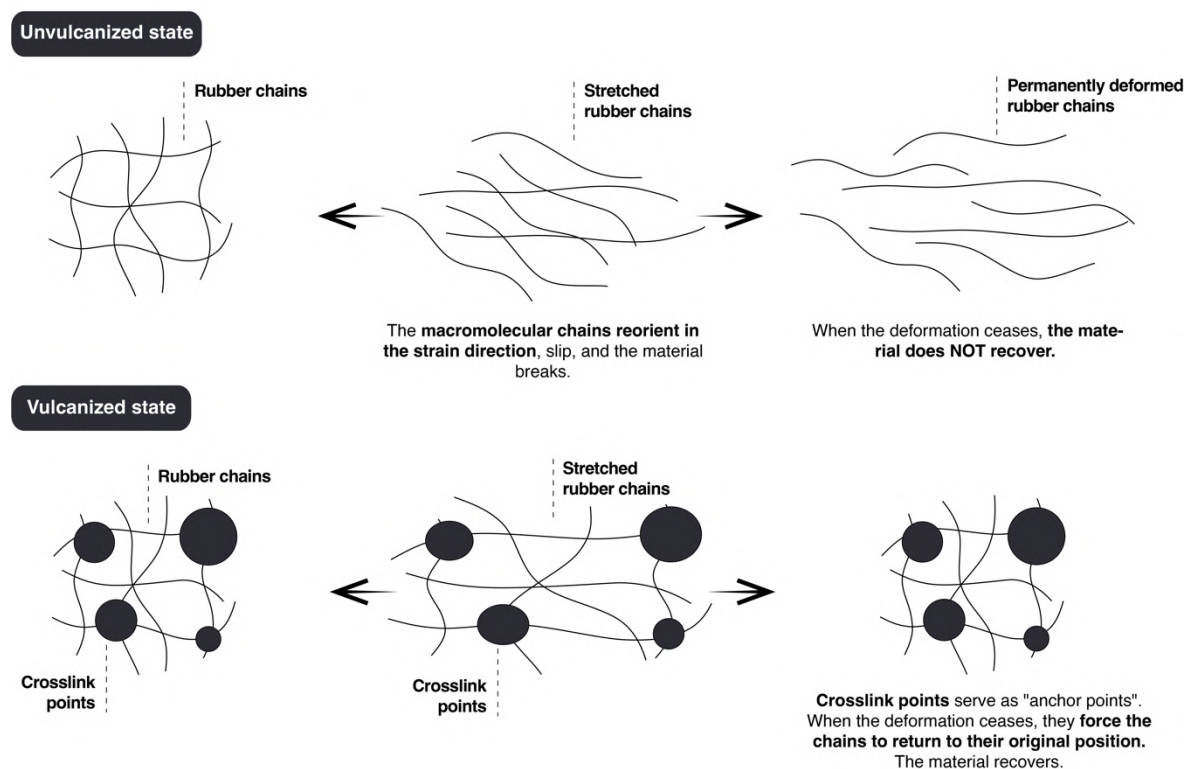


**Figure 1.2.** Polymeric rubber chains before and after vulcanization.

The second widely used vulcanization agents for rubber compounds include organic peroxides. Vulcanization with organic peroxides also results in the formation of covalent crosslinks networks [7]. Nonetheless, these crosslink points are carbon−carbon (C−C) bonds, which are more thermally stable than S-based bonds, but exhibit lower mechanical performance [5].

As previously mentioned, conventional covalent crosslinked elastomers, such as those obtained with S- and peroxide-based vulcanization systems, at the end of their lifetime are particularly critical for the environment because of their reprocessing difficulties. These irreversible crosslinked networks act as "anchor points", preventing

the flow of polymeric chains. Consequently, the material cannot be reshaped [4] and a considerable amount of rubber waste is generated. One of the strategies to solve this issue has been the recovery of end-of-life tires (ELT) for their use as a diluent or reinforcing filler in new composite materials [10–14]. In addition, the selective breaking of crosslinking points, known as devulcanization [15–19], has been extensively studied. However, both strategies have been considered insufficient. Therefore, the redesign of crosslinked rubbers is mandatory. The most recent redesign strategies focus on building dynamic networks [4,20,21].

The creation of crosslinked polymers with dynamic networks has spawned a new generation of polymers known as DYNAMERS (*DYNAmic polyMERS*) [22,23]. The construction of these networks is based on multiple dynamic bonds and/or supramolecular interactions, such as hydrogen bonds [24,25], ionic interactions [26], metal-ligand coordination [27], disulfide exchange [28], and Diels-Alder chemistry [29,30], among other covalent and non-covalent mechanisms and/or combinations between them [31–35]. The reversible nature of these networks can be controlled by an external stimulus, such as temperature, pressure, electrical current, or magnetic field, or further changes in the medium, such as pH [36–38]. In this way, the stimuli-responsive material would be able to release its "anchor points", allowing the flow of its chains until reshaping.

Special elastomers, such as carboxylated rubbers, are potentially useful for the development of DYNAMERS, as they support other vulcanizing agents that promote the formation of ionic crosslinks. The functional crosslinking unit (ion pairs) is capable of regrouping in higher-order structures known as multiplets and clusters [39,40]. The latter structure acts as supramolecular crosslinking points [41]. However, unlike covalent systems, these structures tend to be unstable at higher temperatures [42–44]. Figure 1.3 summarizes the nature of the crosslinks formed by the most common vulcanization agents in rubber recipes (S and organic peroxides) and ionic crosslinks based on metal cations.
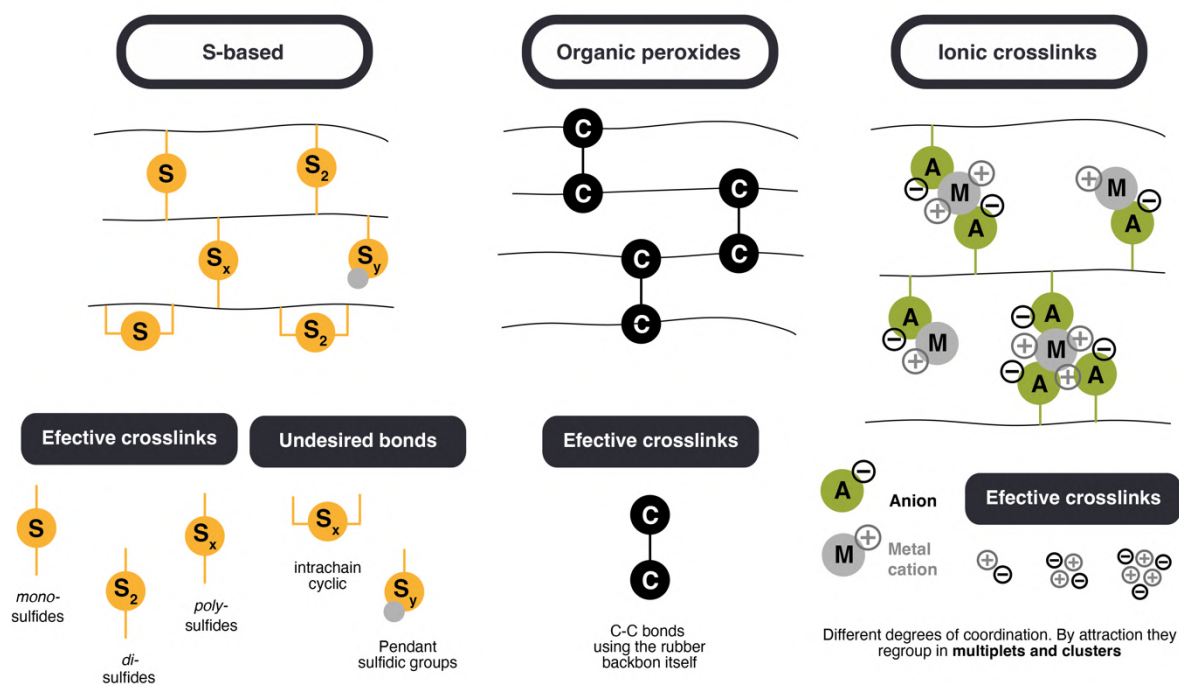
**Figure 1.3.** Functional crosslinking units by S, organic peroxides, and ionic crosslinks.

## 1.2. Ionic Elastomers

When the fundamental crosslinking unit in a vulcanized elastomers is based on ionic interactions, which form a separate phase from the matrix, they are known as ***ionic elastomers*** or ***elastomeric ionomers***.

In 1965, DuPont introduced the term *ionomer* to describe *Surlyn®*, a thermoplastic polymer based on ethylene and partially neutralized methacrylic acid [45,46]. Today, *ionic elastomers*, some block copolymers, and blends of polyolefins with elastic polymers form the thermoplastic elastomers (TPE) group. This family of elastomers combines the elasticity of rubber with the reprocessability of a thermoplastic [46,47]. The schematic in Figure 1.4 summarizes the types of TPEs currently in existence, as well as the nature of the phases that constitute these materials.
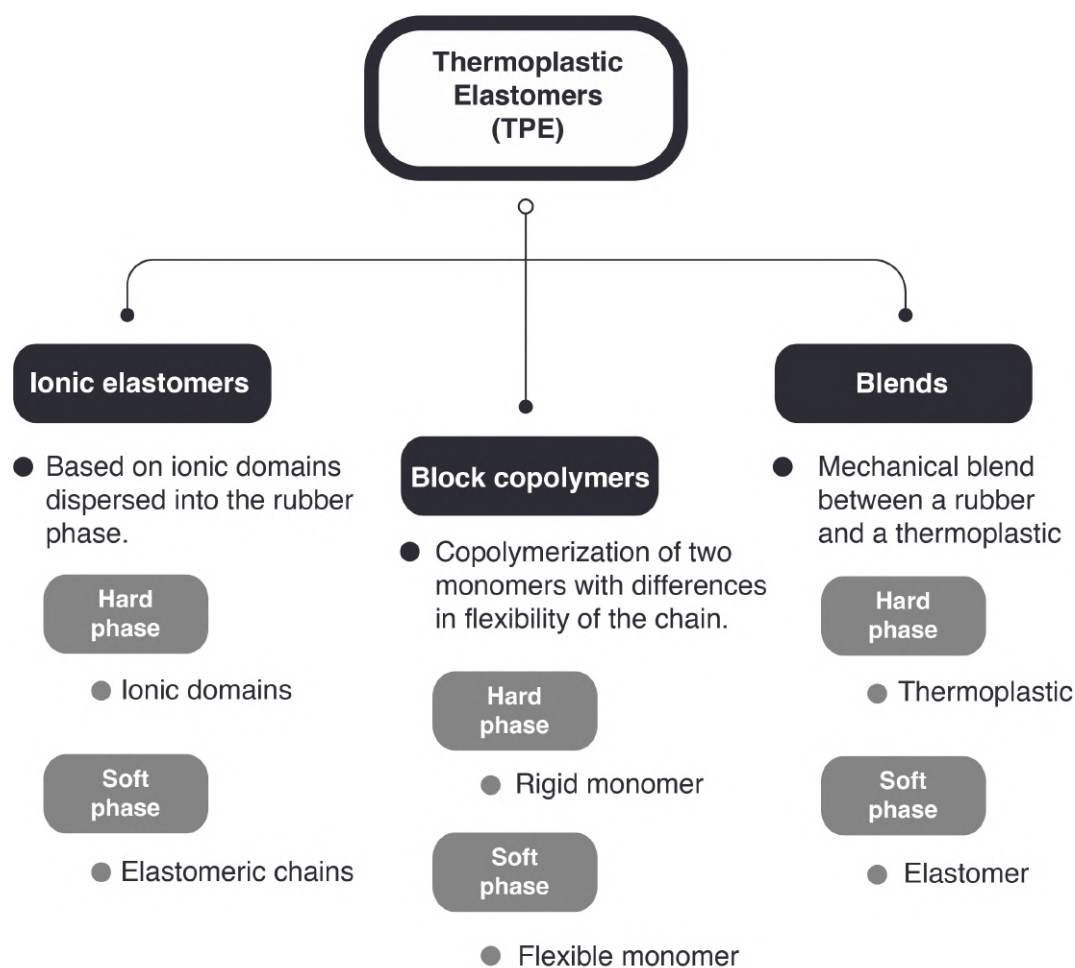
**Figure 1.4.** Classification of TPEs.

In a TPE the elastic behavior is achieved through the presence of at least two separate phases. Both phases are thermodynamically incompatible, leading to phase separation. This implies that polymer networks of flexible chains (soft phase) are interconnected by hard domains [46]. The soft phase, characterized by a low Tg, comprises elastomeric segments with high extensibility. The rigid phase consists of hard domains with limited extensibility that act as crosslinks. In *ionic elastomers*, this phase is complex and follows an order of aggregation that is explained according to a model known as the Eisenberg Model [39,40], illustrated in Figure 1.5.

*Ionic elastomers* usually possess ionizable groups grafted or incorporated into polymer chains (e.g., carboxylic or sulfonic groups), typically not exceeding 15 wt. %

of the material [6]. These groups react with a metallic cation (e.g., $Na^+$, $Mg^{2+}$, $Ca^{2+}$, or $Zn^{2+}$) to provide ionic pairs, the fundamental crosslinking units [41,43,44,48–54]. Ionic pairs tend to aggregate because of their polarity difference from the hydrocarbon chains of the elastomeric matrix, resulting in thermolabile crosslinking.
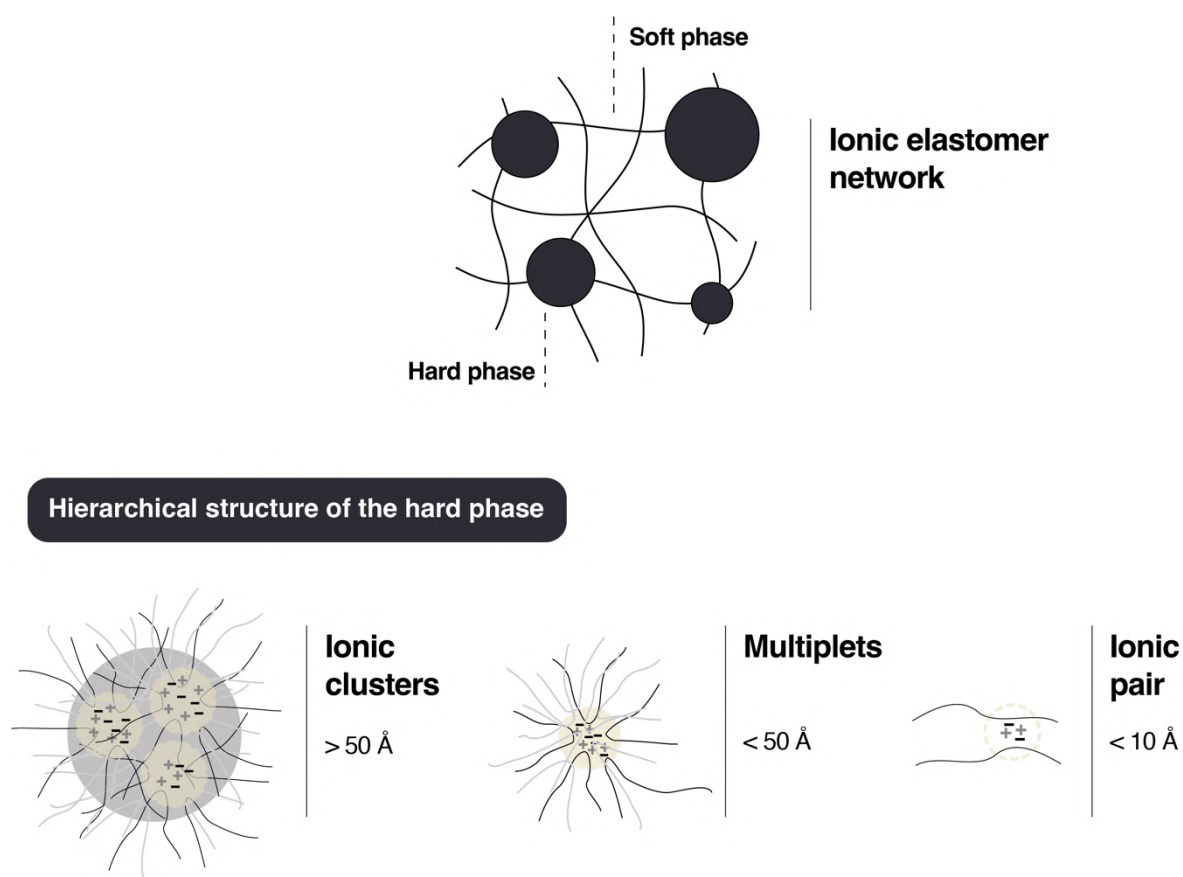


**Figure 1.5**. Structure of *ionic elastomers* according to the Eisenberg model.

Six to eight ion pairs form multiplets. These multiplets are typically dispersed in the matrix [55]. As the ion content increases, the average distance between multiplets decreases, leading to the formation of ionic clusters. Clusters are aggregates of several multiplets and trapped chains. This higher-order association is caused by electrostatic interactions and is affected by the elastic shrinkage forces of the rubber macromolecules. The restricted mobility of elastomer chains in the vicinity of ionic clusters consolidates the hard phase immersed in the rubber matrix [56]. This hard

phase exhibits its own "glass" transition temperature, which is designated as the ionic transition temperature (Ti).

When the material is heated above Ti, the release of trapped chains during long-range "jumping" of ions [57] leads to an increase in the molecular motion of the system, allowing the polymer to be reprocessable. This process is known as ion-hopping and was initially proposed by Cooper [58]. Furthermore, this process is reversible [55]. Upon cooling, the material recrystallizes or vitrifies in its hard phase, retaining its shape and reacquiring the elastomeric properties.

This hierarchical structure gives ionomers outstanding physical properties, which allow them to gain ground in multiple applications below their Ti. They have recently expanded into multifunctional 3D printed parts [59] and advanced applications, such as shape memory elastomers [60,61], dielectric actuators [62,63], coatings [64], and self-healing materials [65–68].

## 1.3. Recyclability of Ionic Elastomers

As TPE, *ionic elastomers* are potentially recyclables. This attribute stems from their unique thermally-responsive ionic domains, which initiate ion-hopping at temperatures higher than Ti. This process releases trapped chains, temporarily transforming the crosslinked structure into a malleable, thermoplastic-like state, thus enabling reprocessability. But what exactly does recycling mean?

According to Directive 2008/98/EC of the European Parliament and of the Council of 19 November 2008, on waste and repealing certain Directives [69,70]:

> **Recycling** *means any recovery operation by which waste materials are reprocessed into products, materials or substances whether for the original or other purposes. It includes the reprocessing of organic material but does not include energy recovery and the reprocessing into materials that are to be used as fuels or for backfilling operations.*

This comprehensive definition encompasses waste recovery operations that could involve repurposing into lower- or higher-quality products. In this context, it is pertinent to differentiate between two approaches of recycling: downcycling and upcycling [71].

Downcycling entails the breakdown of waste materials into their fundamental components or their transformation into materials of lesser quality. Typically, this process results in new products with low quality or value. For example, plastics tend to lose strength and quality when recycled, restricting their subsequent applications. The use of ELT in playground construction or for decorative purposes (such as plant pots) are also forms of downcycling [72].

The primary benefit of downcycling is its capacity to divert waste from landfills and lessen the reliance on pristine materials. However, a notable drawback is the progressive deterioration in the quality of products, which can limit the frequency of their recyclability. Consequently, materials subjected to downcycling are likely to become waste after one recycling cycle [72].

Upcycling, on the other hand, is the process of transforming waste materials or unusable products into new materials or products of greater quality or value. This recycling approach is often viewed as a creative and innovative approach to waste reuse, as it enhances the value of the original material. Upcycling holds particular importance in sustainable development, as it not only reduces waste volume but also curtails the demand for new raw materials. It also enables lower-energy pathways promoting the generation of high-value products. Examples of upcycling include converting old clothes into new fashion items or using ELT powder for the creation of advanced elastomeric materials [73].

A key feature of upcycling is its potential to at least maintain or even improve the performance of the original materials. Moreover, upcycling supports the notion that materials can undergo multiple recycling cycles. Nonetheless, it also faces challenges, including limitations in the scalability and uniformity of the resulting products [73].

The upcycling approach is beginning to be introduced in the scientific literature of general-purpose rubbers. Recently, Yang, et al. [74] explored an innovative approach to recycling waste synthetic running tracks (WSTP) by incorporating them into styrene-butadiene rubber (SBR). This method involves using ground powder of WSTP as a modifier for SBR. The research demonstrated that adding up to 90 parts per hundred rubber (phr) of WSTP significantly increased the tensile strength and elongation at break of SBR. The study also discussed the economic benefits of this recycling method, noting substantial cost savings and positive environmental impacts. This approach not only provides a viable solution for recycling synthetic running track waste but also enhances the performance of SBR, making it a promising method for sustainable material management.

Beyond the approach used, the type of operation applied to achieve the reuse of the waste material can be biological, chemical and/or (thermo-)mechanical (Figure 1.6.) [75]. Biological recycling is based on the degradation and metabolization of polymer chains by microorganisms for subsequent reuse [76]. Chemical recycling is understood as a process where materials are broken down at the molecular level in order to create new products. Unlike other methods, this approach allows the complete transformation of complex substances (macromolecules) into simpler substances (monomers) [77]. Mechanical recycling aims at recovering materials through mechanical processes, such as shredding, grinding, and extrusion [75,78]. These operations can be carried out at RT or temperature-driven (thermomechanical recycling). In the available literature on *ionic elastomers*, essentially chemical recycling and mechanical recycling have been reported.

Using chemical recycling, Shao et al. [79] demonstrated the recyclability of ionically crosslinked SBR via a solution process. The authors developed a new ionic crosslinker using bis[3-(triethoxysilyl)propyl]tetrasulfide (TESPT) and zinc dimethacrylate (ZDMA). The recycling process involved dissolving the initial ionic crosslinked SBR in a mixture of toluene and chloroacetic acid, followed by ultrasonic vibration for 10 h at 90 °C and centrifugation at 10,000 rpm for 5 min. During swelling in toluene,

$H^+$ from the ionization of chloroacetic acid replaced $Zn^{2+}$ in the crosslinked structure, forming zinc chloroacetate, and simultaneously, zinc carboxylate in the crosslinked structure was transformed into the carboxyl group. The reprocessed SBR with ZnO as the crosslinking agent achieved a TS of 3.34 MPa (79 % of the pristine value) and EB of 555 % (53 % of the pristine value).
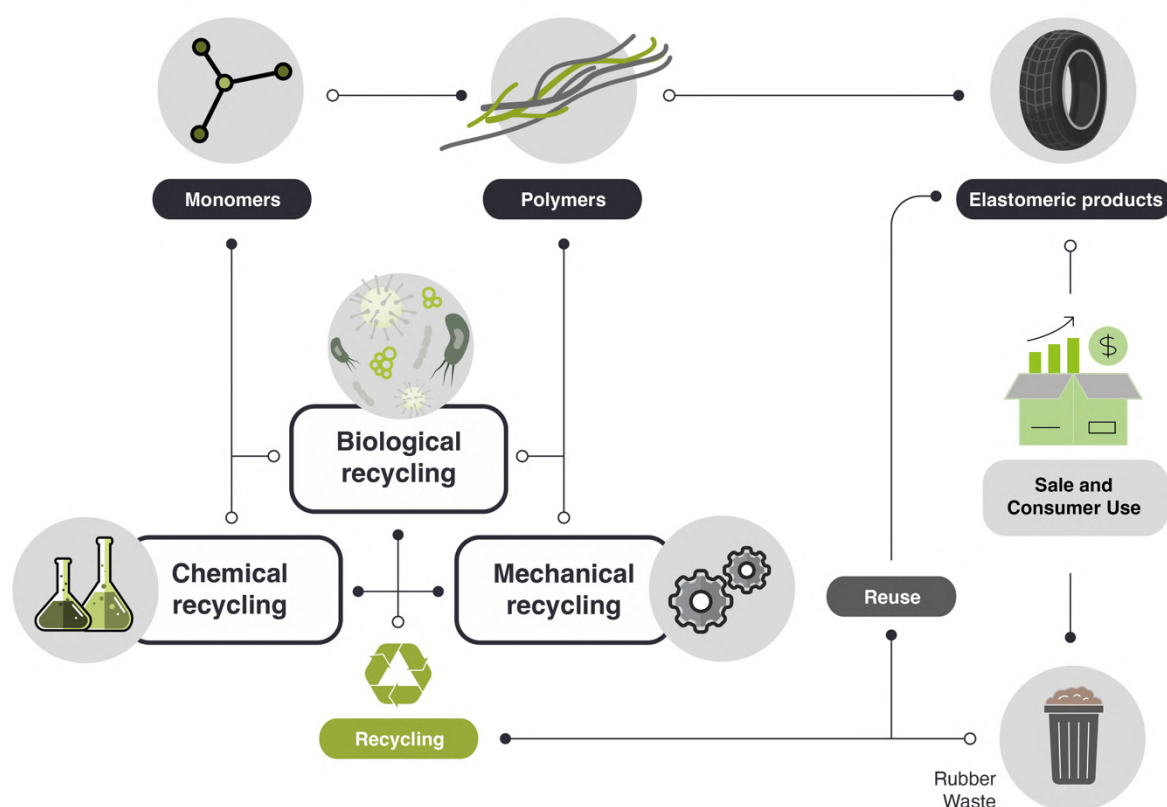


**Figure 1.6.** Recycling operations in elastomeric materials.

The major form of recycled rubber is still ground rubber from mechanical recycling [78]. This is produced either by cryogenic, ambient, or wet grinding. Zainol et al. [80] explored the recyclability of XNBR ionically crosslinked with zinc thiolate (ZT). This method allows for the effective self-healing and recyclability of the material. The recycling process involved cutting the vulcanized rubber into small pieces and masticating them on two-roll mills heated at 80 °C for 5 min. Subsequently, the

rubber was hot-pressed into sheets and shaped for tensile testing. With 30 phr of ZT the full recyclability of its properties was observed at the breaking point. The increase in mechanical performance after three recycling cycles was attributed to changes in the morphology. However, no other evidence was presented, no changes in molecular dynamics were observed, and it was not ruled out that the changes in morphology could be associated with the mastication to which the recycled rubber was subjected to on the two-roll mill.

Identical recycling methodologies have been also used in EPDM grafted citraconic acid with ZnO and zinc stearate (ZnSt) [81], carboxylated SBR (XSBR) ionically crosslinked with ZnO [82], EPDM grafted maleic anhydride (MAH) with zinc acetate (ZnAc) [83] and in XNBR crosslinked by Ni–cysteine and Zn–cysteine complexes [84].

All these works show a strong orientation towards the study of recyclability with tensile mechanical properties. However, although TS and EB are crucial parameters in rubber compounds, they do not represent a functional test in real-world scenarios. This is because most elastomers are not subjected to exclusive uniaxial tensile conditions in practical applications up to more than 500 % deformation. In this sense, relying solely on the recovery of these properties does not provide a comprehensive understanding of the molecular changes that occur when the material undergoes full reprocessing. Future research should include a broader examination of recyclability by considering multiple properties. This doctoral thesis aims to address this gap by conducting an in-depth analysis of molecular dynamics using advanced techniques and analyzing different properties to provide a comprehensive understanding of the recyclability of *ionic elastomers* with an upcycling approach.

## 1.4. Self-healing Elastomers

Inspired by nature, self-healing materials have the ability to repair or restore damage, replicating mechanisms found in living organisms, such as plants and

human skin. To ensure the success of self-healing, three concepts were defined by van der Zwaag et al. [85]: a) localization, b) temporality, and c) mobility. This work introduces a fourth key concept: d) mechanism to classify different generations of self-healing materials (Figure 1.7) [86].
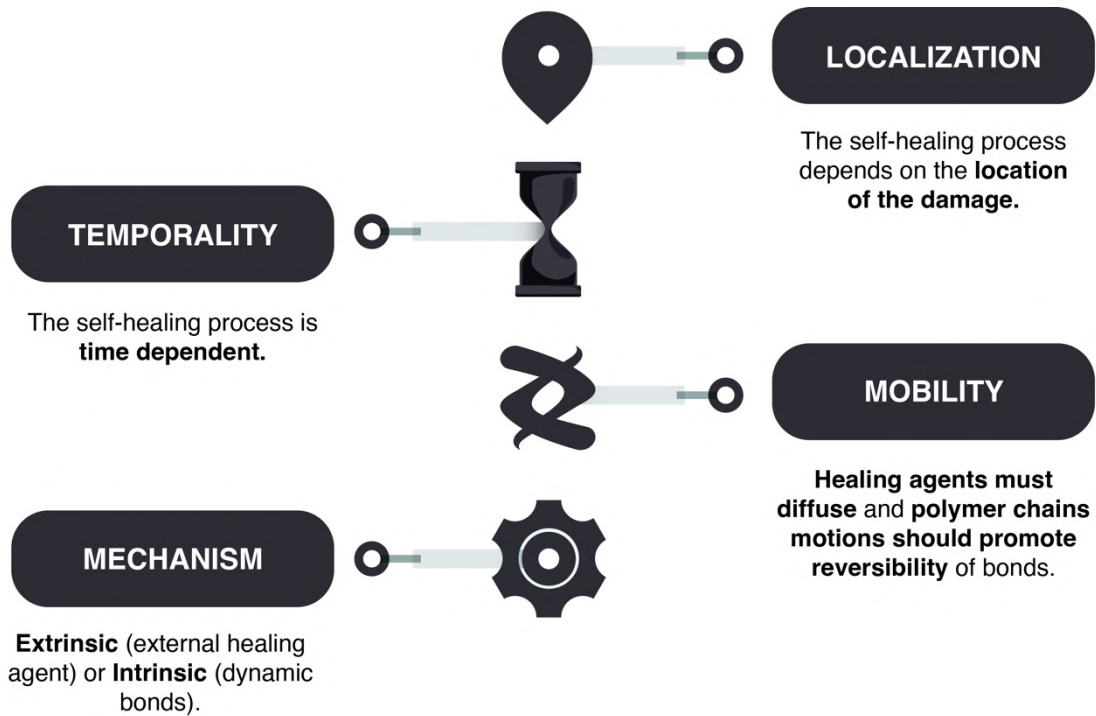


**Figure 1.7.** Key self-healing concepts. Adapted from [86].

The concept of localization refers to the position and/or scale of damage. It can be superficial, such as scratches, (micro) cracks, or cuts; it can be deep, such as the propagation of surface damage, fiber debonding, or delamination, resulting in catastrophic damage, or molecular scale damage, for example, breakage of the material network [87]. The localization and scale of these damages play an essential role when considering the self-healing capability of a material. The aim is to develop a single protocol that ensures healing at all scales; however, specific protocols can be

designed for particular damages according to the intended application of the material.

The second factor, temporality, is given by the time gap between a damage event and its repair. Even in nature, self-healing is time-dependent, not instantaneous. The target is to minimize the time for healing to occur. One way to reduce this time is by conferring mobility to the material, which is the third key concept. Mobility promotes the diffusion of the healing agent to the damaged area as well as the reformation of broken bonds. This concept is key to optimizing others; for example, if the mobility of the agent is not adequate, it will not flow towards the damage, or it will do so slowly.

The last key concept of self-healing is its mechanism. This concept enables classification of self-healing materials into two families: extrinsic and intrinsic. Extrinsic self-healing materials are those in which the process depends on an external agent that is normally dispersed in the form of capsules or vascular systems. These agents are released to seal the damage and do not interact specifically with the matrix. On the other hand, intrinsic self-healing materials are those in which the reversible bonds present in the material can be restored after a damage event [87]. In the case of polymers, extrinsic systems have widely been used in thermosets, mainly in epoxy resins [88–90], while intrinsic mechanisms have widely been considered in elastomers, such as silicones [91], polyurethanes (PU) [92], and general-purpose rubbers [93–95]. At this point, it is important to clarify that the current use of intrinsic and extrinsic terms in the field of self-healing to classify any material according to the type of mechanism involved differs from its use to designate physical quantities. In chemistry, *intrinsic* describes properties independent of size, shape, and quantity (such as density and refractive index), whereas *extrinsic* refers to dependent properties (such as weight and volume). The use of these words has some limitations, despite their extensive validation and widespread use in the field of self-healing [96–100]. All the above motivates the proposal of a new classification based

on the self-healing mechanism and historical development that enables the organization of self-healing materials in four generations (Figure 1.8).



**CAPSULE-BASED**

**(Extrinsic)**

An encapsulated healing agent dispersed in the matrix is released when some damage occurs, sealing it.

**INTRINSIC**

Based on the chemistry of dynamic bonds and reversible supramolecular networks, which can be restored under the influence or not of external stimuli.

1ST GENERATION

4TH GENERATION

2ND GENERATION

3RD GENERATION

**COMBINED**

This new generation presents the combination of different self-healing systems, generally intrinsic.

**VASCULAR BASED**

**(Extrinsic)**

The healing agent relies on a vascular network system (fibers or nanotubes) and is released when some damage occurs, sealing it.

**Figure 1.8.** Generations of self-healing materials. Adapted from [86].

## 1.4.1. Generations of Self-healing Elastomers

Although it was not the first published mechanism (as will be explained later), the first-generation of self-healing materials were based on extrinsic mechanisms and employed encapsulated external healing agents. This generation has the disadvantage of supporting only a single self-healing cycle [96]. To overcome this

limitation, the second generation of self-healing polymeric materials emerged, based on intrinsic mechanisms, using the chemistry of reversible bonds; however, the self-healing capability and mechanical performance of the materials were compromised, with an increase in one indicating a decrease in the other. The intrinsic approach has been studied for all types of polymers, with special emphasis on elastomers [97,98]. Later, further development of extrinsic systems was initiated through healing agents confined in vascular networks, giving way to the third generation of self-healing polymers with a strong inspiration in nature. These systems have been extensively studied in thermosets, but their application in elastomers remains limited, except for a few studies on silicones [101].

Finally, the fourth generation is currently growing fast and aims to overcome the different drawbacks of the previous generations. Hence, its objective is to develop a polymer with excellent mechanical properties, high healing efficiency, and resistance to multiple damage cycles through a combination of different healing mechanisms. However, the road to this point has been long, and there are still some challenges to be overcome.

According to the literature, in the 1970s, Malinskii et al. [102–104] presented one of the first studies on polymer self-healing, specifically in poly(vinyl acetate) (PVAc). Later, Jud et al. [105] and Wool et al. [106,107] further studied the healing of cracks in poly(methyl methacrylate) (PMMA), polystyrene (PS), and hydroxy-terminated polybutadiene (HTPB). Nevertheless, all these works and those in the immediate years were based on chain interdiffusion [108], a well-known concept in polymers that only required a temperature slightly higher than the Tg of the material to occur. Ellul et al. [109] presented the concept of self-adhesion in butyl rubber (IIR), as an essential preliminary step to ensure good contact between the surfaces to be repaired. The concept of autonomic self-healing, as we know it today, was introduced by Dry et al. [110,111] in the early 1990s; mainly in cement and epoxy resins. However, it was not until the publication of White et al. [88] that the definitive impulse for the

development of self-healing polymeric materials began. This work is considered the starting point for modern self-healing polymers.

White et al. [88] achieved self-healing by incorporating a healing agent (dicyclopentadiene, DCPD) embedded in microcapsules and a platinum catalyst (Grubb's catalyst) dispersed in an epoxy resin. Upon the release of the agent and encountering the catalyst, the polymerization of DCPD occurs, sealing the crack. Initially, this method enabled efficiencies of up to 75 % in the recovery of the maximum load in a fracture toughness test. The implementation of this methodology in elastomers, specifically in poly(dimethylsiloxane) (PDMS), was carried out by Keller et al. [112], who used chemistry based on two types of microcapsules. They introduced a high-molecular-weight resin of PDMS functionalized with vinyl groups and a platinum catalyst in one, while in another, they encapsulated an initiator and a PDMS copolymer with active sites that would serve to link the vinyl groups of the functionalized resin by platinum catalyst action. This chemical reaction, also based on the polymerization of external agents, allowed efficiencies of up to 120 % in the recovery of the tear strength. This first generation has been classified in several ways according to the arrangement of healing agents and catalysts. The most widespread classification comprises five types: single-capsules, capsule/dispersed catalysts, phase-separated droplets/capsules, double-capsules, and all-in-one capsules. It is also possible to establish classifications according to encapsulation techniques (for example, *in situ* polymerization, sol-gel reaction, interface polymerization, and emulsion) [113].

The second generation is based on the chemistry of dynamic bonds. Any bond or interaction that is reversible under equilibrium conditions is considered dynamic and can be classified as covalent or non-covalent. Intrinsic self-healing mechanisms of non-covalent nature comprise all those weak interactions that can occur between different families of atoms, such as van der Waals interactions, $\pi$-$\pi$ stacking, dipole-dipole interactions, hydrogen bonding, ionic interactions, metal-ligand coordination, and host-guest interactions. Some authors [114,115] attribute the self-healing

capability to the existence of the shape memory effect (SM). There is debate about whether SM can be considered a self-healing mechanism. However, undoubtedly assists the self-healing process, especially in its initial stages, when the best possible contact between the surfaces is required, contributing to achieving high healing efficiencies. Figure 1.9 summarizes all non-covalent interactions and their basic definitions.
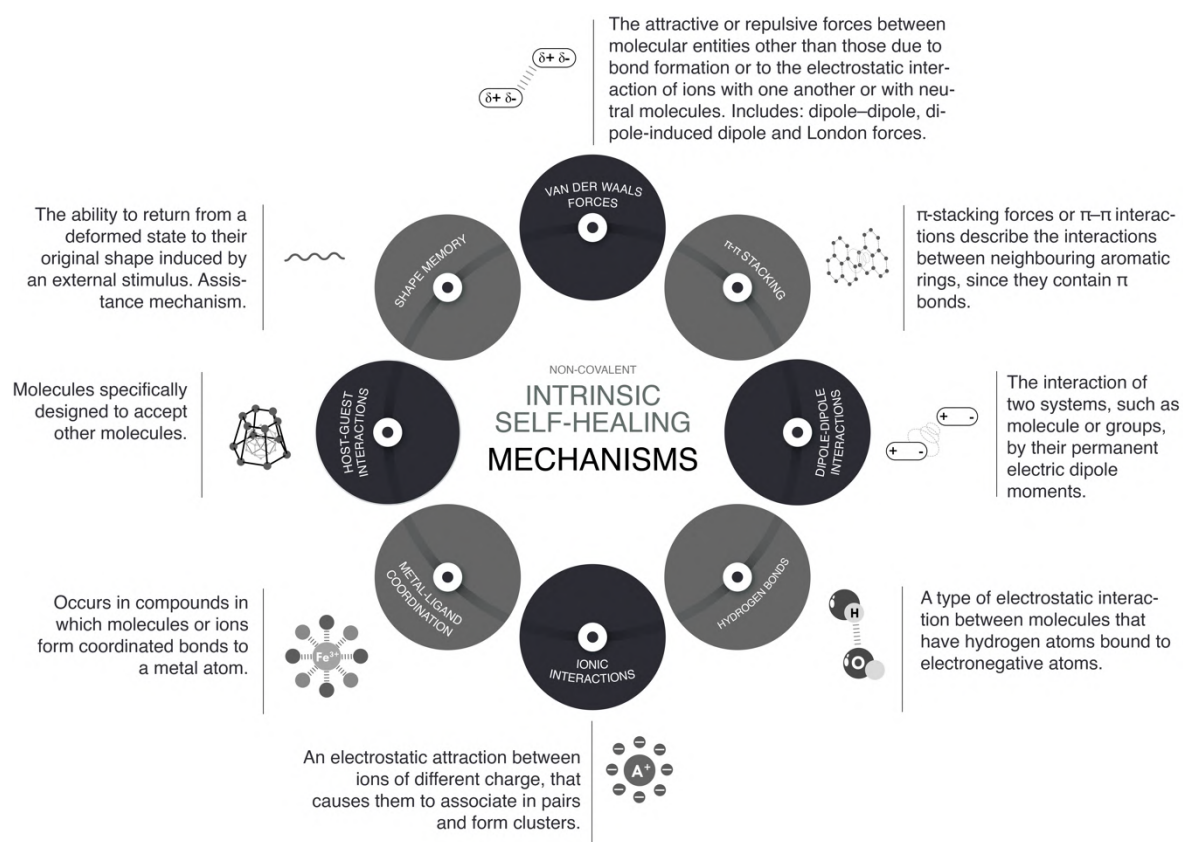


**Figure 1.9.** Non-covalent intrinsic self-healing mechanisms. Adapted from [86].

Non-covalent systems are characterized by a low bonding energy compared to pure covalent systems [116]; therefore, they usually have higher healing efficiencies because they facilitate the restoration of broken bonds, even at room temperature (RT). The non-covalent interactions most commonly used in elastomers are hydrogen bonds [24] and ionic interactions [117].

Intrinsic covalent mechanisms are related to all those chemical bonds that can be formed between different atoms, and can be dynamic under an external stimulus. Figure 1.10 schematically summarizes some of these bonds and their basic definitions. Clear examples are disulfides, which can undergo metathesis reactions, and the Diels-Alder chemistry, where Diels-Alder and retro-Diels–Alder reactions occur at different temperatures. These bonds have higher energy than non-covalent bonds [116]; therefore, their contribution is usually associated with the mechanical performance of the material.
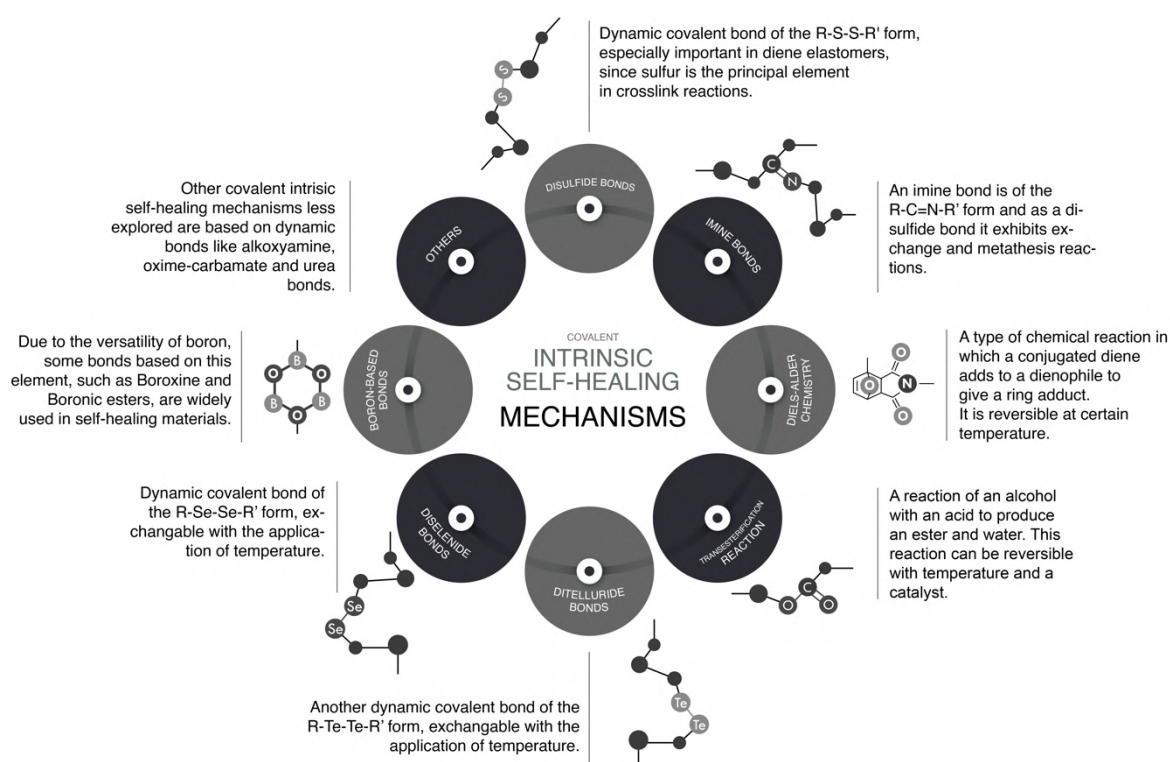


**Figure 1.10.** Covalent intrinsic self-healing mechanisms. Adapted from [86].

Although polymeric materials based on reversible chemistry have been developed in the past, Chen et al. [29] specifically designed the first self-healing polymer based on multi-furan and multi-maleimide monomers (Diels-Alder chemistry). In this study, fracture toughness tests were carried out after healing at temperatures between

120 °C and 150 °C, achieving an efficiency of 57 % in the recovery of the maximum load. Simultaneously, the effect of pressure on the repair process was evaluated, and it was concluded that it had minimal influence on the healing efficiency of this material. This work represents an important development in the field because it shows a recovery of 80 % after subjecting the material to a third damage event, thus proving the occurrence of multiple healing cycles.

Later, Cordier et al. [118] first introduced the intrinsic self-healing methodology into an elastomer designed and synthesized from molecules that could form chains and crosslinks through hydrogen bonds. Therefore, they constructed a supramolecular network capable of self-restoration at RT. In this work, time dependence in the self-healing process was evidenced. Longer times implied greater efficiencies. Therefore, they concluded that self-healing was not an instantaneous process.

The third generation of self-healing materials began with the study by Toohey et al. [119]. Although the concept was explored almost 20 years earlier by Dry et al. [110,111], the definitive stimulus for this generation took considerable time owing to the difficulties of incorporating vascular networks into a polymer matrix. This generation is typically classified according to the nature of the vascular network and its preparation technique. Examples include electrospinning (coaxial electrospinning or emulsion spinning), solution blowing (coaxial solution blowing or emulsion blowing), and tubes and channel networks (micro/nano, such as hollow glass fibers, carbon nanotubes, among others) [101]. Toohey et al. [119] used the methodology previously described by White et al. [88]; however, the healing agent (DCPD) was confined to a net embedded in the epoxy resin coating. The healing efficiency was also measured as the retention of properties in fracture toughness tests, with efficiencies of over 40 % and supporting up to seven healing cycles.

The difficulty of incorporating vascular networks into the matrix has hindered their application in elastomers. Only one group has reported the incorporation of an electrospun vascular network into PDMS [120–123]. Lee et al. [120,121], prepared

two co-axial electrospun networks with polyacrylonitrile (PAN), as shell, and with either dimethylvinyl-terminated dimethylsiloxane (resin monomer) or methylhydrogen dimethylsiloxane (curing agent) as core. Thus, the two core materials interact only upon cutting the PAN shell. The self-healing efficiency was qualitatively evaluated as an anti-corrosive barrier and showed good performance. Thus, the design of resistant vascular networks that do not break during high-shear and conventional processes remains challenging.

The fourth generation is currently emerging in this field. Since the work of Burattini et al. [124], the literature on combined self-healing mechanisms is steadily growing (Figure 1.11), and has focused on intrinsic self-healing mechanisms, always searching for an optimal combination of dynamic bonds, either covalent or non-covalent [125]. This strategy has also been considered for different, but not distant, purposes in elastomers, such as recyclability [126–129].
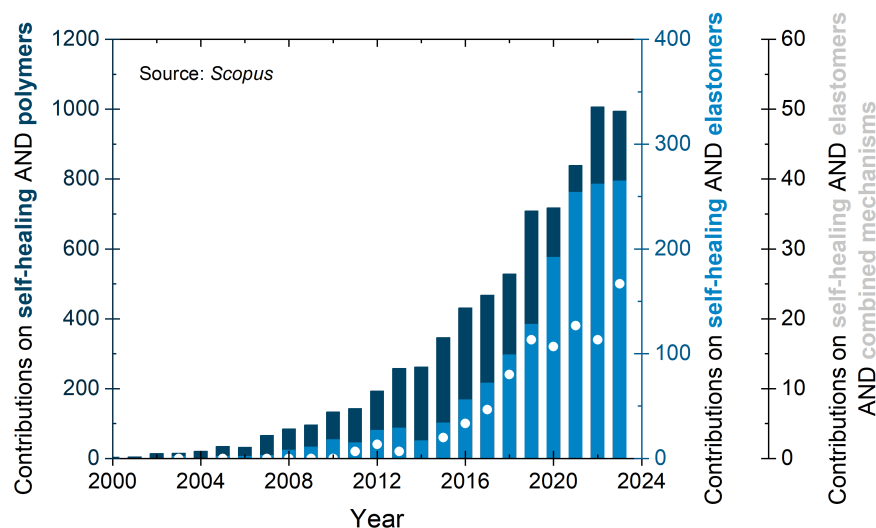


**Figure 1.11.** Evolution of contributions on self-healing elastomers. Adapted from [130].

In their first study, Burattini et al. [124] reported a combination of healing moieties (π–π stacking and hydrogen bonds) in an elastomeric network based on polyimide

and polyurethane with pyrenyl end groups. The $\pi$–$\pi$ stacking was due to the $\pi$-electron-deficient diimide groups and $\pi$-electron-rich pyrenyl units. Meanwhile, hydrogen bonds were formed at the intermolecular level between the terminal residues of the pyrenyl groups in the PU. This material reached a TS of 0.2 MPa, with a healing efficiency higher than 80 %.

However, this new generation does not mean that further developments using previous approaches have ceased. Instead, all available strategies are incorporated into different materials, and their feasibility is studied in both traditional and advanced applications. For example, the use of extrinsic mechanisms has shown a notable increase in coatings [121], instrument panels [131], and sponges [132]; whereas intrinsic mechanisms have turned out to be more versatile for general-purpose elastomers in innovative applications such as nanogenerators [133], sensors [134], conductive elastomers [135], and even tires [95].

### 1.4.2. Current Developments in Self-healing Ionic Elastomers

The development of self-healing *ionic elastomers* occurs mainly within the second and fourth generations of self-healing polymers [136]. In particular, the second generation has more records in the literature [137] using different types of rubber matrices, including natural rubber (NR) and epoxidized NR (ENR) [138–140], SBR and XSBR [141], ethylene-propylene-diene rubber (EPDM) [142], polyisoprene (PI) [62,143–145], IIR [31,65,146–149], PDMS [150], PU [67], and elastomer-based composites [64,66,151,152]. The previous research has demonstrated that self-healing systems relying on intrinsic mechanisms like ionic interactions possess an advantage over other intrinsic mechanisms, such as hydrogen bonds or $\pi$-$\pi$ interactions, by potentially enhancing the mechanical performance of the material significantly. Additionally, compared to covalent mechanisms, it is observed that ionic interactions exhibit their dynamic nature under lower temperature conditions than those required in these alternative systems [4,20,153].

One of the most widely used strategies for the formation of ionic clusters in rubbers has been the *in situ* reaction between methacrylic acid (MAA) and excess $Zn^{2+}$ [154,155] or the grafting of ZDMA [26,94,156]. Xu et al. [140] demonstrated that the *in situ* reaction allows the formation of ionic crosslinks within the NR matrix. The variation in the MAA/ZnO molar ratio fine-tunes the mechanical properties of NR. A key finding was that the TS of NR with an MAA/ZnO ratio of 2:1.4 increased to 1.89 MPa, almost tripling the strength of NR with an MAA/ZnO ratio of 2:1, which only reached 0.64 MPa. These mechanical strength values can be useful for applications that do not require high mechanical performance. The formation of this new ionic network is vital for self-healing, where the diffusion of the NR chains contributes to the healing process. The prepared compounds showed 53 % healing efficiency of TS within 1 min, which increased to 76 % after 5 min. The sample fully recovered after 15 min, demonstrating the effectiveness of the self-healing properties.

In the fourth generation field, ionic interactions have been successfully combined with various non-covalent and covalent systems [26,157,158]. For example, Guo et al. [133] considered the combination of ionic interactions with hydrogen bonds [159], giving rise to a non-covalent network with one of the highest TS and resistance/efficiency ratios reported. They prepared ternary elastomeric complexes of branched poly(ethyleneimine) (bPEI), poly(acrylic acid) (PAA), and poly(ethylene oxide) (PEO) (bPEI/PAA/PEO). These intricated ternary complexes facilitated the formation of electrostatic interactions between bPEI and PAA and hydrogen bonds between PAA and PEO. Owing to the positive effect of both interactions, an elastomeric material was obtained with a TS of 27.4 MPa and a healing efficiency of 92 % at RT in a high-humidity atmosphere.

The same joint mechanisms were explored in a special-purpose rubber, such as brominated butyl rubber (BIIR), with opposite results. Stein et al. [65] designed an elastomeric network of BIIR modified with one uracil and one imidazole moiety. The latter provides ionic groups associated with the so-called ionic clusters. The former, with a bifunctional structure containing two diamidopyridyl moieties, was

responsible for the formation of hydrogen bonds. The incorporation of hydrogen bonds worsened the healing efficiency achieved with only ionic interactions, since they decreased the TS to 5.7 MPa and the healing efficiency to 39 % from a TS of 10.7 MPa and a healing efficiency of 74 % at 70 °C.

More recently, Gong et al. [158] reported the innovative design of 2-aminopyridine (AP) grafted on ENR that integrates a hybrid bond network of ionic and coordination supramolecular bonds. ZDMA was used to provide $Zn^{2+}$ cations. The formed bonds, while sharing identical crosslinking points, exhibit contrasting strengths. Through optical microscopy imaging and temperature-dependent FTIR, the authors demonstrated that the ionic bonds effectively shortened the spatial distance of the ENR chains, enabling them to form a stable, low-energy network. This process also facilitates the reconstruction of coordination bonds because of their shared crosslinking points. The synergistic interplay of these two bond types endows the material with notable mechanical properties, including a low TS of 1.33 MPa and a strain capacity of 600 %, along with a high healing efficiency of 92 % after 3 h at RT. As evidence, self-healing ionomers have a critical drawback, except for a few exceptions. There is a trade-off between how well they can heal and how well they can mechanically perform. This antagonistic relationship between the two properties has made it hard to create fully functional self-healing elastomers. One solution to this problem has been to add fillers that make the self-healing systems stronger, which may (or may not) take part in the healing process.

### 1.4.3. Reinforced Self-healing Ionic Elastomers

In the dynamic landscape of self-healing *ionic elastomers*, a key focus lies on the durability of the materials. This durability is not only given by the reusability provided by the repair process but can also be complemented by a robust mechanical performance for which reinforcing fillers must be included in the rubber recipe.

Reinforcing fillers [160–165] in rubber compounds can be categorized into two distinct groups: conventional and sustainable fillers. Conventional fillers, such as carbon black (CB) and silica, and carbon-based nanoparticles, such as graphene and carbon nanotubes (CNT), have been the cornerstones for enhancing the mechanical properties of these elastomers. Their role in reinforcing the strength and durability of materials is well-established. However, there is a growing interest in exploring sustainable alternatives that offer environmental benefits without sacrificing performance. These sustainable fillers, including cellulose, lignin, and alginate, from natural sources, and waste recovered particles, align with the principles of a CE. Other fillers that act as diluents can be used in the manufacture of rubber compounds to reduce cost, without major effects on the mechanical performance. Figure 1.12 summarizes the most common fillers used in elastomeric compounds.

## Conventional Fillers

The exploration of conventional fillers in the realm of self-healing *ionic elastomers* is always a trend. Traditional fillers, such as CB and silica, and advanced nanomaterials, such as graphene and CNT, have been extensively studied for their potential to reinforce elastomers. These conventional fillers are pivotal for enhancing the mechanical properties of elastomers, contributing to their strength, durability, and overall performance. CB, in particular, has been a mainstay of rubber reinforcement, offering outstanding TS and resistance to wear and tear. While silica enhances the thermal stability and rigidity of the elastomers. Additionally, the advent of nanotechnology has introduced graphene and CNT as innovative fillers, which stand out for their exceptional mechanical properties and the potential to impart novel functionalities to *ionic elastomers.* These conventional fillers play a crucial role in optimizing the performance of self-healing elastomers, making them suitable for a wide range of applications from automotive tires to advanced engineering materials.

Some fillers, such as CB, are not environmentally friendly because of the high pollution generated by their production. Nevertheless, replacing CB in elastomer applications is still not possible, particularly in critical applications that require high mechanical performance. Therefore, conferring self-healing capability to composites reinforced with this type of filler can be a temporary solution to reduce the environmental impact of their use.
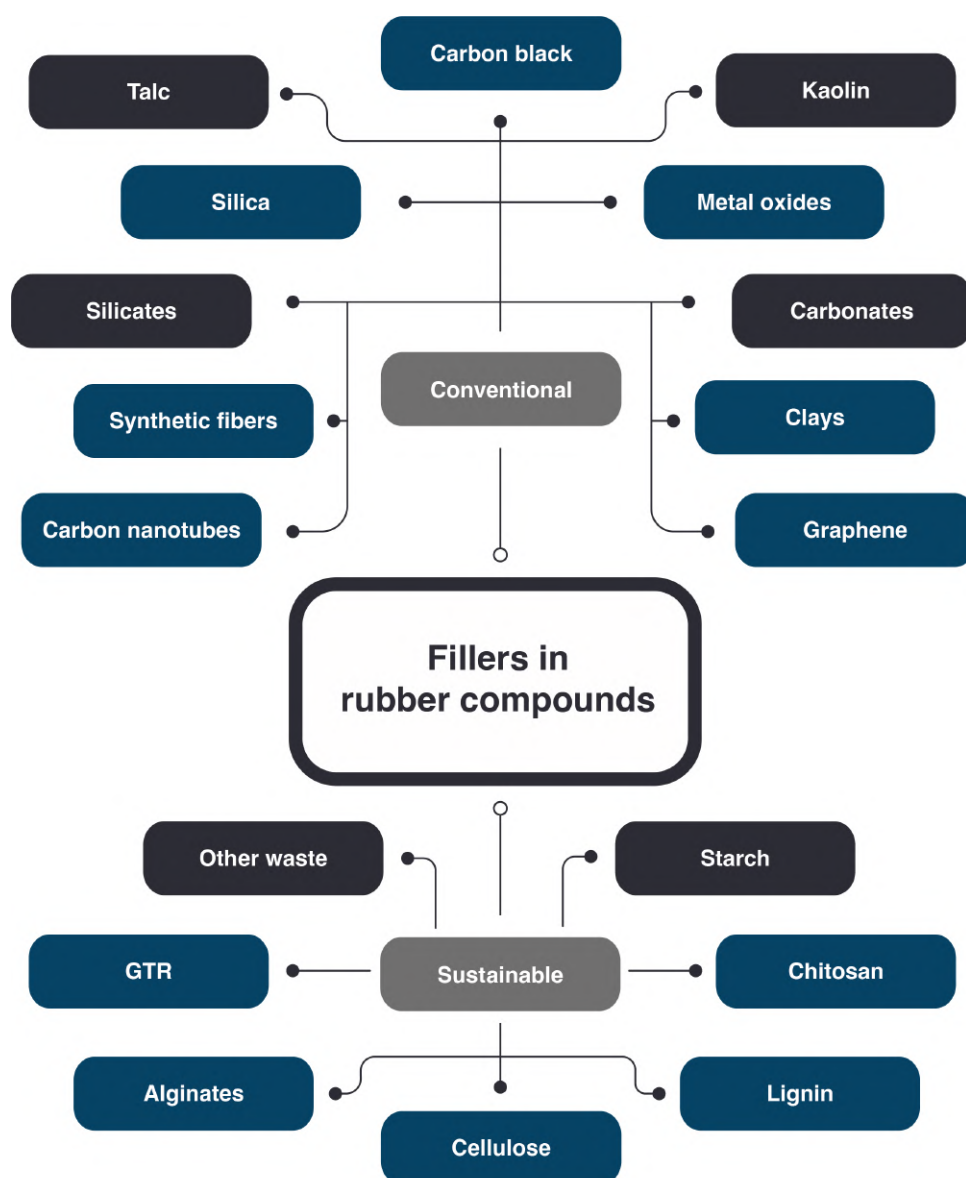


**Figure 1.12.** Fillers in elastomeric compounds. Reinforcing fillers are highlighted in blue, while diluent are highlighted in dark gray.

Zhang et al. [66] delve into the unexplored potential of using CB to reinforce self-healing elastomers, a concept not previously reported due to the complex changes it introduces in the molecular dynamics of the rubber. They focused on a self-healing ionomer based on BIIR grafted with tert-butyl pyridine (BP) into which CB was introduced. This study reveals that the hierarchical microstructure and multilevel molecular dynamics of ionomers are effectively regulated by strong interfacial π-cation interactions between CB and ionic aggregates. This interaction results in a high content of bound rubber, a uniform dispersion of CB, and a compact physical network. While these structural changes have a negligible impact on segmental motion, they significantly enhance the relaxation time and activation energy of ionic clusters, thereby bestowing the ionomer with superior mechanical properties. These structural changes also lead to a higher relaxation temperature, which increases the self-healing temperature. Despite this, the healing efficiency of the ionomer can still be adjusted between 50 % and 100 % depending on the filler content and temperature.

Sattar et al. [166] used a combined mechanism strategy to prepared silica filled ($SiO_2$) NR compounds. Their strategy involves the ionization of natural proteins and lipids of the elastomer to produce ionic crosslinks. A dynamic supramolecular network was formed by adding magnesium sulfate ($MgSO_4$), which provided $Mg^{2+}$ ions, forming electrostatic pairs with the negatively charged lipids arising from acidic ionization. This procedure resulted in healing efficiencies of 79 % at 50 °C, with an excellent TS of 18.5 MPa. The formation of the ionic network was confirmed by Fourier-transform infrared spectroscopy (FTIR) and by comparison with deproteinized NR, in which the repair efficiency was only 52 %.

More recently, Dong et al. [167] used p-phenylenediamine-modified graphene oxide (G-PPD) as a crosslinking agent and reinforcing filler in XNBR. They found that as the content of modified graphene increased, the crosslink density of the XNBR/G-PPD composites increased, leading to enhanced damping properties and thermal conductivity. These composites exhibited high TS and EB values.

Furthermore, the addition of copper sulfate ($CuSO_4$) to the composite resulted in increased tan($\delta$) peak values, which were attributed to the formation of coordination bonds between $Cu^{2+}$, cyano groups in XNBR, and amino groups in G-PPD. This leads to XNBR/G-PPD/$CuSO_4$ composites possessing excellent mechanical properties, along with outstanding self-healing and reprocessing capabilities owing to the presence of dynamic ionic hydrogen bonds and coordination bonds. This study highlights the potential of XNBR/G-PPD and XNBR/G-PPD/$CuSO_4$ composites as thermally conductive damping materials.

**Sustainable Fillers**

Interest in replacing non-sustainable fillers with renewable alternatives, without compromising the performance of rubber compounds, has been growing rapidly. Among the most commercially available and economically accessible renewable alternatives are organic fibers [168]. Cellulose and lignin are the main constituents of most naturally occurring fibers. However, new families of fillers that are beginning to make their way into scientific research on these materials also include chitin/chitosan [169–172], starch [173–177], and alginate [178,179]. The use of materials from waste, such as GTR or CB recovered from ELT, can also be considered as sustainable fillers that add value to waste [180–182], giving another opportunity to trash and contribute to the CE.

Starting with cellulose, this fiber has gained substantial attention owing to its low cost, availability, and performance attributes. Cellulose is a biopolymer composed solely of $\beta$-glucose molecules; therefore, it is considered a homo-polysaccharide [183]. In terms of properties, cellulose (cellulosic fibers) possesses a relatively high tensile modulus (20-70 GPa) a TS (around 1 GPa) counting on the fibril orientation, and better flexibility than glass fibers [184]. There are different types of cellulose; the most interesting forms of cellulose used as fillers in composite preparation are

cellulose (micro- or nano-)crystals and cellulose fibers [168], because of their various interactions with rubber.

Wu et al. [185] present an efficient method to develop robust and self-healable NR/ZDMA/carboxylated cellulose nanofibers (XCNF) composites, constructed through a XCNF-participated ionic supramolecular network. This NR network was generated by the polymerization of ZDMA during controlled peroxide-initiated vulcanization. This study revealed a strong affinity between NR with massive ion clusters and XCNF, enhancing the uniform dispersion of XCNF and its compatibility with NR. Notably, XCNF was integrated into the supramolecular network through non-covalent interactions with NR chains equipped with ionic crosslinks, mitigating the adverse effects of XCNF on the dynamic characteristics of the network. Consequently, the TS of the NR/ZDMA composite with 20 phr of XCNF reaches 4.13 MPa, while maintaining a self-healing efficiency of over 80 %.

Lignin is the second most abundant organic polymer in nature, second only to cellulose. It can be considered the largest reservoir of aromatic compounds on Earth, with great potential for several industrial applications [186]. As a low-cost renewable material, it can be used as an antioxidant, reinforcing agent, plasticizer, UV protectant, and coupling agent in rubber matrices [187]. Its use as a reinforcing filler in rubber compounds is long-standing [188] and has been well-reviewed [187].

As a reinforcing filler in *ionic elastomers*, recently, Zhang et al. [189] develop a cost-effective strategy to create ionomeric elastomer composites with a significant content of lignin, up to 50 wt. %, without requiring purification or chemical modification. This innovative approach utilizes XNBR and enhances the compatibility between elastomer and lignin through the incorporation of ZnO. The resultant lignin/elastomer composites exhibit remarkable mechanical properties, with TS and EB reaching up to 19.6 MPa and 397 %, respectively, especially at a lignin content of 60 phr. These enhanced properties were attributed to the reinforcing effect of the lignin domains and the abundance of sacrificial coordination bonds. Additionally,

the composites possess notable self-repairability, with the repaired sample recovering 94.4 % of its initial TS and 86.3 % of its initial EB after a 2 h repair process at 100 °C.

The last material that joined the group of reinforcing fillers in the self-healing *ionic elastomers* was alginate. It is probably the least explored; however, its two predecessors have shown promising results in advanced applications. Alginic acid or alginate is another widely used naturally-occurring polysaccharide. It is obtained from brown seaweeds (algae) such as Kelp, Gulfweed, Ascophyllum, and Macroalgae [190], which are naturally available in coastal areas of many countries. Brown algae have cell walls with a higher alginate content than red and green macroalgae [191].

The chemical structure of alginate has two isomeric conformations: β-(1-4)-D-mannuronic acid (M blocks) and α-L-guluronic acid (G blocks) [191]. Owing to this and the presence of a free carboxylic group, it can easily bond with a variety of metal ions through ionic, covalent, redox, and/or coordination interactions. Some of the most commonly used cations are divalent ($Ca^{2+}$ and $Mg^{2+}$) and monovalent ($Na^+$).

Utrera-Barrios et al. [179] developed TPE composites with self-healing properties. These composites were based on blends of ENR and polycaprolactone (PCL), reinforced with alginates. The introduction of these natural salts as reinforcing fillers notably enhances the TS of the unfilled rubber, increasing it from 5.6 MPa to 11.5 MPa, while maintaining an impressive EB of approximately 1000 % strain. The composites exhibited thermally assisted self-healing, capable of restoring catastrophic damage and recovering various mechanical properties by up to approximately 100 %. The presence of PCL in the composites facilitated an extrinsic healing mechanism at temperatures above its melting point. Additionally, the inclusion of alginates promotes the formation of hydrogen bonds and ionic interactions, which are crucial for intrinsic self-healing. In the most effective cases, the repair efficiency of the unfilled material increased from approximately 68 % to

approximately 100 % with 20 phr of calcium alginate (Ca-A) after applying a temperature of 110 °C for 12 h.

Regarding the use of waste particles as fillers in *ionic elastomers*, mechano-chemically modified GTR (mGTR) from ELT has been proven to be a feasible solution. Araujo-Morera et al. [192] addressed the common trade-off between the mechanical performance and repairability of self-healing materials by developing hybrid-reinforced self-healing SBR composites. These composites combine the mGTR with CB. A notable finding is that the SBR composite reinforced with 20 phr mGTR and 20 phr CB retains the healing efficiency of unfilled SBR at 80 % while enhancing its TS by 300 %. This represents a successful balance between the two crucial properties. The improved healing capability of the composites was attributed to the synergistic combination of the disulfide bond exchange and reversible ionic clusters formed between the polar groups of mGTR and ZnO.

All of these composites hold potential for widespread applications in various sectors, including automotive, construction, industrial, consumer, medical, electronics, and sporting goods. However, further research is required to ensure the scalability of these materials, with adjustments in recipes tailored to specific applications.

The previous examples provide a short overview of self-healing elastomers evolution. Over the last 20 years, self-healing materials have evolved from simple systems that only support a single healing cycle to systems capable of supporting multiple cycles, being activated through sunlight, UV light, or temperature, being repaired in media other than air, or being healed at RT within a few minutes. Remarkably, all these systems can be processed using conventional techniques and more innovative methods, such as 3D printing [193].

These improvements have mostly arisen over a short period of time. New ideas have evolved from the knowledge gained over previous generations, which are still under study. In the near future, upcoming generations will not be limited to two mechanisms but are likely to explore multiple combinations (three or more) seeking

further positive effects [194]. The use of non-conventional fillers or other additives as carriers of additional healing mechanisms could also be a promising option [195,196], while molecular dynamics studies seem mandatory for simulating interactions between combined mechanisms and for predicting their effect on self-healing capability [197–200].

### 1.4.5. Limitations and Perspectives of Self-healing Elastomers

Despite the advancements and great efforts, self-healing rubbers and self-healing materials in general continue to present serious limitations that should be resolved soon. A comprehensive understanding of the underlying self-healing mechanisms, as well as the optimization of their conditions, is still lacking. The redesign of elastomeric compounds to exhibit this capability requires the consideration of three main conditions [130] (Figure 1.13).

1. The construction of a dynamic but stable and robust network at service temperatures to guarantee excellent mechanical performance,

2. The minimization of components that can hinder the mobility necessary to achieve healing (e.g., secondary irreversible networks) and,

3. Optimization of the appropriate conditions (temporality and external stimulus) for each repair mechanism. In turn, these conditions must be compatible with material stability to avoid deterioration during healing protocols.

Achieving an optimal compromise between these conditions is vital, but not easy. Furthermore, self-healing is not only about what we do but also how we do it. Related to the reproducibility and scalability of self-healing as a property of materials, one of the main limitations is the absence of a unified protocol that permits quantification of the healing capability and, thus, establishing comparisons between systems or families of materials. This limitation becomes more important when trying to compare generations in which the measuring protocols are different.

As an illustrative example, healing within the first generation (encapsulated extrinsic systems) is typically measured using fracture toughness tests. While in the second and fourth (essentially intrinsic systems), healing is predominantly measured by tensile tests [86]. This difference in criteria, even within the same generation, makes it difficult to establish fair comparisons between the materials.
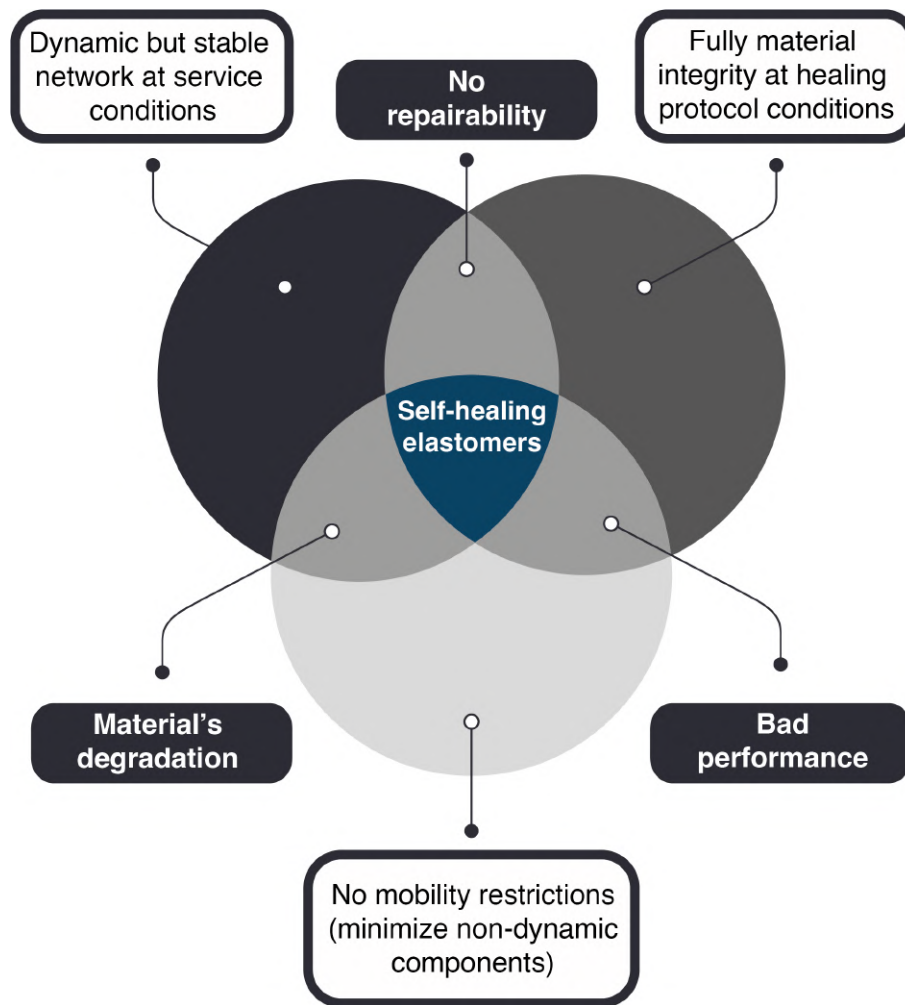


**Figure 1.13.** Venn diagram illustrating optimal healing conditions. Adapted from [130].

Another limitation is related to the type of damage; therefore, there is an urgent need to consider their real scalability. Evaluating the tensile behavior, fracture toughness, and monitoring of superficial cracks are insufficient to ensure the service behavior of self-healing materials. This scalability also refers to the evaluation of

self-healing, not only from the point of view of structural properties, but also regarding key limitations and properties defined for specific applications. Fatigue resistance, thermal and electrical conductivity, aging, and the dichotomy between the dynamic nature of the reversible bonds and the stability of the materials (for example, chemical and thermal) should be considered as soon as possible to make the practical applicability of these strategies a reality.

On this road, it is important not to overlook the economic viability, the reduction of ingredients in rubber recipes, the commercial prospect, and the corresponding life cycle assessment (LCA), which corroborates its environmental impact. When all these conditions are matched, the massive scalability of self-healing materials will be irreversible, and we will have taken one of the definitive steps towards the consolidation of a truly sustainable society.

## 1.5. Summary

**Chapter 1** gives and overview of the key concepts of self-healing and recycling applied to elastomeric materials, with emphasis on *ionic elastomers*. These selected groups of rubbers consist of ionic domains that form a dynamic crosslinked network. This serves as a basis for conferring them intrinsic self-healing capability and recyclability. The chapter also points out the wealth of complex methodologies but also the barriers to scalability and real-world applications. However, there is no doubt that the development of recyclable and self-healing elastomers are crucially needed to advance CE goals. But can we transform this potential into tangible, technology-ready materials using available ingredients and straightforward techniques? This doctoral thesis takes up the charge to respond to this question, taking advantage of the benefits of those ionic networks. By strategic design grounded in feasibility, the aim is to create rubber compounds that check all boxes: high-performance, simple processing, low cost and sustainable attributes, including

intrinsic self-healing capabilities and recyclability, suited for traditional industries to advanced applications, such as soft robotics.

## References

1.  Kaza, S.; Yao, L.C.; Bhada-Tata, P.; Van Woerden, F. What a Waste 2.0: A Global Snapshot of Solid Waste Management to 2050. *What a Waste 2.0: A Global Snapshot of Solid Waste Management to 2050* **2018**, doi:10.1596/978-1-4648-1329-0.

2.  Ikeda, Y.; Kato, A.; Kohjiya, S.; Nakajima, Y. Rubber Science: A Modern Approach. *Rubber Science: A Modern Approach* **2017**, 1–220, doi:10.1007/978-981-10-2938-7.

3.  ASTM International ASTM D1566-21a. Standard Terminology Relating to Rubber 2021.

4.  Wemyss, A.M.; Bowen, C.; Plesse, C.; Vancaeyzeele, C.; Nguyen, G.T.M.; Vidal, F.; Wan, C. Dynamic Crosslinked Rubbers for a Green Future: A Material Perspective. *Materials Science and Engineering: R: Reports* **2020**, *141*, 100561, doi:10.1016/j.mser.2020.100561.

5.  Brydson, J.A. *Rubbery Materials and Their Compounds*; Elsevier Applied Science: London and New York, 1988;

6.  Imbernon, L.; Norvez, S. From Landfilling to Vitrimer Chemistry in Rubber Life Cycle. *Eur Polym J* **2016**, *82*, 347–376, doi:10.1016/j.eurpolymj.2016.03.016.

7.  Akiba, M.; Hashim, A.S. Vulcanization and Crosslinking in Elastomers. *Prog Polym Sci* **1997**, *22*, 475–521, doi:10.1016/S0079-6700(96)00015-9.

8.    Ikeda, Y.; Miyaji, K.; Ohashi, T.; Nakajima, T.; Junkong, P. Vulcanization for Reinforcement of Rubber. *Rubber Chemistry and Technology* **2022**, *95*, 161–174, doi:10.5254/RCT.22.77939.

9.    Mark, J.E.; Erman, B.; Roland, M. *The Science and Technology of Rubber*; Academic Press, 2013;

10.   Zedler, Ł.; Przybysz-Romatowska, M.; Haponiuk, J.; Wang, S.; Formela, K. Modification of Ground Tire Rubber—Promising Approach for Development of Green Composites. *Journal of Composites Science* **2019**, *4*, 2, doi:10.3390/jcs4010002.

11.   Zedler, Ł.; Colom, X.; Cañavate, J.; Saeb, M.; T. Haponiuk, J.; Formela, K. Investigating the Impact of Curing System on Structure-Property Relationship of Natural Rubber Modified with Brewery By-Product and Ground Tire Rubber. *Polymers (Basel)* **2020**, *12*, 545, doi:10.3390/polym12030545.

12.   Zhang, Y.; Zhang, Z.; Wemyss, A.M.; Wan, C.; Liu, Y.; Song, P.; Wang, S. Effective Thermal-Oxidative Reclamation of Waste Tire Rubbers for Producing High-Performance Rubber Composites. *ACS Sustain Chem Eng* **2020**, *8*, 9079–9087, doi:10.1021/acssuschemeng.0c02292.

13.   Hassan, A.A.; Zhang, Z.; Formela, K.; Wang, S. Thermo-Oxidative Exfoliation of Carbon Black from Ground Tire Rubber as Potential Reinforcement in Green Tires. *Compos Sci Technol* **2021**, *214*, 108991, doi:10.1016/j.compscitech.2021.108991.

14.   Formela, K.; Kurańska, M.; Barczewski, M. Recent Advances in Development of Waste-Based Polymer Materials: A Review. *Polymers (Basel)* **2022**, *14*, 1050, doi:10.3390/polym14051050.

15.   Ghorai, S.; Bhunia, S.; Roy, M.; De, D. Mechanochemical Devulcanization of Natural Rubber Vulcanizate by Dual Function Disulfide Chemicals. *Polym*

*Degrad Stab* **2016**, *129*, 34–46, doi:10.1016/J.POLYMDEGRADSTAB.2016.03.024.

16. Aoudia, K.; Azem, S.; Aït Hocine, N.; Gratton, M.; Pettarin, V.; Seghar, S. Recycling of Waste Tire Rubber: Microwave Devulcanization and Incorporation in a Thermoset Resin. *Waste Management* **2017**, *60*, 471–481, doi:10.1016/J.WASMAN.2016.10.051.

17. de Sousa, F.D.B.; Scuracchio, C.H.; Hu, G.H.; Hoppe, S. Devulcanization of Waste Tire Rubber by Microwaves. *Polym Degrad Stab* **2017**, *138*, 169–181, doi:10.1016/J.POLYMDEGRADSTAB.2017.03.008.

18. Seghar, S.; Asaro, L.; Rolland-Monnet, M.; Aït Hocine, N. Thermo-Mechanical Devulcanization and Recycling of Rubber Industry Waste. *Resour Conserv Recycl* **2019**, *144*, 180–186, doi:10.1016/j.resconrec.2019.01.047.

19. Colom, X.; Cañavate, J.; Formela, K.; Shadman, A.; Saeb, M.R. Assessment of the Devulcanization Process of EPDM Waste from Roofing Systems by Combined Thermomechanical/Microwave Procedures. *Polym Degrad Stab* **2021**, *183*, 109450, doi:10.1016/j.polymdegradstab.2020.109450.

20. Wemyss, A.M.; Ellingford, C.; Morishita, Y.; Bowen, C.; Wan, C. Dynamic Polymer Networks: A New Avenue towards Sustainable and Advanced Soft Machines. *Angewandte Chemie International Edition* **2021**, *60*, doi:10.1002/anie.202013254.

21. Bosnjak, N.; Silberstein, M.N. Pathways to Tough yet Soft Materials. *Science (1979)* **2021**, *374*, 150–151, doi:10.1126/science.abl6358.

22. Roy, N.; Bruchmann, B.; Lehn, J.M. DYNAMERS: Dynamic Polymers as Self-Healing Materials. *Chem Soc Rev* **2015**, *44*, 3786–3807, doi:10.1039/c5cs00194c.

23. Zhang, B.; De Alwis Watuthanthrige, N.; Wanasinghe, S. V.; Averick, S.; Konkolewicz, D. Complementary Dynamic Chemistries for Multifunctional

Polymeric Materials. *Adv Funct Mater* **2022**, *32*, 2108431, doi:10.1002/ADFM.202108431.

24. Xie, Z.; Hu, B.L.; Li, R.W.; Zhang, Q. Hydrogen Bonding in Self-Healing Elastomers. *ACS Omega* **2021**, *6*, 9319–9333, doi:10.1021/ACSOMEGA.1C00462.

25. Huang, Q.; Liu, Y.; Li, S.; Zhu, M.; Hao, T.; Zhou, Z.; Nie, Y. Blending Polar Rubber with Polyurethane to Construct Self-Healing Rubber with Multiple Hydrogen Bond Networks. *Polymer (Guildf)* **2022**, *246*, 124768, doi:10.1016/j.polymer.2022.124768.

26. Liu, J.; Xiao, C.; Tang, J.; Liu, Y.; Hua, J. Construction of a Dual Ionic Network in Natural Rubber with High Self-Healing Efficiency through Anionic Mechanism. *Ind Eng Chem Res* **2020**, *59*, 12755–12765, doi:10.1021/ACS.IECR.0C01538.

27. Das, M.; Naskar, K. Development, Characterization and Applications of a Unique Self-Healable Elastomer: Exploring a Facile Metal-Ligand Interaction. *Polymer (Guildf)* **2021**, *237*, 124373, doi:10.1016/J.POLYMER.2021.124373.

28. Huang, J.; Gong, Z.; Chen, Y. A Stretchable Elastomer with Recyclability and Shape Memory Assisted Self-Healing Capabilities Based on Dynamic Disulfide Bonds. *Polymer (Guildf)* **2022**, *242*, 124569, doi:10.1016/J.POLYMER.2022.124569.

29. Chen, X.; Dam, M.A.; Ono, K.; Mal, A.; Shen, H.; Nutt, S.R.; Sheran, K.; Wudl, F. A Thermally Re-Mendable Cross-Linked Polymeric Material. *Science (1979)* **2002**, *295*, 1698–1702, doi:10.1126/SCIENCE.1065879/SUPPL_FILE/1065879S3_THUMB.GIF.

30. Tanasi, P.; Hernández Santana, M.; Carretero-González, J.; Verdejo, R.; López-Manchado, M.A. Thermo-Reversible Crosslinked Natural Rubber: A

Diels-Alder Route for Reuse and Self-Healing Properties in Elastomers. *Polymer (Guildf)* **2019**, *175*, 15–24, doi:10.1016/j.polymer.2019.04.059.

31.   Zhang, L.; Wang, H.; Zhu, Y.; Xiong, H.; Wu, Q.; Gu, S.; Liu, X.; Huang, G.; Wu, J. Electron-Donating Effect Enabled Simultaneous Improvement on the Mechanical and Self-Healing Properties of Bromobutyl Rubber Ionomers. *ACS Appl Mater Interfaces* **2020**, *12*, 53239–53246, doi:10.1021/acsami.0c14901.

32.   Peng, T.; Huang, J.; Gong, Z.; Ding, J.; Chen, Y. Multiple Cross-linked Networks Enhanced ENR-based Composite with Excellent Self-healing Properties. *Polym Adv Technol* **2021**, *32*, 2856–2865, doi:10.1002/pat.5295.

33.   Yeh, C.-M.; Lin, C.-H.; Han, T.-Y.; Xiao, Y.-T.; Chen, Y.-A.; Chou, H.-H. Disulfide Bond and Diels–Alder Reaction Bond Hybrid Polymers with High Stretchability, Transparency, Recyclability, and Intrinsic Dual Healability for Skin-like Tactile Sensing. *J Mater Chem A Mater* **2021**, *9*, 6109–6116, doi:10.1039/D0TA10135D.

34.   Gao, X.; Fan, W.; Zhu, W.; Jiuwei, G.; Zhang, P.; Wang, C.; Wang, X.; Xia, H.; Wang, Z.; Huang, W. Tough and Healable Elastomers via Dynamic Integrated Moiety Comprising Covalent and Noncovalent Interactions. *Chemistry of Materials* **2022**, *34*, 2981–2988, doi:10.1021/acs.chemmater.1c03813.

35.   Jing, T.; Heng, X.; Guifeng, X.; Li, L.; Li, P.; Guo, X. Rapid Self-Healing and Tough Polyurethane Based on the Synergy of Multi-Level Hydrogen and Disulfide Bonds for Healing Propellant Microcracks. *Mater Chem Front* **2022**, *6*, 1161–1171, doi:10.1039/D2QM00047D.

36.   Cerdan, K.; Van Assche, G.; van Puyvelde, P.; Brancart, J. A Novel Approach for the Closure of Large Damage in Self-Healing Elastomers Using Magnetic Particles. *Polymer (Guildf)* **2020**, *204*, doi:10.1016/j.polymer.2020.122819.

37. Zhang, Y.; Khanbareh, H.; Roscow, J.; Pan, M.; Bowen, C.; Wan, C. Self-Healing of Materials under High Electrical Stress. *Matter* **2020**, *3*, 989–1008, doi:10.1016/j.matt.2020.07.020.

38. Guo, H.; Han, Y.; Zhao, W.; Yang, J.; Zhang, L. Universally Autonomous Self-Healing Elastomer with High Stretchability. *Nat Commun* **2020**, *11*, 2037, doi:10.1038/s41467-020-15949-8.

39. Eisenberg, A. Clustering of Ions in Organic Polymers. A Theoretical Approach. *Macromolecules* **1970**, *3*, 147–154, doi:10.1021/ma60014a006.

40. Eisenberg, A.; Hird, B.; Moore, R.B. A New Multiplet-Cluster Model for the Morphology of Random Ionomers. *Macromolecules* **1990**, *23*, 4098–4107, doi:10.1021/ma00220a012.

41. Malmierca, M.A.; González-Jiménez, A.; Mora-Barrantes, I.; Posadas, P.; Rodríguez, A.; Ibarra, L.; Nogales, A.; Saalwächter, K.; Valentín, J.L. Characterization of Network Structure and Chain Dynamics of Elastomeric Ionomers by Means of 1H Low-Field NMR. *Macromolecules* **2014**, *47*, 5655–5667, doi:10.1021/ma501208g.

42. Ibarra, L.; Alzorriz, M. Vulcanization of Carboxylated Nitrile Rubber (XNBR) by a Mixed Zinc Peroxide-Sulphur System. *Polym Int* **2000**, *49*, 115–121, doi:10.1002/(SICI)1097-0126(200001)49:1<115::AID-PI317>3.0.CO;2-X.

43. Ibarra, L.; Rodríguez, A.; Mora-Barrantes, I. Crosslinking of Unfilled Carboxylated Nitrile Rubber with Different Systems: Influence on Properties. *J Appl Polym Sci* **2008**, *108*, doi:10.1002/app.27893.

44. Mora-Barrantes, I.; Malmierca, M.A.; Valentin, J.L.; Rodriguez, A.; Ibarra, L. Effect of Covalent Cross-Links on the Network Structure of Thermo-Reversible Ionic Elastomers. *Soft Matter* **2012**, *8*, 5201–5213, doi:10.1039/c2sm06975j.

45. Reynolds, P.J. A Surlyn® Ionomer as a Self-Healing and Self-Sensing Composite, University of Birmingham: Birmingham, 2012.

46. González Jiménez, A. Materiales Elastoméricos Con Memoria de Forma, Universidad Complutense de Madrid: Madrid, 2017.

47. Legge, N.R. Thermoplastic Elastomers—Three Decades of Progress. *Rubber Chemistry and Technology* **1989**, *62*, 529–547, doi:10.5254/1.3536257.

48. Ibarra, L. The Effect of Crosslinking Type on the Physical Properties of Carboxylated Acrylonitrile Butadiene Elastomers. *J Appl Polym Sci* **1999**, *73*, 927–933, doi:10.1002/(SICI)1097-4628(19990808)73:6.

49. Ibarra, L.; Alzorriz, M. Vulcanization of Carboxylated Nitrile Rubber (XNBR) by Zinc Peroxide. *Polym Int* **1999**, *48*, doi:10.1002/(SICI)1097-0126(199907)48:7<580::AID-PI186>3.0.CO;2-4.

50. Ibarra, L.; Alzorriz, M. Ionic Elastomers Based on Carboxylated Nitrile Rubber and Calcium Oxide. *J Appl Polym Sci* **2002**, *87*, doi:10.1002/app.11468.

51. Ibarra, L.; Alzorriz, M. Effect of Temperature on the Crosslink Densities of Nitrile Rubber and Carboxylated Nitrile Rubber with Zinc Peroxide. *J Appl Polym Sci* **2002**, *86*, 335–340, doi:10.1002/APP.10963.

52. Ibarra, L.; Alzorriz, M. Ionic Elastomers Based on Carboxylated Nitrile Rubber (XNBR) and Zinc Peroxide: Influence of Carboxylic Group Content on Properties. *J Appl Polym Sci* **2002**, *84*, 605–615, doi:10.1002/APP.10313.

53. Ibarra, L.; Alzorriz, M. Ionic Elastomers Based on Carboxylated Nitrile Rubber and Magnesium Oxide. *J Appl Polym Sci* **2007**, *103*, 1894–1899, doi:10.1002/APP.25411.

54.     Ibarra, L.; Rodríguez, A.; Mora-Barrantes, I. Crosslinking of Carboxylated Nitrile Rubber (XNBR) Induced by Coordination with Anhydrous Copper Sulfate. *Polym Int* **2009**, *58*, 218–226, doi:10.1002/PI.2519.

55.     Basu, D.; Das, A.; Stöckelhuber, K.W.; Jehnichen, D.; Formanek, P.; Sarlin, E.; Vuorinen, J.; Heinrich, G. Evidence for an in Situ Developed Polymer Phase in Ionic Elastomers. *Macromolecules* **2014**, *47*, 3436–3450, doi:10.1021/ma500240v.

56.     Utrera-Barrios, S.; Manzanares, R.V.; Araujo-Morera, J.; González, S.; Verdejo, R.; López-Manchado, M.Á.; Santana, M.H. Understanding the Molecular Dynamics of Dual Crosslinked Networks by Dielectric Spectroscopy. *Polymers (Basel)* **2021**, *13*, 3234, doi:10.3390/polym13193234.

57.     Tian, F.; Ohki, Y. Charge Transport and Electrode Polarization in Epoxy Resin at High Temperatures. *J Phys D Appl Phys* **2014**, *47*, 045311, doi:10.1088/0022-3727/47/4/045311.

58.     Cooper, W. Copolymers of Butadiene and Unsaturated Acids: Crosslinking by Metal Oxides. *Journal of Polymer Science* **1958**, *28*, 195–206, doi:10.1002/pol.1958.1202811618.

59.     Engel, K.E.; Kilmartin, P.A.; Diegel, O. Recent Advances in the 3D Printing of Ionic Electroactive Polymers and Core Ionomeric Materials. *Polym Chem* **2022**, *13*, 456–473, doi:10.1039/D1PY01297E.

60.     González-Jiménez, A.; Malmierca, M.A.; Bernal-Ortega, P.; Posadas, P.; Pérez-Aparicio, R.; Marcos-Fernández, Á.; Mather, P.T.; Valentín, J.L. The Shape-Memory Effect in Ionic Elastomers: Fixation through Ionic Interactions. *Soft Matter* **2017**, *13*, 2983–2994, doi:10.1039/C7SM00104E.

61.     González-Jiménez, A.; Bernal-Ortega, P.; Salamanca, F.M.; Valentin, J.L. Shape-Memory Composites Based on Ionic Elastomers. *Polymers (Basel)* **2022**, *14*, 1230, doi:10.3390/POLYM14061230/S1.

62. Naito, K.; Miwa, Y.; Ando, R.; Yashiro, K.; Kutsumizu, S. Evaluation for the Actuation Performance of Dielectric Elastomer Actuator Using Polyisoprene Elastomer with Dynamic Ionic Crosslinks. *Sens Actuators A Phys* **2021**, *332*, 113143, doi:10.1016/j.sna.2021.113143.

63. Bernat, J.; Gajewski, P.; Kołota, J.; Marcinkowska, A. Review of Soft Actuators Controlled with Electrical Stimuli: IPMC, DEAP, and MRE. *Applied Sciences* **2023**, *13*, 1651, doi:10.3390/app13031651.

64. Luo, G.; Pang, B.; Luo, X.; Zeng, X.; Wang, Y.; Zhao, L. Self-Healing and Enhanced Anticorrosion Coatings Based on Graphene-Reinforced Brominated Butyl Rubber Ionomer. *Prog Org Coat* **2023**, *174*, 107245, doi:10.1016/j.porgcoat.2022.107245.

65. Stein, S.; Mordvinkin, A.; Voit, B.; Komber, H.; Saalwächter, K.; Böhme, F. Self-Healing and Reprocessable Bromo Butylrubber Based on Combined Ionic Cluster Formation and Hydrogen Bonding. *Polym Chem* **2020**, *11*, 1188–1197, doi:10.1039/C9PY01630A.

66. Zhang, L.; Zhang, J.; Liu, H.; Wu, Q.; Xiong, H.; Huang, G.; Wu, J. Reinforcing Self-Healing and Re-Processable Ionomers with Carbon Black: An Investigation on the Network Structure and Molecular Mobility. *Compos Sci Technol* **2021**, *216*, 109035, doi:10.1016/J.COMPSCITECH.2021.109035.

67. Da Via, F.; Suriano, R.; Boumezgane, O.; Grande, A.M.; Tonelli, C.; Turri, S. Self-healing Behavior in Blends of PDMS-based Polyurethane Ionomers. *Polym Adv Technol* **2022**, *33*, 556–565, doi:10.1002/pat.5537.

68. Wang, Q.; Li, Y.; Xiao, J.; Xia, L. Intelligent Eucommia Ulmoides Rubber/Ionomer Blends with Thermally Activated Shape Memory and Self-Healing Properties. *Polymers (Basel)* **2023**, *15*, 1182, doi:10.3390/polym15051182.

69. DIRECTIVE 2008/98/EC OF THE EUROPEAN PARLIAMENT AND OF THE COUNCIL of 19 November 2008 on Waste and Repealing Certain Directives. *Official Journal of the European Union* 2008, *OJ L 312*, 3.

70. DIRECTIVE (EU) 2018/851 OF THE EUROPEAN PARLIAMENT AND OF THE COUNCIL of 30 May 2018  Amending Directive 2008/98/EC on Waste. *Official Journal of the European Union* 2018, *OJ L 150*, 109–140.

71. La Mantia, F.P. Polymer Mechanical Recycling: Downcycling or Upcycling? *Progress in Rubber, Plastics and Recycling Technology* **2004**, *20*, 11–24, doi:10.1177/147776060402000102.

72. Helbig, C.; Huether, J.; Joachimsthaler, C.; Lehmann, C.; Raatz, S.; Thorenz, A.; Faulstich, M.; Tuma, A. A Terminology for Downcycling. *J Ind Ecol* **2022**, *26*, 1164–1174, doi:10.1111/JIEC.13289.

73. Korley, L.S.T.J.; Epps, T.H.; Helms, B.A.; Ryan, A.J. Toward Polymer Upcycling-Adding Value and Tackling Circularity. *Science (1979)* **2021**, *373*, 66–69, doi:10.1126/SCIENCE.ABG4503.

74. Yang, W.; Li, Y.; Chen, Y.; Lu, Y.; Jiang, X.; Cui, P.; Hao, W. Upcycling Waste Synthetic Running Tracks in Reinforcement of Styrene-Butadiene Rubber. *J Clean Prod* **2023**, *430*, 139769, doi:10.1016/J.JCLEPRO.2023.139769.

75. Jung, H.; Shin, G.; Kwak, H.; Hao, L.T.; Jegal, J.; Kim, H.J.; Jeon, H.; Park, J.; Oh, D.X. Review of Polymer Technologies for Improving the Recycling and Upcycling Efficiency of Plastic Waste. *Chemosphere* **2023**, *320*, 138089, doi:10.1016/J.CHEMOSPHERE.2023.138089.

76. Ellis, L.D.; Rorrer, N.A.; Sullivan, K.P.; Otto, M.; McGeehan, J.E.; Román-Leshkov, Y.; Wierckx, N.; Beckham, G.T. Chemical and Biological Catalysis for Plastics Recycling and Upcycling. *Nat Catal* **2021**, *4*, 539–556, doi:10.1038/s41929-021-00648-4.

77. Coates, G.W.; Getzler, Y.D.Y.L. Chemical Recycling to Monomer for an Ideal, Circular Polymer Economy. *Nat Rev Mater* **2020**, *5*, 501–516, doi:10.1038/s41578-020-0190-4.

78. Myhre, M.; Saiwari, S.; Dierkes, W.; Noordermeer, J. Rubber Recycling: Chemistry, Processing, and Applications. *Rubber chemistry and technology* **2012**, *85*, 408–449, doi:10.5254/rct.12.87973.

79. Shao, L.; Xu, R.; Wang, J.; Ma, Z.; Ji, Z.; Zhang, W.; Wei, H.; Zhu, C.; Wang, C.; Ma, J. Recyclable and Reprocessable Crosslinked Rubber Enabled by Constructing Ionic Crosslinked Networks. *ACS Sustain Chem Eng* **2020**, *8*, 12999–13006, doi:10.1021/acssuschemeng.0c03863.

80. Zainol, M.H.; Ariff, Z.M.; Omar, M.F.; Ping, T.M.; Shuib, R.K. Self-Healable and Recyclable Nitrile Rubber Based on Thermoreversible Ionic Crosslink Network. *J Appl Polym Sci* **2022**, *139*, doi:10.1002/APP.51948.

81. Kim, J.; Bae, J.; Lee, J.; Lee, Y.; Kim, H. Preparation and Properties of High-performance Recyclable Ethylene Propylene Diene Rubber. *J Appl Polym Sci* **2015**, *132*, doi:10.1002/app.42718.

82. Xu, C.; Huang, X.; Li, C.; Chen, Y.; Lin, B.; Liang, X. Design of "Zn2+ Salt-Bondings" Cross-Linked Carboxylated Styrene Butadiene Rubber with Reprocessing and Recycling Ability via Rearrangements of Ionic Cross-Linkings. *ACS Sustain Chem Eng* **2016**, *4*, 6981–6990, doi:10.1021/acssuschemeng.6b01897.

83. Gong, C.; Cao, J.; Guo, M.; Cai, S.; Xu, P.; Lv, J.; Li, C. A Facile Strategy for High Mechanical Performance and Recyclable EPDM Rubber Enabled by Exchangeable Ion Crosslinking. *Eur Polym J* **2022**, *175*, 111339, doi:10.1016/j.eurpolymj.2022.111339.

84. Das, M.; Sreethu, T.K.; Pal, S.; Naskar, K. Biologically Derived Metal-Cysteine Coordination Complexes Crosslink Carboxylated Nitrile Rubber and

Enable Room Temperature Self-Healing, Stretchability, and Recyclability. *ACS Appl Polym Mater* **2022**, *4*, 6414–6425, doi:10.1021/ACSAPM.2C00840.

85.    van der Zwaag, S.; Brinkman, E. *Self Healing Materials: Pioneering Research in the Netherlands*; IOS Press, 2015; ISBN 1614995141.

86.    Utrera-Barrios, S.; Verdejo, R.; López-Manchado, M.A.; Hernández Santana, M. Evolution of Self-Healing Elastomers, from Extrinsic to Combined Intrinsic Mechanisms: A Review. *Mater Horiz* **2020**, *7*, 2882–2902, doi:10.1039/d0mh00535e.

87.    Blaiszik, B.J.; Kramer, S.L.B.; Olugebefola, S.C.; Moore, J.S.; Sottos, N.R.; White, S.R. Self-Healing Polymers and Composites. *Annu Rev Mater Res* **2010**, *40*, 179–211, doi:10.1146/ANNUREV-MATSCI-070909-104532.

88.    White, S.R.; Sottos, N.R.; Geubelle, P.H.; Moore, J.S.; Kessler, M.R.; Sriram, S.R.; Brown, E.N.; Viswanathan, S. Autonomic Healing of Polymer Composites. *Nature* **2001**, *409*, 794–797, doi:10.1038/35057232.

89.    Blaiszik, B.J.; Sottos, N.R.; White, S.R. Nanocapsules for Self-Healing Materials. *Compos Sci Technol* **2008**, *68*, 978–986, doi:10.1016/J.COMPSCITECH.2007.07.021.

90.    Wu, X.F.; Rahman, A.; Zhou, Z.; Pelot, D.D.; Sinha-Ray, S.; Chen, B.; Payne, S.; Yarin, A.L. Electrospinning Core-Shell Nanofibers for Interfacial Toughening and Self-Healing of Carbon-Fiber/Epoxy Composites. *J Appl Polym Sci* **2013**, *129*, 1383–1393, doi:10.1002/APP.38838.

91.    Jia, X.Y.; Mei, J.F.; Lai, J.C.; Li, C.H.; You, X.Z. A Highly Stretchable Polymer That Can Be Thermally Healed at Mild Temperature. *Macromol Rapid Commun* **2016**, *37*, 952–956, doi:10.1002/MARC.201600142.

92.    Feng, L.; Yu, Z.; Bian, Y.; Lu, J.; Shi, X.; Chai, C. Self-Healing Behavior of Polyurethanes Based on Dual Actions of Thermo-Reversible Diels-Alder

Reaction and Thermal Movement of Molecular Chains. *Polymer (Guildf)* **2017**, *124*, 48–59, doi:10.1016/J.POLYMER.2017.07.049.

93. Wang, D.; Guo, J.; Zhang, H.; Cheng, B.; Shen, H.; Zhao, N.; Xu, J. Intelligent Rubber with Tailored Properties for Self-Healing and Shape Memory. *J Mater Chem A Mater* **2015**, *3*, 12864–12872, doi:10.1039/C5TA01915J.

94. Xu, C.; Cao, L.; Lin, B.; Liang, X.; Chen, Y. Design of Self-Healing Supramolecular Rubbers by Introducing Ionic Cross-Links into Natural Rubber via a Controlled Vulcanization. *ACS Appl Mater Interfaces* **2016**, *8*, 17728–17737, doi:10.1021/ACSAMI.6B05941.

95. Araujo-Morera, J.; Santana, M.H.; Verdejo, R.; López-Manchado, M.A. Giving a Second Opportunity to Tire Waste: An Alternative Path for the Development of Sustainable Self-Healing Styrene–Butadiene Rubber Compounds Overcoming the Magic Triangle of Tires. *Polymers (Basel)* **2019**, *11*, 2122, doi:10.3390/POLYM11122122.

96. Bekas, D.G.; Tsirka, K.; Baltzis, D.; Paipetis, A.S. Self-Healing Materials: A Review of Advances in Materials, Evaluation, Characterization and Monitoring Techniques. *Compos B Eng* **2016**, *87*, 92–119, doi:10.1016/J.COMPOSITESB.2015.09.057.

97. Dahlke, J.; Zechel, S.; Hager, M.D.; Schubert, U.S. How to Design a Self-Healing Polymer: General Concepts of Dynamic Covalent Bonds and Their Application for Intrinsic Healable Materials. *Adv Mater Interfaces* **2018**, *5*, 1800051, doi:10.1002/ADMI.201800051.

98. Wang, Z.; Lu, X.; Sun, S.; Yu, C.; Xia, H. Preparation, Characterization and Properties of Intrinsic Self-Healing Elastomers. *J Mater Chem B* **2019**, *7*, 4876–4926, doi:10.1039/C9TB00831D.

99. Sanka, R.V.S.P.; Krishnakumar, B.; Leterrier, Y.; Pandey, S.; Rana, S.; Michaud, V. Soft Self-Healing Nanocomposites. *Front Mater* **2019**, *6*, 137, doi:10.3389/FMATS.2019.00137.

100. Willocq, B.; Odent, J.; Dubois, P.; Raquez, J.M. Advances in Intrinsic Self-Healing Polyurethanes and Related Composites. *RSC Adv* **2020**, *10*, 13766–13782, doi:10.1039/D0RA01394C.

101. Lee, M.W.; An, S.; Yoon, S.S.; Yarin, A.L. Advances in Self-Healing Materials Based on Vascular Networks with Mechanical Self-Repair Characteristics. *Adv Colloid Interface Sci* **2018**, *252*, 21–37, doi:10.1016/J.CIS.2017.12.010.

102. Malinskii, Y.M.; Prokopenko, V. V.; Ivanova, N.A.; Kargin, V.A. Investigation of Self-Healing of Cracks in Polymers - I. Effect of Temperature and Crosslinks on Self-Healing of Cracks in Polyvinyl Acetate. *Polymer Mechanics* **1970**, *6*, 240–244, doi:10.1007/BF00859196.

103. Malinskii, Y.M.; Prokopenko, V. V.; Ivanova, N.A.; Kargin, V.S. Investigation of Self-Healing of Cracks in Polymers - 2. Effect of Molecular Weight of a Polymer and the Environment on Self-Healing of Cracks in Polyvinyl Acetate. *Polymer Mechanics* **1970**, *6*, 382–384, doi:10.1007/BF00858197.

104. Malinskii, Y.M.; Prokopenko, V. V.; Kargin, V.A. Investigation of the Self-Healing of Cracks in Polymers - 3. Effect of Medium and Layer Thickness on Self-Healing in Polyvinyl Acetate. *Polymer Mechanics* **1970**, *6*, 969–972, doi:10.1007/BF00856916.

105. Jud, K.; Kausch, H.H.; Williams, J.G. Fracture Mechanics Studies of Crack Healing and Welding of Polymers. *J Mater Sci* **1981**, *16*, 204–210, doi:10.1007/BF00552073.

106. Wool, R.P.; O'Connor, K.M. A Theory Crack Healing in Polymers. *J Appl Phys* **1981**, *52*, 5953–5963, doi:10.1063/1.328526.

107. Wool, R.P.; O'Connor, K.M. Time Dependence of Crack Healing. *Journal of Polymer Science: Polymer Letters Edition* **1982**, *20*, 7–16, doi:10.1002/POL.1982.130200102.

108. Zhai, L.; Narkar, A.; Ahn, K. Self-Healing Polymers with Nanomaterials and Nanostructures. *Nano Today* **2020**, *30*, 100826, doi:10.1016/J.NANTOD.2019.100826.

109. Ellul, M.D.; Gent, A.N. The Role of Molecular Diffusion in the Adhesion of Elastomers. *Journal of Polymer Science: Polymer Physics Edition* **1984**, *22*, 1953–1968, doi:10.1002/POL.1984.180221108.

110. Dry, C. Passive Tuneable Fibers and Matrices. *Int J Mod Phys B* **1992**, *6*, 2763–2771, doi:10.1142/S0217979292001419.

111. Dry, C.M.; Sottos, N.R. Passive Smart Self-Repair in Polymer Matrix Composite Materials. *Procedings from SPIE 1916, Smart Structures and Materials 1993: Smart Materials* **1993**, doi:10.1117/12.148501.

112. Keller, M.W.; White, S.R.; Sottos, N.R. A Self-Healing Poly(Dimethylsiloxane) Elastomer. *Adv Funct Mater* **2007**, *17*, 2399–2404, doi:10.1002/ADFM.200700086.

113. Zhu, D.Y.; Rong, M.Z.; Zhang, M.Q. Self-Healing Polymeric Materials Based on Microencapsulated Healing Agents: From Design to Preparation. *Prog Polym Sci* **2015**, *49–50*, 175–220, doi:10.1016/J.PROGPOLYMSCI.2015.07.002.

114. Xu, Y.; Chen, D. Self-Healing Polyurethane/Attapulgite Nanocomposites Based on Disulfide Bonds and Shape Memory Effect. *Mater Chem Phys* **2017**, *195*, 40–48, doi:10.1016/J.MATCHEMPHYS.2017.04.007.

115. Chang, K.; Jia, H.; Gu, S.Y. A Transparent, Highly Stretchable, Self-Healing Polyurethane Based on Disulfide Bonds. *Eur Polym J* **2019**, *112*, 822–831, doi:10.1016/J.EURPOLYMJ.2018.11.005.

116. Hoeben, F.J.M.; Jonkheijm, P.; Meijer, E.W.; Schenning, A.P.H.J. About Supramolecular Assemblies of π-Conjugated Systems. *Chem Rev* **2005**, *105*, 1491–1546, doi:10.1021/CR030070Z.

117. Wang, X.; Liang, D.; Cheng, B. Preparation and Research of Intrinsic Self-Healing Elastomers Based on Hydrogen and Ionic Bond. *Compos Sci Technol* **2020**, *193*, 108127, doi:10.1016/J.COMPSCITECH.2020.108127.

118. Cordier, P.; Tournilhac, F.; Soulié-Ziakovic, C.; Leibler, L. Self-Healing and Thermoreversible Rubber from Supramolecular Assembly. *Nature* **2008**, *451*, 977–980, doi:10.1038/nature06669.

119. Toohey, K.S.; Sottos, N.R.; Lewis, J.A.; Moore, J.S.; White, S.R. Self-Healing Materials with Microvascular Networks. *Nat Mater* **2007**, *6*, 581–585, doi:10.1038/nmat1934.

120. Lee, M.W.; An, S.; Lee, C.; Liou, M.; Yarin, A.L.; Yoon, S.S. Self-Healing Transparent Core–Shell Nanofiber Coatings for Anti-Corrosive Protection. *J Mater Chem A Mater* **2014**, *2*, 7045–7053, doi:10.1039/C4TA00623B.

121. An, S.; Liou, M.; Song, K.Y.; Jo, H.S.; Lee, M.W.; Al-Deyab, S.S.; Yarin, A.L.; Yoon, S.S. Highly Flexible Transparent Self-Healing Composite Based on Electrospun Core–Shell Nanofibers Produced by Coaxial Electrospinning for Anti-Corrosion and Electrical Insulation. *Nanoscale* **2015**, *7*, 17778–17785, doi:10.1039/C5NR04551G.

122. Lee, M.W.; An, S.; Jo, H.S.; Yoon, S.S.; Yarin, A.L. Self-Healing Nanofiber-Reinforced Polymer Composites. 1. Tensile Testing and Recovery of Mechanical Properties. *ACS Appl Mater Interfaces* **2015**, *7*, 19546–19554, doi:10.1021/ACSAMI.5B05998.

123. Lee, M.W.; An, S.; Jo, H.S.; Yoon, S.S.; Yarin, A.L. Self-Healing Nanofiber-Reinforced Polymer Composites. 2. Delamination/Debonding and Adhesive

and Cohesive Properties. *ACS Appl Mater Interfaces* **2015**, *7*, 19555–19561, doi:10.1021/ACSAMI.5B03470.

124. Burattini, S.; Greenland, B.W.; Merino, D.H.; Weng, W.; Seppala, J.; Colquhoun, H.M.; Hayes, W.; MacKay, M.E.; Hamley, I.W.; Rowan, S.J. A Healable Supramolecular Polymer Blend Based on Aromatic π-π Stacking and Hydrogen-Bonding Interactions. *J Am Chem Soc* **2010**, *132*, 12051–12058, doi:10.1021/JA104446R.

125. Jiang, Z.; Bhaskaran, A.; Aitken, H.M.; G Shackleford, I.C.; Connal, L.A.; Jiang, Z.; Bhaskaran, A.; Aitken, H.M.; G Shackleford, I.C.; Connal, L.A. Using Synergistic Multiple Dynamic Bonds to Construct Polymers with Engineered Properties. *Macromol Rapid Commun* **2019**, *40*, 1900038, doi:10.1002/MARC.201900038.

126. Li, L.; Kim, J.K. Thermoreversible Cross-Linking Maleic Anhydride Grafted Chlorobutyl Rubber with Hydrogen Bonds (Combined with Ionic Interactions). *Rubber Chemistry and Technology* **2014**, *87*, 459–470, doi:10.5254/RCT.14.86976.

127. Liu, J.; Wang, S.; Tang, Z.; Huang, J.; Guo, B.; Huang, G. Bioinspired Engineering of Two Different Types of Sacrificial Bonds into Chemically Cross-Linked Cis-1,4-Polyisoprene toward a High-Performance Elastomer. *Macromolecules* **2016**, *49*, 8593–8604, doi:10.1021/ACS.MACROMOL.6B01576.

128. Li, C.; Wang, Y.; Yuan, Z.; Ye, L. Construction of Sacrificial Bonds and Hybrid Networks in EPDM Rubber towards Mechanical Performance Enhancement. *Appl Surf Sci* **2019**, *484*, 616–627, doi:10.1016/J.APSUSC.2019.04.064.

129. Liu, Y.; Tang, Z.; Wu, S.; Guo, B. Integrating Sacrificial Bonds into Dynamic Covalent Networks toward Mechanically Robust and Malleable Elastomers. *ACS Macro Lett* **2019**, *8*, 193–199, doi:10.1021/ACSMACROLETT.9B00012.

130. Utrera-Barrios, S.; Verdejo, R.; López-Manchado, M.Á.; Hernández Santana, M. The Final Frontier of Sustainable Materials: Current Developments in Self-Healing Elastomers. *Int J Mol Sci* **2022**, *23*, 4757, doi:10.3390/IJMS23094757.

131. Chung, U.S.; Min, J.H.; Lee, P.C.; Koh, W.G. Polyurethane Matrix Incorporating PDMS-Based Self-Healing Microcapsules with Enhanced Mechanical and Thermal Stability. *Colloids Surf A Physicochem Eng Asp* **2017**, *518*, 173–180, doi:10.1016/J.COLSURFA.2017.01.044.

132. Lee, M.W.; An, S.; Kim, Y. Il; Yoon, S.S.; Yarin, A.L. Self-Healing Three-Dimensional Bulk Materials Based on Core-Shell Nanofibers. *Chemical Engineering Journal* **2018**, *334*, 1093–1100, doi:10.1016/J.CEJ.2017.10.034.

133. Zhu, Y.; Shen, Q.; Wei, L.; Fu, X.; Huang, C.; Zhu, Y.; Zhao, L.; Huang, G.; Wu, J. Ultra-Tough, Strong, and Defect-Tolerant Elastomers with Self-Healing and Intelligent-Responsive Abilities. *ACS Appl Mater Interfaces* **2019**, doi:10.1021/ACSAMI.9B11041.

134. Guo, Q.; Zhang, X.; Zhao, F.; Song, Q.; Su, G.; Tan, Y.; Tao, Q.; Zhou, T.; Yu, Y.; Zhou, Z.; et al. Protein-Inspired Self-Healable Ti3C2 MXenes/Rubber-Based Supramolecular Elastomer for Intelligent Sensing. *ACS Nano* **2020**, *14*, 2788–2797, doi:10.1021/ACSNANO.9B09802.

135. Li, R.; Fan, T.; Chen, G.; Zhang, K.; Su, B.; Tian, J.; He, M. Autonomous Self-Healing, Antifreezing, and Transparent Conductive Elastomers. *Chemistry of Materials* **2020**, *32*, 874–881, doi:10.1021/ACS.CHEMMATER.9B04592.

136. Wang, S.; Urban, M.W. Self-Healing Polymers. *Nat Rev Mater* **2020**, *5*, 562–583, doi:10.1038/s41578-020-0202-4.

137. Mirabedini, S.M.; Alizadegan, F. Ionomers as Self-Healing Materials. In *Self-Healing Polymer-Based Systems*; Elsevier, 2020; pp. 279–291.

138. Mandal, S.; Hait, S.; Simon, F.; Ghosh, A.; Scheler, U.; Arief, I.; Tada, T.; Hoang, T.X.; Wießner, S.; Heinrich, G.; et al. Transformation of Epoxidized Natural Rubber into Ionomers by Grafting of 1H-Imidazolium Ion and Development of a Dynamic Reversible Network. *ACS Appl Polym Mater* **2022**, *4*, 6612–6622, doi:10.1021/acsapm.2c00976.

139. Thajudin, N.L.N.; Sardi, N.S.; Zainol, M.H.; Shuib, R.K. Room Temperature Self-Healable Natural Rubber. *Journal of Rubber Research 2019 22:4* **2019**, *22*, 203–211, doi:10.1007/S42464-019-00025-8.

140. Xu, C.; Cao, L.; Huang, X.; Chen, Y.; Lin, B.; Fu, L. Self-Healing Natural Rubber with Tailorable Mechanical Properties Based on Ionic Supramolecular Hybrid Network. *ACS Appl Mater Interfaces* **2017**, *9*, 29363–29373, doi:10.1021/ACSAMI.7B09997.

141. Tiwari, S.; Bag, D.S.; Dwivedi, M. Self-healing Thermoplastic Elastomeric Blends of Zinc-ionomer and Styrene–Butadiene–Styrene Block Copolymer and Their Characterization. *Polym Int* **2023**, doi:10.1002/pi.6582.

142. Jin, W.S.; Sahu, P.; Paria, S.; Jeong, S.; Jeon, J.H.; Yun, J.; Lee, J.H.; Park, S.M.; Kim, N. Il; Oh, J.S. Preparation of Self-Healing EPDM/Ionomer Thermoplastic Vulcanizates with Ionic Network for Automotive Application: Effects of Maleic Anhydride Grafted EPDM as Compatibilizer. *Journal of Elastomers & Plastics* **2023**, *55*, 1096–1110, doi:10.1177/00952443231195619.

143. Miwa, Y.; Kurachi, J.; Kohbara, Y.; Kutsumizu, S. Dynamic Ionic Crosslinks Enable High Strength and Ultrastretchability in a Single Elastomer. *Commun Chem* **2018**, *1*, doi:10.1038/s42004-017-0004-9.

144. Miwa, Y.; Kurachi, J.; Sugino, Y.; Udagawa, T.; Kutsumizu, S. Toward Strong Self-Healing Polyisoprene Elastomers with Dynamic Ionic Crosslinks. *Soft Matter* **2020**, *16*, 3384–3394, doi:10.1039/D0SM00058B.

145. Miwa, Y.; Yamada, M.; Shinke, Y.; Kutsumizu, S. Autonomous Self-Healing Polyisoprene Elastomers with High Modulus and Good Toughness Based on the Synergy of Dynamic Ionic Crosslinks and Highly Disordered Crystals. *Polym Chem* **2020**, *11*, doi:10.1039/d0py01034k.

146. Das, A.; Sallat, A.; Böhme, F.; Suckow, M.; Basu, D.; Wießner, S.; Stöckelhuber, K.W.; Voit, B.; Heinrich, G. Ionic Modification Turns Commercial Rubber into a Self-Healing Material. *ACS Appl Mater Interfaces* **2015**, *7*, 20623–20630, doi:10.1021/ACSAMI.5B05041.

147. Suckow, M.; Mordvinkin, A.; Roy, M.; Singha, N.K.; Heinrich, G.; Voit, B.; Saalwächter, K.; Böhme, F. Tuning the Properties and Self-Healing Behavior of Ionically Modified Poly(Isobutylene-Co-Isoprene) Rubber. *Macromolecules* **2018**, *51*, 468–479, doi:10.1021/acs.macromol.7b02287.

148. Mordvinkin, A.; Suckow, M.; Böhme, F.; Colby, R.H.; Creton, C.; Saalwächter, K. Hierarchical Sticker and Sticky Chain Dynamics in Self-Healing Butyl Rubber Ionomers. *Macromolecules* **2019**, *52*, 4169–4184, doi:10.1021/acs.macromol.9b00159.

149. Xiong, H.; Zhang, L.; Gu, S.; Hou, Y.; Wu, Q.; Wu, J. Mechanically Robust and Healable Bromobutyl Rubber Ionomer via Designing the Resonance Isomerization Effect. *Macromolecules* **2023**, doi:10.1021/ACS.MACROMOL.3C00835.

150. Madsen, F.B.; Yu, L.; Skov, A.L. Self-Healing, High-Permittivity Silicone Dielectric Elastomer. *ACS Macro Lett* **2016**, *5*, 1196–1200, doi:10.1021/ACSMACROLETT.6B00662.

151. Le, H.H.; Böhme, F.; Sallat, A.; Wießner, S.; auf der Landwehr, M.; Reuter, U.; Stöckelhuber, K.W.; Heinrich, G.; Radusch, H.J.; Das, A. Triggering the Self-Healing Properties of Modified Bromobutyl Rubber by Intrinsically Electrical Heating. *Macromol Mater Eng* **2016**, *302*, 1600385, doi:10.1002/MAME.201600385.

152. Khimi, S.R.; Syamsinar, S.N.; Najwa, T.N.L. Effect of Carbon Black on Self-Healing Efficiency of Natural Rubber. *Mater Today Proc* **2019**, *17*, 1064–1071, doi:10.1016/J.MATPR.2019.06.513.

153. Utrera-Barrios, S.; Verdejo, R.; López-Manchado, M.; Hernández Santana, M. Self-Healing Elastomers: A Sustainable Solution for Automotive Applications. *Eur Polym J* **2023**, 112023, doi:10.1016/J.EURPOLYMJ.2023.112023.

154. Wu, M.; Yang, L.; Shen, Q.; Zheng, Z.; Xu, C. Endeavour to Balance Mechanical Properties and Self-Healing of Nature Rubber by Increasing Covalent Crosslinks via a Controlled Vulcanization. *Eur Polym J* **2021**, *161*, 110823, doi:10.1016/j.eurpolymj.2021.110823.

155. Mohd Sani, N.F.; Thajudin, N.L.N.; Hayeemasae, N.; Shuib, R.K. Effect of Zn2+ Salt Bonding on Thermo-reversible Self-healing Natural Rubber. *J Appl Polym Sci* **2023**, *140*, doi:10.1002/app.53924.

156. Zhao, M.; Chen, H.; Yuan, J.; Wu, Y.; Li, S.; Liu, R. The Study of Ionic and Entanglements Self-healing Behavior of Zinc Dimethacrylate Enhanced Natural Rubber and Natural Rubber/Butyl Rubber Composite. *J Appl Polym Sci* **2022**, *139*, doi:10.1002/app.52048.

157. Sun, H.; Liu, X.; Liu, S.; Yu, B.; Ning, N.; Tian, M.; Zhang, L. Silicone Dielectric Elastomer with Improved Actuated Strain at Low Electric Field and High Self-Healing Efficiency by Constructing Supramolecular Network. *Chemical Engineering Journal* **2020**, *384*, 123242, doi:10.1016/J.CEJ.2019.123242.

158. Gong, Z.; Huang, J.; Cao, L.; Xu, C.; Chen, Y. Self-Healing Epoxidized Natural Rubber with Ionic/Coordination Crosslinks. *Mater Chem Phys* **2022**, *285*, 126063, doi:10.1016/j.matchemphys.2022.126063.

159. Guo, H.; Fang, X.; Zhang, L.; Sun, J. Facile Fabrication of Roomerature Self-Healing, Mechanically Robust, Highly Stretchable, and Tough Polymers Using Dual Dynamic Cross-Linked Polymer Complexes. *ACS Appl Mater Interfaces* **2019**, *11*, 33356–33363, doi:10.1021/ACSAMI.9B11166.

160. Hamed, G.R. Reinforcement of Rubber. *Rubber Chemistry and Technology* **2000**, *73*, 524–533, doi:10.5254/1.3547603.

161. Ponnamma, D.; Maria, H.J.; Chandra, A.K.; Thomas, S. Rubber Nanocomposites: Latest Trends and Concepts. In; 2013; pp. 69–107.

162. Danafar, F.; Kalantari, M. A Review of Natural Rubber Nanocomposites Based on Carbon Nanotubes. *Journal of Rubber Research* **2018**, *21*, 293–310, doi:10.1007/BF03449176.

163. Fan, Y.; Fowler, G.D.; Zhao, M. The Past, Present and Future of Carbon Black as a Rubber Reinforcing Filler – A Review. *J Clean Prod* **2020**, *247*, 119115, doi:10.1016/J.JCLEPRO.2019.119115.

164. Robertson, C.G.; Hardman, N.J. Nature of Carbon Black Reinforcement of Rubber: Perspective on the Original Polymer Nanocomposite. *Polymers (Basel)* **2021**, *13*, 538, doi:10.3390/polym13040538.

165. Neethirajan, J.; Parathodika, A.R.; Hu, G.-H.; Naskar, K. Functional Rubber Composites Based on Silica-Silane Reinforcement for Green Tire Application: The State of the Art. *Functional Composite Materials* **2022**, *3*, 7, doi:10.1186/s42252-022-00035-7.

166. Sattar, M.A.; Gangadharan, S.; Patnaik, A. Design of Dual Hybrid Network Natural Rubber-SiO2 Elastomers with Tailored Mechanical and Self-Healing

Properties. *ACS Omega* **2019**, *4*, 10939–10949, doi:10.1021/ACSOMEGA.9B01243.

167. Dong, H.; Zhang, Y. Robust, Thermally Conductive and Damping Rubbers with Recyclable and Self-Healable Capability. *Compos Part A Appl Sci Manuf* **2023**, *175*, 107783, doi:10.1016/j.compositesa.2023.107783.

168. Thomas, S.K.; Parameswaranpillai, J.; Krishnasamy, S.; Begum, P.M.S.; Nandi, D.; Siengchin, S.; George, J.J.; Hameed, N.; Salim, Nisa.V.; Sienkiewicz, N. A Comprehensive Review on Cellulose, Chitin, and Starch as Fillers in Natural Rubber Biocomposites. *Carbohydrate Polymer Technologies and Applications* **2021**, *2*, 100095, doi:10.1016/j.carpta.2021.100095.

169. Xu, C.; Nie, J.; Wu, W.; Fu, L.; Lin, B. Design of Self-Healable Supramolecular Hybrid Network Based on Carboxylated Styrene Butadiene Rubber and Nano-Chitosan. *Carbohydr Polym* **2019**, *205*, 410–419, doi:10.1016/J.CARBPOL.2018.10.080.

170. Xu, C.; Nie, J.; Wu, W.; Zheng, Z.; Chen, Y. Self-Healable, Recyclable, and Strengthened Epoxidized Natural Rubber/Carboxymethyl Chitosan Biobased Composites with Hydrogen Bonding Supramolecular Hybrid Networks. *ACS Sustain Chem Eng* **2019**, *7*, 15778–15789, doi:10.1021/ACSSUSCHEMENG.9B04324.

171. Kodsangma, A.; Homsaard, N.; Nadon, S.; Rachtanapun, P.; Leksawasdi, N.; Phimolsiripol, Y.; Insomphun, C.; Seesuriyachan, P.; Chaiyaso, T.; Jantrawut, P.; et al. Effect of Sodium Benzoate and Chlorhexidine Gluconate on a Bio-Thermoplastic Elastomer Made from Thermoplastic Starch-Chitosan Blended with Epoxidized Natural Rubber. *Carbohydr Polym* **2020**, *242*, 116421, doi:10.1016/J.CARBPOL.2020.116421.

172. Han, H.; Zhang, X.; Kuang, W.; Tian, H.; Wang, X. Self-Healing and Recyclable Elastomer Based on Epoxidized Natural Rubber and Carboxylated-

Chitosan. *Composites Communications* **2023**, *40*, 101594, doi:10.1016/J.COCO.2023.101594.

173. Carvalho, A.J.F.; Job, A.E.; Alves, N.; Curvelo, A.A.S.; Gandini, A. Thermoplastic Starch/Natural Rubber Blends. *Carbohydr Polym* **2003**, *53*, 95–99, doi:10.1016/S0144-8617(03)00005-5.

174. Misman, M.A.; Rashid, A.A.; Yahya, S.R. Modification and Application of Starch in Natural Rubber Latex Composites. *Rubber Chemistry and Technology* **2018**, *91*, 184–204, doi:10.5254/rct-18-82604.

175. Wu, J.; Li, K.; Pan, X.; Liao, S.; You, J.; Zhu, K.; Wang, Z. Preparation and Physical Properties of Porous Starch/Natural Rubber Composites. *Starch - Stärke* **2018**, *70*, 1700296, doi:10.1002/STAR.201700296.

176. Du, X.; Zhang, Y.; Pan, X.; Meng, F.; You, J.; Wang, Z. Preparation and Properties of Modified Porous Starch/Carbon Black/Natural Rubber Composites. *Compos B Eng* **2019**, *156*, 1–7, doi:10.1016/j.compositesb.2018.08.033.

177. Sowí Nska-Baranowska, A.; Maciejewska, M.; Duda, P. The Potential Application of Starch and Walnut Shells as Biofillers for Natural Rubber (NR) Composites. *International Journal of Molecular Science* **2022**, *23*, 7968, doi:10.3390/ijms23147968.

178. Shen, Q.; Wu, M.; Xu, C.; Wang, Y.; Wang, Q.; Liu, W. Sodium Alginate Crosslinked Oxidized Natural Rubber Supramolecular Network with Rapid Self-Healing at Room Temperature and Improved Mechanical Properties. *Compos Part A Appl Sci Manuf* **2021**, *150*, 106601, doi:10.1016/J.COMPOSITESA.2021.106601.

179. Utrera-Barrios, S.; Ricciardi, O.; González, S.; Verdejo, R.; López-Manchado, M.Á.; Hernández Santana, M. Development of Sustainable, Mechanically Strong, and Self-Healing Bio-Thermoplastic Elastomers Reinforced with

Alginates. *Polymers (Basel)* **2022**, *14*, 4607, doi:10.3390/POLYM14214607/S1.

180. Fazli, A.; Rodrigue, D. Recycling Waste Tires into Ground Tire Rubber (Gtr)/Rubber Compounds: A Review. *Journal of Composites Science* **2020**, *4*, doi:10.3390/JCS4030103.

181. Alonso Pastor, L.E.; Núñez Carrero, K.C.; Araujo-Morera, J.; Hernández Santana, M.; Pastor, J.M. Setting Relationships between Structure and Devulcanization of Ground Tire Rubber and Their Effect on Self-Healing Elastomers. *Polymers (Basel)* **2021**, *14*, 11, doi:10.3390/POLYM14010011.

182. Nuñez Carrero, K.C.; Alonso Pastor, L.E.; Hernández Santana, M.; María Pastor, J. Design of Self-Healing Styrene-Butadiene Rubber Compounds with Ground Tire Rubber-Based Reinforcing Additives by Means of DoE Methodology. *Mater Des* **2022**, *221*, 110909, doi:10.1016/J.MATDES.2022.110909.

183. Marchessault, R.H.; Sundararajan, P.R. 2 - Cellulose. In *The Polysaccharides*; ASPINALL, G.O., Ed.; Academic Press, 1983; pp. 11–95 ISBN 978-0-12-065602-8.

184. Roy, K.; Pongwisuthiruchte, A.; Chandra Debnath, S.; Potiyaraj, P. Application of Cellulose as Green Filler for the Development of Sustainable Rubber Technology. *Current Research in Green and Sustainable Chemistry* **2021**, *4*, 100140, doi:10.1016/j.crgsc.2021.100140.

185. Wu, M.; Yang, L.; Zheng, Z.; Wan, F.; Teng, X.; Xu, C. Strengthened Self-Healable Natural Rubber Composites Based on Carboxylated Cellulose Nanofibers Participated in Ionic Supramolecular Network. *Int J Biol Macromol* **2022**, *222*, 587–598, doi:10.1016/J.IJBIOMAC.2022.09.192.

186. Keilen, J.J.; Pollak, A. Lignin for Reinforcing Rubber. *Rubber Chemistry and Technology* **1947**, *20*, 1099–1108, doi:10.5254/1.3543321.

187. Roy, K.; Debnath, S.C.; Potiyaraj, P. A Review on Recent Trends and Future Prospects of Lignin Based Green Rubber Composites. *J Polym Environ* **2020**, *28*, 367–387, doi:10.1007/s10924-019-01626-5.

188. Yu, P.; He, H.; Jia, Y.; Tian, S.; Chen, J.; Jia, D.; Luo, Y. A Comprehensive Study on Lignin as a Green Alternative of Silica in Natural Rubber Composites. *Polym Test* **2016**, *54*, 176–185, doi:10.1016/j.polymertesting.2016.07.014.

189. Zhang, G.; Tian, C.; Shi, J.; Zhang, X.; Liu, J.; Tan, T.; Zhang, L. Mechanically Robust, Self-Repairable, Shape Memory and Recyclable Ionomeric Elastomer Composites with Renewable Lignin via Interfacial Metal–Ligand Interactions. *ACS Appl Mater Interfaces* **2022**, *14*, 38216–38227, doi:10.1021/acsami.2c10731.

190. Lee, K.Y.; Mooney, D.J. Alginate: Properties and Biomedical Applications. *Prog Polym Sci* **2012**, *37*, 106–126, doi:10.1016/j.progpolymsci.2011.06.003.

191. Coleman, R.J.; Lawrie, G.; Lambert, L.K.; Whittaker, M.; Jack, K.S.; Grøndahl, L. Phosphorylation of Alginate: Synthesis, Characterization, and Evaluation of in Vitro Mineralization Capacity. *Biomacromolecules* **2011**, *12*, 889–897, doi:10.1021/bm1011773.

192. Araujo-Morera, J.; Utrera-Barrios, S.; Olivares, R.D.; Verdugo Manzanares, R.; López-Manchado, M.Á.; Verdejo, R.; Hernández Santana, M. Solving the Dichotomy between Self-Healing and Mechanical Properties in Rubber Composites by Combining Reinforcing and Sustainable Fillers. *Macromol Mater Eng* **2022**, 2200261, doi:10.1002/mame.202200261.

193. Almutairi, M.D.; Aria, A.I.; Thakur, V.K.; Khan, M.A. Self-Healing Mechanisms for 3D-Printed Polymeric Structures: From Lab to Reality. *Polymers (Basel)* **2020**, *12*, doi:10.3390/polym12071534.

194.  Kuang, X.; Chen, K.; Dunn, C.K.; Wu, J.; Li, V.C.F.; Qi, H.J. 3D Printing of Highly Stretchable, Shape-Memory, and Self-Healing Elastomer toward Novel 4D Printing. *ACS Appl Mater Interfaces* **2018**, *10*, 7381–7388, doi:10.1021/ACSAMI.7B18265.

195.  Lv, C.; Wang, J.; Li, Z.; Zhao, K.; Zheng, J. Degradable, Reprocessable, Self-Healing PDMS/CNTs Nanocomposite Elastomers with High Stretchability and Toughness Based on Novel Dual-Dynamic Covalent Sacrificial System. *Compos B Eng* **2019**, *177*, 107270, doi:10.1016/J.COMPOSITESB.2019.107270.

196.  Lee, W.J.; Cha, S.H. Improvement of Mechanical and Self-Healing Properties for Polymethacrylate Derivatives Containing Maleimide Modified Graphene Oxide. *Polymers (Basel)* **2020**, *12*, 603, doi:10.3390/POLYM12030603.

197.  Balazs, A.C. Modeling Self-Healing Materials. *Materials Today* **2007**, *10*, 18–23, doi:10.1016/S1369-7021(07)70205-5.

198.  Zhang, T.; Mbanga, B.L.; Yashin, V. V.; Balazs, A.C. Effects of Morphology on the Mechanical Properties of Heterogeneous Polymer-Grafted Nanoparticle Networks. *Mol Syst Des Eng* **2017**, *2*, 490–499, doi:10.1039/C7ME00071E.

199.  Chen, J.; Li, F.; Luo, Y.; Shi, Y.; Ma, X.; Zhang, M.; Boukhvalov, D.W.; Luo, Z. A Self-Healing Elastomer Based on an Intrinsic Non-Covalent Cross-Linking Mechanism. *J Mater Chem A Mater* **2019**, *7*, 15207–15214, doi:10.1039/C9TA03775F.

200.  Zhang, Z.; Liu, J.; Li, S.; Gao, K.; Ganesan, V.; Zhang, L. Constructing Sacrificial Multiple Networks to Toughen Elastomer. *Macromolecules* **2019**, *52*, 4154–4168, doi:10.1021/ACS.MACROMOL.9B00116.

**2 Experimental**

# Chapter 2.    Experimental

*Chapter 2 provides an overview of the materials used for the development of the ionic elastomers studied in this doctoral thesis. It also outlines the compounding and vulcanization processes, the methods employed throughout the research for the characterization of rubbers, as well as the recycling and self-healing protocols specifically designed and optimized for the materials developed.*

## 2.1. Materials

A standard rubber recipe is typically composed of different ingredients, as rubber by itself is not commonly used for major practical applications. These ingredients form different systems, among which two are particularly noteworthy: the vulcanization system and the filler system. The first is tasked with overseeing the vulcanization process, while the second plays a key role in enhancing mechanical performance through reinforcing fillers or aiding in cost reduction via diluting fillers. Depending on the specific requirements of a particular application, other ingredients might be employed. A summary of all the materials used in the rubber recipes, along with those necessary for certain characterization methods, is provided below.

### 2.1.1. Carboxylated Nitrile Rubber

Nitrile rubber (NBR) is considered a workhorse in the automotive industry. It is a synthetic rubber produced by the copolymerization of acrylonitrile and butadiene monomers. When a third monomer, acrylic or methacrylic acid, is added to the

copolymerization, it results in a terpolymer called carboxylated nitrile rubber (XNBR).

XNBR has carboxylic groups in its chemical structure, which make it stronger and improve its exceptional chemical resistance to aliphatic hydrocarbons (such as propane, butane, petroleum oil, greases, and fuels) and hydraulic fluids. Carboxylation also positively impacts the overall mechanical performance, particularly abrasion and tear resistance, and heat resistance. As also mentioned in **Chapter 1**, another key aspect of carboxylation is to provide ionic crosslinking moieties. The chemical structure of XNBR is shown in Figure 2.1.
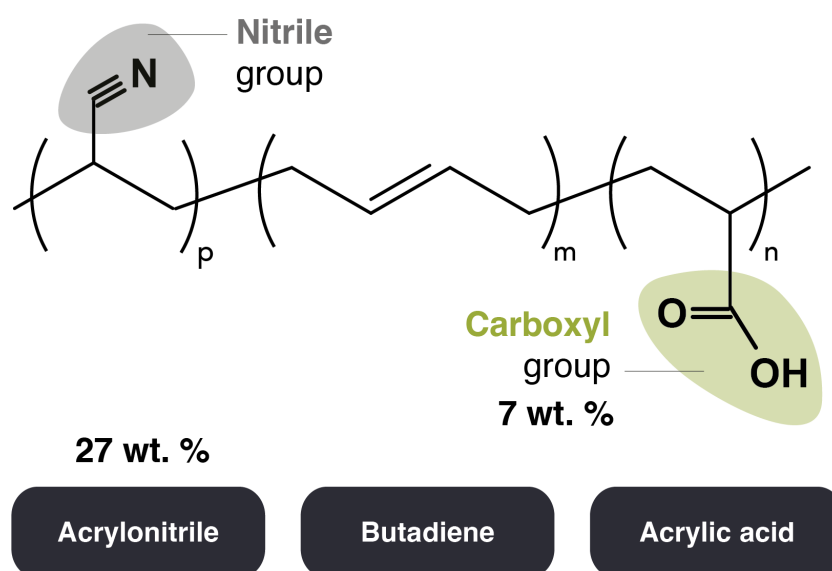


**Figure 2.1.** Chemical structure of XNBR.

A commercial XNBR (Krynac® x750) kindly provided by Arlanxeo was selected for this doctoral thesis. This product is a terpolymer synthesized via cold emulsion polymerization, non-staining stabilized, with an acrylonitrile content of 27 wt. % and 7 wt. %. of carboxyl groups. Supplied in 25 kg bales, with a slight amber color, this rubber is recommended for applications requiring high abrasion and wear

resistance, high modulus, and good adhesion. Table 2.1 summarizes the technical data of this material.

**Table 2.1.** Technical data of XNBR Krynac® x750, provided by Arlanxeo.

| Property | Nominal Value | Test Method |
| --- | --- | --- |
| Mooney viscosity | 47 MU[1] | ISO 289 / ASTM D1646 / ML(1+4) 100 °C |
| Acrylonitrile (ACN) content | 27.0 wt. % | ISO 24698 |
| Carboxyl (COOH) groups | 7.0 wt. % | - |
| Density | 0.99 g cm$^{-3}$ | Internal method |

[1] Mooney Units (MU).

## 2.1.2. Vulcanization System

The vulcanization system for conventional crosslinked rubber involves a large number of additives. Traditional sulfur (S) based systems require a combination of accelerators, activators, and/or retardants [1]. One of the advantages of the methodology employed in this doctoral thesis is that these complex systems are replaced by a single metal oxide (MO). However, this additive not only functions as a vulcanization agent; but above stoichiometric saturation, it acts as a semi-reinforcing filler with a slightly positive impact on mechanical performance. In addition, it also acts as a processing aid in mixing as it tends to slightly reduce the viscosity of the blend during the action of the rollers.

Zinc oxide (ZnO, ExpertQ®, with a specific density of 5.47 g cm$^{-3}$ and a particle size < 5 mm) and Magnesium oxide (MgO, Pharmpur®, with a specific density of

3.58 g cm$^{-3}$ and a particle size $< 150$ mm), both for analysis and supplied by Scharlau, were selected as the crosslinking agents.

For comparative purposes, a covalent network based on a regular S-accelerator system, was also designed. S was acquired from Merck. Stearic acid (SA) as activator was supplied by Alfa Aesar and $n$-cyclohexyl-2-benzothiazole sulfenamide (CBS) from Biosynth Carbosynth was selected as the accelerator. All these additives do not require purification prior to use.

### 2.1.3. Filler System

**Carbon Black**

Carbon black (CB) is a form of elemental carbon manufactured by controlled vapor-phase pyrolysis and partial combustion of hydrocarbons. It is composed of fine particles with a graphitic carbon core and has a complex structure with layered, amorphous regions. This unique composition gives CB a characteristic black color and a range of physical and chemical properties essential for its effectiveness as a filler and dye. For rubber compounds, CB has been widely used because of its ability to improve mechanical properties, abrasion resistance, and tear strength. This makes CB the top reinforcing filler for elastomers [2].

During the manufacturing of rubber composites, it is blended with the matrix, promoting the breakdown of the aggregates and their uniform distribution. This step is vital because poor dispersion can lead to inconsistent performance. An optimized mixing process aligned with the small particle size ($10 - 500$ nm), high surface area, and structure of CB ensures superior filler dispersion and polymer-filler interactions. The primary mechanisms behind CB reinforcement include the following:

1. Hydrodynamic effect: CB particles restrict polymer chain mobility, thereby increasing the viscosity and modulus.

2. Physical crosslinking: Polymer chains adsorb onto the CB surface, providing reinforcement analogous to that provided by chemical crosslinks.

3. Filler networking: CB particles are linked together into a microstructure that resists deformation and crack growth.

For comparative purposes, two types of CB were selected, N234 and N330, both kindly supplied by Birla Carbon and with a particle size between 200-300 μm. N234 has a higher surface area than N330 and is typically used in high-performance applications, especially where abrasion resistance is critical. N330 is a general-purpose CB, often used in tire treads and industrial rubber products, where a balance between wear resistance and cost is required. Table 2.2 summarizes the technical data of the two CBs used.

**Table 2.2.** Technical data of CB N234 and N330, provided by Birla Carbon.

| Property | N234 | N330 | Method | Significance |
|---|---|---|---|---|
| Density (g cm$^{-3}$) | $1.7 - 1.9$ | $1.7 - 1.9$ | N/R | - |
| BET[1] surface area (NSA) (m$^2$ g$^{-1}$) | 119 | 78 | ASTM D1510 | - |
| STSA[2] surface area (m$^2$ g$^{-1}$) | 112 | 75 | ASTM D3265 | - |
| Iodine number (ION) (mg g$^{-1}$) | 120 | 82 | ASTM D3493 | ↑ ION ↑ Surface area |
| Oil absorption number (OAN) [ml (100g)$^{-1}$] | 125 | 102 | ASTM D6556 | ↑ OAN ↑ Structure |

[1] Brunauer-Emmett-Teller (BET) method.

[2] Statistical Thickness External Surface Area (STSA).

**Silica**

Silica, also known as silicon dioxide ($SiO_2$), is a naturally occurring mineral. It is most commonly found in the form of quartz, and is the primary component of sand. In rubber compounding, silica is used in a precipitated, amorphous form, synthesized from the controlled precipitation of a sodium silicate solution [3].

Silica is particularly significant in the tire industry, where it is used to reduce the rolling resistance and improve the fuel efficiency of "green tires" [4]. It is also used in several industrial rubber products, where environmental considerations and color are key factors.

For rubber reinforcement, silica usually requires a silane coupling agent (TESPT) to effectively bond with a non-polar rubber matrix. This is in contrast with CB, which inherently bonds well with rubber owing to its carbon-based structure [5]. However, the choice of a polar rubber such as XNBR makes it possible to dispense with the use of coupling agents (which are generally expensive), thus taking full advantage of the functionalities provided by this reinforcing filler.

Commercially available silica, ZEOSIL® 1165 MP, kindly provided by Solvay, was used in this study. This grade is highly dispersible silica (HDS), which is known to enhance the balance between the tire rolling resistance and grip, with a particle size of $200 - 300$ μm and 2.1 g $cm^{-3}$ of density.


**Cellulose**

Cellulose is a polysaccharide that forms the structural component of the primary cell walls of green plants. It is the most abundant organic polymer on Earth. As stated in **Chapter 1**, cellulose can be obtained in its microcrystalline or nanocrystalline form and as cellulose fibers. Crystalline forms are widely used in rubber research as a natural and renewable alternative for rubber composites [6]. In this doctoral thesis, the use of an alternative less-explored form was intended. Cellulose fibers (CF) with

a particle size of 50 – 350 μm and fiber diameter of 12 – 15 μm from Merck were selected.

## Ground Tire Rubber

As part of the growing environmental concerns derived from inadequate management of tire waste, legislation in Europe has promoted the recovery of ELT, reaching high recovery rates of up to 95 %. Although only a small percentage of this collected amount ends up being recycled, one of the uses that has been gained under this principle is the incorporation into new rubber blends [7]. The marketed granulate is known as ground tire rubber (GTR). This granule is generally composed of tire waste from passenger cars and trucks, which varies substantially in the proportions of the three main rubbers (NR, SBR, and BR). SBR is the main component of passenger tires, while NR is the main component of truck tires.

To obtain GTR from ELT, non-rubber components (mainly textiles and steels) are separated, and the rubber is shredded. For these granules to be useful in the manufacturing of new rubber blends, they must undergo particle size reduction, for which grinding at RT or below the Tg of the rubber can be used. In this doctoral thesis, for comparative purposes, two GTRs were selected from grinding under cryogenic conditions and using water jet technology. Cryogenically ground GTR (Cryo, with a BET surface area of 0.0209 $m^2$ $g^{-1}$) was supplied by Lehigh Technologies, and GTR from water jet technology (WJ, with a BET surface area of 0.1696 $m^2$ $g^{-1}$) by Rubber Jet.

## Toner Cartridge

Directive 2012/19/EU of the European Parliament and the Council of the European Union (EU) was issued on July 4th, 2012 to regulate and mitigate the adverse impacts of waste from electrical and electronic equipment (WEEE) on the

environment and human health [8]. It aims to promote sustainable production and consumption by preventing WEEE and encouraging techniques such as preparation for reuse [9]. Inspired by the use of GTR as an additive in new rubber compounds, in this doctoral thesis we studied the incorporation of toner cartridges as an additive in ionic elastomers. Discarded cartridges (05x Black Noir, Hewlett-Packard) were selected from the collection point of the Institute of Polymer Science and Technology (ICTP), CSIC.

The focus was on two constituents of the cartridge: thermoplastic parts (essentially the casing) and toner powder (TP). The latter, owing to its characteristic black color, is constituted by CB, so it could be used as a reinforcing filler. To properly handle the thermoplastic parts, they were subjected to cryogenic grinding in a ball mill (CryoMill, Retsch) to reduce the particle size and facilitate their incorporation during the mixing process. 9 grinding cycles of 2.5 min duration each, at a frequency of 30 Hz, were used, with a preconditioning step before each cycle of 0.5 min at 5 Hz. The average particle size was 89 µm.

### 2.1.4. Other Materials

Other ingredients used in different experimental techniques throughout the research were toluene (ACS reagent) from Merck, and gasoline 95 and motor oil from Repsol for crosslink density assessment and chemical resistance, respectively. Any other material that has been used in a particular way in any of the chapters of this doctoral thesis will be presented in the corresponding section.

## 2.2. Compounding and Vulcanization

The manufacture of the ionic elastomers followed a three-stage process: first, the design of the rubber recipes; second, the process of mixing XNBR with the selected additives; and finally, vulcanization. For ease of reference, specific recipes are

presented in each corresponding chapter. All of these are expressed in phr (parts per hundred rubber) as a functional unit in the rubber industry.

## 2.2.1. Mixing

The mixing process was conducted in a two-roll mill (MGN-300S, Comerio Ercole S.P.A.) operating at a friction ratio of 1:1.15. Initially, the XNBR was masticated for 4 min. Mastication is a process in which raw rubber is softened and made more workable by mechanically breaking down polymer chains. In this process, the rubber is passed solely through the counter-rotating rolls. After the formation of an elastomeric band, the additives were incorporated in a sequential manner; initially, MO was added, followed by 1/2 of the total filler amount (if any was specified in the recipe), and then the remaining 1/2 was introduced. During this time, transverse cuts were made to the rubber band to promote homogenization of the ingredients. Figure 2.2 summarizes this sequence for the unfilled and filled compounds. To prevent overheating, which could lead to changes in the molecular structure of the rubber such as pre-vulcanization, a water-cooling system was employed through the rolls. The total mixing time was 15 min. The blends were stored in a refrigerator for a minimum of 24 h before characterization.

## 2.2.2. Vulcanization

Vulcanization is the curing process by which rubber acquires its elasticity. The vulcanization process was carried out by compression molding in an automatic press (P 200 P, Collin) operating at 160 °C and 200 bar during the optimum cure time (t90), as determined from the curing curves. Steel molds were used for the sample fabrication.
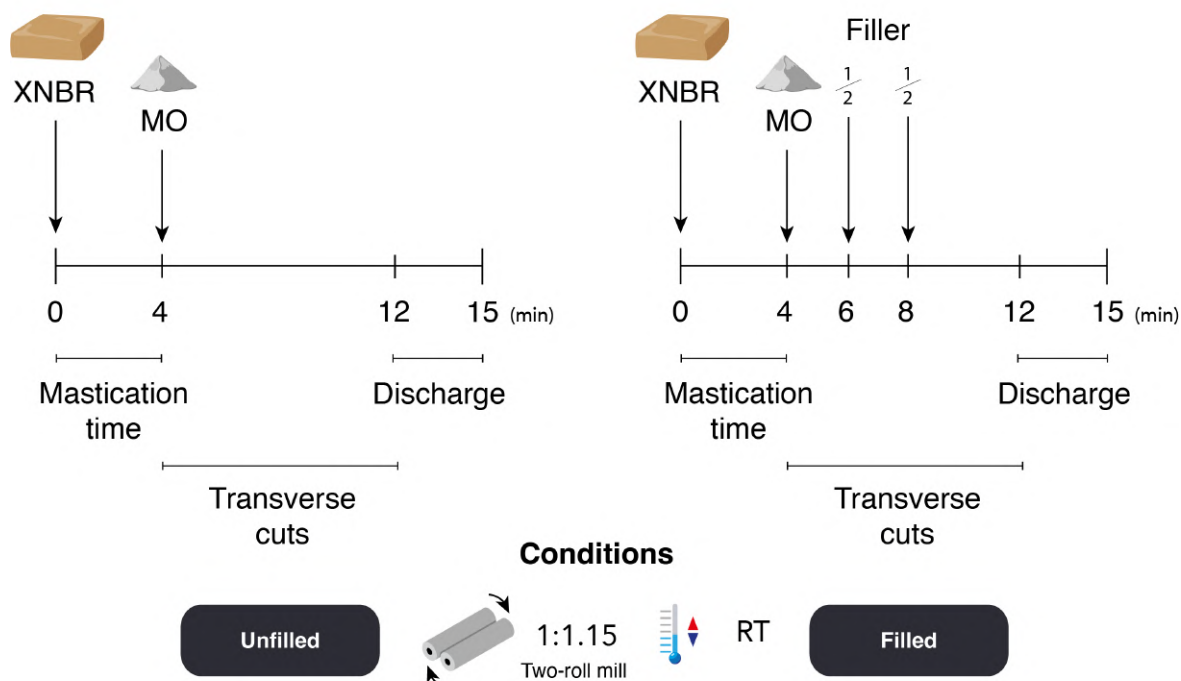
**Figure 2.2.** Scheme of the mixing process.

## 2.3. Characterization Techniques

The characterization techniques have been classified according to the type of property or parameters that can be determined. Five categories have been defined: (1) physico-chemical properties, (2) structural properties, (3) thermal properties, (4) mechanical properties and (5) dynamic properties. Each technique used is presented within its category in alphabetical order.

### 2.3.1. Physico-chemical Properties

**Density**

The densities of the different prepared samples required for crosslink density calculations were determined following the ISO 2781 standard using the hydrostatic weighing method. The values reported for this and all calculations presented in this

section are the average with their respective standard deviations, from at least three different samples.

## Chemical Resistance

To evaluate the chemical resistance of the prepared recipes, five samples (1 cm × 1 cm × 2 mm) were immersed in the targeted solvents for 72 h at RT. Before ($m_i$) and after ($m_f$) immersion, the samples were weighed to determine the mass change ($\Delta m$, %), which was used as an indirect measure of chemical resistance, calculated according to Equation 2.1:

$$\Delta m = 100 \frac{m_f - m_i}{m_i} \qquad \text{Equation 2.1}$$

## Crosslink Density

*Mooney-Rivlin Method:* The stress-strain analysis allows the calculation of the crosslink density ($\nu$) in mol cm$^{-3}$, using the Mooney-Rivlin method [10,11]. For this purpose, the stress ($\sigma$) and strain ($\varepsilon$) values obtained from the tensile tests were used. Subsequently, the reduced stress ($\sigma_{red}$) was plotted as a function of the inverse of the strain ratio ($\lambda^{-1}$, with $\lambda = 1 + \varepsilon$) using Equation 2.2:

$$\sigma_{red} = \frac{\sigma}{\lambda - \lambda^{-2}} = 2C_1 + 2C_2 \left(\frac{1}{\lambda}\right) \qquad \text{Equation 2.2}$$

where $C_1$ represents the contribution of the crosslinking units, $C_2$ denotes the Mooney-Rivlin elastic constant, and is related to the trapped entanglements. From the linear region of the plot, the *y*-intercept is $2C_1$ and the slope is $2C_2$. Consequently, $\nu$ can be calculated by Equation 2.3:

$$2C_1 = N_A \nu k T \qquad \text{Equation 2.3}$$

where $N_A$ is Avogadro's number ($6.02 \times 10^{-23}$ mol$^{-1}$), $k$ is the Boltzmann's constant ($1.38 \times 10^{-23}$ J K$^{-1}$), and $T$ is the temperature (in K).

*Swelling Test:* An equilibrium swelling test was conducted on five samples with a square section of approximately 1 cm × 1 cm × 2 mm. These samples were immersed in the selected solvent (toluene) for 72 h at RT, extracted, and dried in air until the solvent evaporated to a constant mass. The mass after each step was recorded before immersion ($m_1$), after swelling for 72 h ($m_2$), and after evaporation of the absorbed solvent ($m_3$).

Subsequently, $\nu$ was calculated and expressed in mol cm$^{-3}$ using Equation 2.4:

$$\nu = \frac{\rho_r}{M_c} \qquad \text{Equation 2.4}$$

where $\rho_r$ is the rubber density and $M_c$ is the average molecular weight between crosslinks.

The Flory-Rehner expression [12,13] considering the affine model and tetra-functional networks, $f = 4$, was required to calculate $\rho_r\, M_c^{-1}$ according to Equation 2.5:

$$\ln(1 - V_r) + V_r + \chi V_r^2 = -\frac{\rho_r}{M_c} V_s \left( V_r^{\frac{1}{3}} - \frac{2V_r}{f} \right) \qquad \text{Equation 2.5}$$

where $V_s$ is the molar volume of toluene (106.28 cm$^3$ mol$^{-1}$), $\chi$ is the Flory-Huggins interaction parameter between XNBR and toluene (calculated using the expression $0.4132 + 0.4341\,V_r$ [14]), and $V_r$ is the volume fraction of rubber in the recipe, calculated according to Equation 2.6:

$$V_r = \frac{\dfrac{m_3}{\rho_r} - V_f}{\dfrac{m_3}{\rho_r} + \dfrac{m_2 - m_3}{\rho_s}} \qquad \text{Equation 2.6}$$

where $\rho_s$ is the density of toluene (0.867 g cm$^{-3}$) and $V_f$ is the volume fraction of fillers in the rubber recipe (if any), calculated following Equation 2.7:

$$V_f = a \frac{m_1}{\rho_r}$$

Equation 2.7

where $a$ is the weight fraction of the filler in the blend.

## Fourier-transform Infrared Spectroscopy (FTIR)

FTIR was used to verify the formation of the ionic crosslinks. A spectrometer (Spectrum Two, Perkin Elmer) was operated to obtain the IR spectra of the compounds in Attenuated Total Reflectance (ATR) mode from 400 cm$^{-1}$ to 4000 cm$^{-1}$ with a resolution of 4 cm$^{-1}$ and co-adding 4 scans per spectrum.

## Rheometric Properties

The curing properties of the rubber compounds were evaluated using a moving-die rheometer (MDR 2000, Monsanto) according to ASTM D5289-19a. The torque increment was recorded at 160 °C for 60 min at a frequency of 1.7 Hz and an oscillation arc of 0.5°. Approximately 4 g of the uncured rubber sample was sandwiched between polyester films inside the rheometer chamber.

The equipment records the variation in torque as a function of time, resulting in a curing curve. Figure 2.3 shows a theoretical representation of the curing curves. As the material undergoes crosslinking, its stiffness progressively increases, reaching a peak value. This phenomenon is reflected in the curing curve as an increase in torque, which generates three distinct zones on the curve. Zone 1, known as the induction zone, captures the early stages of the process. As the elastomeric material is heated, it becomes more mobile, leading to a decrease in the torque. This decrease serves as an indicator of the viscosity of the blend until the onset of vulcanization. Zone 2,

the actual curing zone, is marked by a continuous increase in torque, indicative of the formation of crosslink points. The rate of this increase is directly related to the vulcanization speed. The final stage, Zone 3, encompasses overcuring. Ideally, the material would *plateau* at this stage, indicating the completion of vulcanization. However, variations, such as reversion (a decrease in torque post-peak value) or the marching modulus (characteristic in ionic systems, where the torque never stabilizes due to the continuous movement of ions), can also be observed. Table 2.3 summarizes the different parameters obtained from those curves.
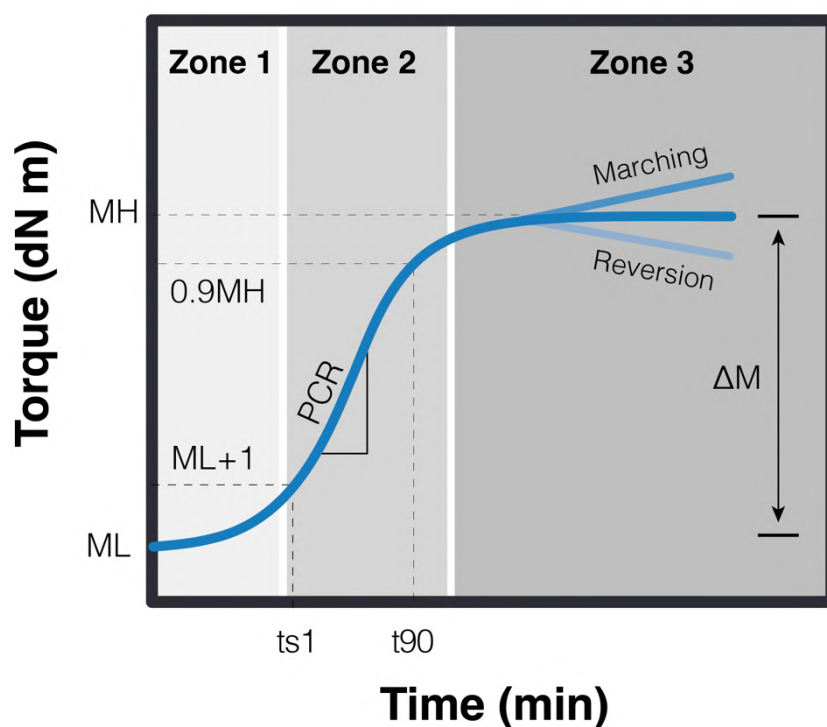


**Figure 2.3.** Theoretical curing (vulcanization) curves of the elastomers.

The marching modulus imposes serious complications in the calculation of t90 because the torque does not stabilize, and different results can be obtained depending on the duration of the test. In this case, the tangent method can be applied to determine a cut-off point with a more realistic optimum curing time.

**Table 2.3.** Parameters obtained from curing curves.

| Property | Description |
|---|---|
| Scorch time, ts1 or ts2 (min) | Time necessary for the torque value to rise one or two units above the minimum. |
| Curing time, t90 (min) | Time at which 90 % of the maximum torque is reached. |
| Minimun torque, ML (dNm) | Correlated with the viscosity of the uncured rubber. |
| Maximun torque, MH (dNm) | The degree of vulcanization. Related to the modulus and hardness of the vulcanizate. |
| $\Delta M = MH - ML$ (dNm) | Corelated with the crosslink density of the rubber. |
| Cure rate index, $CRI = 100 / (t90 - ts1)$ $(min^{-1})$ | Associated with the entire vulcanization rate. |
| Peak cure rate, PCR $(dNm\ min^{-1})$ | Maximum slope in the ascending zone of the curve. Corelated with the fastest rate of crosslink formation. |

## 2.3.2. Structural Properties

**Scanning Electron Microscopy (SEM)**

An environmental SEM (XL30, Phillips) was used to observe the morphology of the samples. The microscope was equipped with a tungsten filament. An acceleration voltage of 25 kV was fixed. Owing to the polymeric character of the samples, the surfaces required sputter-coating with a gold alloy. A cross-section resulting from a cryogenic fracture was observed.

**X-Ray Diffraction (XRD)**

A diffractometer (D8 Advance, Bruker) with Cu-K$\alpha$ radiation (with $\lambda = 1.52$ Å) was used to obtain diffraction patterns over a wide $2\vartheta$ range between 1° and 90° (WAXS) under standard conditions (0.2 s per step) using vulcanized solid samples of 1-2 mm in thickness. The spectra were expressed as a function of the distance in reciprocal space, $q$, according to Equation 2.8:

$$q = \frac{2\pi}{d}$$

Equation 2.8

where $d$ is the distance between structures according to Bragg's law (Equation 2.9):

$$n\lambda = 2d \sin\theta$$

Equation 2.9

## 2.3.3. Thermal Properties

**Differential Scanning Calorimetry (DSC)**

Differential scanning calorimetry (DSC, 214 Polyma, Netzsch) was used to observe the different thermal transitions of the materials. A three-step heating-cooling-heating method was set at a rate of 10 K min$^{-1}$ in the range of $-90$ °C to 160 °C under nitrogen flux (2 mL min$^{-1}$).

**Thermogravimetric Analysis (TGA)**

A thermal analyzer (TGA 2, Mettler Toledo) was used to perform a temperature sweep from RT to 600 °C under a nitrogen atmosphere, and then up to 800 °C in an oxygen atmosphere at a heating rate of 10 °C min$^{-1}$.

## 2.3.4. Mechanical Properties

**Abrasion Resistance**

Abrasion resistance index ($ARI_A$) was calculated according to Equation 2.10 and following the standard procedure in ASTM D5963 (2015), using Method A (non-rotating). An abrasion test was performed using an Abrasimeter DIN. Three samples of each compound were prepared directly via compression molding.

$$ARI_A = \frac{\Delta m_1 d_t}{\Delta m_t d_1} \qquad \text{Equation 2.10}$$

where $\Delta m_1$ is the mass loss of Standard Rubber #1 test piece in mg, $d_1$ is the density of Standard Rubber #1 in mg m$^{-3}$, $\Delta m_t$ is the mass loss of the test rubber piece in mg, and $d_t$ is the density of the test rubber in mg m$^{-3}$.

**Compression Fatigue Testing**

The compressive fatigue response was studied using a tabletop testing system (858, MTS) employing cylindrical samples with a diameter of 16 mm and height of 12.5 mm. A sinusoidal oscillation with an amplitude of 3.1 mm (25 % compressive strain) at a frequency of 10 Hz was set. All experiments were performed for up to 10000 cycles at RT. The final heights were recorded after 5 min and 30 days.

**Cyclic Tensile Testing**

Cyclic tensile tests were conducted using the same type of samples and equipment as the tensile tests, but with an extension rate of 500 mm min$^{-1}$ to 300 % strain up to ten times. To simplify the plots, only the curves of the first three loading and unloading cycles are shown; thereafter, the changes were negligible.

**Hardness**

Hardness is defined as the resistance to indentation and is influenced by the stiffness and viscoelastic characteristics of the elastomer. This parameter is one of the most commonly assessed in the rubber sector. The hardness was measured using a Shore A durometer (Bareiss, Neurtek). The indentation was held for 15 s at RT in accordance with the ISO 7619-1 standard. Tests were conducted on three distinct samples for each rubber composite.

**Tensile Measurements**

Tensile tests were conducted on dumbbell-shaped specimens in accordance with the UNE-ISO 37:2013 standard using a universal testing machine (4204, Instron) equipped with a 50 kN load cell. The tests were performed at an extension rate of 200 mm min$^{-1}$ and initial gauge length of 35 mm. All reported magnitudes are the mean values of the five samples tested and their corresponding standard deviations, while the shown stress-strain curves are the most representative of the mean values. Figure 2.4 shows the theoretical stress-strain curve of elastomers and Table 2.4 summarizes the mechanical parameters.

In the Rubber Science and Technology field [15–17], the stress values recorded at specific strain levels, such as 100 % (M100), 300 % (M300) and 500 % (M500), are often referred to as "modulus". While these terms provide an analogous insight into the stiffness of a material at these deformation levels, they are not moduli in the classical sense, such as Young's modulus. Although the latter magnitude can be calculated using different available models.
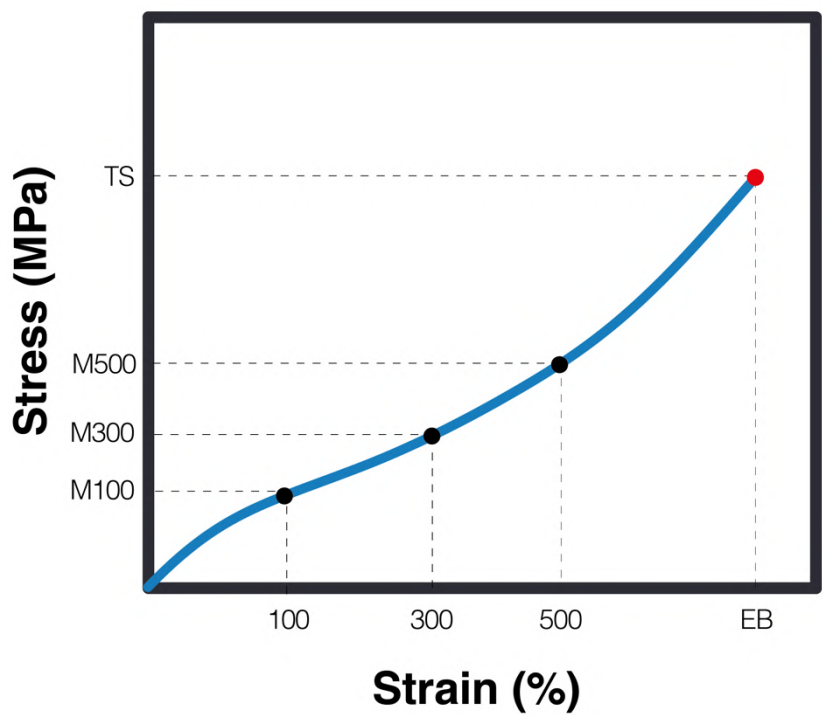
**Figure 2.4.** Theoretical stress-strain curves of elastomers.

**Table 2.4.** Properties obtained from the stress-strain curves of elastomers.

| Property | Description |
| --- | --- |
| Stress at 100 % strain, M100 (MPa) | Correlated with the stiffness. |
| Stress at 300 % strain, M300 (MPa) | Correlated with the stiffness. |
| Stress at 500 % strain, M500 (MPa) | Correlated with the stiffness and the reinforcement index (RI)[1]. |
| Tensile strength, TS (MPa) | Stress at the breaking point ($\sigma_b$). |
| Elongation at break, EB (%) | Strain at the breaking point ($\varepsilon_b$). |

[1] In filled rubbers.

## 2.3.5. Dynamic Properties

**Broadband Dielectric Spectroscopy (BDS)**

Frequency sweeps ranging from $10^{-1}$ Hz to $10^6$ Hz were performed on a high-resolution dielectric analyzer (ALPHA, Novocontrol Technologies) from $-100$ °C to 150 °C in increments of 5 °C. The complex dielectric function in the frequency domain $\varepsilon^*(\omega)$ was obtained as expressed in Equation 2.11 [18,19]:

$$\varepsilon^*(\omega) = \varepsilon'(\omega) - i\varepsilon''(\omega) \qquad \text{Equation 2.11}$$

where $\varepsilon'(\omega)$ is the real part and is proportional to the energy stored reversibly in the system and $\varepsilon''(\omega)$ is the imaginary part and is proportional to the dissipated energy (also known as dielectric loss).

For a supplemental visualization of the effects over the complex dielectric function, the reciprocal of the complex permittivity, $1/\varepsilon^*(w)$, known as the complex electric modulus $M^*(\omega)$, can be used and is expressed as seen in Equation 2.12:

$$M^*(\omega) = M'(\omega) + iM''(\omega)$$

$$M'(\omega) = \frac{\varepsilon'(\omega)}{\left(\varepsilon'(\omega)\right)^2 + \left(\varepsilon''(\omega)\right)^2} \qquad \text{Equation 2.12}$$

$$M''(\omega) = \frac{\varepsilon''(\omega)}{\left(\varepsilon'(\omega)\right)^2 + \left(\varepsilon''(\omega)\right)^2}$$

The analysis of the dielectric spectra and each dielectric relaxation process requires the use of different model functions. One of the most general functions is the Havriliak-Negami function (HN-function) according to Equation 2.13:

$$\varepsilon^*_{HN}(\omega) = \varepsilon_\infty + \frac{\Delta\varepsilon}{(1 + (i\omega\tau_{HN})^\alpha)^\beta} \qquad \text{Equation 2.13}$$

where $\alpha$ and $\beta$ are two parameters related to the symmetric and asymmetric broadening of the complex dielectric function, respectively, with $0 < \alpha$ and $\alpha\beta \leq 1$, $\Delta\varepsilon = \varepsilon_0 - \varepsilon_\infty$ is the dielectric strength, where $\varepsilon_0$ is the relaxed ($\omega = 0$) and $\varepsilon_\infty$ the unrelaxed ($\omega = \infty$) dielectric constant values, respectively; and, finally, $\tau_{HN}$ is the HN relaxation time, related to the position of maximal loss in the HN-function. $\alpha$ and $\beta$ are also related to the overall position of each maximal loss ($\tau_{max} = 1/\omega_{max}$), according to Equation 2.14:

$$\tau_{max} = \tau_{HN} \left[ \sin\left( \frac{\alpha\pi}{2 + 2\beta} \right) \right]^{-\frac{1}{\alpha}} \left[ \sin\left( \frac{\alpha\beta\pi}{2 + 2\beta} \right) \right]^{\frac{1}{\alpha}} \qquad \text{Equation 2.14}$$

Typically, different relaxation processes and contributions from conductivity are combined. If the latter has an electronic origin (such as in electrode- or Maxwell-Wagner-Sillars-polarization), it does not contribute to $\varepsilon'$ but $\varepsilon''$ is directly proportional to the dc-conductivity of the sample ($\sigma_0$) and inversely proportional to $\omega^{-s}$, where $s < 1$. Therefore, a secondary power law (PL) function is required to properly fit the complex dielectric function, as shown in Equation 2.15:

$$\varepsilon^*(\omega) = -ia\left( \frac{\sigma_0}{\varepsilon_v \omega^s} \right) + \varepsilon^*_{HN}(\omega) \qquad \text{Equation 2.15}$$

where $\varepsilon_v$ is the dielectric permittivity of vacuum (a constant value, $\varepsilon_v = 8.854 \times 10^{-12}$ A s V$^{-1}$ m$^{-1}$).

The analysis of dielectric data sometimes requires prior use of the first-order approximation of the Kramers-Kronig relation. Different relaxation processes, especially at high temperatures, can be complex to analyze because their contribution and ionic conductivity can overlap in $\varepsilon''(\omega)$. An elegant way to remove Ohmic conduction from the measured loss spectra is to use a logarithmic derivative, which transforms the real part $\varepsilon'(\omega)$ into an imaginary part $\varepsilon''_{der}$ that is solely based on relaxation phenomena [20–22]. Thus, $\varepsilon''_{der}$ lacks an Ohmic conduction term. This approximation is based on Equation 2.16:

$$\varepsilon''_{der} = -\frac{\pi}{2}\frac{\partial \varepsilon'(\omega)}{\partial \ln \omega} \approx \varepsilon'' \qquad \text{Equation 2.16}$$

**Dynamic Mechanical Analysis (DMA)**

Temperature sweeps from $-100$ °C to $150$ °C were performed using a DMA analyzer (DMA Q800, TA Instruments) in tension mode over rectangular specimens ($20 \times 4 \times 2$ mm). A constant amplitude of 20 μm and frequency of 1 Hz were set at a heating rate of 2 K min$^{-1}$.

## 2.4. Recycling Protocol

Mechanical recycling involved a two-stage protocol. The first stage comprised the reduction of the vulcanized sheet into small fragments by cutting, roughly measuring an area of 1 cm$^2$. These portions were then placed inside a mold in an automatic hot press at 160 °C and 200 bar for an hour to proceed with the (re)molding process. This sequence of actions is termed as one recycling cycle (R1), resulting in the transformation of the material into a new solid sheet with a thickness of 2 mm. This process was repeated for up to three cycles (R3). Figure 2.5. shows a schematic of the two-step recycling protocol.

## 2.5. Self-healing Protocol

The healing protocol consists of two primary steps, as shown in Figure 2.6. First, a rectangular sample was damaged using a razor blade. In the next step, the repairability of the induced damage was explored. For this purpose, the two surfaces resulting from the damage were manually repositioned in a mold that matched the dimensions of the pristine sample. Subsequently, at 200 bar, different temperature and time conditions were applied.
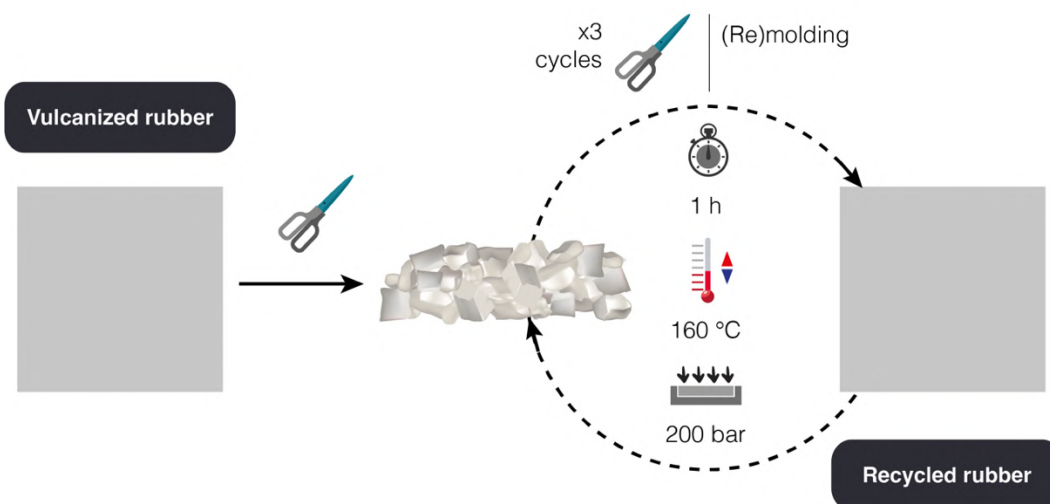
**Figure 2.5.** Schematic representation of the recycling protocol.
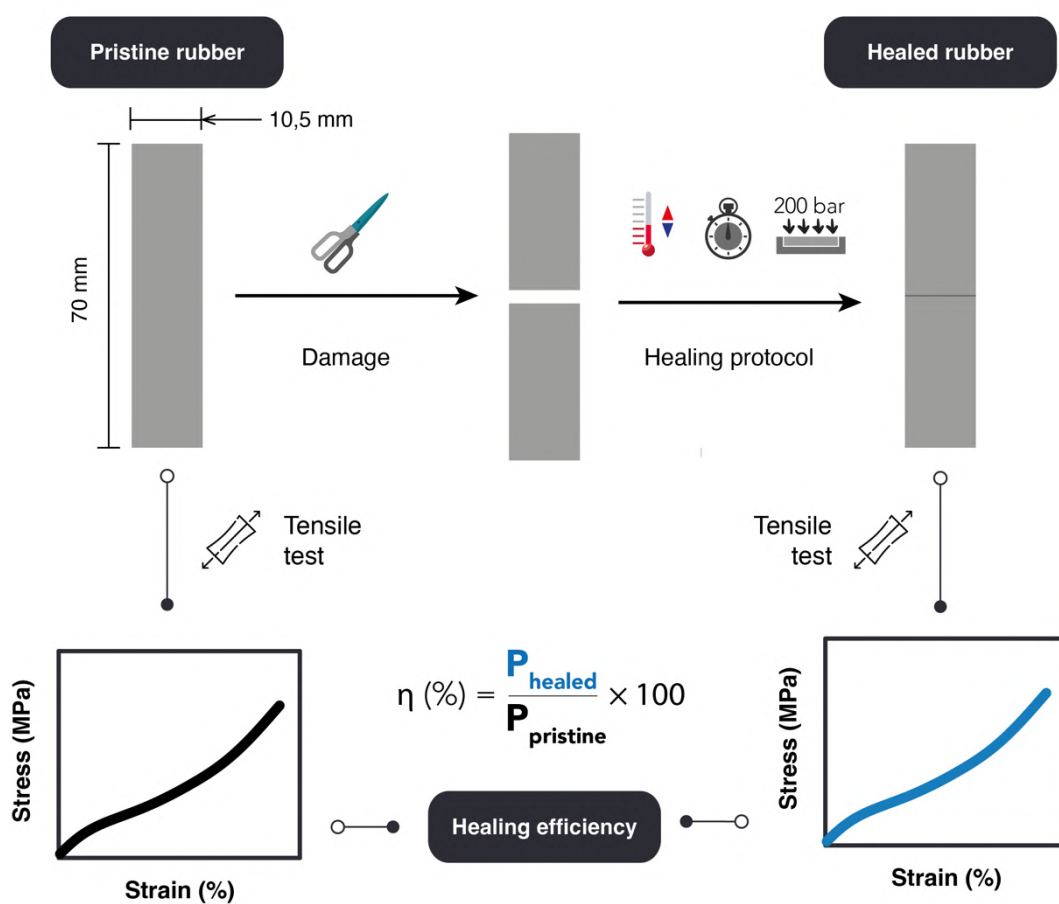


**Figure 2.6.** Schematic representation of the self-healing protocol.

The mechanical properties of the healed compounds were measured, and the healing efficiency ($\eta$) was calculated using Equation 2.17:

$$\eta(\%) = \frac{P_{healed} - P_{damaged}}{P_{pristine} - P_{damaged}} 100 = \frac{P_{healed}}{P_{pristine}} 100 \qquad \text{Equation 2.17}$$

with selected properties before healing ($P_{pristine}$), after damage ($P_{damaged}$), and after healing ($P_{healed}$). As the serious damage of cutting a sample in two pieces leads to a loss of property after damage ($P_{damaged} = 0$), the equation can be simplified into the ratio between the property before and after the healing protocol.

## 2.6. Manufacturing of Soft Robotic Gripper

As it is not a transversal method to the whole doctoral thesis, the procedure related to the assembly and validation of the soft robotic gripper with the prepared ionic elastomers, will be described in the specific chapter where this topic is presented (**Chapter 5**).

## 2.7. Summary

As previously illustrated, the process of developing rubber products and their accurate characterization is complex. Therefore, reducing the number of steps involved and the ingredients used is crucial for real-world scalability. As a summary of **Chapter 2**, Figure 2.7 provides a comprehensive overview of the journey of the developed *ionic elastomers*, from the initial recipe to the final application development.
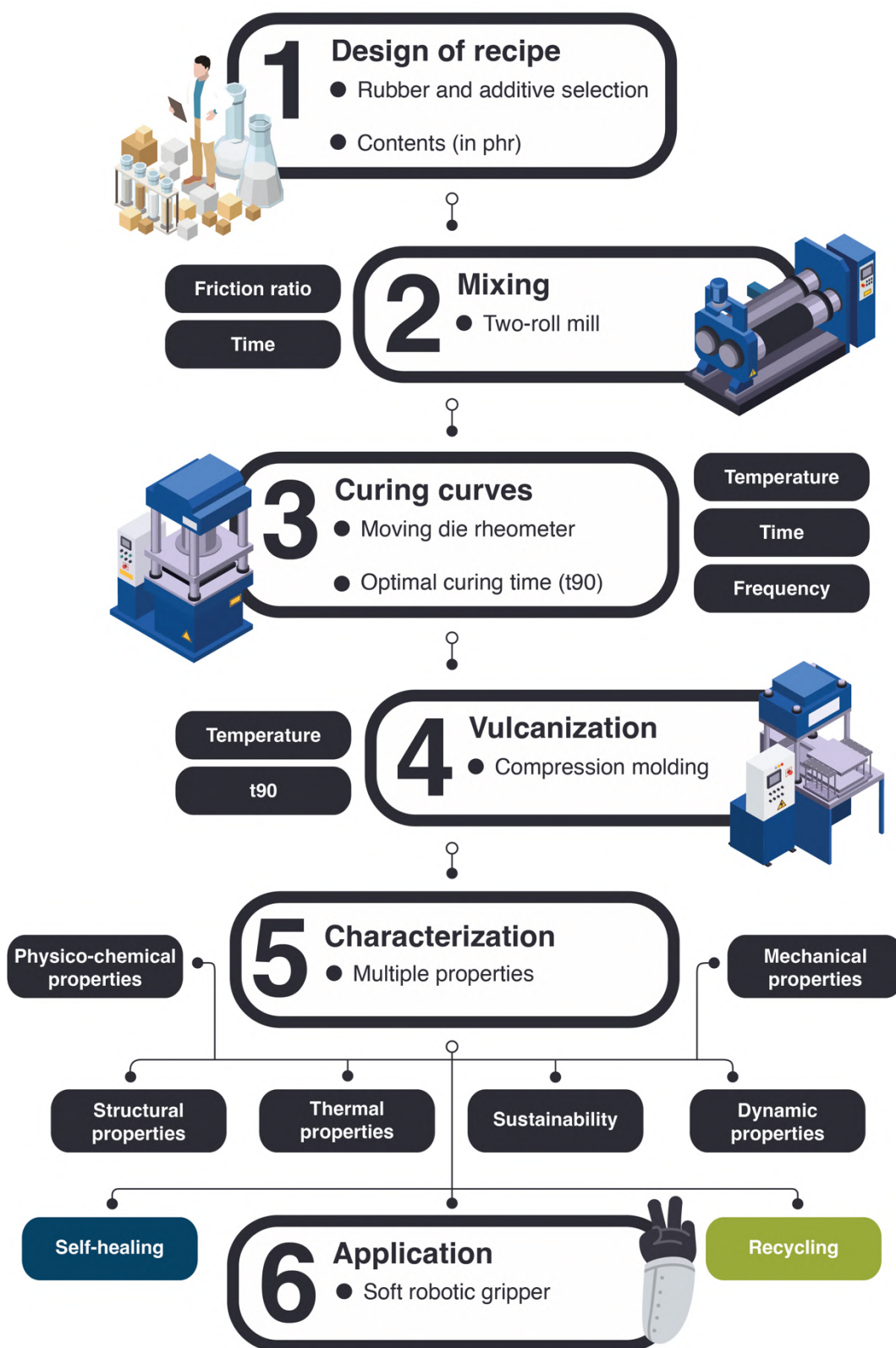
**Figure 2.7.** Schematic of the manufacturing of *ionic elastomers.*

**References**

1. Akiba, M.; Hashim, A.S. Vulcanization and Crosslinking in Elastomers. *Prog Polym Sci* **1997**, *22*, 475–521, doi:10.1016/S0079-6700(96)00015-9.

2. Fan, Y.; Fowler, G.D.; Zhao, M. The Past, Present and Future of Carbon Black as a Rubber Reinforcing Filler – A Review. *J Clean Prod* **2020**, *247*, 119115, doi:10.1016/J.JCLEPRO.2019.119115.

3. Roy, K.; Debnath, S.C.; Potiyaraj, P. A Critical Review on the Utilization of Various Reinforcement Modifiers in Filled Rubber Composites. *Journal of Elastomers & Plastics* **2019**, *52*, 167–193, doi:10.1177/0095244319835869.

4. Neethirajan, J.; Parathodika, A.R.; Hu, G.-H.; Naskar, K. Functional Rubber Composites Based on Silica-Silane Reinforcement for Green Tire Application: The State of the Art. *Functional Composite Materials* **2022**, *3*, 7, doi:10.1186/s42252-022-00035-7.

5. Salina Sarkawi, S.; Kaewsakul, W.; Sahakaro, K.; Dierkes, W.K.; Noordermeer, J.W.M. A Review on Reinforcement of Natural Rubber by Silica Fillers for Use in Low-Rolling Resistance Tyres. *Journal of Rubber Research* **2015**, *18*, 203–233.

6. Utrera-Barrios, S.; Bascuñan, A.; Verdejo, R.; López-Manchado, M.Á.; Aguilar-Bolados, H.; Hernández Santana, M. Sustainable Fillers for Elastomeric Compounds. In *Green-Based Nanocomposite Materials and Applications*; Springer, 2023; pp. 31–61.

7. Araujo-Morera, J.; Verdejo, R.; López-Manchado, M.A.; Hernández Santana, M. Sustainable Mobility: The Route of Tires through the Circular Economy Model. *Waste Management* **2021**, *126*, 309–322, doi:10.1016/J.WASMAN.2021.03.025.

8.    Directive 2012/19/EU of the European Parliament and of the Council of 4 July 2012 on Waste Electrical and Electronic Equipment (WEEE). *Official Journal of the European Union* 2012, *OJ L 197*, 38–71.

9.    Arner, A. Extended Producer Responsibility for Waste Oil, E-Waste and End-of-Life Vehicles. *International Journal of Economics and Financial Research* **2020**, *6*, 223–235.

10.   Mooney, M. A Theory of Large Elastic Deformation. *J Appl Phys* **1940**, *11*, doi:10.1063/1.1712836.

11.   Rivlin, R.S.; Saunders, D. Large Elastic Deformations of Isotropic Materials VII. Experiments on the Deformation of Rubber. *Philosophical Transactions of the Royal Society of London. Series A, Mathematical and Physical Sciences* **1951**, *243*, 251–288, doi:10.1098/rsta.1951.0004.

12.   Flory, P.J.; Rehner, J. Statistical Mechanics of Cross-Linked Polymer Networks II. Swelling. *J Chem Phys* **1943**, *11*, 521–526, doi:10.1063/1.1723792.

13.   Flory, P.J. Statistical Mechanics of Swelling of Network Structures. *J Chem Phys* **1950**, *18*, 108–111, doi:10.1063/1.1747424.

14.   Gaca, M.; Pietrasik, J.; Zaborski, M.; Okrasa, L.; Boiteux, G.; Gain, O. Effect of Zinc Oxide Modified Silica Particles on the Molecular Dynamics of Carboxylated Acrylonitrile-Butadiene Rubber Composites. *Polymers (Basel)* **2017**, *9*, 645, doi:10.3390/POLYM9120645.

15.   Potts, J.R.; Shankar, O.; Murali, S.; Du, L.; Ruoff, R.S. Latex and Two-Roll Mill Processing of Thermally-Exfoliated Graphite Oxide/Natural Rubber Nanocomposites. *Compos Sci Technol* **2013**, *74*, 166–172, doi:10.1016/J.COMPSCITECH.2012.11.008.

16.   Hassan, A.A.; Formela, K.; Wang, S. Enhanced Interfacial and Mechanical Performance of Styrene-Butadiene Rubber/Silica Composites Compatibilized

by Soybean Oil Derived Silanized Plasticization. *Compos Sci Technol* **2020**, *197*, 108271, doi:10.1016/J.COMPSCITECH.2020.108271.

17.     Zhang, S.; Liu, P.; Guo, M.; Yu, Q.; Hu, Y.; Tang, Z.; Guo, B.; Zhou, G. Dual Functions of Inverse Vulcanized Copolymers as Both Vulcanizator and Interfacial Modifier for Improving the Mechanical Properties of Silica Reinforced Rubber Composites. *Compos Sci Technol* **2023**, *239*, 110075, doi:10.1016/J.COMPSCITECH.2023.110075.

18.     Schönhals, A.; Kremer, F. Theory of Dielectric Relaxation. In *Broadband Dielectric Spectroscopy*; Kremer, F., Schönhals, A., Eds.; Springer Berlin Heidelberg: Berlin, Heidelberg, 2003; pp. 1–33 ISBN 978-3-642-56120-7.

19.     Schönhals, A.; Kremer, F. Analysis of Dielectric Spectra. In *Broadband Dielectric Spectroscopy*; Kremer, F., Schönhals, A., Eds.; Springer Berlin Heidelberg: Berlin, Heidelberg, 2003; pp. 59–98 ISBN 978-3-642-56120-7.

20.     Wübbenhorst, M.; Van Turnhout, J. Analysis of Complex Dielectric Spectra. I. One-Dimensional Derivative Techniques and Three-Dimensional Modelling. *J Non Cryst Solids* **2002**, *305*, 40–49, doi:10.1016/S0022-3093(02)01086-4.

21.     Van Turnhout, J.; Wübbenhorst, M. Analysis of Complex Dielectric Spectra. II: Evaluation of the Activation Energy Landscape by Differential Sampling. *J Non Cryst Solids* **2002**, *305*, 50–58, doi:10.1016/S0022-3093(02)01120-1.

22.     Woodward, W.H.H. Broadband Dielectric Spectroscopy - A Practical Guide. In *Broadband Dielectric Spectroscopy: A Modern Analytical Technique*; American Chemical Society, 2021; Vol. 1375, pp. 3–59.

# 3 Rubber Networks

# Chapter 3.    Rubber Networks

*__Chapter 3__ discusses the molecular dynamics of various crosslinked XNBR networks to understand their impact on critical rubber properties. Several compounds were prepared using different crosslinking systems: purely ZnO-based ionic networks, purely S-based covalent networks, and dual networks combining both. Rheometric analysis showed that the ionic network exhibited faster curing times, while the dual networks exhibited higher torques. Chemical resistance tests revealed that this property was not affected by the nature of the crosslinks. Equivalent values were obtained for the purely covalent and purely ionic compounds at equal crosslink densities. In contrast, abrasion resistance is susceptible to the type of crosslinking. Compounds with an ionic phase (individual or combined) exhibited better performance. Overall, the purely ionic networks exhibited an optimal balance of higher curing efficiency and mechanical performance, good chemical and abrasion resistance, and distinct recyclability, making it a suitable sustainable alternative to traditional crosslinked rubbers.*

## 3.1. Motivation

Most of the available studies in XNBR crosslinked networks have explained their behavior using DMA, with a strong focus on the mechanical performance. Powerful BDS, which offers precise and complementary insights for a better understanding of these complex systems across broad frequency and temperature ranges [1–6], has been less explored. However, beyond the in-depth characterization of these networks, the field of Rubber Science and Technology has largely neglected a crucial aspect of the development of crosslinked elastomers: sustainability. The commercial focus for industrial applications is predominantly on maximizing performance using non-dynamic covalent networks, often at the expense of neglecting the balance with environmental impacts. This research gap, in the author's experience, could be

attributed to the limited studies on application-oriented *ionic elastomers*, aligning with CE principles. Therefore, the motivation behind **Chapter 3** is to lay the groundwork for a new perspective in the study of *ionic elastomers*, emphasizing sustainability.

**Chapter 3** discusses the molecular dynamics of various networks to understand their impact on rubber properties. Initially, different purely ionic compounds were prepared, with a focus on optimizing the curing temperature and ZnO content to investigate their baseline properties. This sets the foundation for subsequent assessments. A covalent compound solely vulcanized with S was developed to match the crosslink density of one of the ionic compounds, enabling meaningful comparison between the two types of networks. Subsequently, dual networks combining ionic (ZnO-based) and covalent (S-based) crosslinks have been developed. ZnO served as both an ionic vulcanization agent and an activator for S vulcanization. Special attention was given to two main properties of XNBR: chemical and abrasion resistance. An in-depth study using BDS was conducted to correlate the molecular dynamics of different networks with their performance, thereby complementing the existing knowledge on carboxylated elastomers. The chapter concludes by situating the prepared vulcanizates within the broader context of sustainability. The focus was particularly on the recyclability of the developed compounds, highlighting rubber with the optimal balance of physical properties and recyclability as the starting point for this doctoral thesis.

## 3.2. Results and Discussion

The most important parameter in the vulcanization of rubber is the curing temperature. This value is decisive for the reaction rate. In the ionic networks, crosslinking of the XNBR matrix was carried out according to Equation 3.1:

$$2\ R\text{–}COOH\ +\ ZnO\ \rightarrow [2\ R\text{–}COO^-]\ Zn^{2+}\ +\ H_2O \qquad \text{Equation 3.1}$$
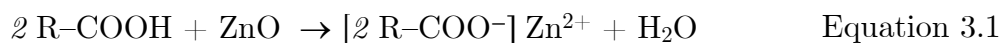
The incorporation of metal ions yields crosslinking bonds between the rubber chains, defined as ionic pairs, and originates from the association of the anionic groups $COO^-$ and $Zn^{2+}$. The selected XNBR had 7 wt. % of carboxyl groups (–COOH); hence, according to Equation 2.7, which considers tetracoordinated ionic crosslinking points, the necessary amount of ZnO to obtain the saturation of these groups in 100 g of XNBR is 6 g. In this context, a base compound of 100 phr XNBR ionically crosslinked with 6 phr ZnO was prepared. This compound was labeled as 6ZnO, and vulcanized at different temperatures (100 °C, 130 °C, 160 °C, and 190 °C) to select the optimum value. Figure 3.1a shows the curing curves obtained and Table 3.1 summarizes the values of the different rheometric parameters.
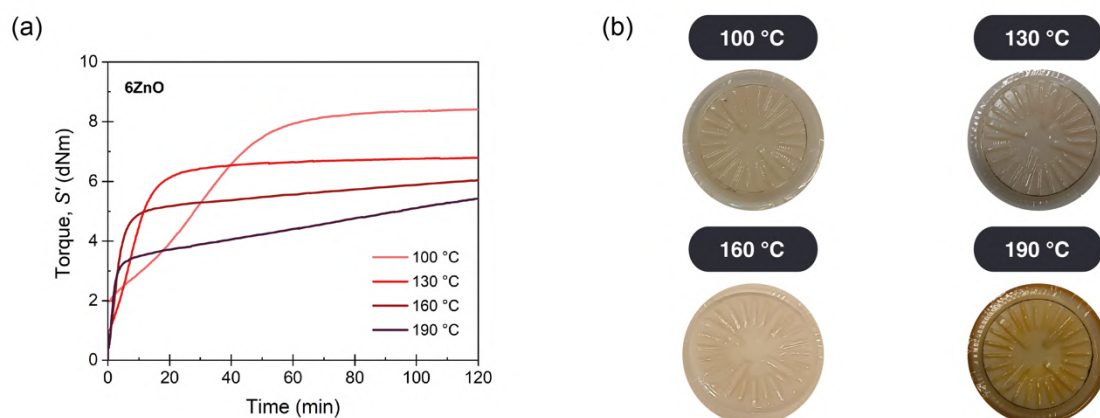


**Figure 3.1.** (a) Curing curves for 6ZnO at different temperatures and (b) 6ZnO impeller obtained at different temperatures.

The motivating factors behind the selection of the optimum temperature were the ΔM and t90 values. As discussed in **Chapter 2**, ΔM, also known as the extent of cure, correlates with the crosslink density, and, consequently, the mechanical performance of the vulcanizate. For the first three temperatures (100 °C, 130 °C,

and 160 °C), the ΔM value hovers around 6 dNm, with minor differences among the samples (less than 0.7 dNm). This similarity suggests that vulcanization at their respective t90 values yields an equivalent mechanical performance for the three systems.

**Table 3.1.** Rheometric properties of 6ZnO at different curing temperatures.

| Property | 100 °C | 130 °C | 160 °C | 190 °C |
|---|---|---|---|---|
| Scorch time, ts1 (min) | 10.6 | 3.8 | 1.6 | 1.2 |
| Curing time, t90 (min) | 53.1 | 17.1 | 8.3 | 3.3 |
| Minimun torque, ML (dNm) | 2.0 | 1.0 | 0.6 | 0.4 |
| Maximun torque, MH (dNm) | 8.5 | 6.9 | 6.4 | 5.4 |
| $\Delta M = MH - ML$ (dNm) | 6.5 | 5.9 | 5.8 | 5.0 |
| Cure rate index, $CRI = 100 / (t90 - ts1)$ (min$^{-1}$) | 2.4 | 7.5 | 14.9 | 47.6 |
| Peak cure rate, PCR (dNm min$^{-1}$) | 0.1 | 0.4 | 0.9 | 1.2 |

The focus then shifted to the t90 value, which indicated the duration of the reaction. Typically, higher temperatures are expected to reduce the reaction time. However, the vulcanization process does not follow a linear relationship. The reaction time started at nearly 1 h for the sample cured at 100 °C and was reduced by more than threefold to 17.1 min at 130 °C. A further increase to 160 °C nearly halves t90 to 8.3 min, a reaction time close to that of more commonly used commercial systems. Although a lower t90 was achieved at 190 °C, the corresponding ΔM value was also lower than that at the other temperatures. This lower degree of cure could be because the high temperature adversely affects the rubber chains and ionic pair stability,

making it less suitable (as evidenced by the coloration of the impeller in Figure 3.1b. Therefore, 160 °C appears to offer a balanced compromise between a sufficient extent of curing and reduced curing time, enhancing the efficiency of the vulcanization.

### 3.2.1. Unraveling the Rubber Networks: Rheometric and Chemical Characterization

The effect of oxide content was subsequently evaluated at a curing temperature of 160 °C. Three compounds were prepared using increasing amounts of ZnO (2.5 phr, 5 phr and 10 phr). For comparison, a pure covalent compound with 1 phr of S (the common vulcanization agent in commercial rubber recipes) was prepared. Table 3.2 summarizes the rubber recipes of the prepared compounds.

**Table 3.2.** Rubber compound recipes (in phr).

| Ingredient | Ionic crosslinks | | | S-based crosslinks | Dual crosslinks | | |
|---|---|---|---|---|---|---|---|
|  | 2.5ZnO | 5ZnO | 10ZnO | 1S | 1S-2.5ZnO | 1S-5ZnO | 1S-10ZnO |
| XNBR | 100 | 100 | 100 | 100 | 100 | 100 | 100 |
| ZnO | 2.5 | 5 | 10 | 0 | 2.5[1] | 5[1] | 10[1] |
| SA[2] | 0 | 0 | 0 | 0 | 1 | 1 | 1 |
| CBS[2] | 0 | 0 | 0 | 0.25 | 0.25 | 0.25 | 0.25 |
| S | 0 | 0 | 0 | 1 | 1 | 1 | 1 |

[1] ZnO acts as an activator (for the S-based network) and vulcanization agent (for the ionic network).

[2] CBS acts as an accelerator and SA as an activator for S vulcanization.

The curing curves (Figure 3.2a) show that each network exhibits a different behavior during vulcanization; the S-based covalent network draws a less pronounced curve, showing a slow vulcanization rate. In contrast, ionic networks exhibit a much faster vulcanization rate. In addition, instead of reaching a *plateau*, the ionic networks curves exhibit a characteristic slightly upward trend (marching modulus) [7,8].
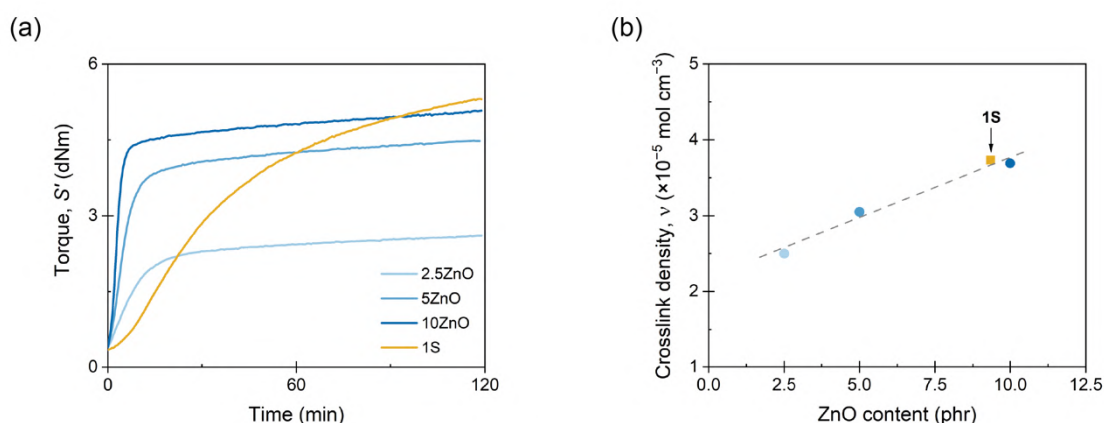


**Figure 3.2.** (a) Curing curves and (b) crosslink densities of prepared compounds.

Table 3.3. summarizes the data obtained from the curing curves. As expected, the MH value increases with the amount of ZnO as a consequence of two main factors: the hydrodynamic effect of a rigid solid in a soft material, and the increase in the ionic crosslink points in the matrix, i.e. higher crosslink density, which causes a greater resistance to shear deformation [9]. Regarding the crosslink density, Figure 3.2b summarizes the obtained values. There is a noticeable trend of increasing crosslink density with the content of ZnO varying from $2.5 \times 10^{-5}$ mol cm$^{-3}$ with 2.5 phr of ZnO to $3.7 \times 10^{-5}$ mol cm$^{-3}$ with 10 phr of ZnO. This increase is attributed to the rise in the number of ionic aggregations, promoted by the higher oxide content in the matrix. Additionally, the results of 1S and 10ZnO stand out because of their similarity; thus, they can be considered equivalent crosslinked networks.

**Table 3.3.** Rheometric properties of ionic and covalent systems.

| Property | 2.5ZnO | 5ZnO | 10ZnO | 1S |
|---|---|---|---|---|
| Scorch time, ts1 (min) | 6.7 | 3.0 | 1.8 | 13.4 |
| Curing time, t90 (min) | 12.7 | 9.9 | 5.7 | 85.0 |
| Minimun torque, ML (dNm) | 0.4 | 0.4 | 0.4 | 0.3 |
| Maximun torque, MH (dNm) | 2.6 | 4.5 | 5.1 | 5.3 |
| $\Delta M = MH - ML$ (dNm) | 2.2 | 4.1 | 4.7 | 5.0 |
| Cure rate index, $CRI = 100 / (t90 - ts1)$ (min$^{-1}$) | 16.7 | 14.4 | 25.6 | 1.4 |
| Peak cure rate, PCR (dNm min$^{-1}$) | 0.1 | 0.4 | 1.1 | 0.02 |
| Crosslink density, $\nu$ ($\times 10^{-5}$ mol cm$^{-3}$) | 2.5 ± 0.1 | 3.1 ±0.2 | 3.7 ± 0.1 | 3.9 ± 0.1 |

The chemical structure of each matrix was verified using FTIR spectroscopy (Figure 3.3). The FTIR spectral analysis provided further insight into the crosslinking process and its impact on the chemical structure of the rubber compounds. Figure 3.3a shows the ATR spectra of a selected sample before and after vulcanization, with pure XNBR as a reference. Every band related to the chemical structure of the rubber backbone is clearly discerned. At high wavenumbers, 2922 cm$^{-1}$ and 2849 cm$^{-1}$, the doublet corresponding to the vibration of the methylene (–CH$_2$) in the polymer backbone was identified, while the medium-intensity band at 2237 cm$^{-1}$ was correlated with the cyano group (–CN) in the acrylonitrile monomer. The bands

at 967 cm$^{-1}$ and 916 cm$^{-1}$ were attributed to the out-of-plane vibrations of the –CH near the double bonds (–CH=CH–) of the *trans* configuration of butadiene and –CH=CH$_2$, respectively.[10] These bands remained constant after vulcanization, indicating the structural integrity of the rubber.

Of particular interest in *ionic elastomers* based on carboxyl groups is the band at 1698 cm$^{-1}$, which corresponds to the carbonyl (C=O) stretching of the acid. This band is directly related to the vulcanization process with metal cations. Depending on the vulcanization system used, any shift in this signal indicates the successful formation of ionic interactions and their nature. In this case, a shift of up to 1588 cm$^{-1}$ is observed after vulcanization. This corresponds to the asymmetric carbonyl stretching of the coordination [11–14]. Additionally, after vulcanization, new peaks appeared at 1417 cm$^{-1}$, associated with the symmetric carbonyl stretching of the coordination [15]. These results confirmed the formation of metal salts during vulcanization.
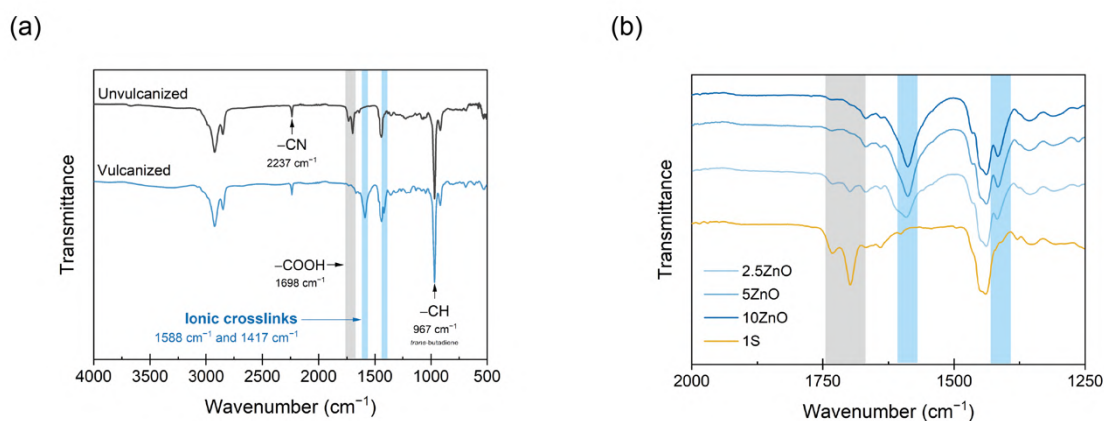


**Figure 3.3.** (a) ATR-IR spectra of the unvulcanized and vulcanized 5ZnO. (b) ATR-IR spectra of the covalent and ionic compounds.

Figure 3.3b shows the infrared spectra of the other compounds in the vulcanized state. In the covalent formulation (1S), the carbonyl signal associated with the

carboxyl groups appeared unchanged at 1700 cm$^{-1}$, indicating that these groups were free in the matrix. For the 2.5ZnO compound, a small signal appeared at 1700 cm$^{-1}$, associated with free carboxyl groups that did not react because the amount of ZnO was below its saturation level. All this evidence confirms a clear difference in the nature of the networks formed with S and ZnO in the XNBR. Having established the basis for the chemical structure and rheometric behavior of compounds vulcanized purely with ionic crosslinks and those vulcanized only with S, the next step in this research focuses on combined networks incorporating both systems. An illustrative scheme of the prepared networks is shown in Figure 3.4.
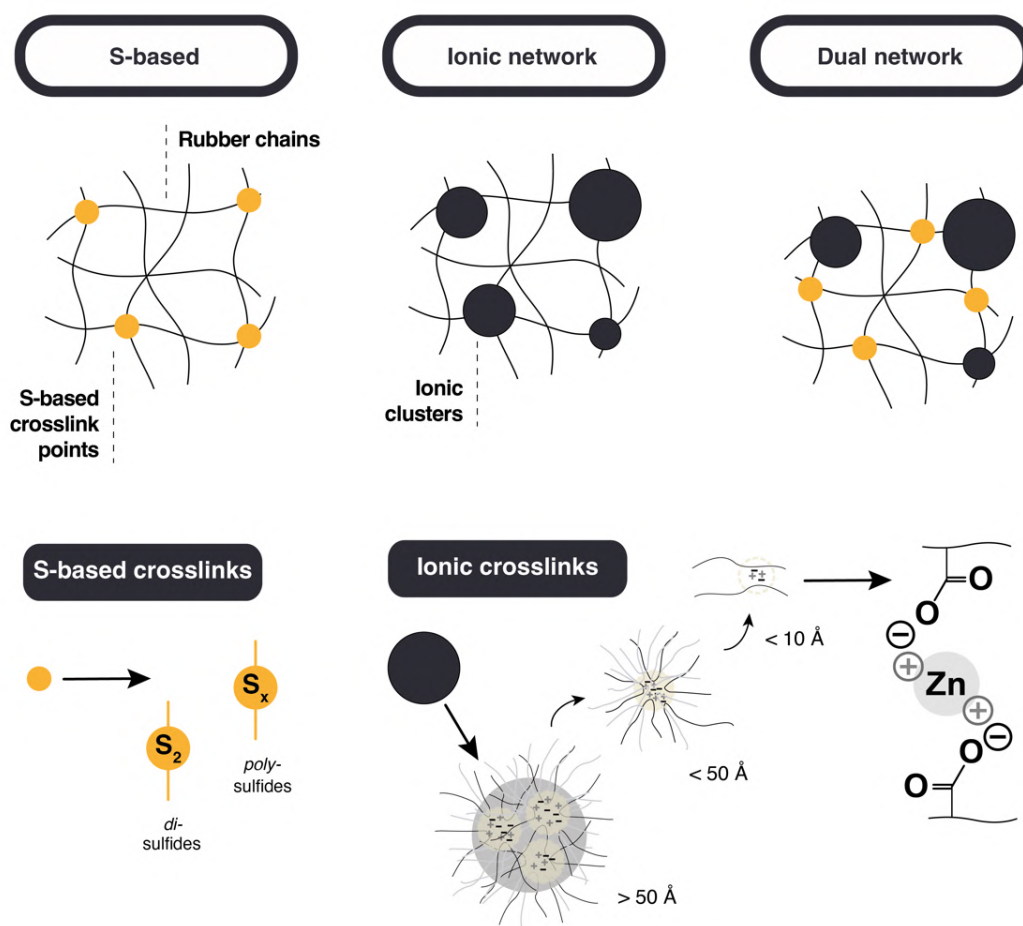


**Figure 3.4.** Scheme of the prepared crosslinked networks.

Figure 3.5 shows the curing curves  The marching modulus for the elastic component (S', Figure 3.5a) and the maximum in the viscous component (S'', Figure 3.5b) curve, are characteristics of dual networks [7,16]. In the curing curve of the dual compound with the highest ZnO content (1S-10ZnO) two slopes were detected in the early stages of vulcanization, confirming the formation of the two distinct networks. This effect is easily observed for $S''$ because of the presence of a peak. After the typical increase in $S''$, because of the initiation of vulcanization, these nets do not reach a *plateau* but start to descend after reaching a maximum value. The descending zone is associated with the covalent network, which increases the elastic component with a corresponding decrease in the viscous component. This behavior was not detected in individual compounds such as 1S and 10ZnO, where $S''$ reached a *plateau,* indicating the end of vulcanization [16,17].
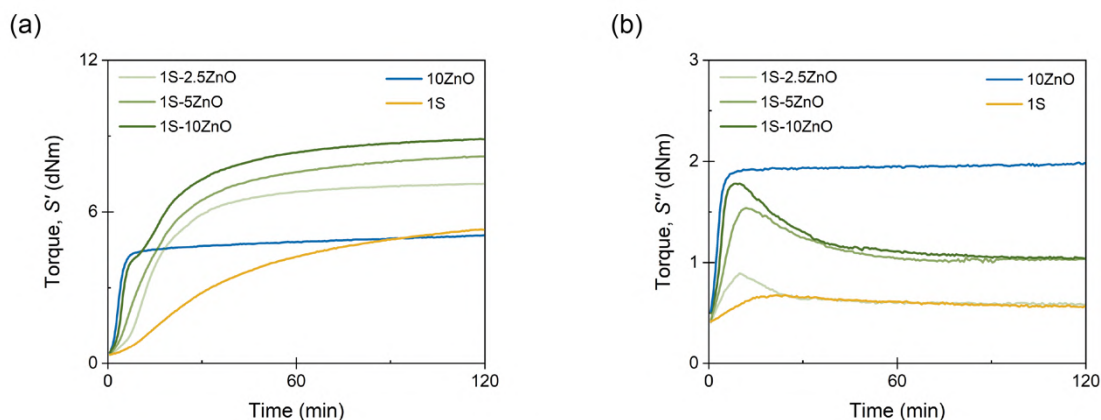


**Figure 3.5.** (a) Elastic component ($S'$) and (b) viscous component ($S''$) of the curing curves of the combined and selected individual networks.

When comparing to individual systems, it is evident that dual networks exhibited higher MH and extent of cure, aligning with increased crosslink density. This value increases from $6.6 \times 10^{-5}$ mol cm$^{-3}$ in 1S-2.5ZnO to $9.0 \times 10^{-5}$ mol cm$^{-3}$ in 1S-10ZnO, about 2.5 times higher than the maximum value in the purely ionic and covalent networks. Dual compounds also exhibited a notable decline in curing

efficiency, with increased t90 and reduced CRI, yet maintain similar PCR values. PCR is linked to the highest slope of the $S'$ curve, reflecting the efficiency of ionic network formation (the one that forms more quickly). Conversely, the higher t90 values and lower CRI are indicative of the overall curing process, where the development of the S-based covalent portion of the network generates a slowing-down effect. Table 3.4 summarizes the rheometric parameters from the curing curves.

**Table 3.4.** Rheometric properties and crosslink density of dual systems at 160 °C.

| Property | 1S-2.5ZnO | 1S-5ZnO | 1S-10ZnO |
|---|---|---|---|
| Scorch time, ts1 (min) | 0.6 | 0.6 | 0.6 |
| Curing time, t90 (min) | 42 | 53 | 45 |
| Minimun torque, ML (dNm) | 0.3 | 0.4 | 0.4 |
| Maximun torque, MH (dNm) | 7.1 | 8.2 | 8.9 |
| $\Delta M = MH - ML$ (dNm) | 6.8 | 7.8 | 8.4 |
| Cure rate index, CRI = 100 / (t90 − ts1) (min$^{-1}$) | 2.4 | 1.9 | 2.2 |
| Peak cure rate, PCR (dNm min$^{-1}$) | 0.4 | 0.3 | 1.0 |
| Crosslink density, $\nu$ (×10$^{-5}$ mol cm$^{-3}$) | 6.6 ± 0.1 | 8.2 ± 0.1 | 9.0 ± 0.2 |

The internal structures of the dual networks were also studied by ATR-IR. Figure 3.6a shows the spectra. Bands associated with ionic bonds appear at 1595 cm$^{-1}$ and 1419 cm$^{-1}$ with increasing amounts of ZnO. In the case of 1S-5ZnO and 1S-10ZnO, there was enough ZnO to promote ionic vulcanization and form clusters. It is important to mention a band located at 1536 cm$^{-1}$, which is present in all

compounds. This band coincides with another in the spectrum of the zinc stearate (ZnSt) powder (Figure 3.6b). ZnSt is a characteristic secondary product of the S-accelerator systems. This confirms that, even at low metal oxide contents, the formation of the sulfur vulcanization activator complex begins and competes with the formation of ionic crosslinks.
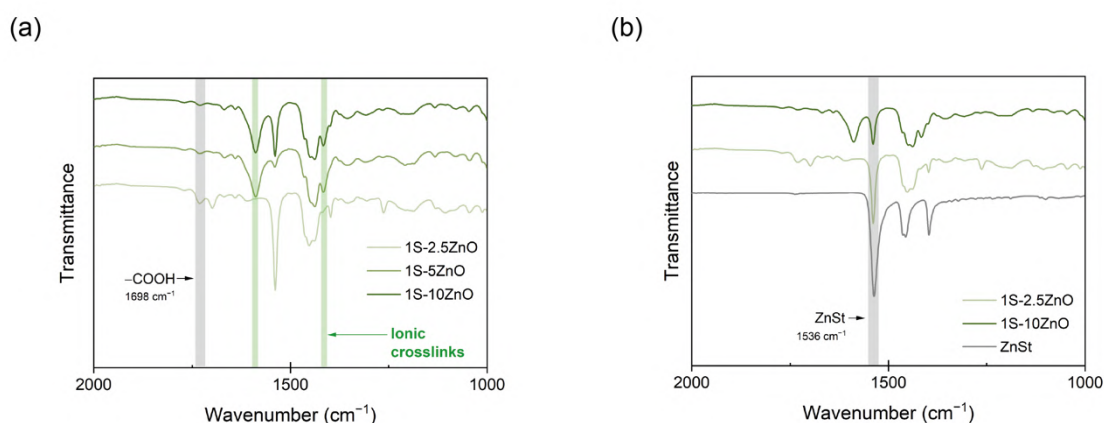


**Figure 3.6.** (a) ATR-IR spectra of dual network compounds. (b) ATR-IR spectra of 1S-2.5ZnO and 1S-10ZnO with ZnSt powder.

### 3.2.2. Assessing the Chemical and Abrasion Resistance of Rubber Networks

Having characterized the internal structure and vulcanization characteristics of XNBR compounds in both individual and dual networks, the focus now shifts to an application-oriented analysis. Emphasis is placed on evaluating two critical properties of XNBR: chemical resistance and abrasion resistance. These properties are of relevance, especially when considering practical applications of the chosen rubber in the automotive industry, particularly for the manufacture of gaskets and hoses [18].

XNBR, with its intrinsic chemical structure enriched by nitrile (–CN) and carboxyl (–COOH) functional groups, shows high resistance to non-polar solvents, which makes it invaluable in the automotive industry for the manufacture of critical

components such as seals and hoses in contact with oils and fuels. To comprehensively evaluate this chemical resistance, specimens of each formulation were immersed in two liquids: (1) motor oil and (2) gasoline, which are critical solvents in the applications of this rubber. The results of this test are shown in Figure 3.7.
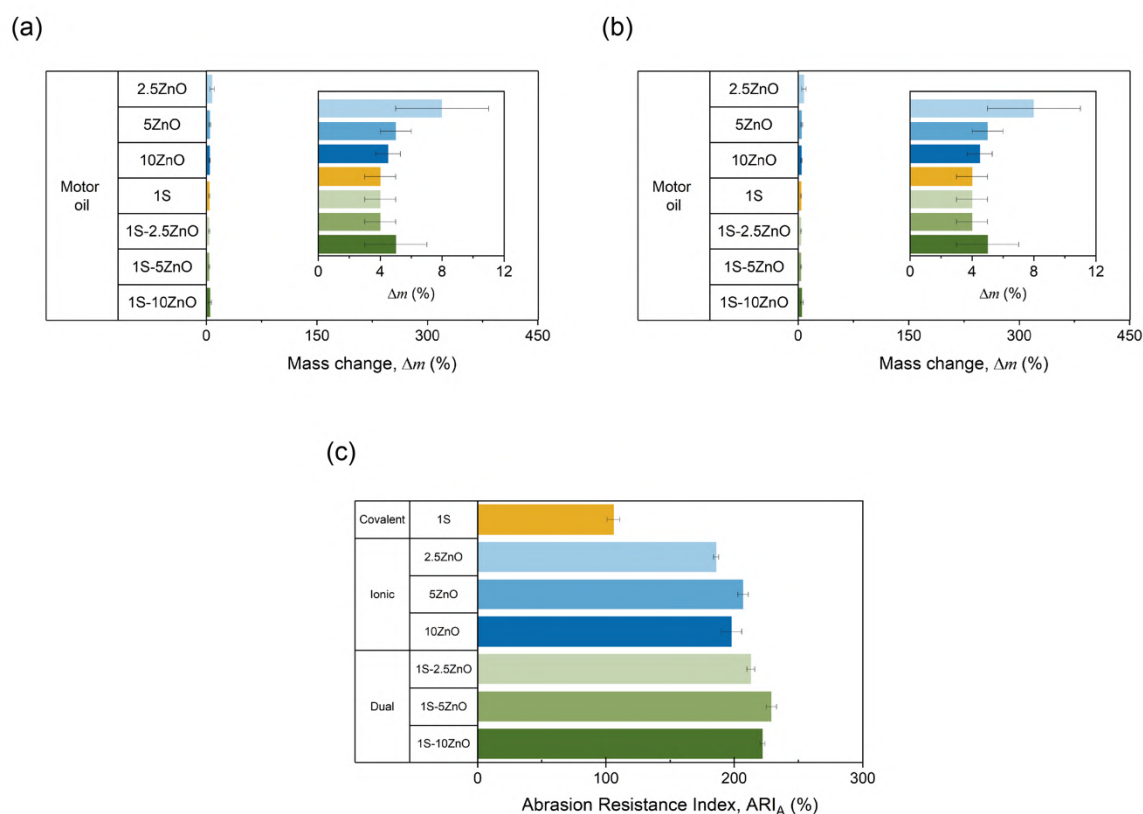


**Figure 3.7.** Chemical resistance in (a) motor oil and (b) gasoline, and (c) abrasion resistance index ($ARI_A$) of covalent, ionic, and dual-network compounds.

Both types of individual crosslinked matrices showed similar chemical resistances, regardless of the solvent. In general, it was observed that all compounds had less mass change in the case of motor oil, followed by gasoline. Thus, their resistance to oil was higher. At equal crosslink densities (1S and 10ZnO), it was observed that the type of ionic or covalent system did not affect the chemical resistance of the material. In contrast, an increase in chemical resistance was observed with increasing ZnO

content. This behavior may be correlated with an increase in the crosslink density, which restricts the diffusion of the solvent into the matrix [19,20]. Therefore, the crosslink density appears to be a more decisive factor in the chemical resistance of the prepared compounds than the nature of the crosslinking system itself.

This can be confirmed by examining the results of dual networks. The combination of crosslinking systems yielded the highest chemical resistance, with reductions of up to 26 % in compound swelling. This can be ascribed to the synergistic effect of the presence of the two types of networks, which significantly increase the crosslink density, further hindering the diffusion of the solvent into the matrix. A similar effect can be observed in other systems with certain similarities, such as Interpenetrated Polymeric Networks (IPN), in which two crosslinked nets are mixed and physically interlaced on a molecular scale [21].

The second property followed was abrasion resistance (AR). AR is the ability of a material to maintain its structure and shape after suffering damage from erosion and/or surface wear. This characteristic is important in the case of materials that require a use in which the shape is essential; therefore, the surface resistance would facilitate shape retention and, thus, its functionality. In XNBR, the functional groups of the matrix promote secondary interactions that form strong bonds, causing high abrasion resistance compared with other rubbers [18]. Even though the chemical resistance appears to be more dependent on the crosslink density than on the type of crosslinked network, it is in the abrasion resistance where their differences are indisputable.

Figure 3.7d shows that the individual ionic compound had a higher abrasion resistance index (198 ± 8 %) than its covalent counterpart (106 ± 7 %). This 86 % increase was correlated with bond strength. In the case of an ionic network, the bonds have greater intensity and are stronger than those in the case of a S-based network [9,22]. In this case, the dual networks yielded slightly higher abrasion resistance values than pure ionic compounds. A maximum is reached for the 1S-5ZnO

compound with an ARI$_A$ of 229 ± 4 %. This represents increments of just 15 %, even when the crosslink density of the dual systems was significantly higher.

This outcome is encouraging because it suggests that for applications demanding robust AR, opting for purely ionic networks may be a viable choice. Specially after careful consideration of other factors related to scalability and sustainability. These include the benefits of using fewer additives in simpler yet efficient recipes, and the thermoformable nature of ionic clusters, which could enhance recyclability or enable self-healing capabilities. These aspects will be explored in the upcoming sections. Before proceeding with tests on recyclability and self-healing capabilities, a fundamental aspect crucial for these applications is examined: mobility. In this context, the focus now shifts to molecular dynamics.

### 3.2.3. Revisiting the Molecular Dynamics of Rubber Networks

This section provides a comprehensive exploration of the molecular motion of 1S, 10ZnO, and 1S-10ZnO using DMA and BDS. This analysis is crucial for revealing the underlying mechanisms governing the physical characteristics of rubber, such as its glass transition temperature and segmental relaxation behavior, and not only contributes to the fundamental understanding of these compounds, but also informs practical applications, such as recyclability and self-healing.

A preliminary assessment of the dynamics of the 1S, 10ZnO and 1S-10ZnO compounds was performed using DMA. Figure 3.8a shows two common relaxation zones in the normalized tan(δ) curve. The α relaxation or segmental relaxation is related to the motions of chain segments and is associated with the Tg (around −1.09 °C for 1S, −0.92 °C for 10ZnO and 4.43 °C for 1S-10ZnO). This relaxation exhibits changes in the shape of the peak, being slightly wider for the ionic (10ZnO) and dual compound (1S-10ZnO), versus the covalent one (1S), as well as being shifted to higher temperatures (see Figure 3.8a inset). This could be associated with a greater restriction of the ionic domains as a consequence of the trapped chains in

the clusters and the performance of these clusters as reinforcing points [23], as well as the higher crosslink density in the dual network.
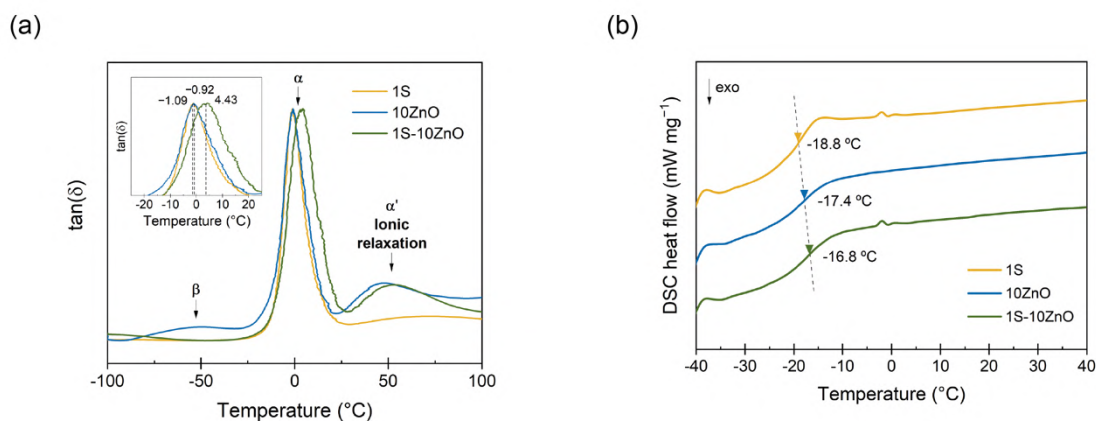


**Figure 3.8.** (a) tan(δ) curve (at 1 Hz) from DMA and (b) DSC spectra of the prepared compounds.

A complementary analysis of the glass transition was performed using DSC (Figure 3.8b). The values obtained for the thermal Tg corroborate the trend of DMA, in which the purely ionic (10ZnO) and dual (1S-10ZnO) networks are presented as more restricted systems than the purely covalent (1S) one. The thermal Tg by DSC was found at −18.8 °C for 1S, −17.4 °C for 10ZnO and −16.8 °C for 1S-10ZnO (all the values reported refer to the mid-points, however, the trend is maintained both at the onset and endpoint).

Besides α relaxation, a second process was detected using DMA (Figure 3.8a). At higher temperatures, the ionic relaxation, α′, around 50 °C, which is not present in the covalent compound (1S), is irrefutable proof of the presence of ionic clusters [2,4,8,11,18] in the purely ionic compound and in the dual one. As introduced in **Chapter 1**, according to the Eisenberg model [24,25], ionic pairs in the matrix are capable of forming associations called multiplets. If the proportion of multiplets is high, the ionic domains create clusters that reduce the mobility of polymeric chains.

This association is caused by electrostatic interactions and is affected by the elastic shrinkage forces of rubber macromolecules. The restricted mobility of elastomer chains in the vicinity of ionic groups results in the formation of a hard phase immersed in a polar matrix. This heterogeneity results in a distinct "ionic domain" with its own "glass/ionic transition". This zone would be more restricted owing to the higher density of crosslinks and the presence of a second network of sulfur bonds (in 1S-10ZnO), which would shift its maximum towards higher values compared to 10ZnO. All these factors could have a noticeable effect on the mechanical properties of the prepared materials. Figure 3.9 shows the stress-strain curves of the three selected compounds.
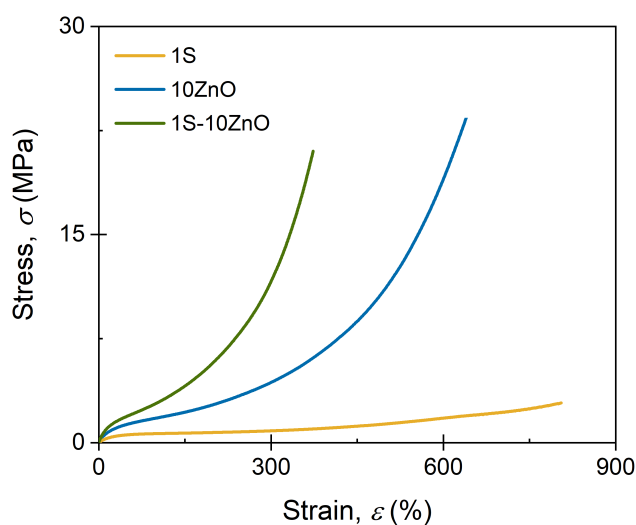


**Figure 3.9.** Stress-strain curves of the selected compounds.

The presence of ionic domains resulted in a noticeable difference in the tensile performance. Thus, compound 1S exhibited high deformability and low maximum strength owing to the higher lability of its bonds. In contrast, it is evident that the ionic domains have a strengthening effect. This behavior can be related to the bond energy. In covalent bonds, such as monosulfide (–S–), disulfide (–S–S–), polysulfide

($-S_x-$), and carbon-carbon ($-C-C-$), among others, the weaker bond tends to give higher TS owing to a mechanism of stress dissipation; however, in ionic bonds, the strength of the electrostatic interactions and the formation of clusters that trap polymer chains (stiffening it) have a greater effect on the performance of the material, generating a considerable increase in mechanical resistance with a detriment to the deformability [8,22].

The differences between 1S-10ZnO and 10ZnO, on the other hand, are interesting. As expected, the higher crosslink density of the dual network (Table 3.4) resulted in lower deformability and higher stiffness (higher M100 and M300), but not higher mechanical strength. These differences could be associated with the compromise between the role of ZnO as a vulcanizing agent (for the ionic network) and S activator (for the covalent network). While in the ionic network all the ZnO goes to create ionic clusters, in the dual network, part of the ZnO is consumed in the creation of the activator complex and the secondary products (ZnSt) in the crosslinking reaction with sulfur. Thus, the density of ionic crosslinks (i.e., the number of clusters) in the dual array is lower than that in the ionic array, resulting in a lower TS. In this way, one can corroborate that not all ZnO in 1S-10ZnO contributes to ionic bonds, as it does in 10ZnO.

A systematic analysis was further performed using BDS to gain a deeper understanding of the dynamics of the three compounds under study. In theory, dielectric and dynamic mechanical analyses should reflect the same motions of the chains and chain segments if the referred motion implies a dipole motion. However, some differences in the intensities and frequencies of the relaxations could be distinguished. In this study, a third weaker relaxation at low temperatures can be detected, β relaxation, which is associated with short-range cooperative motions in the polymeric chain. By DMA it was only detected in 10ZnO (Figure 3.8a), but here it can be corroborated that it is common to all three networks. Figure 3.10 shows the dielectric loss spectra of the β and α relaxations at different temperatures over a wide frequency range. These two relaxations can be confirmed as thermally activated

processes, as evidenced by their shift towards higher frequencies with increasing temperature.
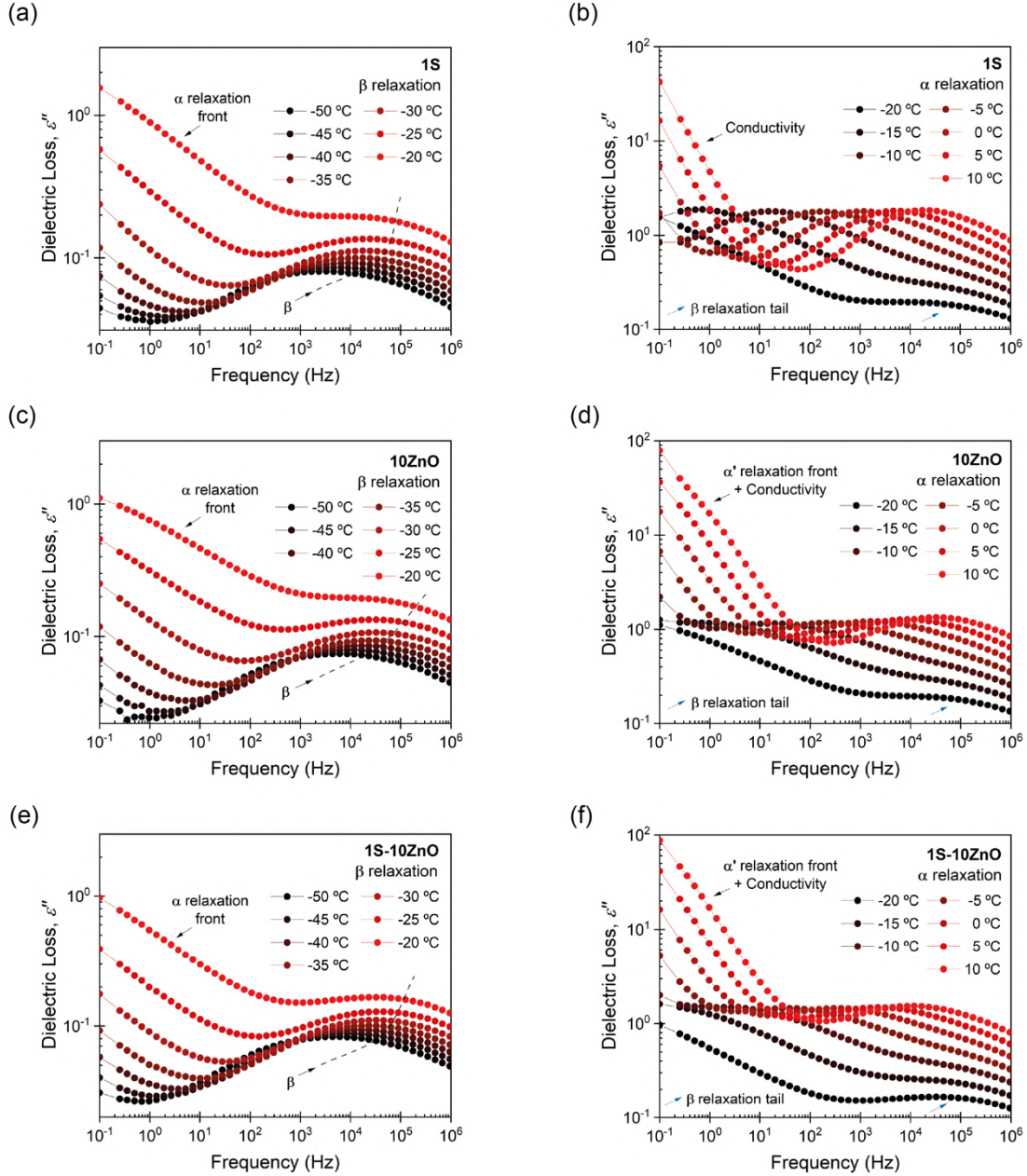


**Figure 3.10.** β and α relaxations in (a,b) 1S, (c,d) 10 ZnO, and (e,f) 1S-10 ZnO.

At high temperatures and low frequencies, both the electrode polarization (EP), which partially blocks the charge exchange between the sample and the electrodes,

and the accelerated movement of ions generate long capacitances that translate into high dielectric constants and into a considerable increase in conductivity. This behavior partially masks the third relaxation (ionic relaxation) in the permittivity spectrum ($\varepsilon''$). To unmask this effect two ways can be followed: (1) the use of the modulus formalism or (2) the calculation of $\varepsilon''$ from the derivative of $\varepsilon'$ ($\varepsilon''_{der}$ lacks the Ohmic conduction term). In this **Chapter 3**, the modulus ($M''$) formalism was chosen [26] (Figure 3.11a and Figure 3.11b).
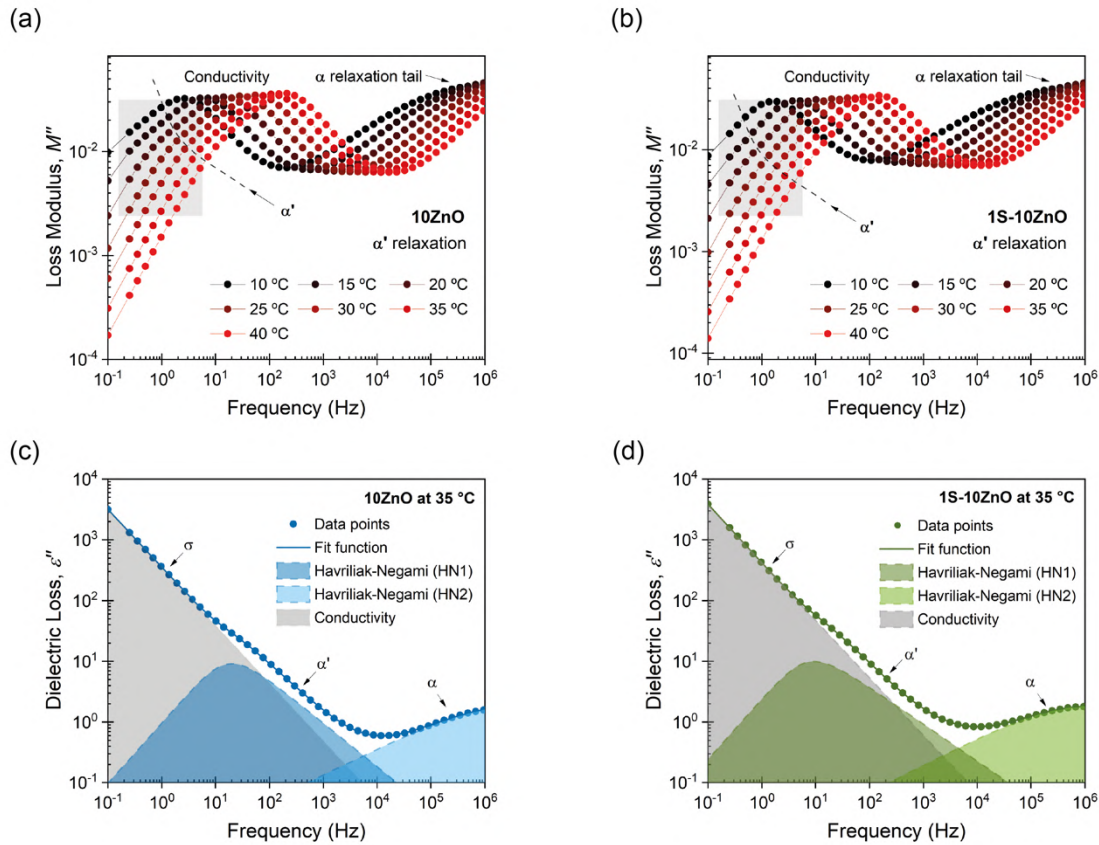


**Figure 3.11.** α' relaxation determined by means of modulus ($M''$) in (a) 10ZnO and (b) 1S-10ZnO and by means of dielectric loss ($\varepsilon''$) in (c) 10ZnO and (d) 1S-10ZnO at 35 °C. The dashed lines in (c) and (d) indicate the fitting of HN and the PL functions.

Both variables ($\varepsilon''$ and $M''$) describe the same electrical relaxation phenomenon; however, under different conditions, a specific form offers more information with

respect to the physical processes that occur. The $M''$ formalism "converts" conductivity into a peak associated with the ac conduction and suppresses the effects of dc conduction and EP. The frequency range below the peak in $M''$ corresponds to the zone dominated by EP and the movement of charge carriers over long distances. With the suppression of the contribution of EP, the second effect can be detected from changes in the size and shape of the peak. This physical process, called long-range ionic hopping, is related to large-scale molecular motions between ionic domains, that is, relaxation of the clusters [27].

The individual ionic compound 10ZnO exhibits an irregular and asymmetric peak with an observable shoulder in the low frequency range (1 Hz to 10 Hz) (Figure 3.11a). This shoulder indicates the presence of a third α' relaxation attributed to the hard ionic domains [2,4,28,29], as observed by DMA. In the dual-network 1S-10ZnO, this shoulder is less notorious (with respect to 10ZnO) because of the dual role of ZnO in the compound, as a vulcanizing agent for ionic network and as activator for S-based network (Figure 3.11b).

Other authors have not been able to detect ionic relaxations through dielectric studies, but a third relaxation (at lower temperatures than those observed by DMA, 50 °C to 70 °C lower) has been associated with the Maxwell-Wagner-Sillars (MWS) relaxation [30]. This relaxation is characteristic of multiphase systems, where each phase has a different dielectric constant and conductivity. If one considers the ionic clusters as polarizable entities, they will appear as heterogeneous with respect to the matrix, exhibiting this physical phenomenon. In our case, the obtained data coincided with those observed by DMA. Hence, either way, both analyzes are conclusive on the presence of a distinct phase (the ionic domains, i.e. the clusters).

For comparative purposes, and with the intention of discerning the effect of the molecular dynamics on the physical properties of the individual and dual crosslinked compounds, we selected a convenient temperature at which each relaxation was well resolved in the frequency domain. Figure 3.12 summarizes all the relaxations at the

designated temperature (−30 °C for β relaxation, 0 °C for α relaxation, and 35 °C for α' relaxation).
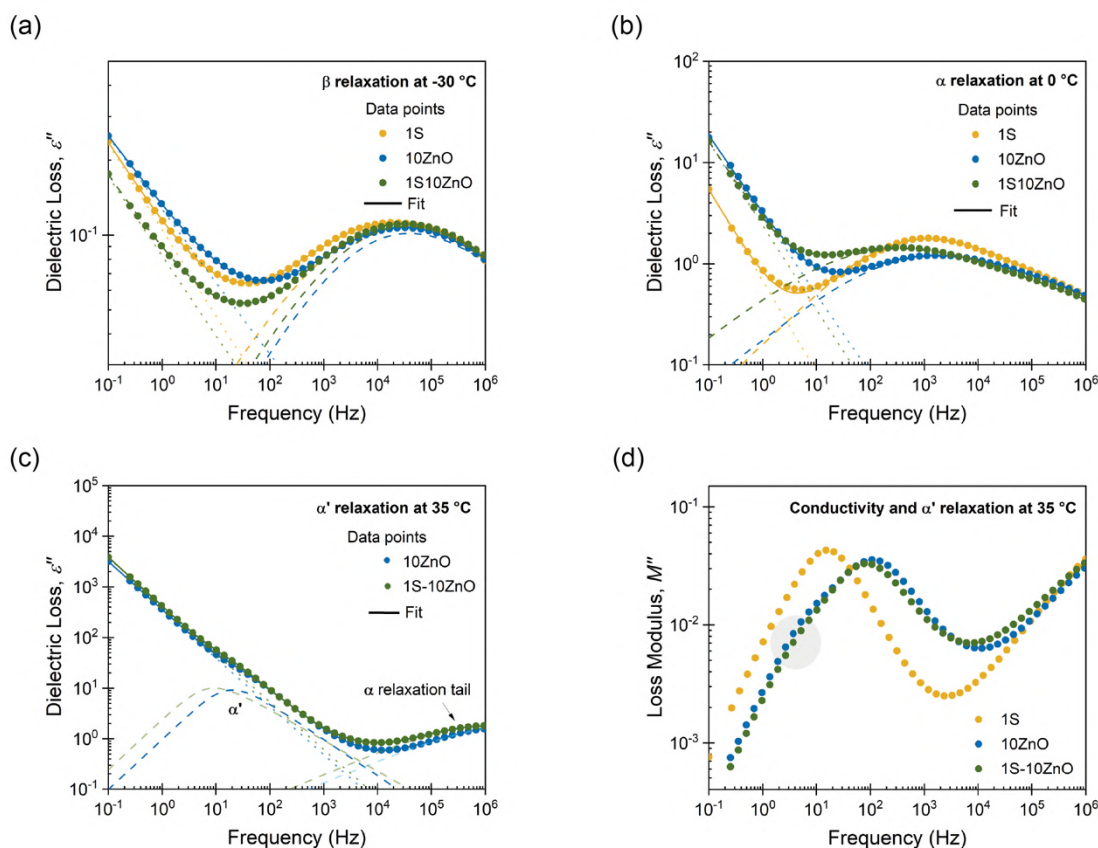


**Figure 3.12.** (a) β, (b) α, and (c) α' relaxation of 1S, 10ZnO, and 1S-10ZnO at selected temperatures and (d) $M''$ of the compounds at selected temperatures. The dashed lines indicate the fitting of HN and the dotted lines indicate the PL functions.

The β relaxation is slightly affected by the type of network (individual or dual) because the covalent (1S) and dual compound (1S-10ZnO) seems more restricted at this low temperature. This relaxation can be fitted using an HN function and a power law for the high-frequency tail (front) of α relaxation. Table 3.5. summarizes the fitting parameters of all relaxations at the chosen temperature. The nature of the crosslinks also influences both α and α' relaxation, as also seen by DMA. A more restricted network was achieved in the dual system (1S-10ZnO), as evidenced by the

shift of the dielectric loss to lower frequencies in the segmental relaxation zone (Figure 3.12.b). The increase in $\tau_{HN}$ and in $\Delta\varepsilon$ (Table 3.5) corroborate this trend. It is expected that the dual system, which shows the highest crosslink density, would present more groups involved in the vulcanization and consequently the dielectric strength as well as the restrictions in the rubber chains mobility would increase.

**Table 3.5.** HN fitting parameters of compounds at selected temperatures.

| Parameters | 1S | 10ZnO | 1S-10ZnO |
|---|---|---|---|
| β relaxation at −30 °C | | | |
| $\sigma_0$ (S/cm) | $8.26 \times 10^{-16}$ | $4.83 \times 10^{-16}$ | $2.32 \times 10^{-15}$ |
| $\Delta\varepsilon$ | 0.87 | 0.79 | 0.84 |
| $\tau_{max}$ (s) | $6.54 \times 10^{-5}$ | $4.04 \times 10^{-6}$ | $4.45 \times 10^{-6}$ |
| $\tau_{HN}$ (s) | $2.50 \times 10^{-5}$ | $1.85 \times 10^{-5}$ | $1.77 \times 10^{-5}$ |
| α | 0.38 | 0.41 | 0.39 |
| β | 0.60 | 0.52 | 0.57 |
| α relaxation at 0 °C | | | |
| $\sigma_0$ (S/cm) | $3.62 \times 10^{-13}$ | $2.30 \times 10^{-12}$ | $1.59 \times 10^{-12}$ |
| $\Delta\varepsilon$ | 10.16 | 8.52 | 10.57 |
| $\tau_{max}$ (s) | $1.35 \times 10^{-4}$ | $8.70 \times 10^{-5}$ | $4.40 \times 10^{-4}$ |
| $\tau_{HN}$ (s) | $4.12 \times 10^{-4}$ | $3.54 \times 10^{-4}$ | $1.95 \times 10^{-3}$ |
| α | 0.53 | 0.44 | 0.42 |
| β | 0.53 | 0.52 | 0.52 |
| $\alpha'$ relaxation at 35 °C | | | |
| $\sigma_0$ (S/cm) | - | $2.62 \times 10^{-10}$ | $3.30 \times 10^{-10}$ |
| $\Delta\varepsilon$ | - | 21.36 | 25.25 |
| $\tau_{max}$ (s) | - | $7.79 \times 10^{-3}$ | $1.7 \times 10^{-2}$ |
| $\tau_{HN}$ (s) | | $1.0 \times 10^{-3}$ | $2.5 \times 10^{-3}$ |
| α | - | 1 | 1 |
| β | - | 0.72 | 0.6 |

This slowing down of segmental dynamics is a consequence of growing cooperativity. It is evident that as the free volume decreases (owing to the crosslinks), more cooperation is required to accomplish segmental motions. Hence, restrictions on the segmental motion of the rubber chains and the lower free volume convert the vulcanizate into a stiffer material, which can be critical for recyclability and self-healing. α relaxation can be fitted using an HN function and a power law for the contributions of conductivity and the high-frequency tail (front) of α' relaxation. Moreover, α' relaxation (Figure 3.12.c) confirms the formation of ionic domains in the dual network. These ionic domains impose greater restrictions on the trapped chains within the ionic clusters. At this point, the differences in the conductivity peaks of the compounds that have an ionic phase compared to those of the purely covalent phase are also interesting (Figure 3.12d). This could also be an irrefutable proof of the presence of multiple ions, which increases the ionic conductivity, reflected in a peak shift towards higher frequencies [27].

### 3.2.4. Assessing Recyclability of the High Performance Compounds

Finally, a visual recyclability test was performed on the 10ZnO and 1S-10ZnO compounds, as the vulcanizates exhibited the best overall performance. The straightforward two-step mechanical recycling protocol described in **Chapter 2** was applied to both compounds. Figure 3.13 shows images of the samples before and after the recycling test. The dual network compound (1S-10ZnO) presents a critical scenario in terms of recyclability. The coexistence of ionic (ZnO-based) and covalent (S-based) crosslinks in this network created a complex and rigid structure that impeded the recycling process. When the ionic transition temperature is exceeded, the polymer chains released from the clusters encounter restricted mobility imposed by the non-dynamic network of S crosslinks. Thus, the total mobility of the system cannot be guaranteed.
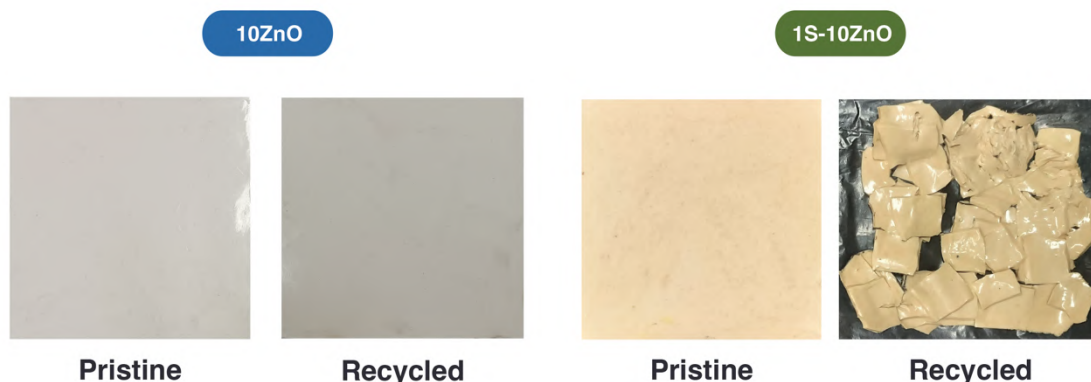
**Figure 3.13.** Recyclability tests for 10ZnO and 1S-10ZnO.

The dual nature of crosslinks, which is beneficial for slightly improving chemical or abrasion resistance, results in a network that is mechanically resistant but not amenable to reprocessing. This limitation highlights a crucial trade-off in the design of vulcanized networks: the integration of non-dynamic covalent bonds for enhanced performance can inadvertently lead to a decrease in environmental sustainability. Consequently, although 1S-10ZnO exhibits commendable performance characteristics, its lack of recyclability is a significant drawback, especially in a world where the demand for sustainable and eco-friendly materials is rapidly increasing.

In contrast, 10ZnO (a purely ionic network) showed promising results in terms of recyclability. The inherent nature of the ionic networks in 10ZnO, characterized by its rapid curing rate and significant mechanical performance, extends to an impressive capacity for recycling. The ionic bonds formed in this network, facilitated by ZnO, contribute to unique structural flexibility above the ionic transition temperature, which allows for effective material recovery and reuse. For all the reasons stated above, 10ZnO was chosen as the comparative basis for subsequent analysis in this doctoral thesis. Starting with recyclability, this characteristic will be analyzed through an in-depth characterization of multiple properties in **Chapter 4**.

## 3.3. Summary

Ionic networks have emerged as a superior choice for the study of XNBR vulcanizates, demonstrating an optimal balance of key properties. These networks exhibit good mechanical performance, which is crucial for applications requiring strength and durability. Additionally, they are characterized by a faster curing process, which enhances the production efficiency. Although slightly outperformed by dual networks in chemical and abrasion resistance, ionic networks still maintain a high level of resistance, making them suitable for scenarios in which a negligible liquid effect is required or where surface wear is a concern. The significant advantage of ionic networks is their higher mobility, which is favorable for reprocessing and recyclability. This aligns well with current sustainability trends and environmental considerations, making ionic networks not only a functionally superior choice but also environmentally responsible. In conclusion, considering the combination of superior curing efficiency and mechanical performance, good abrasion and chemical resistance, distinct recyclability, and potential repairability, ionic networks stand out as the most advantageous option in the realm of XNBR vulcanizates. Figure 3.14 shows a representative schematic that summarizes **Chapter 3**.
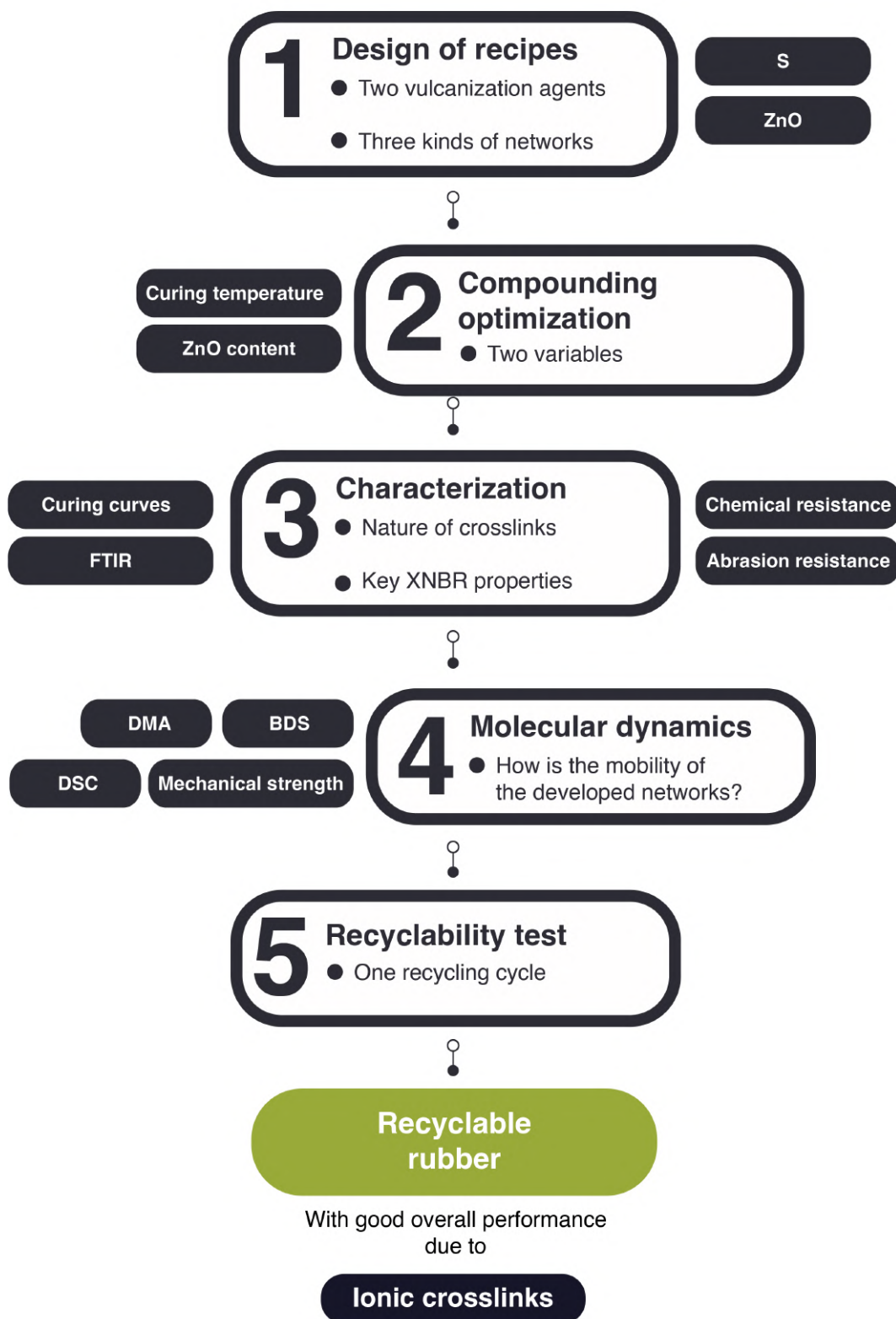
**Figure 3.14.** Schematic representation of **Chapter 3**.

## References

1.  Hernández, M.; Ezquerra, T.A.; Verdejo, R.; López-Manchado, M.A. Role of Vulcanizing Additives on the Segmental Dynamics of Natural Rubber. *Macromolecules* **2012**, *45*, 1070–1075, doi:10.1021/ma202325k.

2.  Basu, D.; Das, A.; Stöckelhuber, K.W.; Jehnichen, D.; Formanek, P.; Sarlin, E.; Vuorinen, J.; Heinrich, G. Evidence for an in Situ Developed Polymer Phase in Ionic Elastomers. *Macromolecules* **2014**, *47*, 3436–3450, doi:10.1021/ma500240v.

3.  Hernández, M.; Valentín, J.L.; López-Manchado, M.A.; Ezquerra, T.A. Influence of the Vulcanization System on the Dynamics and Structure of Natural Rubber: Comparative Study by Means of Broadband Dielectric Spectroscopy and Solid-State NMR Spectroscopy. *Eur Polym J* **2015**, *68*, 90–103, doi:10.1016/j.eurpolymj.2015.04.021.

4.  Gaca, M.; Pietrasik, J.; Zaborski, M.; Okrasa, L.; Boiteux, G.; Gain, O. Effect of Zinc Oxide Modified Silica Particles on the Molecular Dynamics of Carboxylated Acrylonitrile-Butadiene Rubber Composites. *Polymers (Basel)* **2017**, *9*, 645, doi:10.3390/POLYM9120645.

5.  Ortega, L.; Cerveny, S.; Sill, C.; Isitman, N.A.; Rodriguez-Garraza, A.L.; Meyer, M.; Westermann, S.; Schwartz, G.A. The Effect of Vulcanization Additives on the Dielectric Response of Styrene-Butadiene Rubber Compounds. *Polymer (Guildf)* **2019**, *172*, 205–212, doi:10.1016/J.POLYMER.2019.03.073.

6.  Podgórski, M.; Spurgin, N.; Mavila, S.; Bowman, C.N. Mixed Mechanisms of Bond Exchange in Covalent Adaptable Networks: Monitoring the Contribution of Reversible Exchange and Reversible Addition in Thiol–Succinic Anhydride Dynamic Networks. *Polym Chem* **2020**, *11*, 5365–5376, doi:10.1039/D0PY00091D.

154

7. Ibarra, L.; Rodríguez, A.; Mora-Barrantes, I. Crosslinking of Unfilled Carboxylated Nitrile Rubber with Different Systems: Influence on Properties. *J Appl Polym Sci* **2008**, *108*, doi:10.1002/app.27893.

8. Mora-Barrantes, I.; Malmierca, M.A.; Valentin, J.L.; Rodriguez, A.; Ibarra, L. Effect of Covalent Cross-Links on the Network Structure of Thermo-Reversible Ionic Elastomers. *Soft Matter* **2012**, *8*, 5201–5213, doi:10.1039/c2sm06975j.

9. Ibarra, L.; Alzorriz, M. Ionic Elastomers Based on Carboxylated Nitrile Rubber and Magnesium Oxide. *J Appl Polym Sci* **2007**, *103*, 1894–1899, doi:10.1002/APP.25411.

10. Socrates, G. *Infrared and Raman Characteristic Group Frequencies: Tables and Charts*; John Wiley & Sons, 2004; ISBN 0470093072.

11. Laskowska, A.; Zaborski, M.; Boiteux, G.; Gain, O.; Marzec, A.; Maniukiewicz, W. Ionic Elastomers Based on Carboxylated Nitrile Rubber (XNBR) and Magnesium Aluminum Layered Double Hydroxide (Hydrotalcite). *Express Polym Lett* **2014**, *8*, 374–386, doi:10.3144/expresspolymlett.2014.42.

12. Krzemińska, S.M.; Smejda-Krzewicka, A.A.; Leniart, A.; Lipińska, L.; Woluntarski, M. Effects of Curing Agents and Modified Graphene Oxide on the Properties of XNBR Composites. *Polym Test* **2020**, *83*, 106368, doi:10.1016/J.POLYMERTESTING.2020.106368.

13. Brozoski, B.A.; Coleman, M.M.; Painter, P.C. Local Structures in Ionomer Multiplets. A Vibrational Spectroscopic Analysis. *Macromolecules* **1984**, *17*, 230–234, doi:10.1021/MA00132A019.

14. Painter, P.C.; Brozoski, B.A.; Coleman, M.M. FTIR Studies of Calcium and Sodium Ionomers Derived from an Ethylene–Methacrylic Acid Copolymer. *J Polym Sci B Polym Phys* **1982**, *20*, 1069–1080, doi:10.1002/POL.1982.180200614.

15. Song, Z.; Wang, J.; Tao, Q.; Yu, Y.; Zhang, H.; Hu, C.; Cen, H.; Zheng, X.; Hu, T.; Wu, C. Zn-Salt Poly(Styrene–Ran–Cinnamic Acid) Ionomer as a Polystyrene with Improved Impact Toughness, Heat Resistance, and Minimally Compromised Processability. *J Appl Polym Sci* **2022**, *139*, 52041, doi:10.1002/APP.52041.

16. Ibarra, L.; Alzorriz, M. Vulcanization of Carboxylated Nitrile Rubber (XNBR) by a Mixed Zinc Peroxide-Sulphur System. *Polym Int* **2000**, *49*, 115–121, doi:10.1002/(SICI)1097-0126(200001)49:1<115::AID-PI317>3.0.CO;2-X.

17. Ibarra, L.; Alzorriz, M. Ionic Elastomers Based on Carboxylated Nitrile Rubber (XNBR) and Zinc Peroxide: Influence of Carboxylic Group Content on Properties. *J Appl Polym Sci* **2002**, *84*, 605–615, doi:10.1002/APP.10313.

18. Utrera-Barrios, S.; Araujo-Morera, J.; Pulido de Los Reyes, L.; Verdugo Manzanares, R.; Verdejo, R.; López-Manchado, M.Á.; Hernández Santana, M. An Effective and Sustainable Approach for Achieving Self-Healing in Nitrile Rubber. *Eur Polym J* **2020**, *139*, 110032, doi:10.1016/j.eurpolymj.2020.110032.

19. Sombatsompop, N. Investigation of Swelling Behavior of NR Vulcanisates. *Polymer - Plastics Technology and Engineering* **1998**, *37*, doi:10.1080/03602559808006910.

20. Sujith, A.; Unnikrishnan, G.; Radhakrishnan, C.K.; Padmini, M. Interaction of Silica and Carbon Black Fillers with Natural Rubber/Poly(Ethylene-Co-Vinyl Acetate) Matrix by Swelling Studies. *Polym Compos* **2007**, *28*, 705–712, doi:10.1002/pc.20340.

21. Silverstein, M.S. Interpenetrating Polymer Networks: So Happy Together? *Polymer (Guildf)* **2020**, *207*, 122929, doi:10.1016/j.polymer.2020.122929.

22. Chokanandsombat, Y.; Sirisinha, C. MgO and ZnO as Reinforcing Fillers in Cured Polychloroprene Rubber. *J Appl Polym Sci* **2013**, *128*, 2533–2540, doi:10.1002/APP.38579.

23. Schönhals, A. Molecular Dynamics in Polymer Model Systems. *Broadband Dielectric Spectroscopy* **2003**, 225–293, doi:10.1007/978-3-642-56120-7_7.

24. Eisenberg, A. Clustering of Ions in Organic Polymers. A Theoretical Approach. *Macromolecules* **1970**, *3*, 147–154, doi:10.1021/ma60014a006.

25. Eisenberg, A.; Hird, B.; Moore, R.B. A New Multiplet-Cluster Model for the Morphology of Random Ionomers. *Macromolecules* **1990**, *23*, 4098–4107, doi:10.1021/ma00220a012.

26. Wübbenhorst, M.; Van Turnhout, J. Analysis of Complex Dielectric Spectra. I. One-Dimensional Derivative Techniques and Three-Dimensional Modelling. *J Non Cryst Solids* **2002**, *305*, 40–49, doi:10.1016/S0022-3093(02)01086-4.

27. Tian, F.; Ohki, Y. Charge Transport and Electrode Polarization in Epoxy Resin at High Temperatures. *J Phys D Appl Phys* **2014**, *47*, 045311, doi:10.1088/0022-3727/47/4/045311.

28. Fritzsche, J.; Das, A.; Jurk, R.; Stöckelhuber, K.W.; Heinrich, G.; Klüppel, M. Relaxation Dynamics of Carboxylated Nitrile Rubber Filled with Organomodified Nanoclay. *Express Polym Lett* **2008**, *2*, 373–381, doi:10.3144/expresspolymlett.2008.44.

29. Zhang, L.; Wang, H.; Zhu, Y.; Xiong, H.; Wu, Q.; Gu, S.; Liu, X.; Huang, G.; Wu, J. Electron-Donating Effect Enabled Simultaneous Improvement on the Mechanical and Self-Healing Properties of Bromobutyl Rubber Ionomers. *ACS Appl Mater Interfaces* **2020**, *12*, 53239–53246, doi:10.1021/acsami.0c14901.

30. Atorngitjawat, P.; Runt, J. Dynamics of Sulfonated Polystyrene Ionomers Using Broadband Dielectric Spectroscopy. *Macromolecules* **2007**, *40*, 991–996, doi:10.1021/MA061516R.

# 4 Recyclable Rubber

# Chapter 4.    Recyclable Rubber

*In **Chapter 3**, it was shown that ionic crosslinking offers a route to rubber reprocessability due to the dynamism of ion pairs. **Chapter 4** provides a comprehensive overview of the recyclability of XNBR, highlighting the changes in molecular dynamics through multiple recycling cycles beyond tensile tests. The uniquely recyclable XNBR incorporating 10 phr of ZnO as a multifunctional additive was designed using a simple, scalable, two-step recycling process. Evidence of the delicate balance between crosslink density and molecular entanglements that affects the dynamics of the recycled material was found. Recycling also restricts the molecular dynamics near the ionic domains, attributed to a higher crosslink density (from $3.7 \times 10^{-5}$ mol cm$^{-3}$ in the pristine sample to $6.0 \times 10^{-5}$ mol cm$^{-3}$ after the third cycle) caused by a decreased ionic cluster size (the aggregation number drops from 12.2 to 6.9). Remarkably, negligible differences ($<10$ %) in compressive fatigue behavior and enhanced chemical resistance in different solvents (up to a ~350 % increase in motor oil) were also observed, ensuring suitable performance in conditions closer to service. This chapter demonstrates the feasibility of XNBR recycling and provides a broad understanding of this material at the molecular level.*

## 4.1. Motivation

The vast majority of studies in the area of reprocessability/recycling of elastomers have focused on the analysis of mechanical recovery. In the realm of *ionic elastomers*, only a few authors have attempted to go beyond tensile test evaluation to assess the changes in the ionic phase of this type of material with temperature (but without a focus on recyclability) using advanced techniques such as DMA [1], $^1$H low-field Nuclear Magnetic Resonance (NMR) [2], and Small-Angle X-ray Scattering (SAXS) [3]. However, to the author best knowledge, no comprehensive study has analyzed

the changes that occur in the material network through different recycling cycles and using various characterization techniques.

The aim of **Chapter 4** is to answer a critical question: Can the dynamic and reversible nature of ionic elastomers retain the characteristics of their network after each recycling cycle? The answer to this question is crucial for understanding the true potential of these materials in achieving sustainable rubber. For this purpose, two key design fronts were addressed: material composition and the recycling process. **Chapter 3** describes the design of a uniquely recyclable XNBR using only a single metal oxide (ZnO). This multifunctional design accomplishes three critical roles: it serves as a crosslinking agent, reinforcing filler, and processing aid. Complementarily, a straightforward recycling methodology consisting of only two simple steps (cutting and (re)molding) was developed. The simplicity of this process design not only fosters ease of execution, but also ensures scalability, which is a prevailing challenge in the recycling of elastomeric materials. Here, the samples were recycled up to three times, and the materials obtained after each recycling cycle were systematically evaluated at the molecular level using DMA, XRD, and BDS. The changes in the molecular dynamics with recycling cycles were correlated with the morphology and physical (crosslink density), mechanical (tensile and compressive fatigue), and chemical (solvent resistance) properties of rubber.

## 4.2. Results and Discussion

In this chapter, the single recipe based on 100 phr XNBR and an excess of 10 phr of ZnO was prepared and identified as 10ZnO. This compound was chosen based on prior optimization, where the 10ZnO composition exhibited the most favorable combination of properties: high curing rate, excellent mechanical strength, good balance of chemical resistance, and abrasion resistance, but especially the ability to be recyclable. This material was recycled three times following the procedure

described in **Chapter 2**, as illustrated in Figure 4.1. Each sample obtained per cycle was fully characterized.
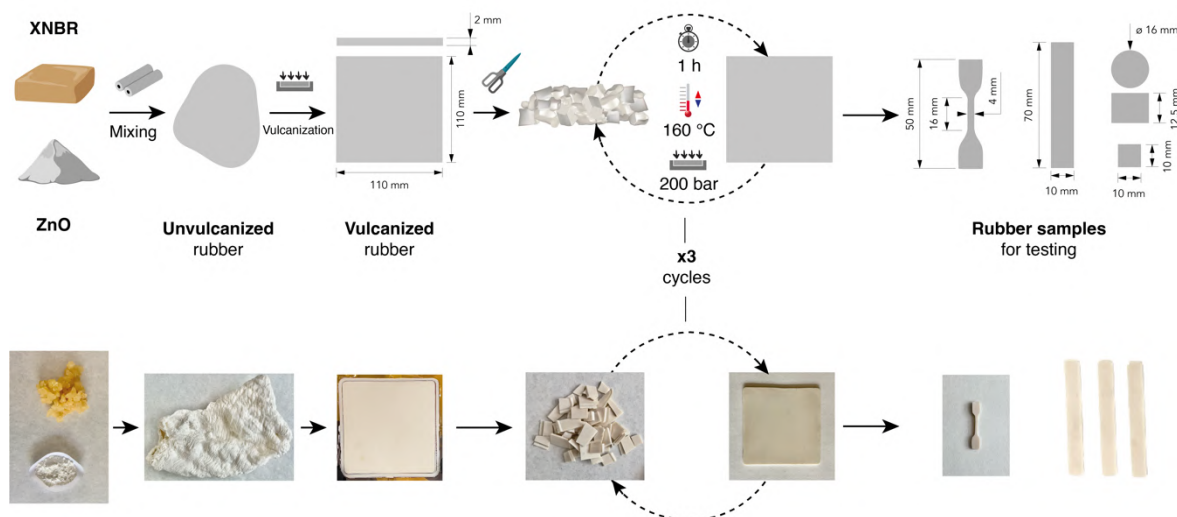


**Figure 4.1.** Schematic representation of the compounding, vulcanization, and recycling processes of the samples prepared in this chapter.

## 4.2.1. Looking at Recyclability Through Molecular Dynamics

The first step was to corroborate the characteristic structure of the *ionic elastomers* after each recycling cycle using DMA. Figure 4.2 shows the temperature-dependent behavior of storage *(E')* and loss modulus *(E'')* for the selected system before and after each recycling cycle (R1, R2, and R3), respectively. The *E'* values exhibited two clear drops, one near 0 °C and a smaller one between 25 °C and 50 °C. Meanwhile, the *E''* curve displays another broader and more diffuse peak at lower temperatures of approximately −35 °C, indicating the presence of a third thermally activated process. These three zones should correspond to the three relaxations that were detected in 10ZnO and discussed in the previous chapter.

(a)
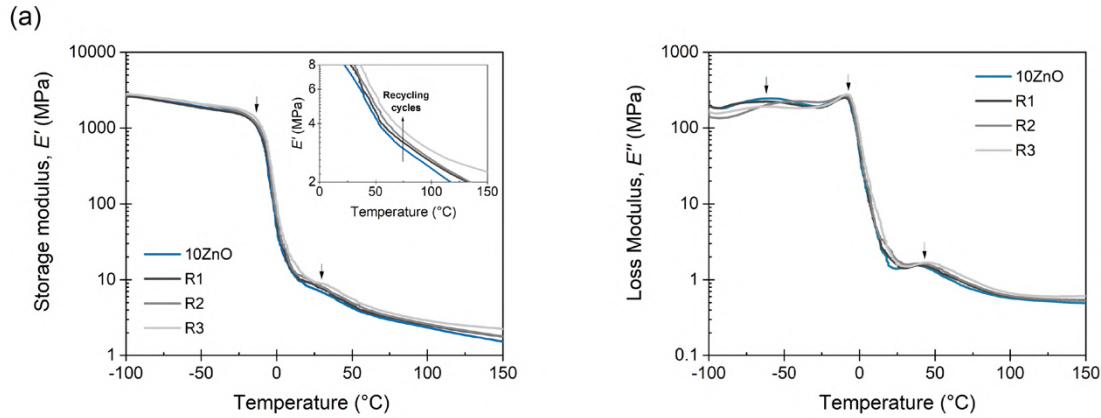


**Figure 4.2.** $E'$ and $E''$ for the selected system before and after each recycling cycle (R1, R2, and R3).

To verify the nature of these zones, the $\tan(\delta)$ values were plotted (Figure 4.3a), confirming the existence of three relaxation processes designated as $\beta$, $\alpha$, and $\alpha'$ in all samples. As stated in the previous chapter, the first relaxation, $\beta$, is believed to be associated with short-range non-cooperative motions, but its full nature is still unclear, despite some attempts to explain its origin in NBR [4]. However, being a sub-Tg relaxation in a crosslinked rubber, it has not aroused enough scientific interest because no elastomeric application performs at temperatures below Tg. The material loses applicability due to its excessive brittleness. The second, $\alpha$, is related to the segmental motion of the material during glass transition. The third, $\alpha'$, is the ionic relaxation, due to the chemical nature of the characteristic ionic domains, present in this type of elastomer [1]. It is important to note that not all types of ionic linkages or coordination complexes contribute to the manifestation of the high-temperature relaxation phenomenon (above Tg). This is only observed when ionic linkages contribute to the formation of clusters, that is, the formation of a hard phase with its own glass/ionic transition [5]. In this sense, it is confirmed that the material can maintain its two-phase structure, formed by amorphous domains of rubber chains and ionic domains, represented by clusters with trapped chains.

(a)



(b)

(c)

(d)
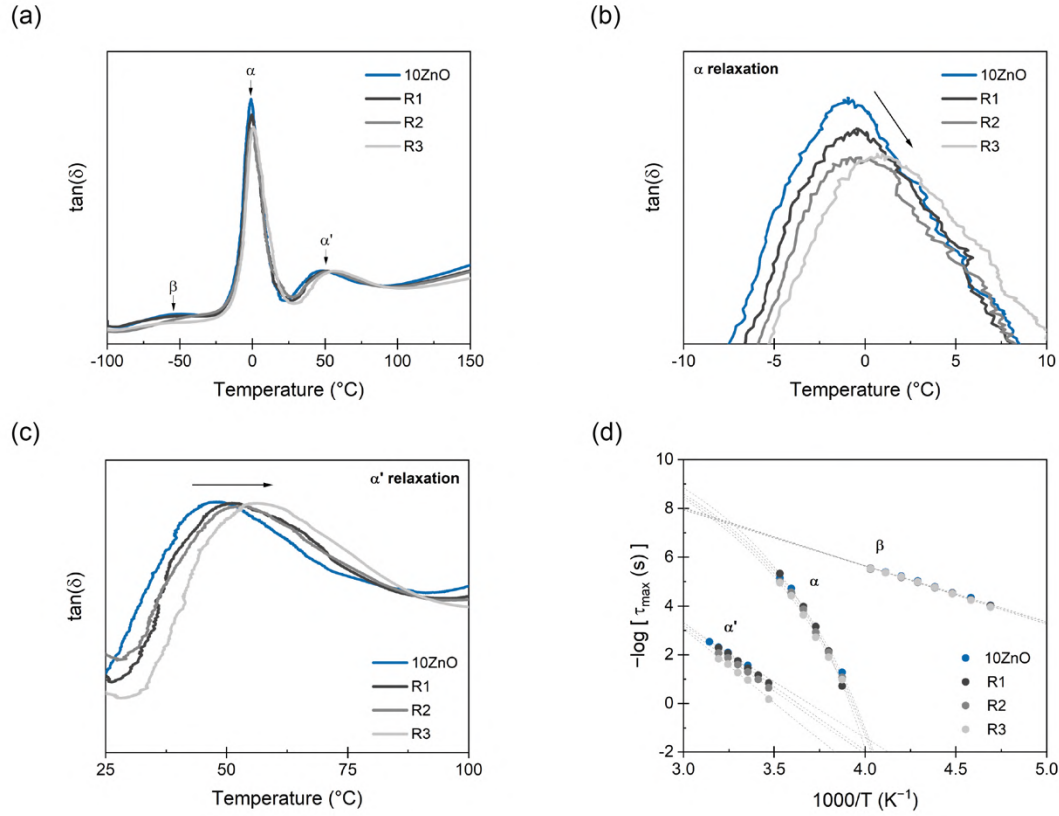
**Figure 4.3.** (a) tan(δ) as a function of temperature, (b) inset of α relaxation, and (c) inset of α' relaxation by DMA. (d) Activation diagram for pristine 10ZnO and each recycled sample. The dashed lines represent the fit by the VFTH and Arrhenius functions.

With the recycling cycles, the α relaxation exhibits a decrease in the intensity of tan(δ) (Figure 4.3b), which is probably related to an increase in the elastic component of the material and a shift towards higher temperatures. This behavior can be attributed to an increase in the crosslink density during recycling. The α' relaxation remained unchanged in intensity but shifted towards higher temperatures (Figure 4.3c). This trend may suggest a more restricted mobility in the vicinity of the ionic domains, possibly due to changes in the morphology of multiplets and clusters with the cycles. To gain further insight, this analysis was complemented with BDS.

The activation diagram of the studied samples (Figure 4.3d) was obtained from the values of $\tau_{max}$ of each relaxation. It can be concluded that recycling cycles do not

seem to have a considerable influence on β relaxation. This may be related to the local character of these motions, which are not directly affected by the overall elastomeric amorphous phase or by the ionic domains of the material. However, changes in the main relaxations (α and α') were more evident. To gain a deeper insight into the behavior of the material, two mathematical functions were used to fit the activation diagrams, providing further elucidation of the underlying mechanisms governing the relaxation motions. For the $\alpha$ relaxation, a Vogel-Fulcher-Tammann-Hesse (VFTH) function was used according to Equation 4.1:

$$\tau_{max} = \tau_0 \exp\left(\frac{B}{T - T_0}\right) \qquad \text{Equation 4.1}$$

where $T_0$ is the Vogel temperature and $B$ and $\tau_0$ are empirical parameters with $B$ related to the fragility strength ($D$), according to Equation 4.2:

$$B = DT_0 \qquad \text{Equation 4.2}$$

The classification of strong or fragile behavior is closely related to the cooperativity of segmental chain movements. Fragile materials are characterized by high cooperativity (typically with rigid backbones) and a marked departure from the Arrhenius behavior. Fragility results in low $D$ and high fragility index ($m$) values, indicating a greater apparent activation energy required for their molecular motions. Conversely, materials with low cooperativity exhibit the opposite trend, where their molecular dynamics are more easily activated, leading to higher $D$ values and lower $m$ values [6], the latter of which can be estimated using Equation 4.3:

$$m = \left.\frac{\partial \log \tau\,(T)}{\partial\left(\frac{T_g}{T}\right)}\right|_{T=T_g} = \frac{DT_0 T_g}{\ln 10\,(T_g - T_0)^2} \approx 16 + \frac{590}{D} \qquad \text{Equation 4.3}$$

The analysis of these two parameters has significant implications for the development and design of polymeric materials with tailored properties because the

cooperativity of segmental chain movements is a crucial factor in determining their mechanical and thermal behavior. For α' relaxation, an Arrhenius function was used, as shown in Equation 4.4:

$$\tau_{max} = \tau_0 \exp\left(\frac{-E_a}{RT}\right)$$

Equation 4.4

where $E_a$ is the activation energy and $R$ is the universal gas constant (8.314 J K$^{-1}$ mol$^{-1}$). Table 4.1 lists all parameters obtained from the fittings.

The results of the polymer relaxation analysis are quite revealing. Although the short-range motions between the dipoles (β relaxation) remained unaffected by the recycling process, the effects on the segmental dynamics (α relaxation) and ionic relaxation (α' relaxation) were significant. All obtained values showed an initial effect during the first recycling cycle (R1). For α relaxation, the higher values of $T_0$ and $m$ (lower $B$ and $D$) reflect an apparent increase in the stiffness of the polymer chains after the first cycle, i.e. a more fragile polymer backbone. The same trend was also observed for α', which reached $E_a$ values of 101 kJ mol$^{-1}$ compared to 85 kJ mol$^{-1}$ for the original sample. However, the subsequent recycling cycles (R2 and R3) reversed this trend in α relaxation. A priori, these results seem to be inconsistent with the shift towards higher temperatures, as seen in the tan(δ) values obtained by DMA. Nevertheless, these results may indicate that factors other than the pure value of the crosslink density can influence the molecular dynamics. For further analysis, the crosslink density values were calculated using the Flory-Rehner and Mooney-Rivlin methods. The latter is particularly useful because it considers two contributions, the first from the chemically crosslinked network product of vulcanization ($\propto 2C_1$); and the second from the intrinsic molecular entanglements between polymer chains ($\propto 2C_2$) [7]. Table 4.2 shows the mean values.

**Table 4.1.** VFTH and Arrhenius fitting parameters for each dielectric relaxation.

| Parameter | 10ZnO | R1 | R2 | R3 |
|---|---|---|---|---|
| **β relaxation** | | | | |
| Activation energy, $E_a$ (kJ mol$^{-1}$) | 45 ± 1 | 44 ± 1 | 45 ± 1 | 46 ± 1 |
| **α relaxation** | | | | |
| $B$ | 1574 ± 29 | 1466 ± 45 | 1657 ± 40 | 1699 ± 54 |
| Vogel temperature, $T_0$ (K) | 204 ± 1 | 210 ± 2 | 203 ± 2 | 202 ± 2 |
| Fragility strength, $D$ | 7.7 ± 0.1 | 7.0 ± 0.3 | 8.2 ± 0.3 | 8.4 ± 0.3 |
| Fragility index, $m$ | 93 ± 4 | 101 ± 4 | 88 ± 3 | 86 ± 2 |
| **α' relaxation** | | | | |
| Activation energy, $E_a$ (kJ mol$^{-1}$) | 85 ± 2 | 101 ± 2 | 100 ± 3 | 116 ± 5 |

**Table 4.2.** Mooney-Rivlin constants and crosslink density values.

| Sample | $2C_1^{(1)}$ | $2C_2^{(2)}$ | $\nu_{Mooney\text{-}Rivlin}{}^{(3)}$ $(\times\ 10^{-4}\ \mathbf{mol\ cm^{-3}})$ | $\nu_{swelling}{}^{(4)}$ $(\times\ 10^{-5}\ \mathbf{mol\ cm^{-3}})$ |
|---|---|---|---|---|
| 10ZnO | 0.31 ± 0.01 | 0.91 ± 0.05 | 1.2 ± 0.1 | 3.7 ± 0.1 |
| R1 | 0.45 ± 0.06 | 1.23 ± 0.12 | 1.8 ± 0.2 | 4.8 ± 0.1 |
| R2 | 0.49 ± 0.05 | 1.15 ± 0.10 | 2.0 ± 0.2 | 5.8 ± 0.1 |
| R3 | 0.55 ± 0.06 | 1.04 ± 0.15 | 2.2 ± 0.2 | 6.0 ± 0.6 |

[1] $C_1$ represents the contribution of the crosslinking units.

[2] $C_2$ is the Mooney-Rivlin elastic constant and is related to the trapped entanglements.

[3] Crosslink density calculated by the Mooney-Rivlin method (see **Chapter 2**, Section 2.3.1).

[4] Crosslink density calculated by the swelling method (see **Chapter 2**, Section 2.3.1).

The Flory-Rehner and Mooney-Rivlin results confirmed the increase in crosslink density with recycling cycles, supporting the DMA observations. The Mooney-Rivlin values provided further insight into the trends observed by the BDS. The increase in $2C_1$ values with recycling cycles validates the increase in crosslink density, whereas $2C_2$ showed a maximum value after the first recycling cycle (R1). This suggests that, during the first stage of recycling, there was a simultaneous increase in the crosslink density and molecular entanglements in the rubber chains, resulting in increased chain rigidity and polymer fragility. However, the subsequent cycles led to a decrease in the number of molecular entanglements. This may be due to increased mobility associated with greater exposure to ion-hopping movements and/or chain scission resulting from continuous cuts made during the recycling protocol, allowing shorter chains (with fewer topological constraints to confine them) to release such entanglements [8]. These results indicate that entanglements and network defects significantly influence the molecular dynamics of recycled materials.

As mentioned above, the invariance in the α' relaxation intensity observed by DMA suggests that the nature of the ion pairs involved in rubber crosslinking is the same. This was evidenced by FTIR-ATR (Figure 4.4a), where no substantial changes in the bands corresponding to the ionic salts (at 1590 cm−1 and 1415 cm−1) were observed with the recycling cycles. Nevertheless, the relaxation shift towards higher temperatures suggests some changes in the morphology and aggregation of this restricted region. The XRD diffractograms (Figure 4.4b) show a shift in the maximum of the ionic domains' region ($q$ values from ~0.1 to 0.7 Å, related to periodic distances between ~63 and 9 Å) [9–11] towards higher $q$ values with the recycling cycles. The observed shift, which indicates a reduction in the spacing between multiplets and clusters, may be attributed to a decrease in the size and number of larger aggregates and a more homogeneous dispersion of the particles throughout the rubber matrix. This results in a loss of electronic contrast, which accounts for the decrease in scattered intensity [9]. To further illustrate this phenomenon, the aggregation number was estimated, which is defined as the number

of carboxylates (or ionic pairs) associated with ionic interactions. Based on the FTIR results, where the band associated with the carboxyl groups completely disappeared (at ~1700 cm$^{-1}$), it can be assumed that all the groups participated in at least one ionic interaction, given that the matrix was completely saturated. The theoretical aggregation number at RT was calculated using the ratio between the concentration of carboxyl groups present in the rubber matrix (~1.53 × 10$^{-3}$ mol cm$^{-3}$) and the ionic crosslink density obtained by Mooney-Rivlin [11]. The results show that the aggregation number decreases almost by half with the number of recycling cycles, from 12.2 for 10ZnO to 6.9 in R3 (Figure 4.4c). This indicates that the number of ion pairs involved in each higher-order structure decreases as a consequence of their redistribution, leading to an increase in the number of smaller aggregates and, hence, the crosslink density.
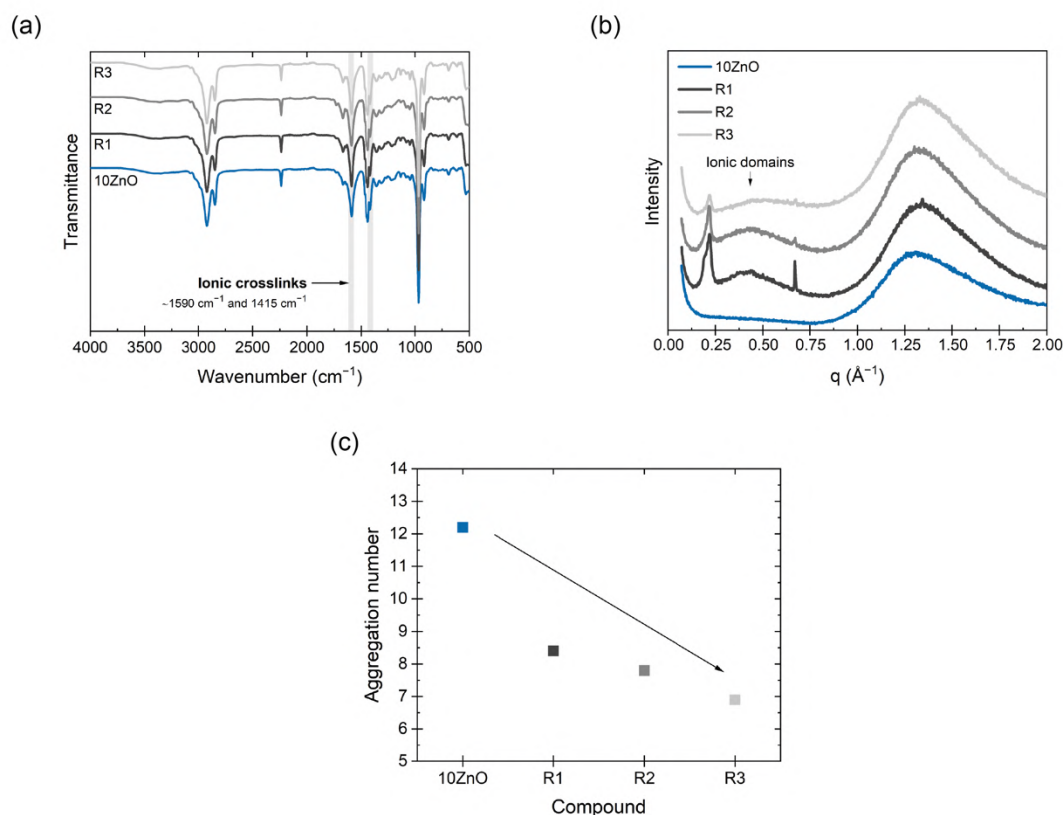


**Figure 4.4.** (a) FTIR-ATR spectra, (b) XRD diffractograms, and (c) aggregation numbers for the pristine 10ZnO and recycled samples.

The SEM micrographs obtained in this study provided compelling evidence highlighting the remarkable effects of recycling on the Zn-based crosslinked XNBR network. Figure 4.5a shows the presence of large white dots corresponding to ZnO particles and aggregates that were uniformly distributed in the XNBR matrix in the original compound (10ZnO) and the first (R1) and third (R3) recycling cycle samples. The significant decrease in the number and size of these white dots in R3 indicates that more residual ZnO was converted to $Zn^{2+}$ salt [12]. It has been suggested that the movement of ions with increasing temperature (ion-hopping) frees some carboxylated groups (R–COO$^-$) and allows the formation of smaller domains distributed throughout the matrix. This is in line with the redistribution of larger clusters and formation of smaller domains, resulting in an increase in the crosslink density and stiffness of the material. These findings provide a pathway for the tunability of recyclable ionically crosslinked XNBR through the control of excess ZnO and/or entanglement (with partial substitution of recycled by virgin material), leading to the development of sustainable materials with improved mechanical properties. Figure 4.5b shows a schematic representation of the proposed model of changes during the recycling cycles.

### 4.3.2. Beyond Tensile Testing: How Does Recycling Affect the XNBR Performance?

Various properties of practical interest (i.e., tensile strength, hysteresis, compressive fatigue behavior, and chemical resistance) and their correlation with changes at the molecular level were studied. Figure 4.6a and Figure 4.6b show the results of the uniaxial tensile tests (M300, TS, and EB). Starting with the M300 values, it can be seen that the material becomes stronger with recycling cycles owing to the increased crosslink density and stiffness.
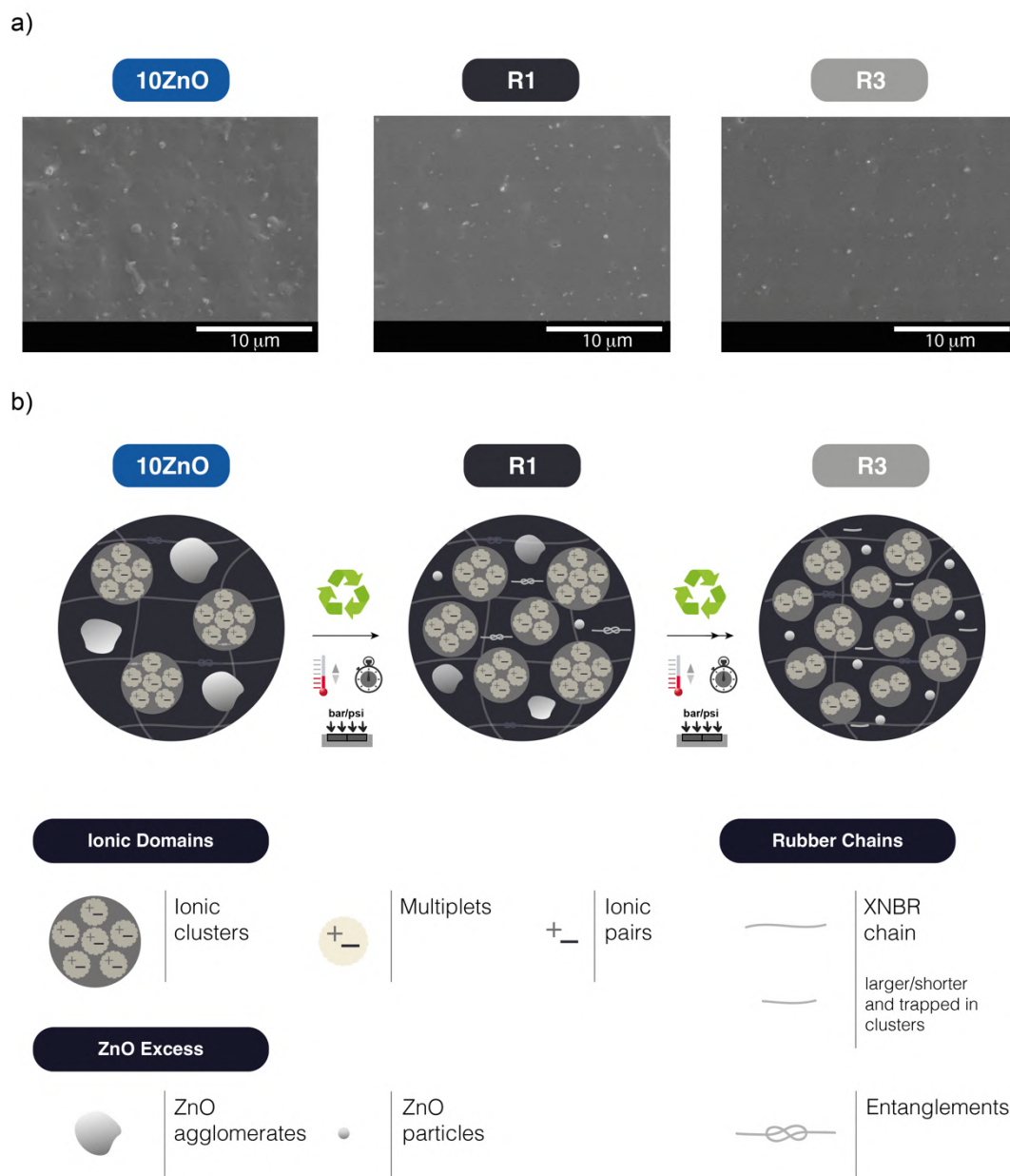
**Figure 4.5.** (a) 10ZnO, R1, and R3 photomicrographs obtained using SEM. (b) Schematic representation of molecular changes during recycling cycles.

Additionally, the compound maintained its initial properties at the breaking point after two cycles (~21 MPa in TS and ~590 % in EB). The subsequent decrease in TS and EB (~14 MPa and ~460 %, respectively) could be a consequence of the reduction in the molecular entanglements that provide mechanical resistance to rubber, as stated previously. However, although there may be a decrease in the TS

after multiple recycling cycles, the properties achieved in R3 are still competitive compared to many other available elastomeric matrices, considering only one additional ingredient in the rubber recipe [13–15]. It is important to note that even after three cycles, the material did not lose its typical hyperelastic behavior, as shown by the stress-strain curves in Figure 4.6c. Hence, the XNBR/ZnO system studied herein can be used in other mechanically demanding products, thus closing the loop of resource consumption.



**Figure 4.6.** (a) M300 and crosslink density, (b) TS and EB, and (c) stress–strain curves of pristine 10ZnO and recycled materials. (d) Cyclic tensile curves at 300 % strain.

From another point of view, the loss of properties at the breaking point can be compensated for by preparing new blends using the recycled material as a partial replacement for the virgin material. Thus, a compromise between the crosslink

density and molecular entanglements can be found, which allows the maintenance of the mechanical behavior at the fracture point during a greater number of recycling cycles.
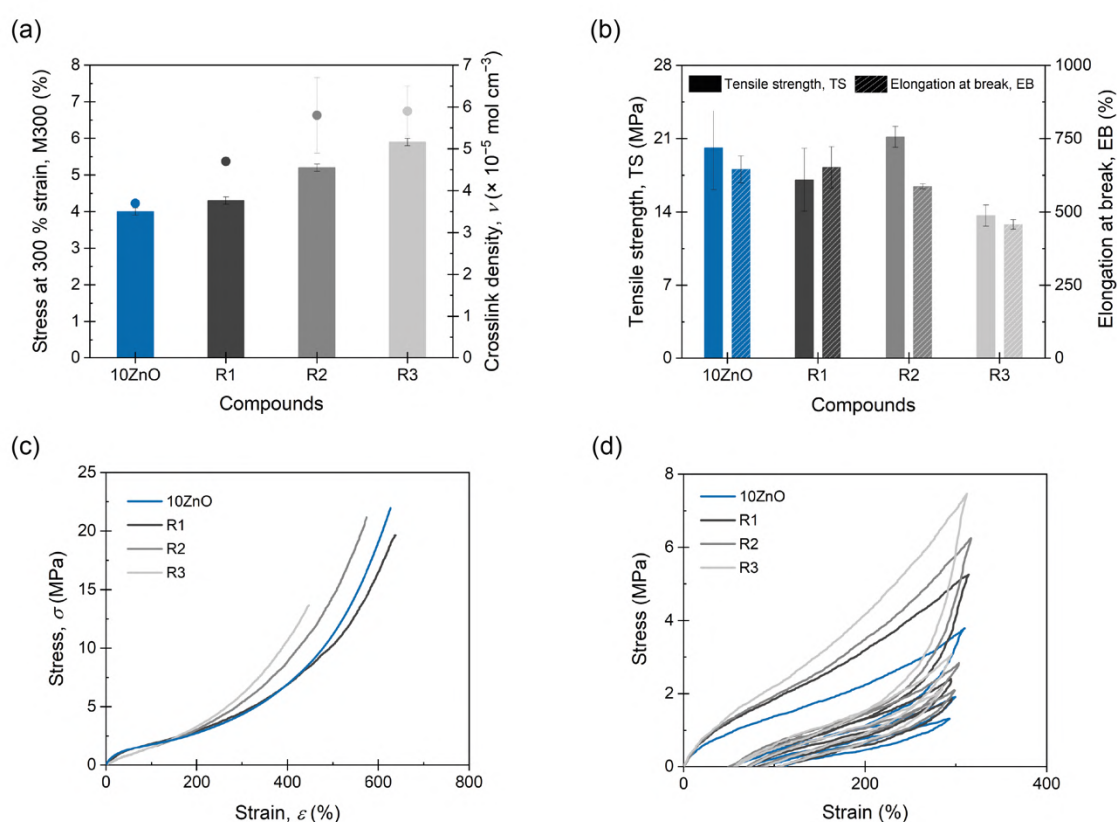
Hysteresis loops were also performed and the results are shown in Figure 4.6d. A well-known phenomenon of stress softening was observed in all the cases. Although this phenomenon in gums is still a subject of debate, it is generally accepted that it is due to the breaking of crosslinking points or chains during deformation, or permanent local orientation after recovery [16,17]. The hysteresis loops increased in area as the recycling cycles progressed, suggesting an increase in the crosslink density of the material. This finding reinforces previous observations that the strength of the material (at low and medium strains) can be improved by recycling.

Compressive fatigue tests showed slightly different mechanical responses for the virgin and recycled materials. Stress decay over compression load cycling was observed (Figure 4.7a), with a higher stress level for the recycled rubber (approximately 10 %). Moreover, the sinusoidal displacement conditions (Figure 4.7b) and measured permanent sets after 5 min (10.40 mm pristine vs 10.55 mm recycled, on average) highlighted the enhanced hysteresis loop after recycling (Figure 4.7c) already at 25 % strain level and higher elastic response, respectively. In line with the observations in the cycled tensile mode, these results suggest a higher crosslink density in the recycled material.

The study of chemical resistance is another crucial aspect for ensuring the viability of recycling XNBR, a highly sought-after elastomer owing to its excellent resistance to petroleum-derived fluids. For this reason, a study of the mass change of XNBR samples after immersion in two non-polar solvents (motor oil and gasoline) was carried out. The results obtained, as shown in Figure 4.7d, reveal an undeniable trend of decreasing mass change as the number of recycling cycles increases, which perfectly correlates with the increase in the crosslink density.
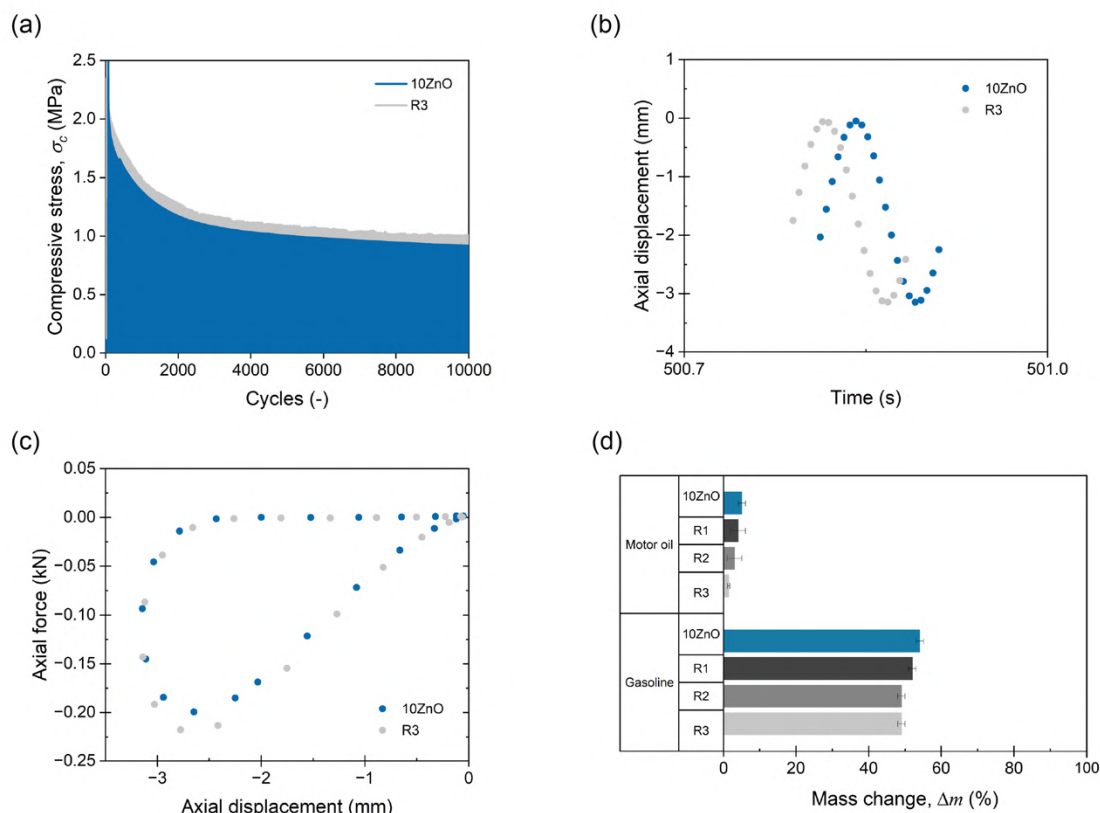
**Figure 4.7.** Compressive fatigue test results (a) stress vs fatigue cycles, (b) axial force vs axial displacement for 5000th loading and unloading cycle and (c) axial displacement vs time for 10ZnO and R3. (d) Mass change in different non-polar solvents.

These observations provide straightforward evidence of the close relationship between the molecular structure, crosslink density, and mechanical behavior of the material, including its tensile and compressive fatigue strengths, as well as other functional properties, such as chemical resistance. These results have significant implications for the future development of XNBR materials with improved mechanical properties, increased sustainability, and enhanced chemical resistance, which are essential for widespread industrial application.

## 4.3. Summary

The results discussed in this chapter mark a significant step towards sustainable polymers by understanding the recyclability of XNBR beyond the conventional uniaxial tensile analysis and provide a breakthrough in the well-known field of *ionic elastomers.* In summary, the results show that XNBR crosslinked with ZnO can be effectively recycled and reused through a simple and easily scalable process involving only two steps: cutting and (re)molding. The feasibility and practicality of this strategy provides a sustainable solution for rubber waste. The benefits of this process include 100 % recycled material to produce new samples (after the first cycle), leaving the door open for further optimization of the recycling methodology through complementary approaches such as the partial substitution of virgin material. Moreover, this study offers valuable insights into molecular-level changes during each recycling cycle, providing a comprehensive understanding of the overall material properties. The results demonstrated that the uniaxial tensile properties of the developed XNBR/ZnO compound were minimally affected after three recycling cycles; however, this effect was more pronounced during the third cycle, probably owing to a decrease in molecular entanglements in the rubber network, according to the Mooney-Rivlin analysis. However, the material stiffness increases owing to a sustained increase in the crosslink density and a decrease in the size of the ionic domains (a higher number of smaller ionic aggregates), causing restricted molecular dynamics in the vicinity of the ionic phase, as demonstrated by DMA, BDS, and XRD. The trade-off between molecular dynamics and entanglements allows the material to maintain its overall behavior, even under compressive fatigue conditions. These findings suggest that recycling of purely ionically crosslinked XNBR is not only possible but also offers significant advantages in terms of sustainability and performance at room temperature. These results provide a promising avenue for future research and development in this area, ultimately contributing to the CE. Figure 4.8 shows a representative schematic summarizing **Chapter 4**.
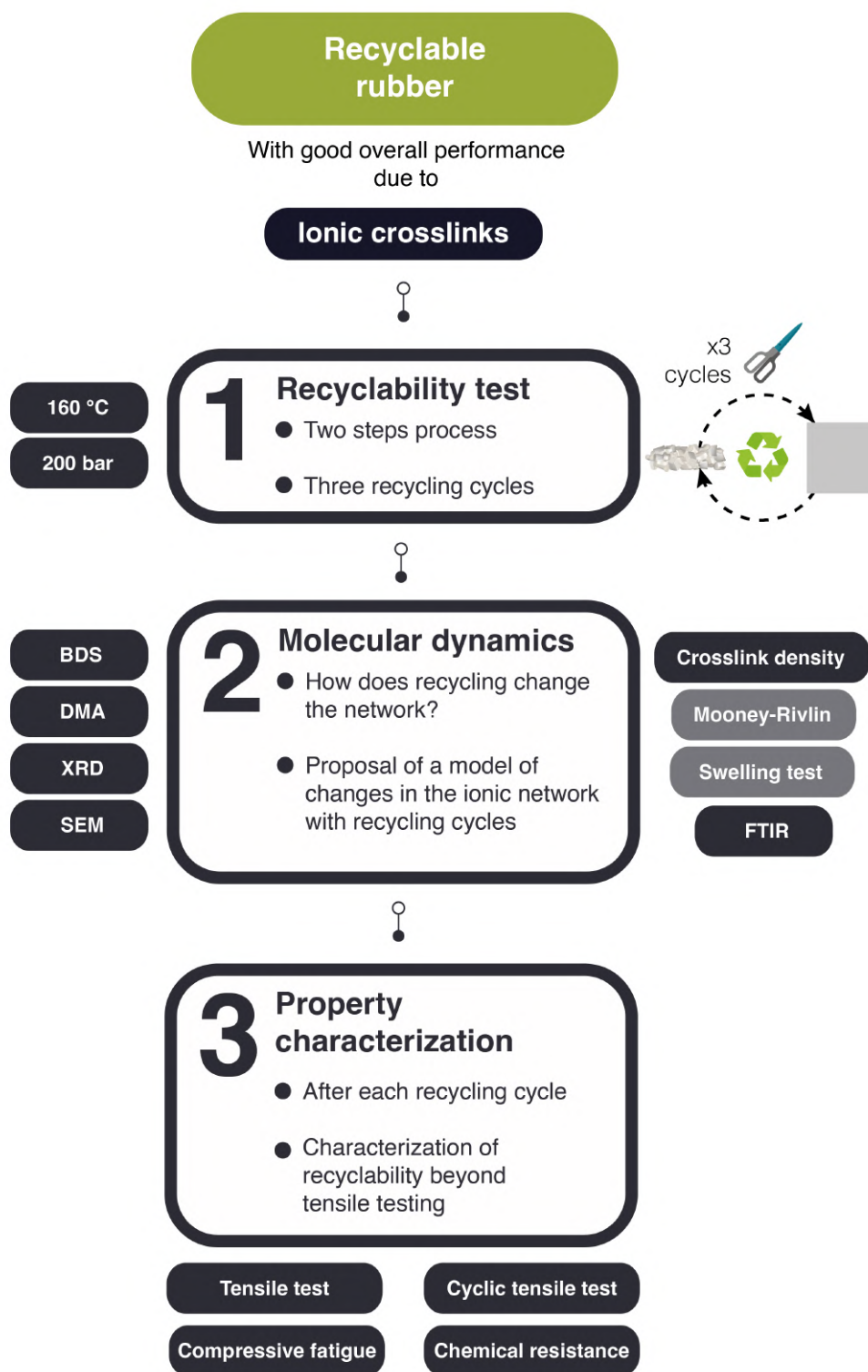
**Figure 4.8.** Schematic representation of **Chapter 4**.

## References

1.  Basu, D.; Das, A.; Stöckelhuber, K.W.; Jehnichen, D.; Formanek, P.; Sarlin, E.; Vuorinen, J.; Heinrich, G. Evidence for an in Situ Developed Polymer Phase in Ionic Elastomers. *Macromolecules* **2014**, *47*, 3436–3450, doi:10.1021/ma500240v.

2.  Malmierca, M.A.; González-Jiménez, A.; Mora-Barrantes, I.; Posadas, P.; Rodríguez, A.; Ibarra, L.; Nogales, A.; Saalwächter, K.; Valentín, J.L. Characterization of Network Structure and Chain Dynamics of Elastomeric Ionomers by Means of 1H Low-Field NMR. *Macromolecules* **2014**, *47*, 5655–5667, doi:10.1021/ma501208g.

3.  Vislavath, P.; Billa, S.; Praveen, S.; Bahadur, J.; Sudarshan, K.; Patro, T.U.; Rath, S.K.; Ratna, D. Heterogeneous Coordination Environment and Unusual Self-Assembly of Ionic Aggregates in a Model Ionomeric Elastomer: Effect of Curative Systems. *Macromolecules* **2022**, *55*, 6739–6749, doi:10.1021/ACS.MACROMOL.2C00784.

4.  Basu, D.; Banerjee, S.S.; Chandra Debnath, S.; Malanin, M.; Amirova, L.; Dubois, P.; Heinrich, G.; Das, A. Unusual Low Temperature Relaxation Behavior of Crosslinked Acrylonitrile-Butadiene Co-Polymer. *Polymer (Guildf)* **2021**, *212*, 123309, doi:10.1016/j.polymer.2020.123309.

5.  Utrera-Barrios, S.; Manzanares, R.V.; Araujo-Morera, J.; González, S.; Verdejo, R.; López-Manchado, M.Á.; Santana, M.H. Understanding the Molecular Dynamics of Dual Crosslinked Networks by Dielectric Spectroscopy. *Polymers (Basel)* **2021**, *13*, 3234, doi:10.3390/polym13193234.

6.  Sanz, A.; Nogales, A.; Ezquerra, T.A. Influence of Fragility on Polymer Cold Crystallization. *Macromolecules* **2010**, *43*, 29–32, doi:10.1021/ma902289k.

7.  Gruendken, M.; Blume, A. Network Formation of Low Molecular Weight 'Liquid' Polymers Studied by Gel Permeation Chromatography and Stress-

Strain Analysis According to Mooney-Rivlin. *Polym Test* **2023**, *118*, 107897, doi:10.1016/J.POLYMERTESTING.2022.107897.

8.  Valentín, J.L.; Posadas, P.; Fernández-Torres, A.; Malmierca, M.A.; González, L.; Chassé, W.; Saalwächter, K. Inhomogeneities and Chain Dynamics in Diene Rubbers Vulcanized with Different Cure Systems. *Macromolecules* **2010**, *43*, doi:10.1021/ma1003437.

9.  Sun, C.X.; Van Der Mee, M.A.J.; Goossens, J.G.P.; Van Duin, M. Thermoreversible Cross-Linking of Maleated Ethylene/Propylene Copolymers Using Hydrogen-Bonding and Ionic Interactions. *Macromolecules* **2006**, *39*, 3441–3449, doi:10.1021/ma052691v.

10. Mordvinkin, A.; Suckow, M.; Böhme, F.; Colby, R.H.; Creton, C.; Saalwächter, K. Hierarchical Sticker and Sticky Chain Dynamics in Self-Healing Butyl Rubber Ionomers. *Macromolecules* **2019**, *52*, 4169–4184, doi:10.1021/acs.macromol.9b00159.

11. Alonso Malmierca, M. Elastómeros Iónicos Con Memoria de Forma: Estructura, Dinámica y Propiedades. Tesis doctoral, Universidad Complutense de Madrid: Madrid, 2013.

12. Xu, C.; Huang, X.; Li, C.; Chen, Y.; Lin, B.; Liang, X. Design of "Zn2+ Salt-Bondings" Cross-Linked Carboxylated Styrene Butadiene Rubber with Reprocessing and Recycling Ability via Rearrangements of Ionic Cross-Linkings. *ACS Sustain Chem Eng* **2016**, *4*, 6981–6990, doi:10.1021/acssuschemeng.6b01897.

13. Imbernon, L.; Norvez, S. From Landfilling to Vitrimer Chemistry in Rubber Life Cycle. *Eur Polym J* **2016**, *82*, 347–376, doi:10.1016/j.eurpolymj.2016.03.016.

14. Wemyss, A.M.; Bowen, C.; Plesse, C.; Vancaeyzeele, C.; Nguyen, G.T.M.; Vidal, F.; Wan, C. Dynamic Crosslinked Rubbers for a Green Future: A

Material Perspective. *Materials Science and Engineering: R: Reports* **2020**, *141*, 100561, doi:10.1016/j.mser.2020.100561.

15.  Utrera-Barrios, S.; Verdejo, R.; López-Manchado, M.; Hernández Santana, M. Self-Healing Elastomers: A Sustainable Solution for Automotive Applications. *Eur Polym J* **2023**, 112023, doi:10.1016/J.EURPOLYMJ.2023.112023.

16.  Diani, J.; Fayolle, B.; Gilormini, P. A Review on the Mullins Effect. *Eur Polym J* **2009**, *45*, 601–612, doi:10.1016/J.EURPOLYMJ.2008.11.017.

17.  Li, Z.; Xu, H.; Xia, X.; Song, Y.; Zheng, Q. Energy Dissipation Accompanying Mullins Effect of Nitrile Butadiene Rubber/Carbon Black Nanocomposites. *Polymer (Guildf)* **2019**, *171*, 106–114, doi:10.1016/J.POLYMER.2019.03.043.

# 5 Self-healing Rubber

# Chapter 5.   Self-healing Rubber

*Chapter 3 and Chapter 4 delved into the advantages of ionic crosslinking for obtaining vulcanized rubbers with a higher cure rate, robust mechanical performance (including tensile and compressive fatigue), and good chemical and abrasion resistance. Notably, the prepared ionic elastomers are recyclable, preserving many of their key properties even after undergoing three recycling cycles. Building on this foundation, Chapter 5 aims to deepen our understanding of the sustainability of ionic elastomers by exploring their self-healing capabilities. Furthermore, this chapter aims to unlock the potential of these materials in cutting-edge applications, specifically in soft robotics. In this field, current materials face challenges related to load capacity, durability, and sustainability. Starting from the previously optimized material (with ZnO), another vulcanizing agent, magnesium oxide (MgO), was explored to expand the availability of mechanically robust, self-healing, and recyclable ionic elastomers based on XNBR. The designed materials exhibited excellent mechanical properties, including a TS exceeding 19 MPa and remarkable deformability, with an EB of over 650 %. Moreover, these materials showed high self-healing capabilities, with 100 % recovery efficiency of TS and EB at 110 °C after 3 h to 5 h, and full recyclability, preserving their mechanical performance even after three recycling cycles. Furthermore, they were also moldable and readily scalable. Tendon-driven soft robotic grippers were successfully developed out of ionic elastomers, illustrating the potential of self-healing and recyclability in the field of soft robotics.*

## 5.1. Motivation

The 4th industrial revolution requires a significant increase in the use of robotic automation with the goal of improving productivity and efficiency. Among robotic automations, soft robots are particularly well-suited for applications that require real

and safe human-robot collaboration and manipulation of fragile or sensitive objects [1]. The integration of soft robotics into different sectors holds the potential to transform processes, ensuring not only increased efficiency, but also enhanced safety and versatility in industrial environments.

## 5.1.1. A Brief Introduction to Soft Robotics

Soft robots are robotic devices made primarily of highly flexible materials, allowing for movement and operation that mimics biological organisms more closely than traditional rigid robots. Unlike conventional robots constructed from hard materials, such as metals and plastics, soft robots are often made from elastomers, gels, or other pliable substances.

Many soft robots are designed by drawing inspiration from biological organisms such as octopuses, starfish, worms, and even humans, leading to innovative solutions in movement and problem-solving. The outstanding compliance of soft robots allows them to flexibly deform and adapt their shapes upon contact with objects, making them ideal candidates for delicate handling tasks, such as electronic components and food items. Soft robots can achieve a wide range of motions such as crawling, bending, twisting, and squeezing, which can be challenging for traditional rigid robots. Figure 5.1 summarizes the key characteristics of soft robots.

However, the load capacity of soft robots remains a significant challenge because of the inherent properties of soft materials, which are characterized by a Young's modulus below 1 GPa [2]. Several approaches have been explored to address this limitation, including the reinforcement of the elastic structure with high-strength fibers [3,4] or using variable stiffness technology, such as particle jamming [5–7], soft actuator coupling [8,9], and stiffness-controlled materials [10]. Unfortunately, these methods tend to complicate soft gripping systems and do not always provide a sustainable solution for soft robotics.
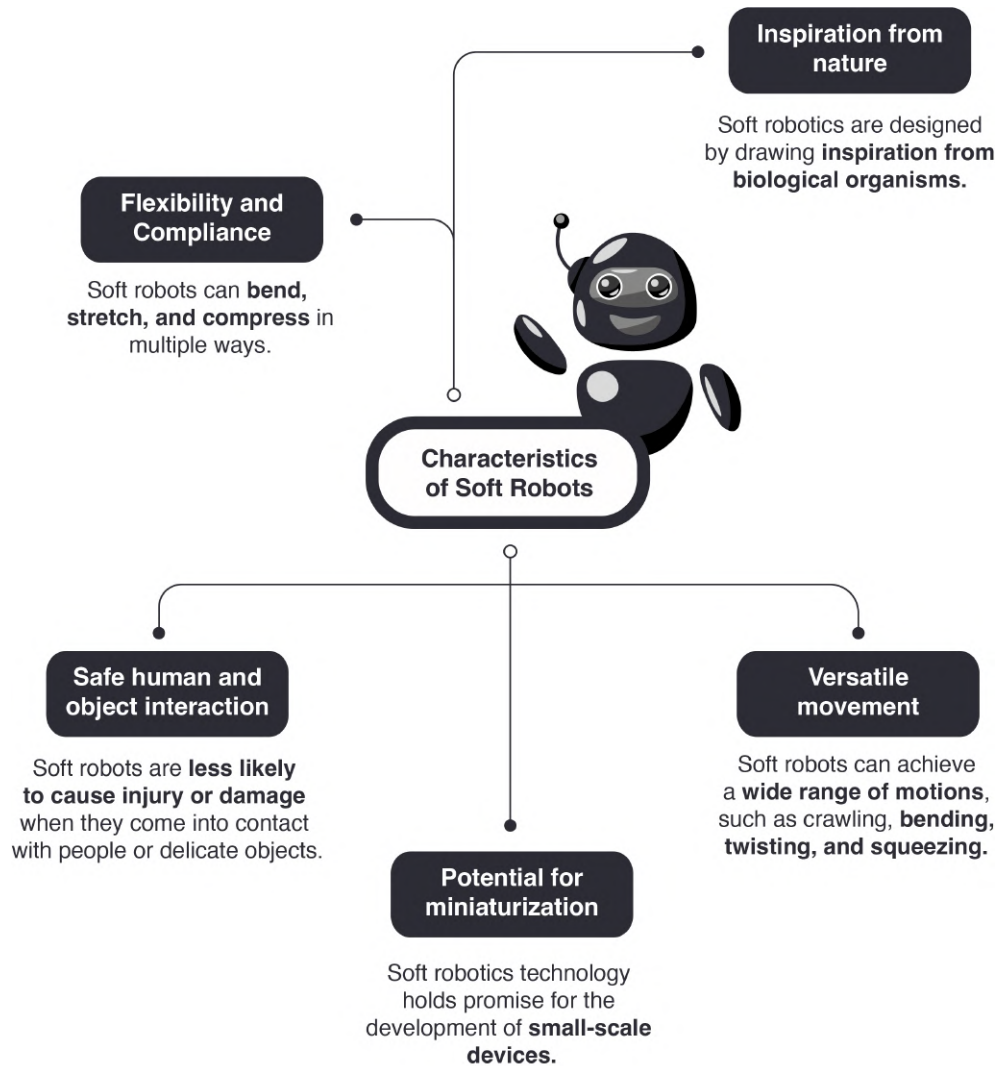
**Figure 5.1.** Key characteristics of soft robots.

The lifetimes of soft robots and their lack of recyclability are additional key concerns that should be addressed before economically and environmentally viable industrial implementation [11,12]. As previously mentioned, soft robotic parts are predominantly fabricated from elastomers such as silicones and PU. These elastomers are vulnerable to sharp objects that cause cuts, tears, and punctures. Furthermore, fatigue can lead to microdamage, which can quickly amplify large-scale issues. Overloading is another frequent challenge due to the inherently low mechanical strength of these materials [12]. In addition, most commercial elastomers

present significant challenges in reprocessing and recycling because of their permanently crosslinked structures [13]. This combination of non-optimal recyclability and limited lifetime hampers their overall sustainability [14]. However, the integration of self-healing and recyclable polymers presents a viable solution, enabling recovery from macroscopic damage, reducing maintenance requirements, minimizing environmental impacts, and extending their operational lifecycle [12]. Figure 5.2 summarizes the main challenges in soft robotics applications.



**Figure 5.2.** Challenges in soft robots applications.

## 5.1.2. Self-healing Polymers in Soft Robots

Several self-healing polymers based on different dynamic chemistries including hydrogen bonding [15–17] or disulfide metathesis [18,19] and extrinsic mechanisms [20], h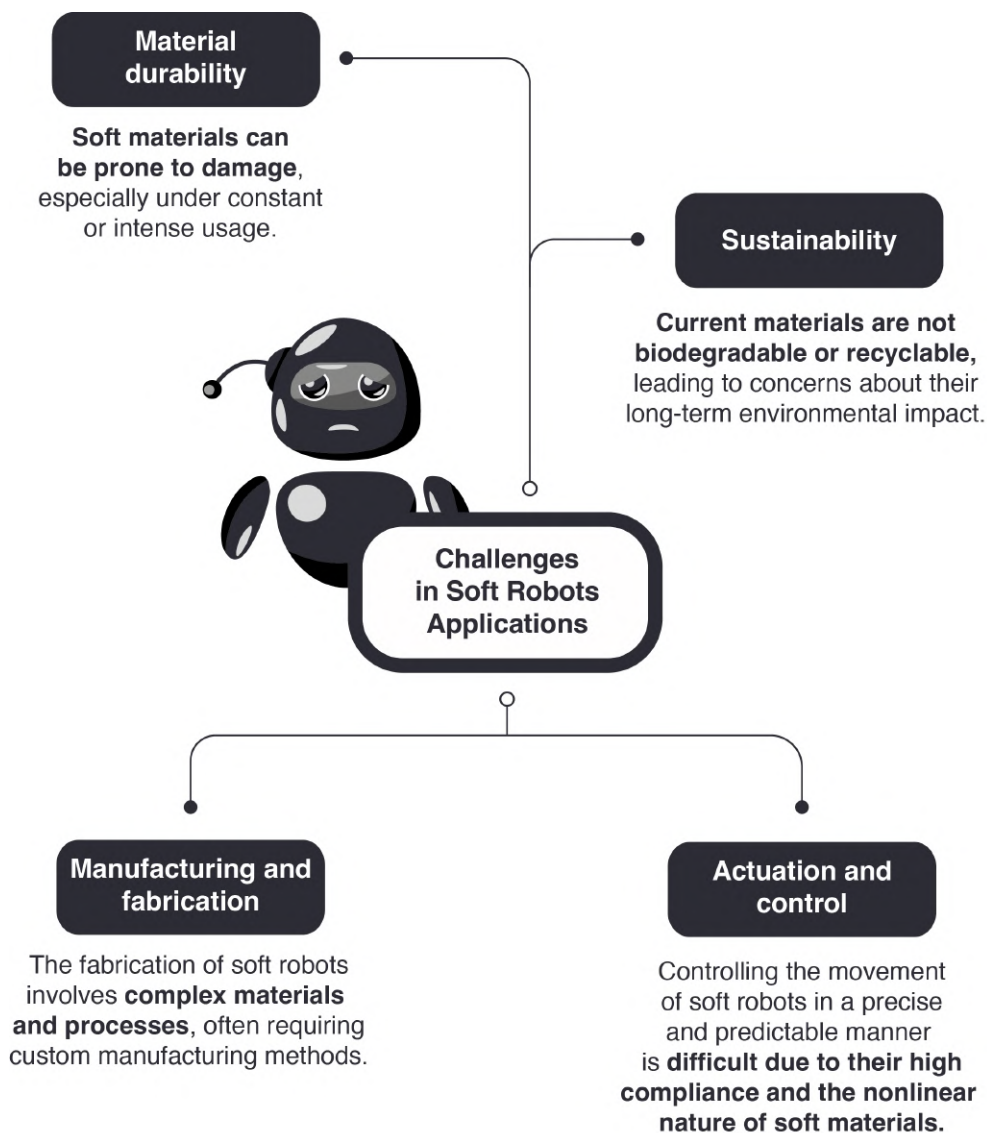ave been used in soft robotics [12]. Despite these advancements, the potential application of well-established general-purpose self-healing rubbers remains unexplored. Additionally, the mechanical performance of the materials available in the current state-of-the-art has its limitation. This includes low moduli, low fracture stress, and non-negligible viscous effects. This stems from the low bond energy of the reversible crosslinks, which leads to the breaking of the bonds at low stresses. Although the resulting self-healing soft robotics can generate large deformations, their payload is limited. For soft robots to be competitive, they must be able to withstand forces comparable to those of traditional rigid robotics. In addition, they must be controlled in terms of the position or force. Time-dependent behaviors that result from viscous effects in materials largely complicate their control or make them impossible to control. Hence, there is a clear need for self-healing elastomers in soft robotics that combine excellent mechanical properties and self-healing capabilities.

In this context, *ionic elastomers* based on general-purpose rubbers present a promising avenue in the field of soft robotics, because they are a unique class of polymeric materials that combine the processability of thermoplastics with the elasticity of rubber. In **Chapter 5**, three *ionic elastomers* based on XNBR were designed using a metal oxide (MO), as a crosslinking agent, semi-reinforcing filler, and processing aid, all at once. All the materials were thoroughly characterized to evaluate their rheometric, thermal, and mechanical properties, as well as their molecular structure and dynamics. After characterization, the material with the best overall performance was used for the fabrication of tendon-driven soft robotic grippers. The simplicity in the selection of a widely available rubber, recipe design, and straightforward manufacturing technique not only promotes ease of execution but also ensures potential scalability.

## 5.2. Results and Discussion

Three XNBR-based compounds were prepared using ZnO and MgO as vulcanizing agents (Table 5.1). The recipes were designed to investigate three key parameters: i) increasing the content of the same MO (1.25MgO and 10MgO), ii) equal crosslink density (1.25MgO and 10ZnO) and iii) equal MO contents (10MgO and 10ZnO).

**Table 5.1.** Rubber recipes based on ZnO and MgO (in phr).

| Ingredient | 1.25MgO | 10MgO | 10ZnO | Role |
|------------|---------|-------|-------|------|
| XNBR | 100 | 100 | 100 | Rubber matrix |
| ZnO | - | - | 10 | Crosslinking agent |
| MgO | 1.25 | 10 | - | |

### 5.2.1. How do Metal Cations Shape the Ionic Elastomer Properties?

As demonstrated in the previous chapters, the XNBR/MO system promotes the formation of ionic crosslinks through the interaction between the carboxyl groups in the main chain of rubber and the divalent metal cations in the chosen MO (in this case, $Mg^{2+}$ and $Zn^{2+}$). The initial step in the characterization involved the analysis of the curing (Figure 5.3a) and stress-strain curves (Figure 5.3b). The elastic component of the torque (S') as a function of time was monitored to track the progress of the vulcanization reaction. Table 5.2 summarizes the curing and mechanical properties of the compounds.
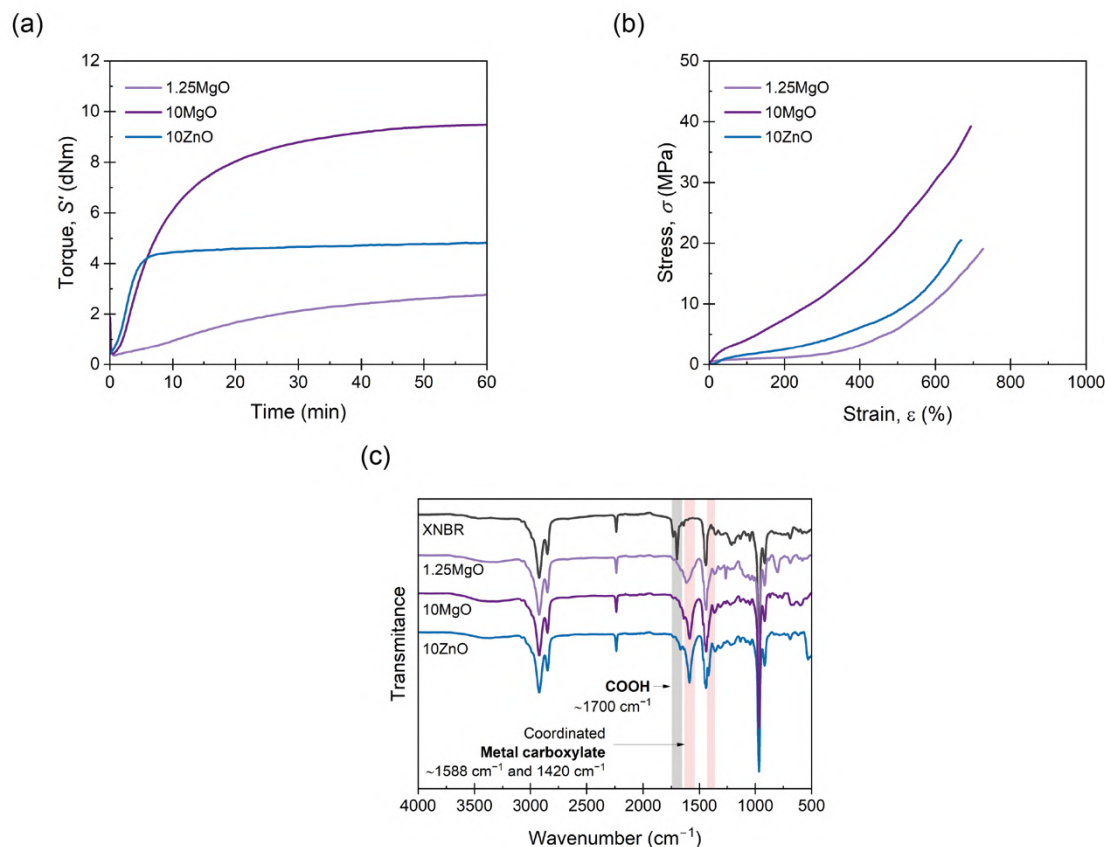
**Figure 5.3.** (a) Curing curves (160 °C) and (b) mechanical properties of the cured *ionic elastomers*. (c) ATR spectra of the prepared samples as well as that of pure XNBR.

The curing curves revealed that increasing the MgO content from 1.25 phr to 10 phr resulted in a slight increase in ML from 0.35 dNm to 0.42 dNm. However, a significant increase was observed in the MH, from 2.76 dNm to 9.48 dNm, as well as in the CRI and the PCR. A higher MgO content provided a higher probability of encountering carboxyl groups for the ion pair, leading to a more efficient curing process and a faster cure rate. This enhanced curing efficiency resulted in increased torque, viscosity, and crosslink density, and improved mechanical performance with higher stress at low (M100) and medium strains (M300), an increase in TS from 19 MPa to 39 MPa, with a minor reduction (~4 %) in EB.

When comparing compounds with equal crosslink densities, it was found that 10ZnO exhibited higher MH, CRI, and PCR than its 1.25MgO counterpart. This was

attributed to the excess ZnO in the recipe. As stated previously, according to stoichiometric calculations, 6 phr of ZnO are required to saturate all carboxyl groups in XNBR. This could result in an excess of ZnO, which acts as a semi-reinforcing filler. The reinforcing character of ZnO has been widely reported in rubber-related literature [21,22]. Long before its recognition as a S vulcanization activator in the early 1920s, ZnO was already used as a non-black filler in rubbers [23]. Its semi-reinforcing characteristics have been described in NR [24], chlorinated NR (Cl-NR) [25], and SBR [26]. This explains why 10ZnO behaves as a stiffer material with higher M100 and M300. However, the TS remained close to approximately 19 MPa for 1.25MgO and 21 MPa for 10ZnO, because of their equal crosslink densities.

With similar MO contents, MgO exhibited superior mechanical properties compared to ZnO, as evidenced by the ultimate state of cure ($\Delta M$), M100, M300, and TS, but a slower cure rate. The improved mechanical performance can be attributed to the nature of the cations. Smaller cations (lower ionic radii, $r$), such as $Mg^{2+}$, can form stronger bonds due to electrostatic attraction (higher forces, $F$) between charged ions (Coulomb's law, $F \propto^{-1} r^2$). The generally accepted smaller ionic radius of $Mg^{2+}$ (0.65 Å) compared to that of $Zn^{2+}$ (0.74 Å) [27–29] results in stronger ionic interactions and better mechanical performance. Another important consideration in this context is the electronic configuration of both cations. The electronic configuration of $Mg^{2+}$ is [He] ($1s^2 2s^2 2p^6$), whereas that of $Zn^{2+}$ is [Ar]$3d^{10}$ ($1s^2 2s^2 2p^6 3s^2 3p^6 3d^{10}$). Although both cations have their outermost orbital filled, in the case of $Zn^{2+}$, the ligands bind to an outer shell of the ions, leading to a reduced electrostatic strength due to the greater distance from the nucleus. Similar effects were described for XNBR modified with 2,6-diaminopyridine (DAP) by Das et al. [30] The effect of several metal salts, such as cobalt(II) nitrate hexahydrate ($Co(NO_3)_2 6H_2O$, $Co^{2+}$), nickel(II) nitrate hexahydrate ($Ni(NO_3)_2 6H_2O$, $Ni^{2+}$), and zinc(II) nitrate hexahydrate ($Zn(NO3)26H2O$, $Zn^{2+}$), was explored. With smaller ionic radii, such as $Ni^{2+}$ (0.69 Å), double TS was achieved compared to $Zn^{2+}$. This outcome was attributable to the electronic configuration and size of the cations.

**Table 5.2.** Curing and mechanical properties of the *ionic elastomers.*

| Property | 1.25MgO | 10MgO | 10ZnO |
|---|---|---|---|
| Scorch time, ts1 (min) | 15.2 | 2.6 | 1.8 |
| Curing time, t90 (min) | 44.9 | 26.4 | 7.3 |
| Minimun torque, ML (dNm) | 0.4 | 0.4 | 0.4 |
| Maximun torque, MH (dNm) | 2.8 | 9.48 | 4.8 |
| $\Delta M = MH - ML$ (dNm) | 2.4 | 9.01 | 4.4 |
| Cure rate index, CRI $= 100$ / (t90 $-$ ts1) (min$^{-1}$) | 3.4 | 4.18 | 18.2 |
| Peak cure rate, PCR (dNm min$^{-1}$) | 0.068 | 0.84 | 1.1 |
| Stress at 100 % strain, M100 (MPa) | $0.5 \pm 0.2$ | $3.9 \pm 0.6$ | $1.7 \pm 0.1$ |
| Stress at 300 % strain, M300 (MPa) | $1.5 \pm 0.3$ | $10.5 \pm 0.5$ | $4.0 \pm 0.1$ |
| Tensile strength, TS (MPa) | $19 \pm 2$ | $39 \pm 1$ | $21 \pm 5$ |
| Elongation at break, EB (%) | $741 \pm 24$ | $705 \pm 12$ | $664 \pm 45$ |
| Crosslink density, $\nu$ ($\times\ 10^{-5}$ mol cm$^{-3}$) | $3.57 \pm 0.02$ | $7.8 \pm 0.2$ | $3.7 \pm 0.1$ |

In contrast, the faster curing of the compounds with ZnO could be attributed to the higher affinity of the carboxyl groups to form interactions with divalent cations. Similar results were reported by Dudev and Lim [31], who computed the formation free energies of $Zn^{2+}$ and $Mg^{2+}$ using different gas-phase ligands. They found that the formation free energies of compounds with $Zn^{2+}$ were always lower (by $24-77$ kcal mol$^{-1}$) than those of compounds with $Mg^{2+}$. This implies that ligands (in which carboxylate groups are included) prefer $Zn^{2+}$ to $Mg^{2+}$. However, they also claimed that Zn complexes are more stable than Mg compounds, but this seems to differ from our initial observations based on the better mechanical performance of MgO compounds.

The FTIR spectra analysis provided further insight into the crosslinking process and its impact on the chemical structure of the rubber compounds. Figure 5.3c shows the ATR spectra of the prepared samples as well as that of XNBR (without additives) as a reference. Every band related to the chemical structure of the rubber backbone was clearly discerned and were already explained in detail in **Chapter 3**. These bands remained constant after vulcanization, indicating the structural integrity of the rubber.

Of particular interest in ionic elastomers based on carboxyl groups is the band at 1698 cm$^{-1}$, which corresponds to the carbonyl (C=O) stretching of carboxylic acid. This band is directly related to the vulcanization process with metal oxides. Depending on the vulcanization system used, any shift in this signal indicates the successful formation of ionic interactions and their nature. In this case, a shift of up to 1586 cm$^{-1}$ was observed in 10MgO, i.e., in the presence of the $Mg^{2+}$ cation (magnesium carboxylate salt), and up to 1588 cm$^{-1}$ in 10ZnO, i.e., in the presence of the $Zn^{2+}$ cation (zinc carboxylate salt). This change corresponds to the asymmetric carbonyl stretching of the coordination [32–35]. Interestingly, in the case of 1.25MgO, a new broad band centered at 1616 cm$^{-1}$ was observed, with a shoulder peak at 1580 cm$^{-1}$. This suggested the coordination with the metal cation, even though the MgO content was below stoichiometric saturation (~3.25 phr, 1:2 ratio).

This indicates the possibility of higher-order coordination, such as hexacoordinated coordination (1:3 ratio), which would explain the saturation effect even at a lower MgO content [34]. Additionally, after vulcanization, new peaks appeared at 1420 cm$^{-1}$ for the compounds with MgO and at 1417 cm$^{-1}$ for those with ZnO, associated with the symmetric carbonyl stretching of the coordination [36]. These results confirmed the formation of the metal salts during vulcanization with both vulcanization agents.

To gain further insight into the structural differences and their impact on the performance of the *ionic elastomers*, BDS was performed. Figure 5.4 show the 3D plots of the conduction-free dielectric loss with respect to temperature and frequency.
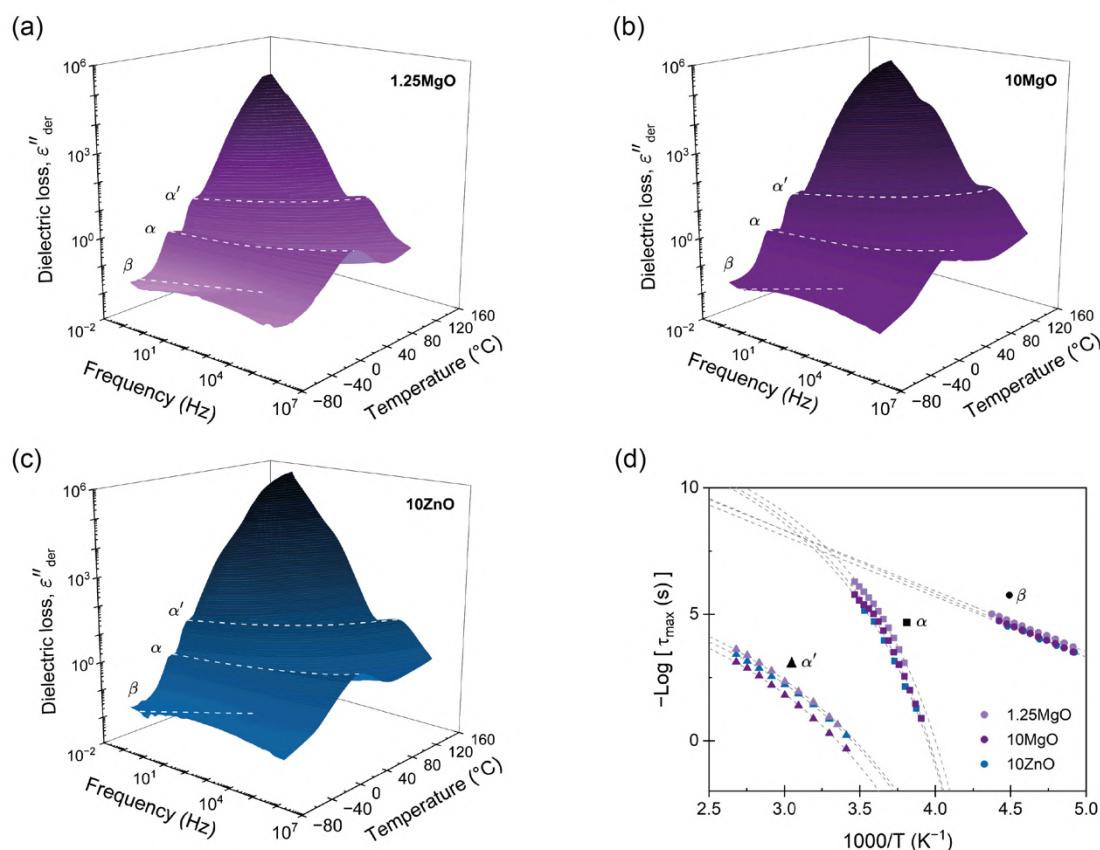


**Figure 5.4.** 3D plots of conduction-free dielectric loss ($\varepsilon''_{der}$) with respect to temperature and frequency for (a) 1.25MgO, (b) 10MgO) and (c) 10ZnO. (d) Activation plot.

Three distinct relaxations were revealed: 1) β, at low temperatures, associated with short-range motions; 2) α, or segmental relaxation, associated with cooperative motions of the polymer chains as a result of the glass transition, and 3) α', or ionic relaxation, at high temperatures, associated with the separated phase formed by the ionic clusters and the trapped rubber chains. The three identified relaxations can be well described by the HN formalism, as shown in **Chapter 2**. This approach enabled the generation of an activation plot (Figure 5.4d). To analyze the activating behavior, the data points were fitted using two distinct functions: a Vogel-Fulcher-Tammann-Hesse (VFTH) for the α and α' relaxations, and Arrhenius for the β relaxation. The dashed lines in each dataset point represent the fitting results obtained using these functions, as described by Equation 4.1 (VFTH) and Equation 4.4 (Arrhenius). Table 5.3 summarizes the parameters obtained.

The results of this study revealed some interesting findings. In terms of the β relaxation, no substantial variation in the activation energy value (46 kJ mol$^{-1}$, 48 kJ mol$^{-1}$ and 45 kJ mol$^{-1}$) was observed. β relaxation is not usually reported or discussed in recent studies on XNBR-based ionomers [32,37–40], neither by DMA nor by BDS. However, the limited available research attributes its origin to the rotational motions of side groups [41]. Additionally, recent investigations on non-carboxylated nitrile rubber (NBR) have associated its behavior with the local non-cooperative motions of the macromolecule [42]. In this context, Fritzsche et al. [41] reported an increase in the activation energy of β relaxation with increasing the filler content in rubber composites (i.e., with increasing constraints); however, no further explanation was given beyond the uncertainties inherent to the linear region. In our case, it seems that the intramolecular and/or intermolecular interactions within the polymer chains (i.e., van der Waals forces, electrostatic forces, and hydrogen bonds) were not affected by the presence of agglomerates (increasing MO content). Further exploration is required to gain a deeper understanding of this relaxation behavior.

**Table 5.3.** Fitting parameters from the activation plot of *ionic elastomers.*

| Parameter | 1.25MgO | 10MgO | 10ZnO |
|---|---|---|---|
| **β relaxation** | | | |
| Activation energy, $E_a$ (kJ mol$^{-1}$) | 46 ± 1 | 48 ± 1 | 45 ± 1 |
| **α relaxation** | | | |
| $B$ | 1477 ± 30 | 1552 ± 30 | 1574 ± 29 |
| Vogel temperature, $T_0$ (K) | 204 ± 1 | 204 ± 1 | 204 ± 1 |
| Fragility strength, $D$ | 7.2 ± 0.1 | 7.6 ± 0.2 | 7.7 ± 0.1 |
| Fragility index, $m$ | 98 ± 1 | 94 ± 2 | 93 ± 1 |
| **α' relaxation** | | | |
| $B$ | 1932 ± 36 | 1843 ± 24 | 1743 ± 14 |
| Vogel temperature, $T_0$ (K) | 183 ± 2 | 191 ± 2 | 189 ± 1 |
| Fragility strength, $D$ | 10.6 ± 0.2 | 9.6 ± 0.2 | 9.2 ± 0.1 |
| Fragility index, $m$ | 72 ± 1 | 77 ± 2 | 80 ± 1 |

For the α relaxation, no significant variations in the parameters derived from the VFTH fit were observed, indicating that the segmental relaxation, which involves the mobility of rubber segments that neither participate in the ionic interaction nor are in its vicinity, remains unaltered. This supports the model of a separate ionic phase with its own thermal transition. The results for α' relaxation showed a stark contrast. To gain further insight into the analysis, the fragility index ($m$) was calculated as a measure of the stiffness of the polymer backbone associated with each relaxation, according to Equation 4.3.

An increase in the Vogel temperature ($T_0$) was observed in the compounds containing higher MO contents (10MgO and 10ZnO). This observation corresponds to a decrease in flexibility attributable to excess oxides, a hallmark of materials exhibiting fragile behavior. These materials are characterized by increased cooperativity, lower $D$ values, and high $m$ values, which are related to the higher apparent activation energy necessary for their molecular motions. Instead, 1.25MgO demonstrated a behavior with lower cooperativity, where the activation of its molecular dynamics was more readily facilitated. This was reflected in the higher $D$ values and diminished $m$. These results hold significant implications, as they may aid in predicting the self-healing behavior. When subjected to identical conditions, 1.25 MgO is expected to exhibit a superior healing response, achieving higher efficiencies than 10ZnO and 10MgO, owing to its enhanced flexibility and mobility. These findings highlight the critical interplay between the composition, molecular dynamics, and self-healing in the development of advanced functional rubbers.

A more nuanced investigation was carried out using BDS. This step forward in the examination involved identifying the α' relaxation process at a constant frequency of 100 Hz in the temperature-sweep domain, as shown in Figure 5.5a. This approach allowed the identification of the temperature associated with the maximum ionic relaxation, that is, the ionic transition temperature. This critical value sets the lower limit of the temperature employed in the self-healing protocol, thereby providing a crucial parameter for efficient material healing. According to the acquired data, the

ionic transition temperature was identified to be ~55 °C for the compounds with equivalent crosslink density (1.25MgO and 10ZnO). However, a higher temperature around ~65 °C was observed for 10MgO. At this frequency, the relaxation temperature seems to be predominantly influenced by the crosslink density and, consequently, the number of ionic interactions.
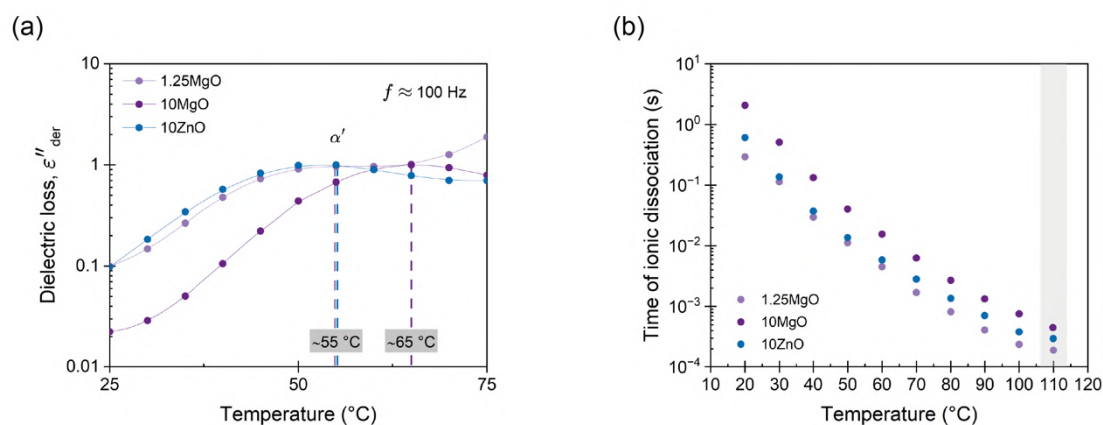


**Figure 5.5.** (a) Conduction-free dielectric loss ($\varepsilon''_{der}$) with respect to temperature at 100 Hz. (b) Time of ionic dissociation of the prepared compounds.

From these observations, a subsequent analysis was performed, plotting the variation in ionic dissociation time (obtained from the $\tau_{max}$ values associated with each $\alpha'$ relaxation) against temperature, as shown in Figure 5.5b. This led to the discovery that the first temperature at which the ionic dissociation times among all composites approach each other equivalently (with negligible differences of around 1-2 × 10$^{-3}$ s between them) is 110 °C. Based on these BDS findings, an insightful turn towards self-healing optimization was made. By embracing this approach, the traditional trial-and-error optimization process was avoided, offering a thorough analysis of the ionic dissociation times of the compounds. The insights derived from the BDS determined 110 °C as the minimum temperature for the self-healing process. This temperature selection is grounded not in conjecture but in the understanding of the molecular dynamics of the materials under specific conditions. This represents a

potentially transformative approach for optimizing healing protocols in future studies. Thus, the focus has now shifted to the study of the healing process.

### 5.2.2. Unveiling the Self-Healing and Recyclability of Ionic Elastomers

The healing capabilities of the compounds were calculated with respect to M300, TS, and EB at 110 °C for 3 h (Figure 5.6a). All *ionic elastomers* were able to fully recover their M300 values after the healing protocol. This is an interesting result from the point of view of recovering functionalities, as most commercial applications of these materials usually operate at lower to medium strains.
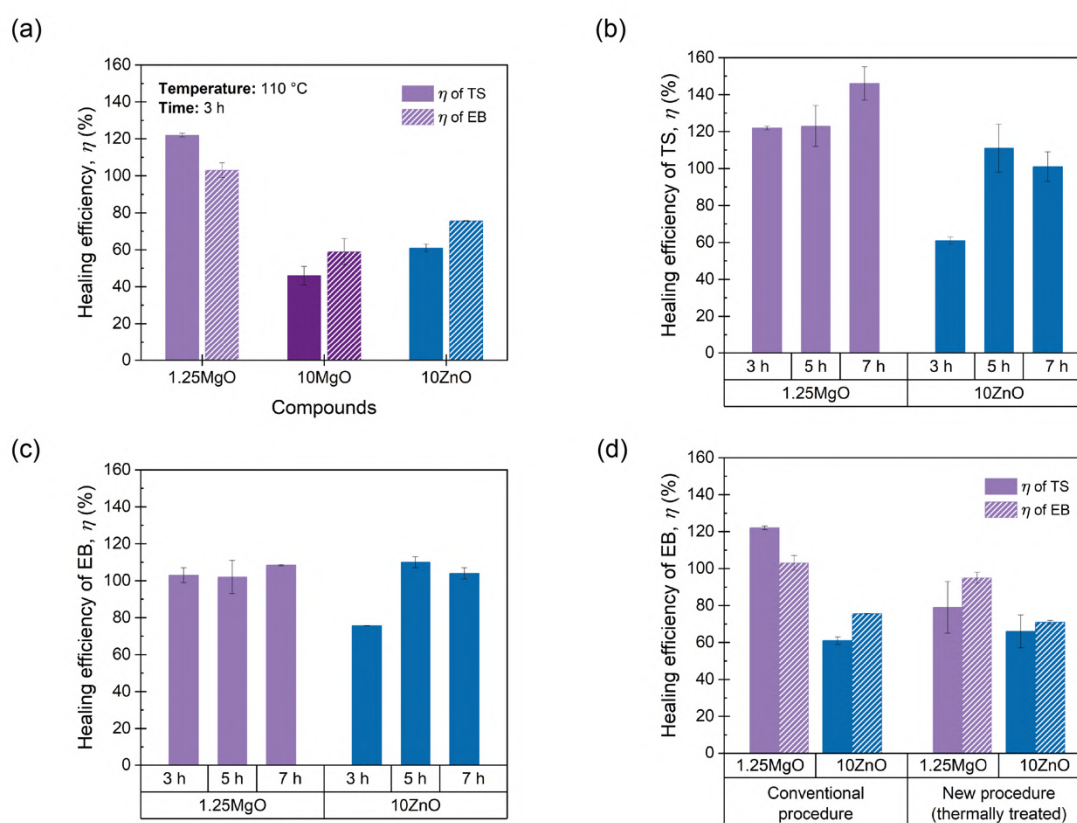


**Figure 5.6.** (a) Healing efficiency at fixed temperature (110 °C) and time (3 h). (b) Optimization of healing efficiency of (b) TS and (c) EB at different times. (d) Healing efficiencies calculated using conventional and new procedures.

The behavior of the properties at the breaking point was different. As the MgO content increased, there was a marked decrease in repairability [43–46]. This demonstrates an antagonistic relationship between the MgO content and healing capability. Specifically, 10MgO exhibited a lower efficiency of 46 % in TS and 59 % in EB compared to 1.25MgO, which achieved values above 100 % in both cases, surpassing its pristine state. This effect correlates well with the stiffness of the compounds.

To further elaborate this, the study was complemented by DMA measurements. Figure 5.7 shows the $E'$ and $E''$ moduli of the three prepared *ionic elastomers*. At the healing temperature (110 °C), a remarkable increase (over a decade) in the $E'$ values of 10MgO was observed, indicating higher stiffness and low diffusivity (i.e., constraints). This high stiffness and low diffusivity would be responsible for the considerable decrease in self-healing efficiency. Similar results were reported by Tierney and Register [47] for ethylene-methacrylic acid (E/MAA) ionomers with $Na^+$ cations. They found that excess acidic groups (below the stoichiometric ratio) accelerated the ion-hopping mechanism through a plasticizing effect of the ionic units, resulting in a reduction in viscosity. This implies that the diffusivity of the ionic group decreases significantly as the level of neutralization increases. All these factors will be key to the study of phenomena such as self-healing and recycling.
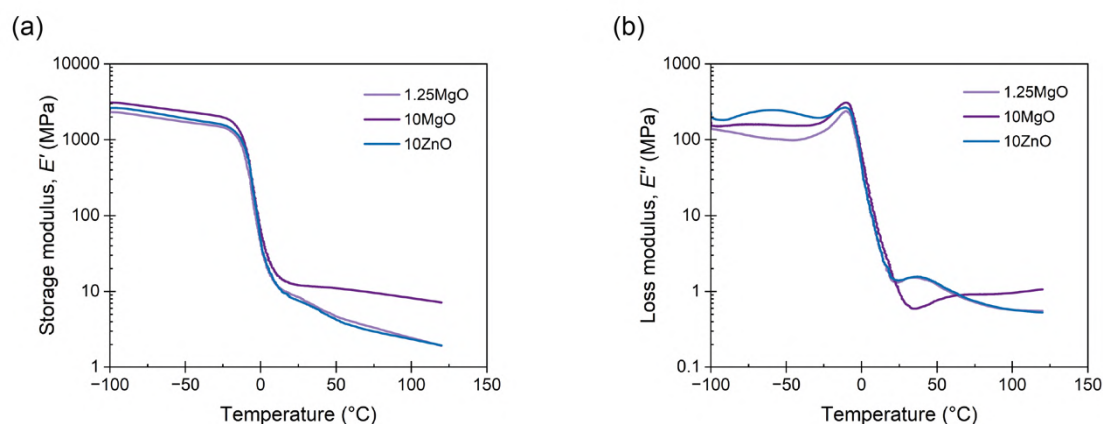


**Figure 5.7.** $E'$ and $E''$ for the three prepared *ionic elastomers*.

At equal crosslink densities, 10ZnO reached healing efficiencies of 61 % in TS and 76 % in EB. The presence of excess ZnO could decrease the free volume available for the motions of the XNBR chains, acting as barriers to mobility and reducing repair efficiency, due to a slowing down of the ion-hopping mechanism. This finding highlights that the crosslink density alone is not the sole influence on the molecular dynamics in the self-healing process. Factors such as the free volume, steric hindrance, neutralization degree, and binding energy also play pivotal roles.

Comparing the two compounds with equal MO contents (10MgO and 10ZnO), a better self-repairing capacity was observed for the compound with ZnO, which could be explained by its lower crosslink density and ionic interaction nature (higher ionic radius, lower ionic interaction), requiring less intense conditions to achieve higher efficiencies. Similar results have been previously reported. Hirasawa et al. [48] studied the effects of different cations on the ionomer structure of poly(ethylene-co-methacrylic acid) (EMAA). The ionic interaction strengths of different cations ($Na^+$, $K^+$, $Mg^{2+}$, $Zn^{2+}$, $Co^{2+}$, $Cu^{2+}$, and $Mn^{2+}$) were correlated with the melt flow rate (MFR) at different degrees of neutralization. The MFR decreased (viscosity increased) with increasing neutralization (i.e., crosslink density). This decrease was considerably higher for alkaline and alkaline earth metal salts than for the transition metal salts. This result shows that the ionic interactions in the ionomers are stronger in $Mg^{2+}$ than in $Zn^{2+}$, as evidenced by the increase in viscosity in the molten state. In this context, a higher viscosity results in lower chain interdiffusion and thus a lower self-healing capacity, as demonstrated by the results of this investigation. Figure 5.8a and 5.9b provide a schematic summary of the differences observed between the ionic networks and a simplified depiction of the Eisenberg model applied to the MO (assuming equal coordination numbers).

Considering these findings and the requirement to determine the optimal healing time, 10MgO was excluded from the subsequent stage of time optimization. Figure 5.6b and Figure 5.6c present the efficiency results with respect to TS and EB by extending the healing protocol time to 5 and 7 h. The results reveal that at 5 h,

10ZnO is capable of fully heal (efficiencies up to 100 % in TS and EB). Concurrently, 1.25MgO can achieve complete repair (efficiencies above 100 %) at all time intervals studied.
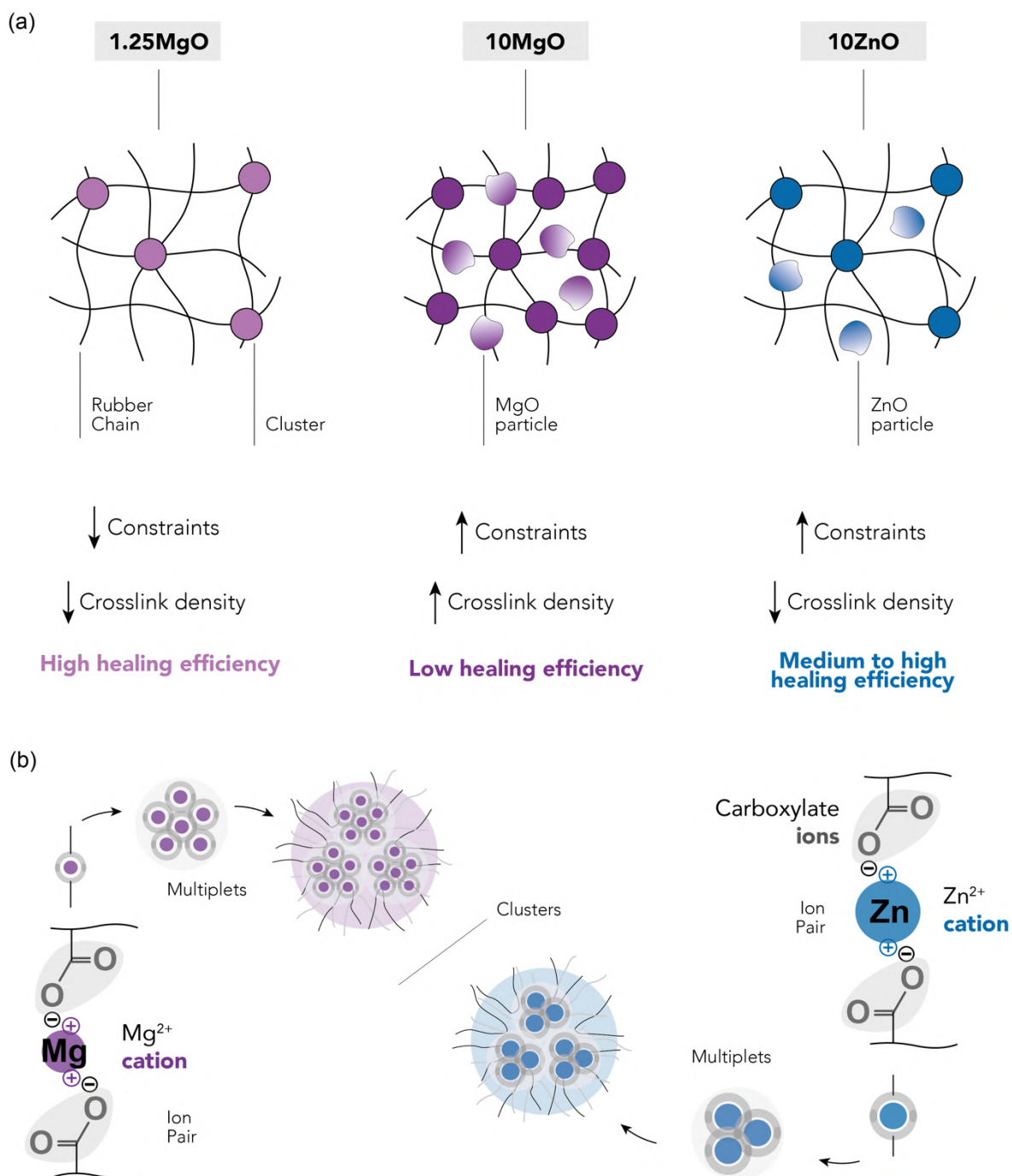


**Figure 5.8.** Scheme of (a) different networks and (b) Eisenberg model for each MO.

At this point in the study, one intriguing aspect to be discussed relates to the possibility of achieving healing efficiencies exceeding 100 %. This raises a compelling question: How can a material that has undergone total macroscopic damage and subsequent repair exhibit performance surpassing that of pristine samples? The influence of the healing protocol, notably the applied temperature, on material properties plays a significant role beyond healing. To understand the extent of this effect, a new procedure was proposed [46], whereby pristine specimens were subjected to heat treatment under the same healing protocol but without inducing macroscopic rupture with a razor blade. The application of temperature to the pristine material induced an increase in the crosslink density, potentially leading to an enhancement in the mechanical properties of the material, as demonstrated with the recycling cycles in **Chapter 4**. Bearing this in mind, from a physical and comparative standpoint, it could be considered reasonable to employ the heat-treated material rather than the pristine material as the reference point for calculating the healing efficiency. The newly calculated efficiency value was more realistically focused on the damage, thus suppressing the effect of the temperature. Nevertheless, in the aforementioned study, the repair mechanism was based on disulfide bond exchange, which is a dynamic but covalent mechanism that is inherently different from ionic interactions. This brings us to an interesting question: does temperature influence ionic interactions in the same way as it affects sulfur bonds? To answer this question, the new procedure was applied to the samples prepared in the current study. The efficiencies of 1.25MgO and 10ZnO (at 110 °C for 3 h) were recalculated (Figure 5.6d). In the case of TS, 79 % (1.25MgO) and 66 % (10ZnO) were obtained, and for EB, 95 % (1.25MgO) and 71 % (10ZnO) were obtained, respectively. This is still an outstanding (successful repair) but more realistic numerical result for the damage recovery process, without considering the thermal effect.

To contextualize the significance of these outcomes, it is important to compare the present results on mechanical properties and self-healing efficiency with recent studies (last 3 years) on healable *ionic elastomers*. However, it is crucial to point

out that making direct comparisons between self-healing studies is not always entirely fair because there are no international standards. As noted in **Chapter 1**, this is one of the major issues to be resolved in this field [49]. Objective assessments require that vulcanization processes, self-healing mechanisms and protocols (time, temperature, pressure, etc.), and variables in mechanical tests (sample size and shape, crosshead speed, temperature, etc.) be equivalent.

In light of these considerations, in terms of the mechanical properties and self-healing efficiency, the designed ionic elastomers exhibited competitive values when compared to the available literature. However, beyond the numerical results, the simplicity of the process introduced, the use of low-cost ingredients, and the optimization of repair conditions place this development in an advantageous position. Zainol et al. [50] developed XNBR compounds using the same zinc-carboxylate metal-ligand interaction but with ZT and dicumyl peroxide (DCP) in their recipes. Employing a considerably higher amount of ZT (30 phr), a TS of up to 8 MPa was achieved, coupled with a healing efficiency of 98 %, at a higher temperature (150 °C), but with a reduced repair time (just 10 min).

Naskar et al. [51] prepared self-healable and extremely stretchable ionic elastomer based on the dynamic metal–ligand coordination between 1-(3-aminopropyl) imidazole (API ligand) and $Zn^{2+}$ metal ion moieties incorporated onto the XNBR rubber backbone, with zinc chloride ($ZnCl_2$). With 3 phr of $Zn^{2+}$, an excellent healing performance of 91.2 % was achieved at RT after 24 h, with a TS of 5.7 MPa.

Recently, Das et al. [52] investigated the ionic crosslinking of XNBR with Ni-cysteine and Zn-cysteine complexes. Compared to the Ni-cysteine compound, the XNBR cured with the Zn-cysteine complex exhibited outstanding extensibility, recyclability, and TS of 3.8 MPa, which is distinctly lower than that of the ZnO- and MgO-based compounds prepared in the present study. However, they reported an impressive healing efficiency of 89.5 % after 24 h at RT. This stands in contrast

to the present doctoral thesis, which requires considerably shorter times but higher temperatures.

In contrast to zinc-carboxylate metal-ligand coordination, Wagje and Das [53] investigated alternate metal cations. In their study, XNBR was crosslinked through a copper (I)-carboxylate metal-ligand interaction using anhydrous copper chloride (CuCl). Employing 20 phr of CuCl, the best mechanical performance was obtained, with a TS of 5.41 MPa and 251 % EB. However, this blend could not self-repair under the tested conditions. Conversely, at a lower CuCl content (5 phr), TS was reduced to 1.95 MPa, while the self-healing efficiencies reached up to 75 % following a 70 °C and 48 h protocol. This underscores the balance between the mechanical strength and self-healing ability.

In this doctoral thesis, this trade-off is addressed, producing materials with both superior mechanical properties and high self-healing efficiencies resulting from meticulously optimized repair conditions.

It is a fact that the studies mentioned highlight the multifaceted nature of approaches in the field of *ionic elastomers* and the versatility of methodologies that can be employed. The available research underscores the critical importance of content optimization to ensure the best balance between mechanical strength and self-healing efficiency. Moreover, while these recent investigations offer a vast wealth of knowledge, a key distinction is evident: their focus was not predominantly application-oriented. In contrast, this doctoral thesis prioritizes this aspect for soft robotics applications, ensuring not only scientific rigor, but also practical applicability. Furthermore, as evident from the variety of crosslinking agents and their costs, it is imperative to consider the feasibility of scalability in material designs. The present work addresses this by striving for simplicity and cost-effectiveness; however, a comprehensive LCA for these compounds is still necessary to gain a clearer understanding of the sustainability of the material and the devised process.

The recyclability of the developed compounds was also analyzed to provide sustainability to the soft actuator. The evolution of different mechanical properties (M300, TS, and EB) and crosslink densities with the number of recycling cycles was followed. Figure 5.9 shows the obtained values.
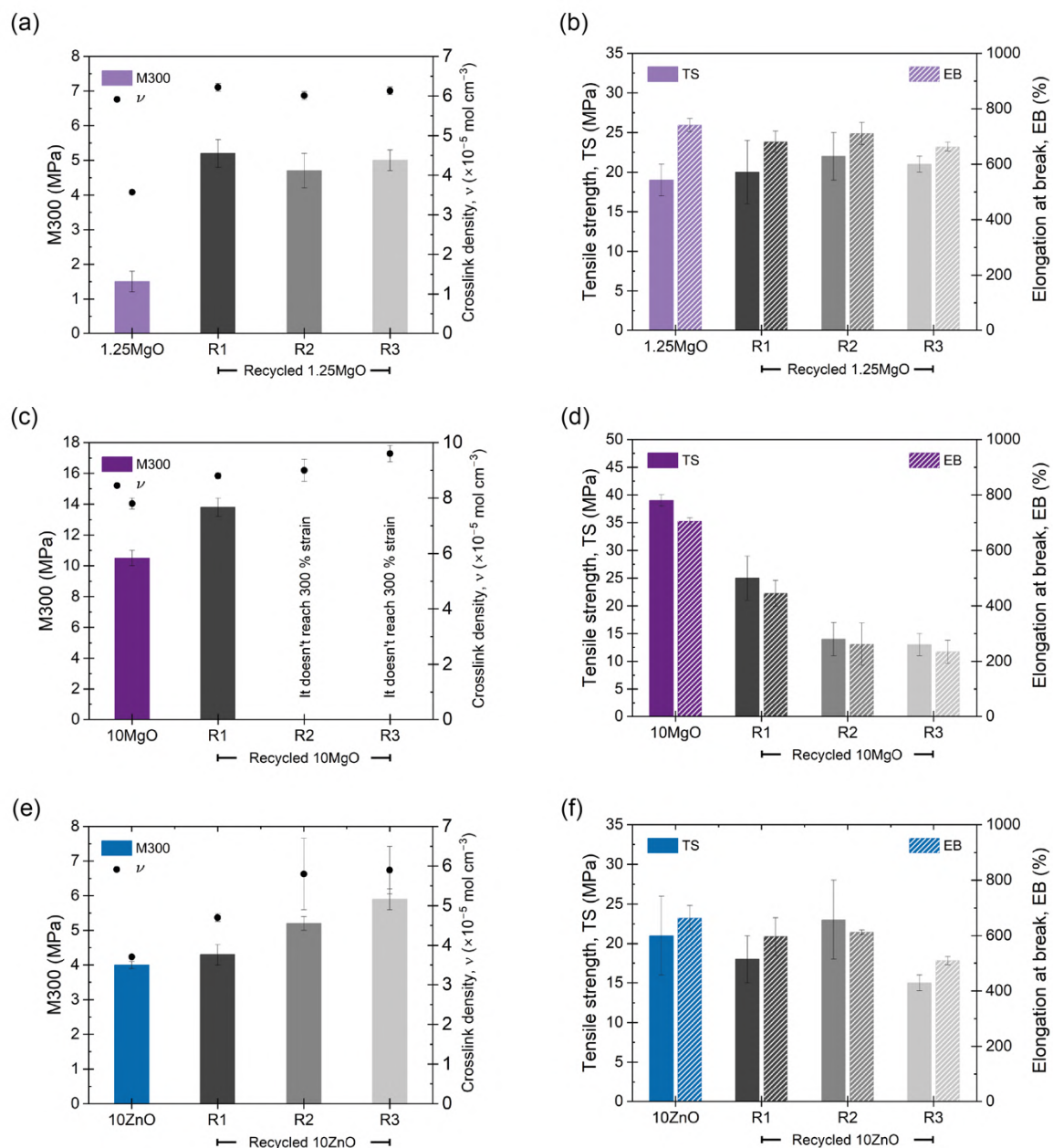


**Figure 5.9.** Evolution of the mechanical properties (M300, TS, and EB) and crosslink densities of (a, b) 1.25MgO, (c, d) 10MgO, and (e, f) 10ZnO over three recycling cycles.

The results of 10ZnO were discussed in detail in the previous **Chapter 4**. With each recycling cycle, an increase in the crosslink density was determined by swelling, with a notable decrease in the volume of the solvent absorbed in the recycled samples. This could be associated with the redistribution of ionic aggregates into smaller structures around the matrix, as previously explained. Compounds with the same crosslink density (1.25MgO and 10ZnO) showed promising behavior, with 10ZnO retaining approximately 75 % of its initial properties and 1.25MgO successfully retaining both properties (TS and EB) even after R3. Nonetheless, 10MgO exhibited a limited recyclability. A noticeable decrease in TS recovery with recycling cycles was observed, and 300% elongation was not reached at R2 and R3. However, its net TS and EB recovery values remained above 12 MPa and 200 % strain, respectively, which may be useful in several rubber applications.

### 5.2.3 Assembly and Validation of the Soft Robotic Gripper

To complete the study from an application-oriented perspective, the next step has been the implementation of the developed materials in an advanced application, such as soft robotics. A tendon-driven soft robotic gripper prototype that imitates a human hand was designed. This part of the study involved two main stages: assembly and validation testing. The assembly and actuation process consisted of five steps. Figure 5.10 shows a schematic representation of this procedure.

*Step 1:* Design and molding of the fingers (actuators). The rubber compound with optimal mechanical strength, self-healing efficiency, and recyclability was selected for compression molding of the five actuators using a hydraulic press and an aluminum mold at 160 °C and 15 bar. An additional time of 8 min was added to t90 to ensure proper vulcanization (+1 min for each mm of thickness in addition to the curing curve impellers). Two sizes were prepared: a smaller with three phalanges for thumb simulation and a larger with four phalanges for the other fingers.

**Step 1**

Design and molding
of the fingers
**(actuators).**

**Actuator**

Compression
molding

7 mm

30°

3 mm

95 mm

15 mm

20 mm

**Step 2**

Design and manufacture
of the **hand base**

PLA filaments

3D printer

**Hand
base**

**Step 3**

Integration of
**tendon-driven actuation**
mechanism

Teflon
tubing

(1)

(2)

Nylon
cords

2 mm

Knot
(3)

**Step 4**

**Assembly** of actuators
and hand base

Final
Assembly

**Step 5**

Code and
**actuaction**

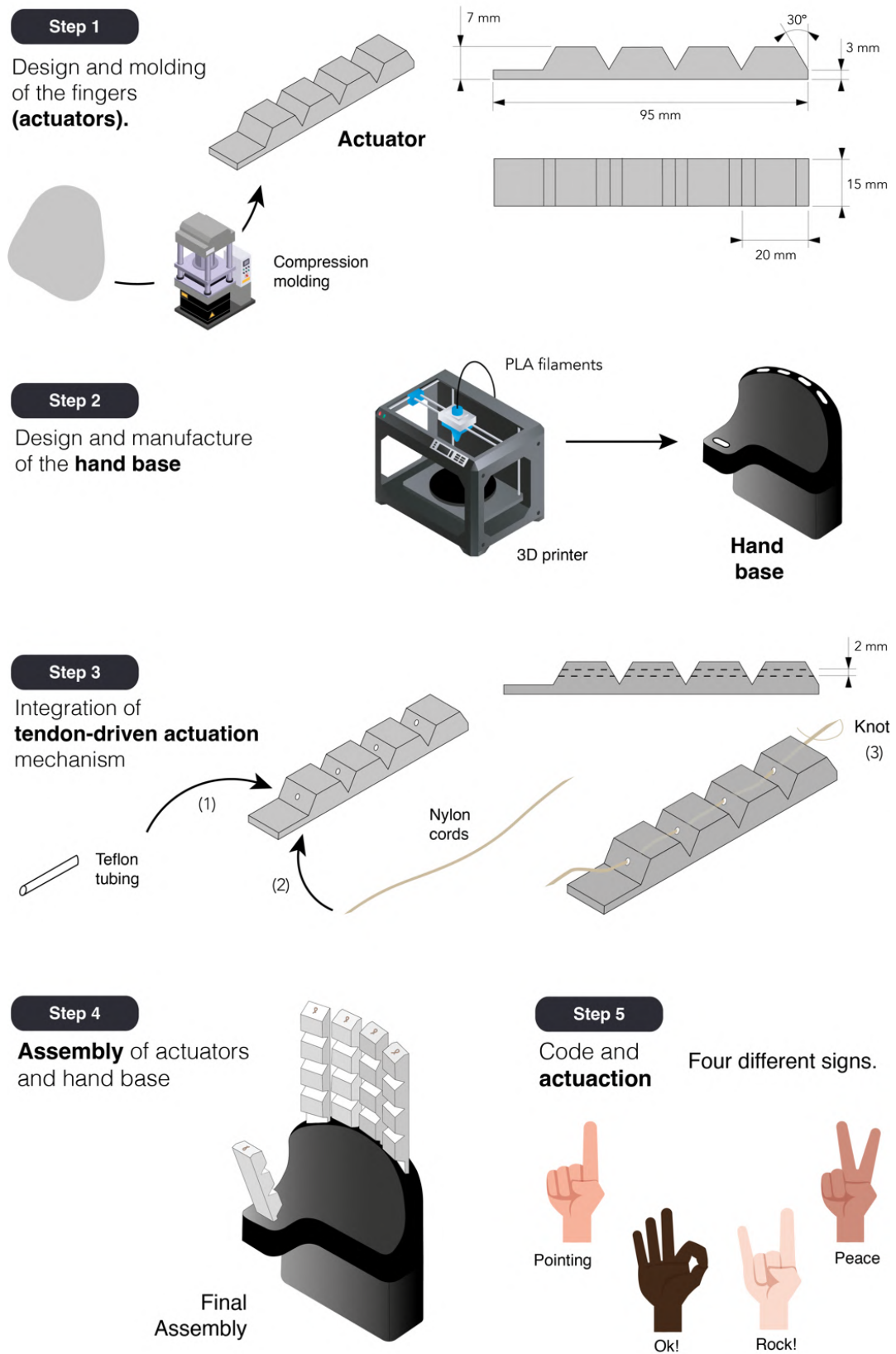Four different signs.

Pointing

Ok!

Rock!

Peace

**Figure 5.10.** Schematic representation of soft robotic gripper assembly.

*Step 2:* Design and manufacture of the hand base. The base, corresponding to the palm of the hand and a portion of the forearm, was designed using the commercial CAD/CAE engineering software, Autodesk Inventor. This piece was subsequently produced using additive manufacturing techniques with black poly(lactic acid) (PLA) filaments on a fused filament fabrication 3D printer (Ultimaker 2).

*Step 3:* Integration of tendon-driven actuation mechanism. The tendon-driven actuation mechanism was then embedded in the five actuators. A commercial nylon cord with a diameter of 0.5 mm was threaded through small PTFE tubes with an inner diameter of 1 mm, which were inserted into each phalanx. The cords were fixed to the top of the finger by using a manually tied knot.

*Step 4:* Assembly of actuators and hand base. Both parts were assembled and firmly affixed to a wooden base. The cords of the tendon-driven actuation mechanism were connected to servo motors (Dynamixel) that pulled the strings to generate the bending motion. The elastic energy stored in the actuators facilitates the return to its original position upon the release of pressure on the cords.

*Step 5:* Code and actuation. Instructions for finger movements were controlled using an Arduino Uno. The Arduino code contains different predefined finger movements.

After the assembly and code development, the second phase involved validation testing. An RGBD camera tracked the deformation of five marks placed on the side of a larger actuator (four phalanges). The camera recorded the position of each mark according to different movement instructions, thus generating a bending angle-time graph. For movement tracking, the actuator was positioned horizontally with the top tip facing right, and actuation was executed in the direction towards a 90° angle with respect to the horizontal. Figure 5.11 shows a schematic representation of this phase.

The final choice for manufacturing soft robotic grippers considers the balance between mechanical performance, healing capability, and recyclability. While 10MgO exhibited exceptional mechanical performance, its limitations in self-healing

and recycling make it less suitable for long-term durability and sustainability. The high stiffness of 10MgO may also hinder its use for handling delicate products. 10ZnO showed good mechanical performance and healing ability, but longer healing times and recycling difficulties after the third cycle may pose challenges in applications where quick repairs and consistent recyclability are crucial. However, this can be compensated by its shorter vulcanization time. 1.25MgO is another suitable choice. Despite having a slightly lower mechanical performance than other compounds, it still possesses competitive values when considering the most elastomeric materials used in soft robotics. One of the main disadvantages is its low curing rate; however, its short healing time and ability to maintain its properties through multiple recycling cycles can significantly extend the lifespan of the robotic hand, reduce maintenance costs, and improve sustainability. Figure 5.12 shows the final assembly of the soft robotic gripper developed using the optimized compound in this study.
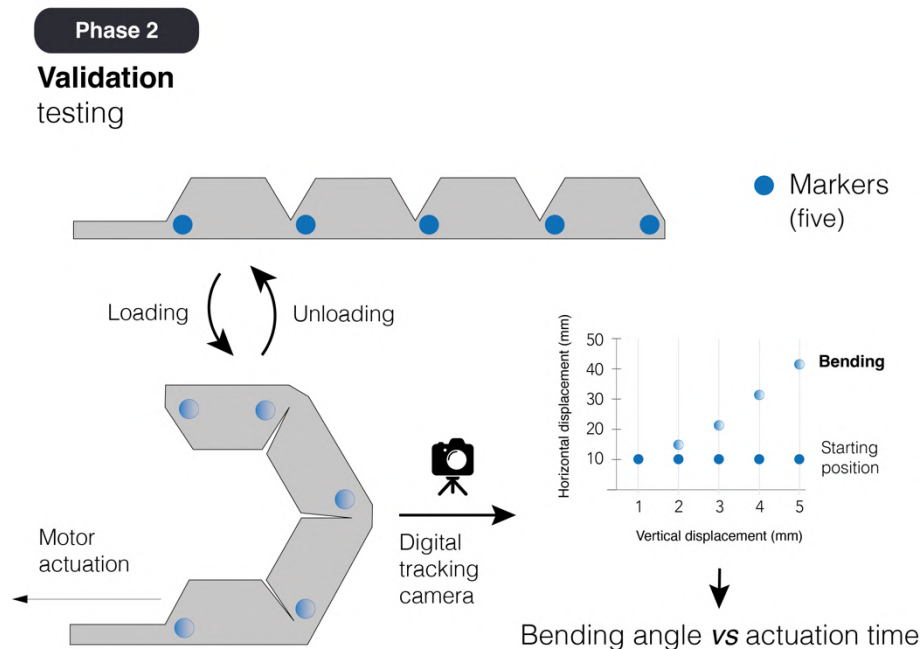


**Figure 5.11.** Schematic representation of the validation testing.

Following the assembly process detailed earlier, the precision of the soft robotic gripper in performing intricate movements was confirmed. It was successfully actuated to form distinct gestures like the universally recognized "pointing", "ok", "rock!" and "peace" signs. These positions not only show the ability of the soft robot to mimic human hand movements but also underscore the efficacy of using the *ionic elastomer* with its optimum flexibility and elastic response for adequate performance.
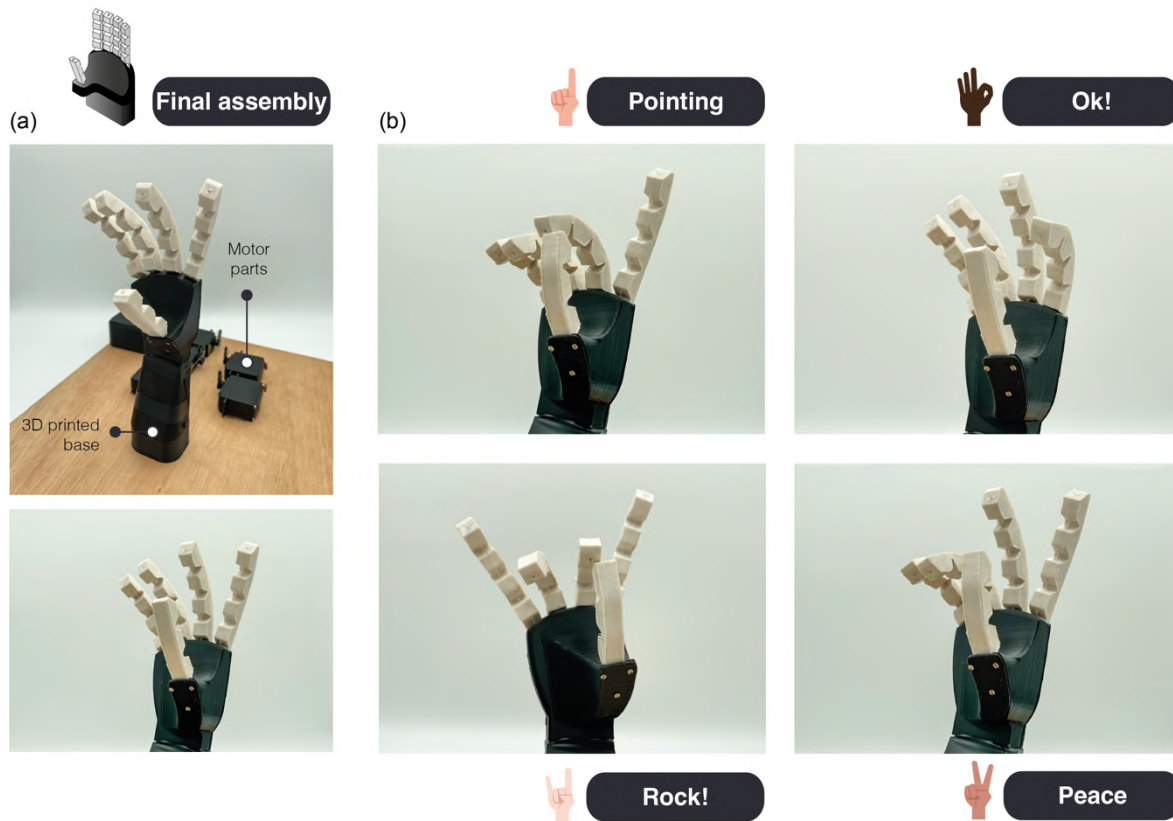


**Figure 5.12.** (a) Final assembly of gripper and (b) actuation of four programmed positions (pointing, ok, rock, and peace signs).

For the validation stage, two experimental tests were conducted using a motion-tracking setup. These tests included a response test (Figure 5.13a) and a stress relaxation test (Figure 5.13b) at the system level, where the bending angle was followed as a function of time. In the response test, the actuator was initially bent

to an angle of 50 °, after which the tension on the tendon was completely released (Figure 5.13c). Next, the response of the actuator was investigated by tracking how quickly it recovered to its initial (unbent) position. This test provides information regarding the dynamics of the selected material in soft robotics applications. It can be observed that only after 80 ms, the actuator reaches back its initial position. Quick responses such as these are crucial in soft robotic grippers, as they guarantee rapid grasping actions, ultimately resulting in increased throughput in industrial applications.
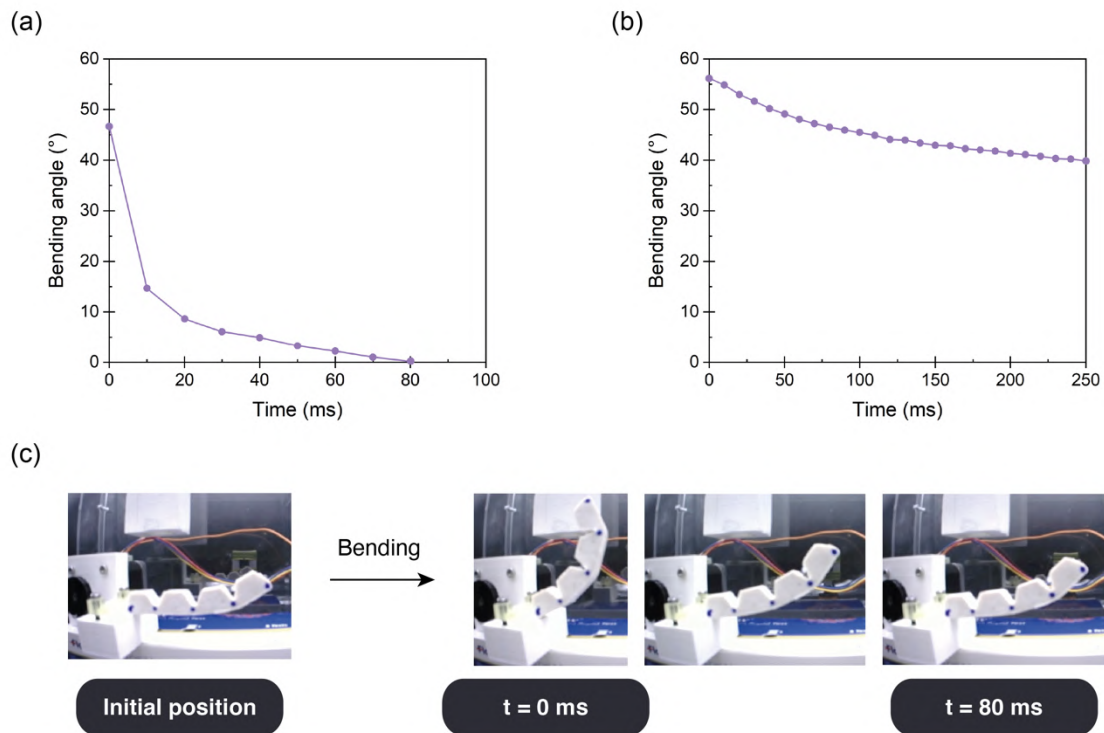


**Figure 5.13.** Bending angle vs time for the (a) response and (b) stress relaxation tests of the selected ionic rubber. (c) Images of the validation process.

In the second experiment, a stress relaxation test was performed on the soft bending actuator level by placing it at a 55° bending angle by tensioning the tendon. Subsequently, the bending angle was monitored over time, while maintaining the

tendon in a fixed position. Due to stress relaxation in the material, the bending angle is slightly reduced over time. After 250 ms, this angle was reduced to 40°. Although this dynamic effect can be partially mitigated by the adaptability of the soft gripper, it is undesirable in gripper applications where a high position accuracy is required. This effect results from the viscoelastic behavior of the *ionic elastomers*. Reversible/dynamic polymer networks, in general, suffer from viscoelastic behavior, which impacts their applications. Although the materials have a relatively low loss modulus at RT, experiments at the actuator level indicate that the viscous component is far from negligible. Therefore, future work should focus on minimizing these viscous effects, as they can affect the controllability of soft robotic systems. However, the approach introduced in this doctoral thesis aids in the sustainable creation of soft robotic parts using healable and recyclable materials and ensures that they have the capability to perform quickly with precision, a key requirement in practical real-world applications.

## 5.3. Summary

**Chapter 5** discusses the potential of XNBR-based compounds employing ZnO and MgO as vulcanizing agents, effectively demonstrating how a single ingredient can drastically influence the mechanical and physical properties of rubber, while concurrently addressing issues of sustainability and recyclability. The research found that a higher MO content increases the vulcanization efficiency, leading to a higher cure rate and degree of crosslinking, and thus enhanced mechanical performance. A comparative analysis of the equal crosslink densities revealed that excess ZnO imparts stiffness owing to its function as a semi-reinforcing filler. In contrast, equal MO contents induced superior mechanical properties in the MgO compound compared to ZnO, owing to the stronger electrostatic attraction of its smaller cations. A significant innovation of this study is the use of BDS to determine the optimal temperature for a self-healing protocol, diverging from the traditional trial-

and-error approaches typically employed for optimization. The compound with just 1.25 phr of MgO boasts the highest self-healing performance, achieving a healing efficiency of up to 79% for TS and up to 95% for EB at 110 °C within 3 h using an updated and fairer method for determining the repair efficiency. The ionic rubber also maintained full recyclability (100 % recovery of the maximum mechanical properties) over three recycling cycles. Despite exhibiting the lowest TS among the prepared compounds, 1.25MgO still delivered an impressive 19 MPa of TS, coupled with an EB exceeding 700 %, which are outstanding values in the field of soft matter. These findings have significant implications for the selection of elastomeric materials in areas such as soft robotics, where the load capacity, sustainability, resilience, self-healing, and recycling abilities are crucial. A soft robotic gripper was successfully assembled, demonstrating the practical application of these findings. These outcomes significantly advance our understanding of the behavior and properties of XNBR-based compounds, particularly within the scope of *ionic elastomers*. It unlocks the potential of this behavior in advanced applications, such as soft robotics, where the use of conventional ionic rubbers is no longer just a possibility, but a tangible reality. Figure 5.14 shows a representative schematic summarizing **Chapter 5**.
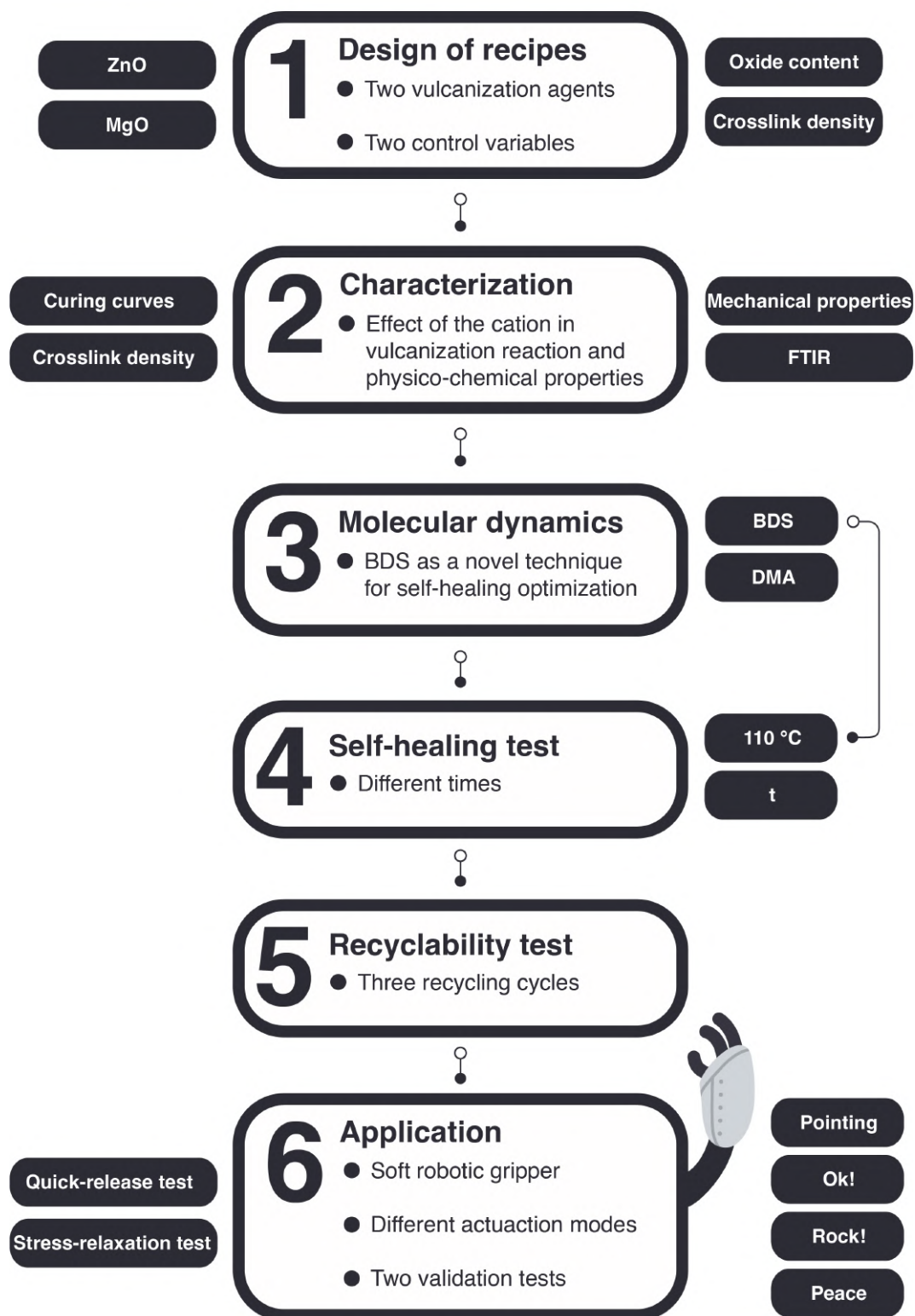
**Figure 5.14.** Schematic representation of **Chapter 5**.

## References

1. Chen, X.; Zhang, X.; Huang, Y.; Cao, L.; Liu, J. A Review of Soft Manipulator Research, Applications, and Opportunities. *J Field Robot* **2022**, *39*, 281–311, doi:10.1002/ROB.22051.

2. Rus, D.; Tolley, M.T. Design, Fabrication and Control of Soft Robots. *Nature* **2015**, *521*, 467–475, doi:10.1038/nature14543.

3. Chen, L.; Yang, C.; Wang, H.; Branson, D.T.; Dai, J.S.; Kang, R. Design and Modeling of a Soft Robotic Surface with Hyperelastic Material. *Mech Mach Theory* **2018**, *130*, 109–122, doi:10.1016/J.MECHMACHTHEORY.2018.08.010.

4. Yang, C.; Kang, R.; Branson, D.T.; Chen, L.; Dai, J.S. Kinematics and Statics of Eccentric Soft Bending Actuators with External Payloads. *Mech Mach Theory* **2019**, *139*, 526–541, doi:10.1016/J.MECHMACHTHEORY.2019.05.015.

5. Brown, E.; Rodenberg, N.; Amend, J.; Mozeika, A.; Steltz, E.; Zakin, M.R.; Lipson, H.; Jaeger, H.M. Universal Robotic Gripper Based on the Jamming of Granular Material. *Proc Natl Acad Sci U S A* **2010**, *107*, 18809–18814, doi:10.1073/PNAS.1003250107.

6. Wei, Y.; Chen, Y.; Ren, T.; Chen, Q.; Yan, C.; Yang, Y.; Li, Y. A Novel, Variable Stiffness Robotic Gripper Based on Integrated Soft Actuating and Particle Jamming. *Soft Robot* **2016**, *3*, 134–143, doi:10.1089/SORO.2016.0027.

7. Jiang, P.; Yang, Y.; Chen, M.Z.Q.; Chen, Y. A Variable Stiffness Gripper Based on Differential Drive Particle Jamming. *Bioinspir Biomim* **2019**, *14*, 036009, doi:10.1088/1748-3190/AB04D1.

8. Al Abeach, L.A.T.; Nefti-Meziani, S.; Davis, S. Design of a Variable Stiffness Soft Dexterous Gripper. *Soft Robot* **2017**, *4*, 274–284, doi:10.1089/SORO.2016.0044.

9.  Al-Fahaam, H.; Nefti-Meziani, S.; Theodoridis, T.; Davis, S. The Design and Mathematical Model of a Novel Variable Stiffness Extensor-Contractor Pneumatic Artificial Muscle. *Soft Robot* **2018**, *5*, 576–591, doi:10.1089/SORO.2018.0010.

10. Zhang, Y.F.; Zhang, N.; Hingorani, H.; Ding, N.; Wang, D.; Yuan, C.; Zhang, B.; Gu, G.; Ge, Q. Fast-Response, Stiffness-Tunable Soft Actuator by Hybrid Multimaterial 3D Printing. *Adv Funct Mater* **2019**, *29*, 1806698, doi:10.1002/ADFM.201806698.

11. Hartmann, F.; Baumgartner, M.; Kaltenbrunner, M.; Hartmann, F.; Baumgartner, M.; Kaltenbrunner, M. Becoming Sustainable, The New Frontier in Soft Robotics. *Advanced Materials* **2021**, *33*, 2004413, doi:10.1002/ADMA.202004413.

12. Terryn, S.; Langenbach, J.; Roels, E.; Brancart, J.; Bakkali-Hassani, C.; Poutrel, Q.A.; Georgopoulou, A.; George Thuruthel, T.; Safaei, A.; Ferrentino, P.; et al. A Review on Self-Healing Polymers for Soft Robotics. *Materials Today* **2021**, *47*, 187–205, doi:10.1016/J.MATTOD.2021.01.009.

13. Imbernon, L.; Norvez, S. From Landfilling to Vitrimer Chemistry in Rubber Life Cycle. *Eur Polym J* **2016**, *82*, 347–376, doi:10.1016/j.eurpolymj.2016.03.016.

14. Roels, E.; Terryn, S.; Iida, F.; Bosman, A.W.; Norvez, S.; Clemens, F.; Van Assche, G.; Vanderborght, B.; Brancart, J. Processing of Self-Healing Polymers for Soft Robotics. *Advanced Materials* **2022**, *34*, 2104798, doi:10.1002/adma.202104798.

15. Cao, J.; Zhou, C.; Su, G.; Zhang, X.; Zhou, T.; Zhou, Z.; Yang, Y. Arbitrarily 3D Configurable Hygroscopic Robots with a Covalent–Noncovalent Interpenetrating Network and Self-Healing Ability. *Advanced Materials* **2019**, *31*, 1900042, doi:10.1002/ADMA.201900042.

16.    Guo, M.; Wu, Y.; Xue, S.; Xia, Y.; Yang, X.; Dzenis, Y.; Li, Z.; Lei, W.; Smith, A.T.; Sun, L. A Highly Stretchable, Ultra-Tough, Remarkably Tolerant, and Robust Self-Healing Glycerol-Hydrogel for a Dual-Responsive Soft Actuator. *J Mater Chem A Mater* **2019**, *7*, 25969–25977, doi:10.1039/C9TA10183G.

17.    Gao, Y.; Fang, X.; Tran, D.; Ju, K.; Qian, B.; Li, J. Dielectric Elastomer Actuators Based on Stretchable and Self-Healable Hydrogel Electrodes. *R Soc Open Sci* **2019**, *6*, doi:10.1098/RSOS.182145.

18.    Deng, J.; Kuang, X.; Liu, R.; Ding, W.; Wang, A.C.; Lai, Y.C.; Dong, K.; Wen, Z.; Wang, Y.; Wang, L.; et al. Vitrimer Elastomer-Based Jigsaw Puzzle-Like Healable Triboelectric Nanogenerator for Self-Powered Wearable Electronics. *Advanced Materials* **2018**, *30*, 1705918, doi:10.1002/ADMA.201705918.

19.    He, Q.; Wang, Z.; Wang, Y.; Song, Z.; Cai, S. Recyclable and Self-Repairable Fluid-Driven Liquid Crystal Elastomer Actuator. *ACS Appl Mater Interfaces* **2020**, *12*, 35464–35474, doi:10.1021/ACSAMI.0C10021.

20.    Zhang, P.; Li, G. Healing-on-Demand Composites Based on Polymer Artificial Muscle. *Polymer (Guildf)* **2015**, *64*, 29–38, doi:10.1016/J.POLYMER.2015.03.022.

21.    Fisher, H.L. Natural and Synthetic Rubbers. *J Chem Educ* **1942**, *19*, 522–530, doi:10.1021/ED019P522.

22.    Chandrasekaran, C. *Essential Rubber Formulary: Formulas for Practitioners*; William Andrew Publishing: Norwich, NY, 2007; ISBN 0815517092.

23.    Maghami, S.; Dierkes, W.K.; Noordermeer, J.W.M. Functionalized SBRs in Silica-Reinforced Tire Tread Compounds: Evidence for Interactions between Silica Filler and Zinc Oxide. *Rubber Chemistry and Technology* **2016**, *89*, 559–572, doi:10.5254/RCT.16.84810.

24. González, N.; Del Àngels Custal, M.; Rodríguez, D.; Riba, J.R.; Armelin, E. Influence of ZnO and TiO2 Particle Sizes in the Mechanical and Dielectric Properties of Vulcanized Rubber. *Materials Research* **2017**, *20*, 1082–1091, doi:10.1590/1980-5373-MR-2017-0178.

25. Parvathi, K.; Ramesan, M.T. Tailoring the Structural, Electrical and Thermal Properties of Zinc Oxide Reinforced Chlorinated Natural Rubber/Poly (Indole) Blend Nanocomposites for Flexible Electrochemical Devices. *Journal of Polymer Research* **2023**, *30*, 1–15, doi:10.1007/S10965-022-03427-2.

26. Araujo-Morera, J.; López-Manchado, M.A.; Verdejo, R.; Hernández Santana, M. Unravelling the Effect of Healing Conditions and Vulcanizing Additives on the Healing Performance of Rubber Networks. *Polymer (Guildf)* **2022**, *238*, 124399, doi:10.1016/J.POLYMER.2021.124399.

27. Shannon, R. Revised Effective Ionic Radii and Systematic Studies of Interatomic Distances in Halides and Chalcogenides. *Acta Crystallographica Section A* **1976**, *32*, 751–767.

28. Liu, Z.; Shao, G.; Chen, W.; Shen, L.; Cheng, Y.; Liang, X.; Xiang, W. Effect of the Replacement of Zn2+ with Mg2+ in Ca14Zn6Ga10O35:Mn4+. *Opt Mater Express* **2018**, *8*, 2532–2541, doi:10.1364/OME.8.002532.

29. DuChanois, R.M.; Heiranian, M.; Yang, J.; Porter, C.J.; Li, Q.; Zhang, X.; Verduzco, R.; Elimelech, M. Designing Polymeric Membranes with Coordination Chemistry for High-Precision Ion Separations. *Sci Adv* **2022**, *8*, 9436, doi:10.1126/SCIADV.ABM9436.

30. Das, M.; Pal, S.; Naskar, K. Exploring Various Metal-Ligand Coordination Bond Formation in Elastomers: Mechanical Performance and Self-Healing Behavior. *Express Polym Lett* **2020**, *14*, 860–880, doi:10.3144/expresspolymlett.2020.71.

31. Dudev, T.; Lim, C. Metal Selectivity in Metalloproteins: Zn2+ vs Mg2+. *Journal of Physical Chemistry B* **2001**, *105*, 4446–4452, doi:10.1021/JP004602G.

32. Laskowska, A.; Zaborski, M.; Boiteux, G.; Gain, O.; Marzec, A.; Maniukiewicz, W. Ionic Elastomers Based on Carboxylated Nitrile Rubber (XNBR) and Magnesium Aluminum Layered Double Hydroxide (Hydrotalcite). *Express Polym Lett* **2014**, *8*, 374–386, doi:10.3144/expresspolymlett.2014.42.

33. Krzemińska, S.M.; Smejda-Krzewicka, A.A.; Leniart, A.; Lipińska, L.; Woluntarski, M. Effects of Curing Agents and Modified Graphene Oxide on the Properties of XNBR Composites. *Polym Test* **2020**, *83*, 106368, doi:10.1016/J.POLYMERTESTING.2020.106368.

34. Brozoski, B.A.; Coleman, M.M.; Painter, P.C. Local Structures in Ionomer Multiplets. A Vibrational Spectroscopic Analysis. *Macromolecules* **1984**, *17*, 230–234, doi:10.1021/MA00132A019.

35. Painter, P.C.; Brozoski, B.A.; Coleman, M.M. FTIR Studies of Calcium and Sodium Ionomers Derived from an Ethylene–Methacrylic Acid Copolymer. *J Polym Sci B Polym Phys* **1982**, *20*, 1069–1080, doi:10.1002/POL.1982.180200614.

36. Song, Z.; Wang, J.; Tao, Q.; Yu, Y.; Zhang, H.; Hu, C.; Cen, H.; Zheng, X.; Hu, T.; Wu, C. Zn-Salt Poly(Styrene–Ran–Cinnamic Acid) Ionomer as a Polystyrene with Improved Impact Toughness, Heat Resistance, and Minimally Compromised Processability. *J Appl Polym Sci* **2022**, *139*, 52041, doi:10.1002/APP.52041.

37. Salaeh, S.; Das, A.; Wießner, S. Design and Fabrication of Thermoplastic Elastomer with Ionic Network: A Strategy for Good Performance and Shape Memory Capability. *Polymer (Guildf)* **2021**, *223*, 123699, doi:10.1016/J.POLYMER.2021.123699.

38.    Chatterjee, T.; Hait, S.; Bhattacharya, A.B.; Das, A.; Wiessner, S.; Naskar, K. Zinc Salts Induced Ionomeric Thermoplastic Elastomers Based on XNBR and PA12. *Polymer-Plastics Technology and Materials* **2019**, *59*, 141–153, doi:10.1080/25740881.2019.1625389.

39.    Paran, S.M.R.; Naderi, G.; Mosallanezhad, H.; Movahedifar, E.; Formela, K.; Saeb, M.R. Microstructure and Mechanical Properties of Carboxylated Nitrile Butadiene Rubber/Epoxy/XNBR-Grafted Halloysite Nanotubes Nanocomposites. *Polymers (Basel)* **2020**, *12*, 1192, doi:10.3390/POLYM12051192.

40.    Gaca, M.; Pietrasik, J.; Zaborski, M.; Okrasa, L.; Boiteux, G.; Gain, O. Effect of Zinc Oxide Modified Silica Particles on the Molecular Dynamics of Carboxylated Acrylonitrile-Butadiene Rubber Composites. *Polymers (Basel)* **2017**, *9*, 645, doi:10.3390/POLYM9120645.

41.    Fritzsche, J.; Das, A.; Jurk, R.; Stöckelhuber, K.W.; Heinrich, G.; Klüppel, M. Relaxation Dynamics of Carboxylated Nitrile Rubber Filled with Organomodified Nanoclay. *Express Polym Lett* **2008**, *2*, 373–381, doi:10.3144/expresspolymlett.2008.44.

42.    Basu, D.; Banerjee, S.S.; Chandra Debnath, S.; Malanin, M.; Amirova, L.; Dubois, P.; Heinrich, G.; Das, A. Unusual Low Temperature Relaxation Behavior of Crosslinked Acrylonitrile-Butadiene Co-Polymer. *Polymer (Guildf)* **2021**, *212*, 123309, doi:10.1016/j.polymer.2020.123309.

43.    Hernández, M.; Grande, A.M.; Dierkes, W.; Bijleveld, J.; Van Der Zwaag, S.; García, S.J. Turning Vulcanized Natural Rubber into a Self-Healing Polymer: Effect of the Disulfide/Polysulfide Ratio. *ACS Sustain Chem Eng* **2016**, *4*, 5776–5784, doi:10.1021/ACSSUSCHEMENG.6B01760.

44.    Grande, A.M.; Martin, R.; Odriozola, I.; van der Zwaag, S.; Garcia, S.J. Effect of the Polymer Structure on the Viscoelastic and Interfacial Healing Behaviour

of Poly(Urea-Urethane) Networks Containing Aromatic Disulphides. *Eur Polym J* **2017**, *97*, 120–128, doi:10.1016/J.EURPOLYMJ.2017.10.007.

45. Zhang, Y.; Zheng, J.; Ma, W.; Zhang, X.; Du, Y.; Li, K.; Liu, Y.; Yu, G.; Jia, Y. Ultra-Low-Temperature Self-Healing Polyurethane with Enhanced Strength and Elongation Based on Dual Synergetic Crosslinking Strategy. *Eur Polym J* **2022**, *175*, 111394, doi:10.1016/J.EURPOLYMJ.2022.111394.

46. Araujo-Morera, J.; Utrera-Barrios, S.; Olivares, R.D.; Verdugo Manzanares, R.; López-Manchado, M.Á.; Verdejo, R.; Hernández Santana, M. Solving the Dichotomy between Self-Healing and Mechanical Properties in Rubber Composites by Combining Reinforcing and Sustainable Fillers. *Macromol Mater Eng* **2022**, 2200261, doi:10.1002/mame.202200261.

47. Tierney, N.K.; Register, R.A. The Role of Excess Acid Groups in the Dynamics of Ethylene−Methacrylic Acid Ionomer Melts. *Macromolecules* **2002**, *35*, 6284–6290, doi:10.1021/MA020396U.

48. Hirasawa, E.; Yamamoto, Y.; Tadano, K.; Yano, S. Effect of Metal Cation Type on the Structure and Properties of Ethylene Ionomers. *J Appl Polym Sci* **1991**, *42*, 351–362, doi:10.1002/APP.1991.070420207.

49. Utrera-Barrios, S.; Verdejo, R.; López-Manchado, M.Á.; Hernández Santana, M. The Final Frontier of Sustainable Materials: Current Developments in Self-Healing Elastomers. *Int J Mol Sci* **2022**, *23*, 4757, doi:10.3390/IJMS23094757.

50. Zainol, M.H.; Ariff, Z.M.; Omar, M.F.; Ping, T.M.; Shuib, R.K. Self-Healable and Recyclable Nitrile Rubber Based on Thermoreversible Ionic Crosslink Network. *J Appl Polym Sci* **2022**, *139*, doi:10.1002/APP.51948.

51. Das, M.; Baran Bhattacharya, A.; Parathodika, R.; Naskar, K. Room Temperature Self-Healable and Extremely Stretchable Elastomer with Improved Mechanical Properties: Exploring a Simplistic Metal-Ligand

Interaction. *Eur Polym J* **2022**, *174*, 111341, doi:10.1016/j.eurpolymj.2022.111341.

52. Das, M.; Sreethu, T.K.; Pal, S.; Naskar, K. Biologically Derived Metal-Cysteine Coordination Complexes Crosslink Carboxylated Nitrile Rubber and Enable Room Temperature Self-Healing, Stretchability, and Recyclability. *ACS Appl Polym Mater* **2022**, *4*, 6414–6425, doi:10.1021/ACSAPM.2C00840.

53. Wajge, S.W.; Das, C. Generating Crosslinking Network in XNBR Based on Copper (I)–Carboxylate Interaction. *Polym Adv Technol* **2023**, *34*, 998–1007, doi:10.1002/PAT.5947.

# 6 Rubber Composites

# Chapter 6.    Rubber Composites

*Chapter 6 delves into a comparative analysis of ionically crosslinked XNBR reinforced with both conventional and sustainable fillers. A key focus is placed on understanding the impact of traditional fillers like carbon black (N234 and N330) and silica, and sustainable options such as cellulose and GTR, on the mechanical, thermal, self-healing and recyclability properties of the rubber. All fillers are examined at a fixed content of 10 phr to ensure a fair comparison, set against a standard matrix base on 100 phr XNBR and 5 phr ZnO. Additionally, a novel approach involving the incorporation of toner cartridges waste as an integral additive in the rubber recipe was explored. This provided insights into the challenges and opportunities of revaluing waste from electrical and electronic equipment (WEEE) in new rubber composites, with an upcycling perspective. This chapter not only uncovers the nuanced effects of various fillers on different properties but also underscores the potential and environmental significance of utilizing sustainable and recycled materials in the rubber industry, contributing to the advancement of eco-friendly ionic elastomers.*

## 6.1. Motivation

As the demand for mechanical performance and environmental sustainability increases, the development of eco-friendly reinforced rubbers is gaining ground. A key challenge in this area is the dichotomy faced when incorporating reinforcing fillers into rubbers [1]. These additives, while enhancing certain properties, can significantly restrict the mobility of macromolecular chains, adversely affecting recyclability and self-healing capabilities [2]. Achieving a trade-off between reinforcement and repair efficiency remains a persistent challenge in the design of sustainable rubbers [3–7].

**Chapter 6** provides a comparative analysis of several reinforcing fillers in XNBR-based *ionic elastomers.* Two main approaches have been followed to revisit the

intricate balance between the strength of the reinforced *ionic elastomer* and its inherent recyclability and self-healing. These approaches are centered on: (1) the use of conventional and sustainable reinforcing fillers into the rubber recipe and (2) the full integration of a waste product both as matrix and reinforcement, resulting in a ionic elastomer-based thermoplastic vulcanizate (TPV). Figure 6.1 shows a schematic representation of the two approaches.
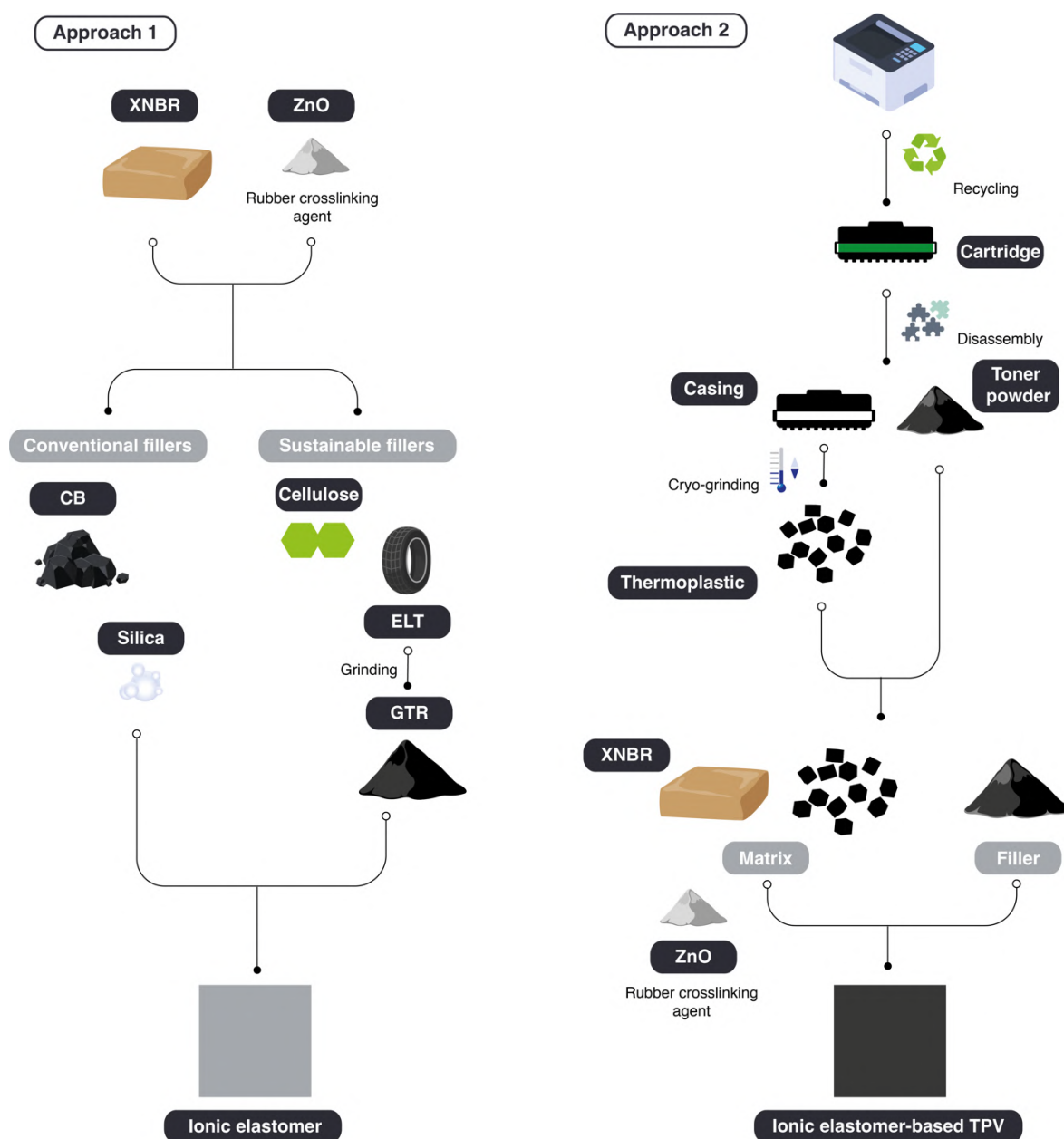


**Figure 6.1.** Schematic representation of the approaches in **Chapter 6**.

In the context of the first approach, in *ionic elastomers* the incorporation of fillers often compete with the ionic cluster formation due to reduced free volume within the matrix, implying a decrease in the crosslink density. Lower crosslink density means lower mechanical performance [8]. Several studies have tried to address this limitation with conventional fillers from a mechanical performance perspective; however, sustainability aspects (recyclability and/or repairability) have often been largely overlooked [9–11]. This means that the effects of incorporating different reinforcing fillers on the overall recyclability, self-healing ability and mechanical performance of ionically crosslinked XNBR is a question mark.

The second approach is driven by the escalating issue of toner cartridge waste disposal. A substantial portion of the approximately 370 million inkjet cartridges and 135 million toner cartridges sold annually in the EU are not recycled [12]. However, the reuse of WEEE, including waste toner, has been promoted in a wide-range of materials and applications such as asphalt binders [13,14], asphalt cement [15], foamed concrete [16], as a carbon source for the production of ferrous components [17] useful in lithium-ion batteries [18], supercapacitors [19], and pigments [20], as well as other carbon by-products such as graphene oxide quantum dots [21] and carbon electrodes for perovskite solar cells [22]. But their use in polymeric materials remains limited.

The reuse of other electronic wastes such as scrap computer plastics (SCP) (i.e., monitors, keyboards, and other hardware), mainly consisting of acrylonitrile-butadiene-styrene co-polymers (ABS), have been explored in NBR blends [23,24], but no formal studies have been found in the recent literature on the use of toner cartridge waste as an active ingredient in rubber recipes.

By addressing these research gaps, the approaches presented in **Chapter 6** are intended to contribute to the development of sustainable materials that uniquely combine robust mechanical properties with environmental viability, a challenging yet crucial goal in the realm of crosslinked rubbers.

## 6.2. Results and Discussion

### 6.2.1. Reinforcing Fillers in Ionic Elastomers

The impact of three conventional fillers, CB (N234 and N330) and silica, and three sustainable fillers, cellulose and GTR (cryo and WJ), was examined. Both Cryo-GTR and WJ-GTR were chemically modified by a sulfuric acid ($H_2SO_4$) treatment previously optimized in the research group and reported in the literature [25]. In previous chapters of this doctoral thesis, it has been established that excess ZnO plays different roles in *ionic elastomers*. One of these roles is interesting to bring up: the effect as a reinforcing additive. Recognizing this, an opportunity was identified to further optimize the recipe by substituting that function of ZnO with sustainable fillers. Therefore, this initial approach is grounded in a unfilled compound with a reduced ZnO content (5 phr). To provide a robust comparative basis, conventional fillers were also included. Table 6.1 summarizes the prepared recipes.

**Table 6.1.** Recipes for reinforced *ionic elastomers* (in phr).

| | | Conventional fillers | | | Sustainable fillers | | |
|---|---|---|---|---|---|---|---|
| Ingredient | 5ZnO | 10N234 | 10N330 | 10Sil | 10Cel | 10Cryo | 10WJ |
| XNBR | 100 | 100 | 100 | 100 | 100 | 100 | 100 |
| ZnO | 5 | 5 | 5 | 5 | 5 | 5 | 5 |
| N234 | - | 10 | - | - | - | - | - |
| N330 | - | - | 10 | - | - | - | - |
| Silica | - | - | - | 10 | - | - | - |
| Cellulose | - | - | - | - | 10 | - | - |
| Cryo-GTR | - | - | - | - | - | 10 | - |
| Cryo-WJ | - | - | - | - | - | - | 10 |

The first step in the characterization of the rubber composites was to obtain the curing curves. Figure 6.2 shows the $S'$ and $S''$ components of the torque derived from the curing curves for all the composites prepared. Table 6.2 summarizes the rheometric properties and the crosslink density obtained after the vulcanization.
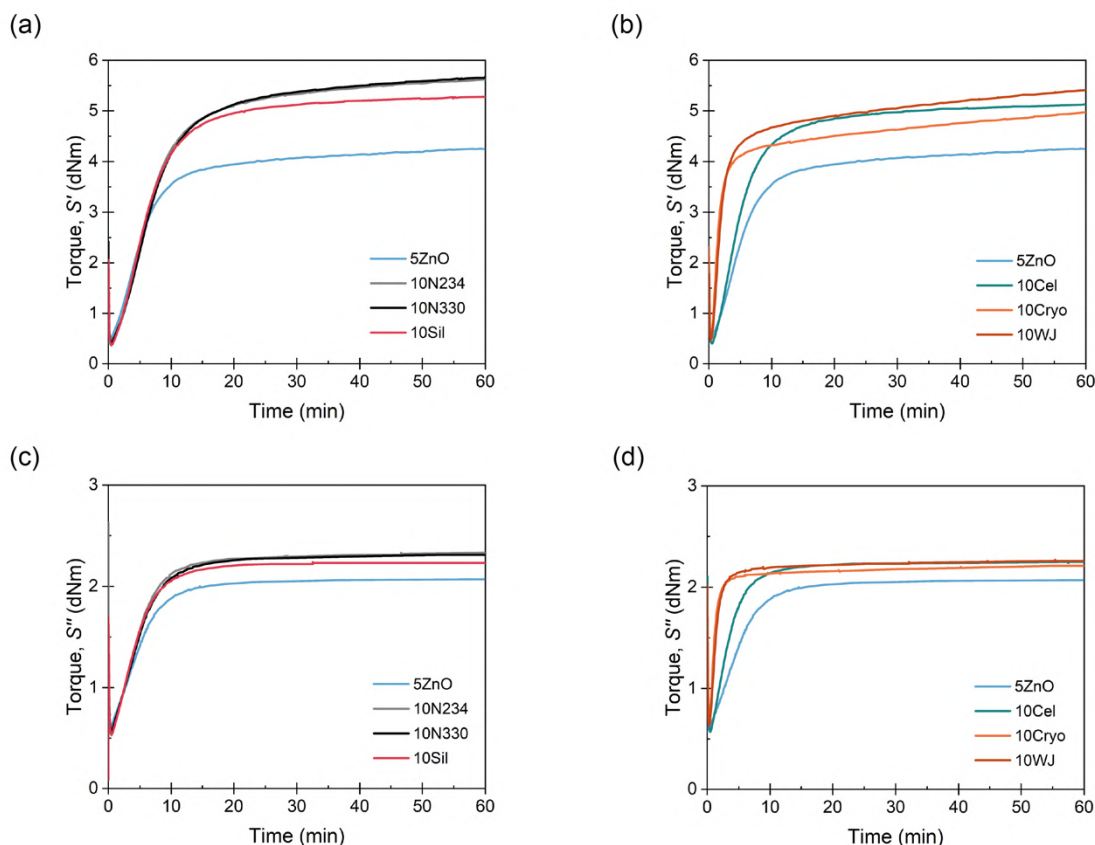


**Figure 6.2.** (a, b) $S'$ and (c, d) $S''$ of the curing curves of the *ionic elastomers* reinforced with conventional and sustainable fillers.

All the fillers used, conventional and sustainable, have a reinforcing character. This is evidenced by an increase in the ΔM value. Within the conventional fillers, the two CB show the highest reinforcing character. The MH value increases from 4.5 dNm for the unfilled composite (5ZnO) to 5.6 dNm and 5.7 dNm for N234 and N330. This would be related to better heat dissipation, a characteristic of reinforcing fillers.

**Table 6.2.** Rheometric properties and crosslink density of the filled *ionic elastomers* (in phr).

| Property | | Conventional fillers | | | Sustainable fillers | | |
|---|---|---|---|---|---|---|---|
| | 5ZnO | 10N234 | 10N330 | 10Sil | 10Cel | 10Cryo | 10WJ |
| Scorch time, ts1 (min) | 3.0 | 3.3 | 3.4 | 2.5 | 3.1 | 1.0 | 1.1 |
| Curing time, t90 (min) | 9.9 | 11.5 | 11.7 | 10.5 | 8.4 | 2.7 | 3.9 |
| Minimun torque, ML (dNm) | 0.4 | 0.4 | 0.4 | 0.4 | 0.4 | 0.5 | 0.5 |
| Maximun torque, MH (dNm) | 4.5 | 5.6 | 5.7 | 5.1 | 5.2 | 5.0 | 5.4 |
| $\Delta$M = MH − ML (dNm) | 4.1 | 5.2 | 5.3 | 4.7 | 4.8 | 4.5 | 5.0 |
| Cure rate index, CRI = 100 / (t90 − ts1) (min$^{-1}$) | 14.4 | 12.2 | 12.0 | 12.5 | 18.9 | 58.8 | 35.7 |
| Peak cure rate, PCR (dNm min$^{-1}$) | 0.4 | 0.5 | 0.5 | 0.5 | 0.7 | 1.8 | 2.1 |
| Crosslink density, $\nu$ ($\times 10^{-5}$ mol cm$^{-3}$) | 3.1 ± 0.2 | 10 ± 1 | 9.2 ± 0.9 | 11.0 ± 0.1 | 7.7 ± 0.3 | 9.7 ± 0.5 | 11.0 ± 0.1 |

The $\Delta M$ value also increases from 4.1 dNm to 5.2 dNm (10N234) and 5.3 dNm (N330), respectively. For the sustainable fillers, the greatest reinforcing effect is observed with the incorporation of GTR-WJ (10WJ), reaching MH values of up to 5.4 dNm and $\Delta M$ of 5.0 dNm, close to those obtained by CB. Positively, the incorporation of fillers does not have a negative effect on the viscosity of the composites. In all cases, the ML value remains constant around $0.4 - 0.5$ dNm. This is a positive result, since in rubbers it is expected that the incorporation of any additive of reinforcing character generates an increase in the viscosity of the sample, with the inherent difficulties of highly viscous composites during the processing stage.

In terms of curing efficiency, conventional fillers do not seem to have significant effects on ts1, t90, CRI and PCR values. In the case of t90 the differences are less than 2 min, while PCR remains practically constant. For sustainable fillers the effect is completely opposite. The incorporation of sustainable fillers seems to show an increase in curing efficiency. The t90 values decrease notably and the CRI and PCR increase both for 10Cel and for the two composites with GTR (10Cryo and 10WJ), this effect being notably higher in the latter. This could be associated with the functional groups present in the surface. Both cellulose and chemically modified Cryo-GTR and WJ-GTR are characterized by many oxygenated groups on their surface [25,26]. In polar rubbers (such as XNBR) these groups can have an accelerating effect on vulcanization [27].

The behavior of the viscous torque component curve ($S''$) confirms the formation of a single network, in this case, the one formed by the ionic bonds characteristic of the XNBR/ZnO system. On the other hand, the increase in the plateau value of $S''$ is consistent with the incorporation of the filler. Any additive added to a rubber contributes to the viscous response in the viscoelastic behavior of the crosslinked polymer [28,29].

As for the crosslink density, all the fillers increase this value compared to the unfilled system (5ZnO), increasing from $3.1 \times 10^{-5}$ mol cm$^{-3}$ to $11.0 \times 10^{-5}$ mol cm$^{-3}$, corresponding to 10Sil and 10 WJ. In the case of silica, its behavior is particularly interesting. The hydrophilic character of this filler makes it incompatible with most non-polar general-purpose rubbers, such as NR, SBR, and BR [30]. Coupling agents are usually required to improve compatibility and unlock the full reinforcing power of this filler [31–33]. In general-purpose but polar rubbers, such as CR, NBR or XNBR, no coupling agents are required as the filler is naturally compatible with the matrix [34,35]. This superior compatibility would be causing higher interactions between the filler and the rubber, which partially disrupts the formation of ionic clusters [36]. For this reason, the MH and $\Delta$M values do not increase to the same level as the CB, but the crosslink density does reach a maximum value, not due to a higher effective formation of chemical crosslinks, but probably to physical crosslinking points resulting from the filler-rubber interactions. This effect would extend to both types of GTR.

The next step in the characterization of the prepared composites was the study of the crosslinked structure. For this purpose, the samples were analyzed by DMA. As continually mentioned in previous chapters, *ionic elastomers* based on XNBR/ZnO are characterized by the formation of a separate phase, i.e. the ionic clusters, with their own thermal transition (Ti). In this sense it is interesting to know the effect of fillers on this transition, since this value is key for the self-healing and recyclability of the material. Figure 6.3 shows the results of $E'$, $E''$ and tan($\delta$) for composites with conventional and sustainable fillers.

The reinforcing effect of the fillers is confirmed by the increase in the value of $E'$ at RT (see inset in Figure 6.3a and 6.2b) for both types. Two notable drops are visualized in the $E'$ curve, associated with two thermal transitions, while the $E''$ curves confirm the third transition at subzero temperatures (Figure 6.3c and 2d). As described in previous chapters, these three transitions correspond to $\beta$ relaxation, $\alpha$

relaxation and α' relaxation with increasing temperature. Being α and α' particularly relevant as they are associated to Tg and Ti, respectively.
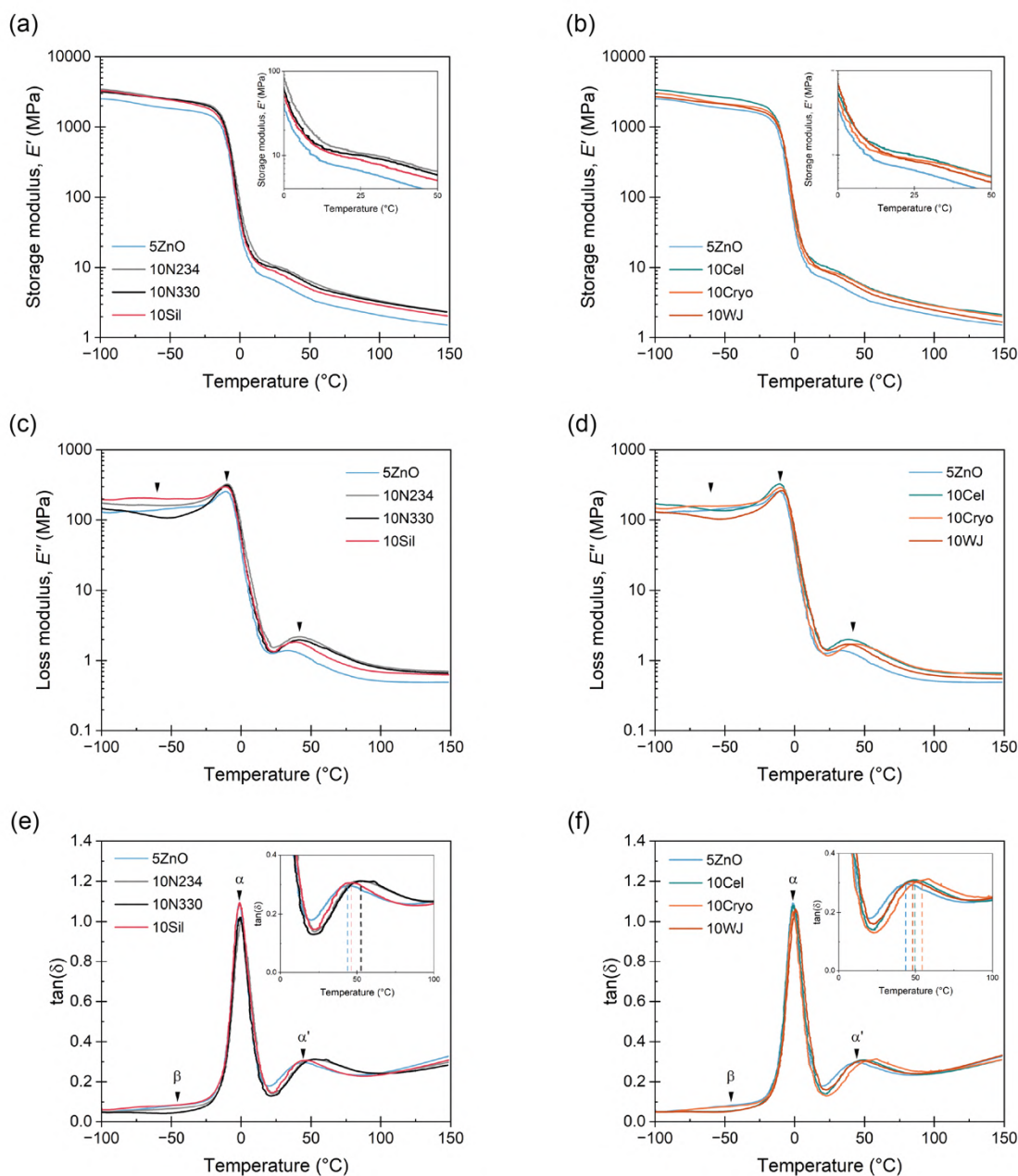


**Figure 6.3.** $E'$, $E''$ and tan(δ) of the prepared *ionic elastomers* reinforced with conventional and sustainable fillers.

To follow the changes in the two main transitions caused by both types of fillers, tan(δ) was plotted as a function of temperature (Figure 6.3e and 6.2f). Table 6.3 summarizes the temperature values of both transitions (Tg and Ti) determined at the maximum of the peak corresponding to tan(δ).

**Table 6.3.** Thermal properties of the unfilled and filled *ionic elastomers* (in phr).

| Compound | Tg DMA (°C)[1] | Ti DMA (°C)[1] | Tg DSC (°C)[2] | Td (°C)[3] |
|---|---|---|---|---|
| 5ZnO | −1.3 | 44.9 | −21.5 | 402.9 |
| **Conventional fillers** | | | | |
| 10N234 | −0.2 | 52.4 | −17.9 | 423.3 |
| 10N330 | −0.2 | 52.2 | −18.6 | 423.5 |
| 10Sil | −1.0 | 45.7 | −18.8 | 394.0 |
| **Sustainable fillers** | | | | |
| 10Cel | −1.1 | 50.0 | −19.3 | 422.3 |
| 10Cryo | −1.1 | 54.1 | −17.4 | 419.3 |
| 10WJ | 0.4 | 48.1 | −16.6 | 417.5 |

[1] Maximum of the relaxation (Maximum of tan(δ) by DMA).

[2] Thermal Tg (Midpoint by DSC).

[3] First degradation zone (Onset by TGA). Td pure XNBR: 391.4.

In the case of α relaxation, a slight increase in Tg is observed in presence of the fillers. This effect is more evident in the composites with CB and WJ-GTR. Tg increases from −1.3 °C in 5ZnO to −0.2 °C in 10N234 and N330, and to 0.4 °C in 10WJ. This change is consistent with the higher values of MH and ΔM reported for

these composites, which implies that the reinforcing character of these fillers is higher and would be imposing some minor restrictions on the mobility of the amorphous polymeric chains. For α' relaxation all fillers have a more restrictive effect on the mobility of the ionic phase, except silica. With increases between 4 °C and 10 °C of Ti. This effect is again particularly important for CB, N234 and N330, going from 44.9 °C to 52.4 °C and 52.2 °C, respectively. 10Sil, on the other hand, remains constant, with a difference of less than 1 °C. As for the sustainable fillers, they generate a restriction on both relaxations, but the secondary interactions that could form between the functional groups on the surface of this fillers and the different functional groups of XNBR (carboxyl and nitrile), as well as the filler-filler interactions themselves (agglomerates), could make it difficult to analyze the behavior of the material.

DSC and TGA scans were performed to further investigate the effects of the fillers on the thermal properties of the prepared composites. Figure 6.4 shows the results obtained and Table 6.3 summarizes the values of the thermal Tg (Tg determined by DSC) and the main degradation temperature (Td). The effects of the fillers on thermal Tg are evident. In this case, all types increase the Tg between 2 °C and 5 °C, which would be associated with the increase of the restrictions on the mobility of the macromolecular chains, due to the reinforcing character previously mentioned. This effect would be higher in the fillers that reported the highest values of MH and ΔM (CB and WJ-GTR) and lower for the fillers that reported the lowest values (cellulose and Cryo-GTR), correlating very well the three parameters.

Regarding the thermal stability of the material, almost all fillers improve the degradation temperature of 5ZnO up to 15 °C and above. 10Sil, on the other hand, decreases this value by almost 8 °C. This is probably another indicator of a decreased ionic phase, due to an increase in filler-rubber interactions.
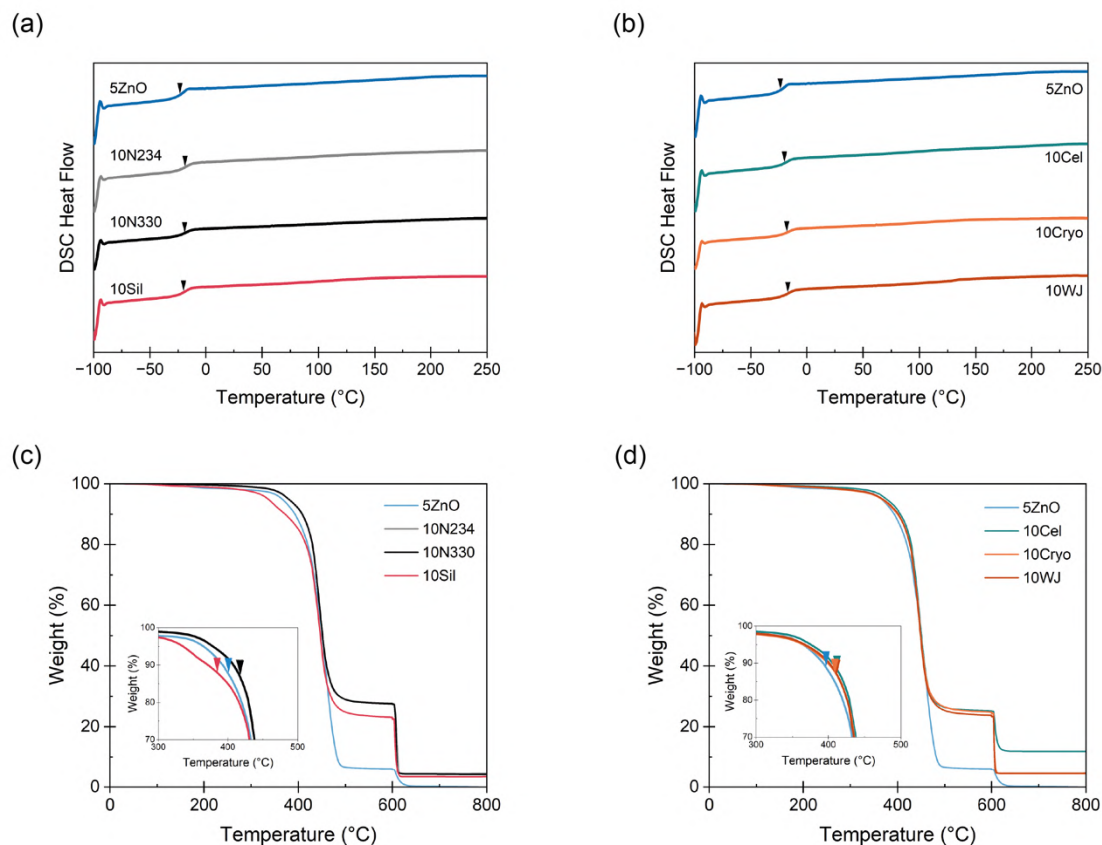
**Figure 6.4.** (a, b) DSC spectra and (c, d) thermogravimetric curves of the prepared *ionic elastomers* reinforced with conventional and sustainable fillers.

The complete characterization of the prepared composites required the analysis of the tensile mechanical properties as well as the hardness of the prepared materials. Figure 6.5 shows the stress-strain curves for composites filled with conventional and sustainable systems. Table 6.4 summarizes all the properties that can be obtained from these curves.

The incorporation of fillers has a remarkable effect on the mechanical properties of the unfilled *ionic elastomer* (5ZnO). All the modulus values at different strain rates (M100, M300 and M500) and, consequently, the hardness increase. As a measure of the reinforcing capacity, a tensile reinforcement index (RI) was calculated as the ratio between the M500 values of the filled and the unfilled composites. The

reinforcing character of conventional fillers (N234, N330, Silica) and the sustainable WJ-GTR was evident, with about a two-fold increase in M500 values.
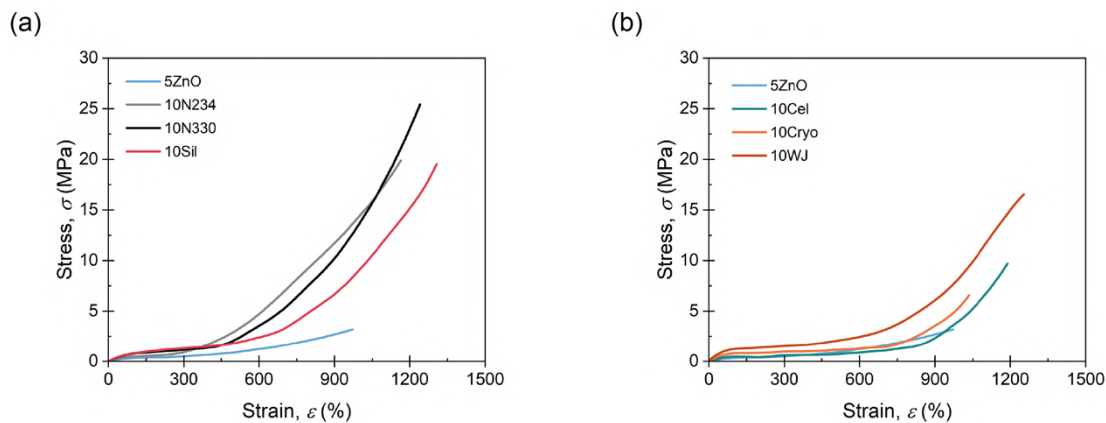


**Figure 6.5.** Stress-strain curves of the prepared *ionic elastomers* reinforced with (a) conventional and (b) sustainable fillers.

This effect was also manifest in the values at the breaking point. Conventional fillers reached equivalent TS between 21 MPa and 25 MPa, and equivalent EB between 1260 % and 1341 %. On the other hand, WJ-GTR achieves reinforcement values close to silica, increasing the TS up to 17 MPa (10WJ), in addition to a slight increase in EB. *Ionic elastomers* reinforced with cellulose and cryo-GTR (10Cel and 10Cryo) exhibit a more modest reinforcing character but increase the TS of the base composite more than twofold to 8.9 MPa and 7.0 MPa, respectively, without a detriment in the deformability of the material. This reinforcing character was further explored through the Payne effect.

**Table 6.4.** Mechanical properties of the filled *ionic elastomers* (in phr).

| Property | | Conventional fillers | | | Sustainable fillers | | |
|---|---|---|---|---|---|---|---|
| | 5ZnO | 10N234 | 10N330 | 10Sil | 10Cel | 10Cryo | 10WJ |
| Stress at 100 % strain, M100 (MPa) | $0.5 \pm 0.1$ | $0.7 \pm 0.2$ | $0.8 \pm 0.3$ | $0.8 \pm 0.2$ | $0.9 \pm 0.2$ | $0.9 \pm 0.1$ | $1.0 \pm 0.3$ |
| Stress at 300 % strain, M300 (MPa) | $0.8 \pm 0.2$ | $1.0 \pm 0.1$ | $1.2 \pm 0.2$ | $1.2 \pm 0.2$ | $1.1 \pm 0.3$ | $1.1 \pm 0.1$ | $1.5 \pm 0.3$ |
| Stress at 500 % strain, M500 (MPa) | $1.0 \pm 0.1$ | $2.3 \pm 0.6$ | $2.2 \pm 0.4$ | $1.8 \pm 0.2$ | $1.3 \pm 0.3$ | $1.3 \pm 0.1$ | $1.9 \pm 0.3$ |
| Reinforcement index, RI $\phantom{x}$ RI = M500$_{\text{filled}}$ / M500$_{\text{unfilled}}$ | - | 2.3 | 2.2 | 1.8 | 1.3 | 1.3 | 1.9 |
| Tensile strength, TS (MPa) | $3.5 \pm 0.3$ | $23 \pm 5$ | $25 \pm 1$ | $21 \pm 2$ | $8.9 \pm 0.9$ | $7.0 \pm 1$ | $17 \pm 2$ |
| Elongation at break, EB (%) | $1100 \pm 81$ | $1267 \pm 88$ | $1260 \pm 32$ | $1341 \pm 105$ | $1173 \pm 34$ | $1073 \pm 60$ | $1349 \pm 102$ |
| Hardness (Shore A) | $39 \pm 5$ | $46 \pm 4$ | $47 \pm 2$ | $46 \pm 4$ | $41 \pm 3$ | $41 \pm 1$ | $44 \pm 1$ |

**Analyzing the Payne Effect in Reinforced Ionic Elastomers**

The reinforcement in filled rubbers is linked to the interaction between the matrix and the filler, along with the dispersion of the solid particles within the matrix. Key indicators of this reinforcement behavior include the bound rubber, which refers to polymer chains adsorbed on the filler surface, and the strain-dependence of the modulus.

According to Payne's theory, rubber reinforcement is influenced by four factors: three are strain-independent – (i) the rubber network, linked to crosslink density, (ii) the hydrodynamic effect arising from the mechanical hindrance to deformation caused by (spherical) particles in the rubber matrix, and (iii) the filler-rubber interactions, where filler particles act as physical polyfunctional crosslink sites and immobilize parts of the rubber within the filler structure, thus contributing to stiffness. The fourth factor is strain-dependent, associated with (iv) the filler-filler interactions (filler network). Figure 6.6 illustrates the contributions.
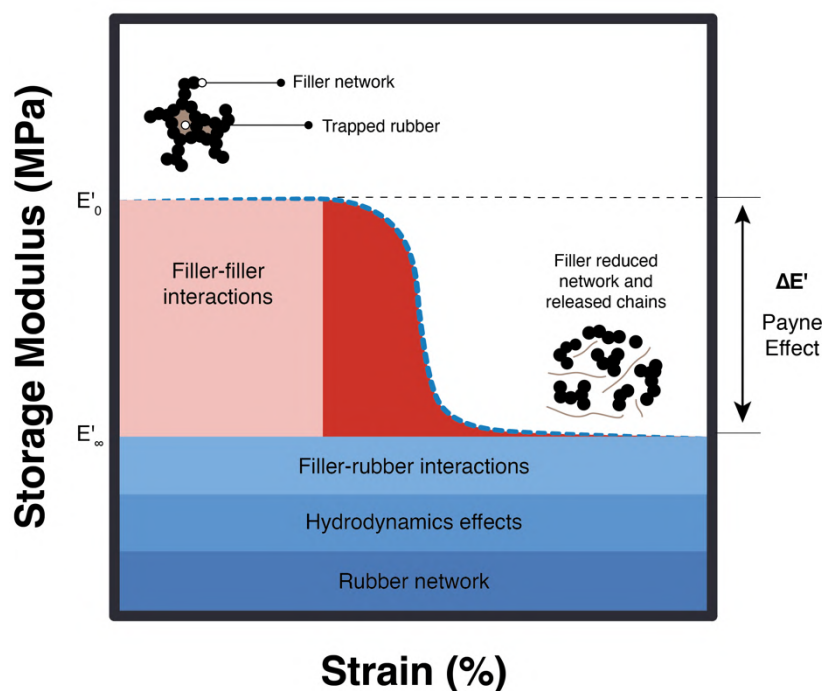


**Figure 6.6.** The Payne effect.

The decrease in $E'$ with increasing strain is called the Payne effect. This reduction is attributed to the gradual breakdown of weak filler-filler interactions (like hydrogen bonds and Van der Waals forces) in a nonlinear regime. Concurrently, rubber trapped within the filler network, known as occluded rubber, is released, enhancing mobility and thereby reducing $E'$. The Payne effect ($\Delta E$), representing the difference between the modulus at low deformations ($E'_0$) and at very high deformations ($E'_\infty$), serves as an indicator of filler-filler interactions. To study this effect, strain sweeps from 0.01 % to 40 % were conducted using DMA at a fixed temperature of 30 °C and a frequency of 1 Hz. Figure 6.7 and Table 6.5 summarizes the results obtained.
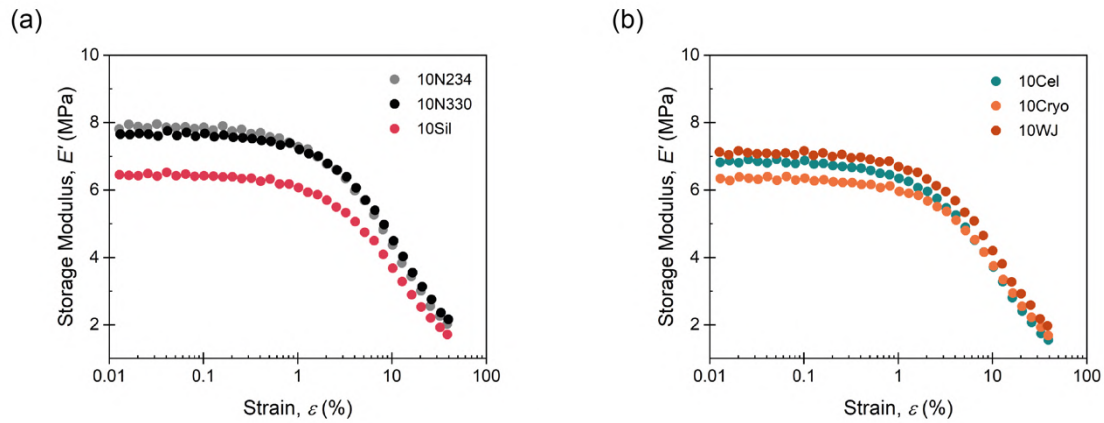


**Figure 6.7.** Strain sweeps by DMA of the *ionic elastomers* reinforced with (a) conventional and (b) sustainable fillers.

The strain sweeps show interesting trends. With conventional fillers, a higher $\Delta E$ is observed for the 10N234 and N330 composites. This would accuse that the mechanism of CB reinforcement in these composites would be strongly influenced by the formation of a distributed filler network in the XNBR matrix. Such filler network is broken with strain, increasing the Payne effect. In contrast, the 10Sil composite exhibited the lowest $\Delta E$. This could be a clear example of the above mentioned factor related to the compatibility of the matrix with silica, due to its polar characters. The increase in the filler-rubber interactions would decrease the Payne

effect. In this sense, the reinforcement provided by the silica in the *ionic elastomer* would be due to its interaction with the matrix, in accordance with previously discussed trends on rheometric properties and crosslink density.

For sustainable systems, the 10Cel composite exhibits the highest $\Delta E$. This may be caused by the large number of polar groups on the cellulose surface (essentially hydroxyl) that promote the formation of intramolecular hydrogen bonds [37,38]. As these intermolecular interactions increase, filler agglomerates increase and thus the Payne effect [39]. Regarding the composites with GTR, a higher Payne effect is observed in 10WJ. This is consistent with its superior mechanical properties and would be indicative that WJ-GTR is able to form a more effective filler network, while having better filler-rubber interactions (higher $E'_\infty$) [36].

**Table 6.5.** Payne effect of the reinforced *ionic elastomers.*

| Compound | $E'_0$ (MPa) | $E'_\infty$ (MPa) | $\Delta E$ (MPa) |
|---|---|---|---|
| 5ZnO | 6.10 | 1.82 | 4.28 |
| **Conventional fillers** | | | |
| 10N234 | 7.81 | 2.02 | 5.79 |
| 10N330 | 7.66 | 2.17 | 5.49 |
| 10Sil | 6.45 | 1.72 | 4.73 |
| **Sustainable fillers** | | | |
| 10Cel | 6.82 | 1.54 | 5.28 |
| 10Cryo | 6.34 | 1.69 | 4.65 |
| 10WJ | 7.13 | 1.97 | 5.16 |

## Reinforcing vs Sustainability: What Happened to Self-Healing Capacity and Recyclability?

Up to this point, it has been observed that the conventional fillers, as expected, are the ones that provide a greater reinforcing effect; on the other hand, the sustainable fillers are promising, being particularly relevant the WJ-GTR for its closeness to the performance of the conventional ones, with the advantage of its recovered waste character. It is now imperative to analyze how these fillers impact the sustainability of the prepared *ionic elastomers*. Starting with self-healing, Table 6.6 shows the results obtained under the optimized BDS protocol described in **Chapter 5**.
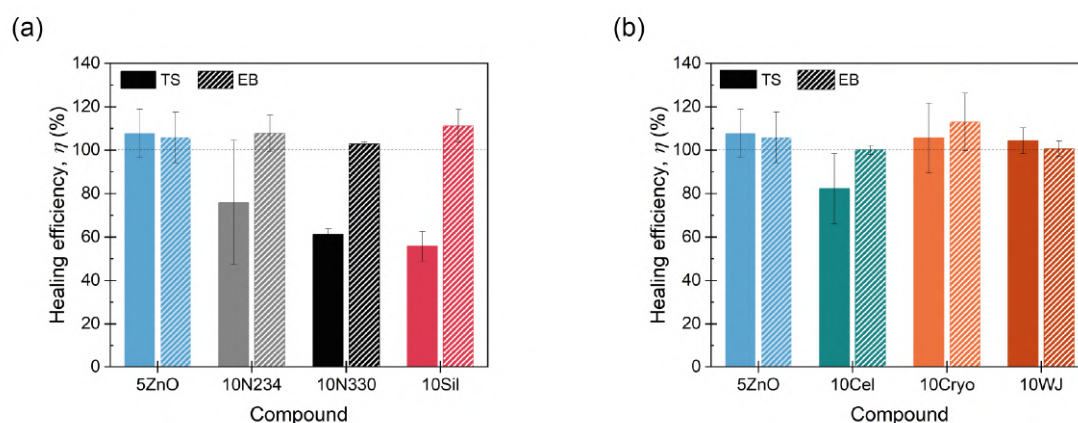


**Figure 6.8.** Healing efficiency at fixed temperature (110 °C) and time (3 h) of the prepared *ionic elastomers* reinforced with (a) conventional and (b) sustainable fillers.

The addition of fillers poses a challenge, as it impedes a key concept of self-healing: mobility [2]. Focusing on conventional fillers, a decrease in self-healing capacity is evident. The classic trade-off between mechanical reinforcement and repair efficiency becomes apparent: as one improves, the other diminishes [1,3]. Despite this, the repair efficiencies observed in 10N234 (76 %), 10N330 (61 %), and 10Sil (57 %) remain competitive, considering their substantial mechanical reinforcement. Besides,

all systems with conventional fillers successfully restore their deformability (EB) with 100 % efficiency.

The effects of sustainable fillers are radically different and represent the major finding of this **Chapter 6**. Despite the reinforcing character of cellulose and the two GTR, the healing efficiency is not substantially affected. In the particular case of 10Cel, a TS efficiency of 83 % is achieved, which, although slightly lower than 5ZnO, represents a very good result (> 80 %) in the context of self-healing materials; but the most outstanding results are obtained with the GTRs. Both 10Cryo and 10WJ can fully restore TS and EB (efficiencies of 100 %). This is particularly interesting considering that 10WJ exhibited a reinforcement index almost equivalent to conventional systems. In this sense, this prepared recipe represents a great accomplishment, having achieved the desired trade-off between reinforcement and healing efficiency, so elusive in the context of reinforced rubbers using sustainable fillers. This healing capability could be due to the presence of polar groups on its surface caused by the previously optimized chemical treatment [25]. These polar groups offer new sites (healing moieties) for the ion-hopping mechanism, which would favor the dynamics of the ionic transition, in addition to the formation of sacrificial secondary interactions, such as hydrogen bonds, which is another intrinsic healing mechanism widely used in rubber-based self-healing materials.

Regarding the recyclability of the composites, Figure 6.9 and Figure 6.10 show the stress-strain curves after a recycling cycle for all the reinforced *ionic elastomers*, with conventional and sustainable filler, respectively. The first notable outcome is that all the composites can maintain the hyperelastic behavior characteristic of crosslinked rubbers. Moreover, except for the 10N330 and 10Sil, it can be stated that each sample is capable of fully recycling, recovering about 100 % of their properties at the breaking point.
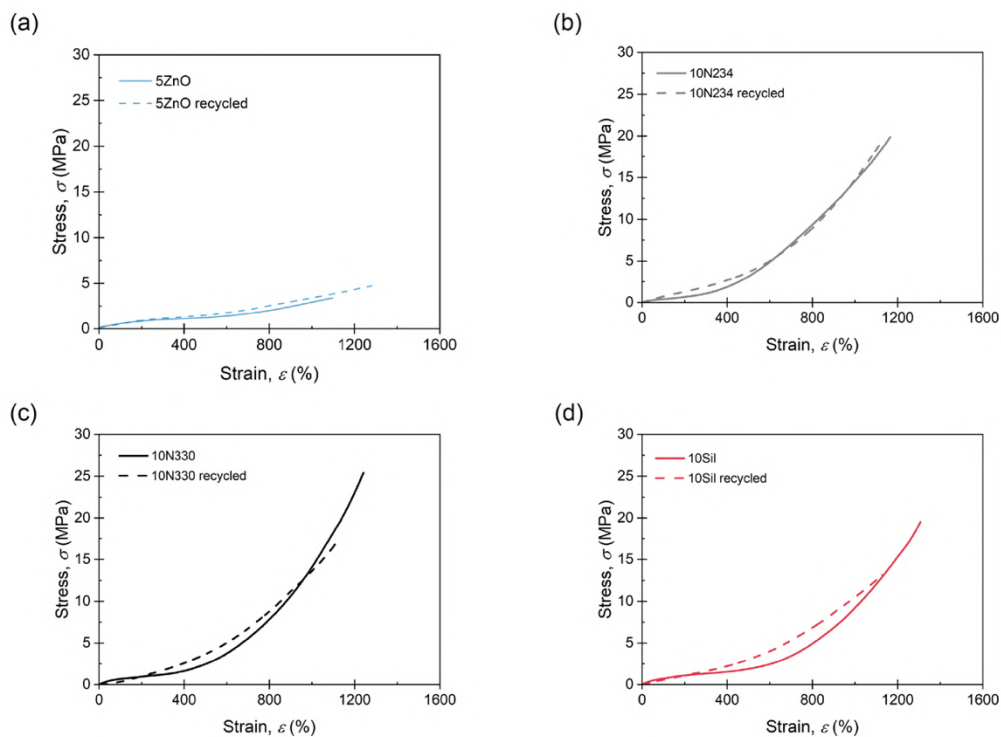
**Figure 6.9.** Stress-strain curves of the prepared *ionic elastomers* reinforced with conventional fillers before and after the recycling protocol.
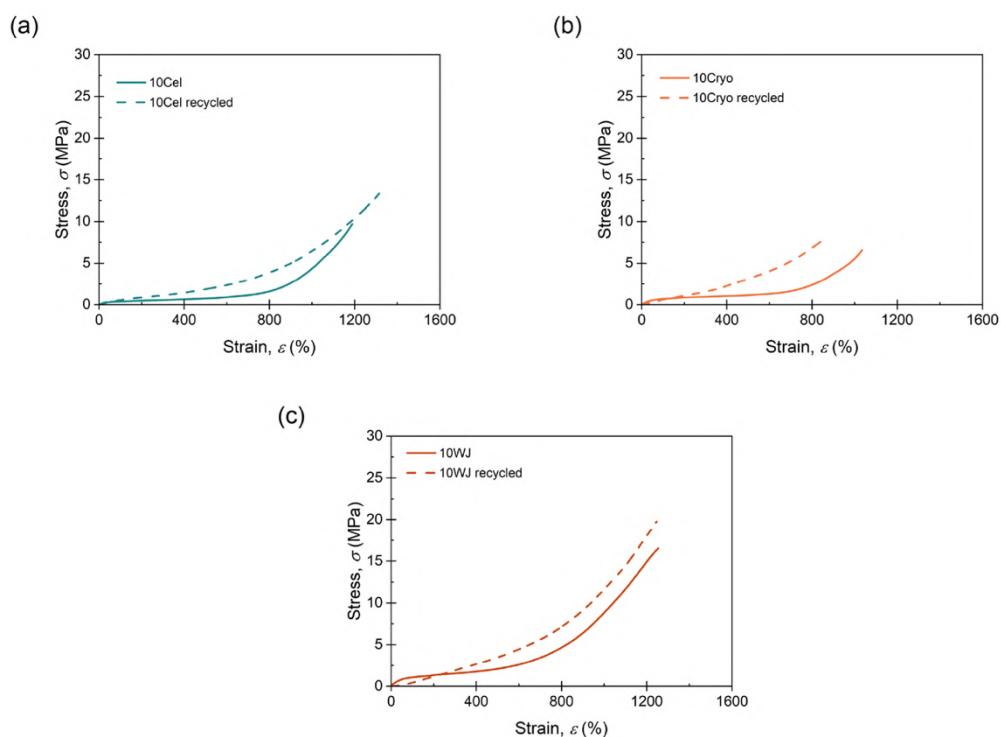


**Figure 6.10.** Stress-strain curves of the prepared *ionic elastomers* reinforced with sustainable fillers before and after the recycling protocol.

This approach presents a significant breakthrough: the identification of a sustainable filler that almost matches conventional fillers in performance, yet far surpasses them in terms of sustainability. WJ-GTR not only reinforced the unfilled *ionic elastomer* but also excels in critical aspects of recyclability and self-healing. These advancements have been realized while concurrently reducing the ZnO content, perfectly aligning with our initial motivation to develop more sustainable and efficient elastomer solutions. This discovery marks a pivotal step forward in the field, offering a path to more environmentally responsible rubbers without major effects on mechanical performance, and indeed, enhancing sustainability.

## 6.2.2. Toner Cartridge Waste as an Additive in Ionic Elastomer Recipe

This section turns its attention to the second approach: utilizing toner cartridge waste as an integral additive in *ionic elastomers*. For the preparation of the materials, the black thermoplastic cartridge components, identified as high-impact polystyrene (HIPS), and toner powder, were selected. The objective is that the thermoplastic components blend with the XNBR as a combined matrix, while the toner powder serves as a reinforcing filler. This resulted in a ionic elastomer-based TPV.

A constant XNBR/thermoplastic ratio of 90/10 was selected since higher thermoplastic contents significantly impair the elasticity of the material [40]. The following analysis delves into the recipe, mechanical properties, and self-healing abilities of these unique composites, aiming to unfold the potential of toner waste in rubber manufacturing. Table 6.6 summarizes the prepared recipes.

The curing curves and parameters are shown in Figure 6.11a and Table 6.7, respectively. According to the curing parameters, a decrease in $\Delta M$ value was observed with the incorporation of the TP. This reduction could be attributed to two phenomena. First, the thermoplastic nature of some of the components in TP. with a softening point far below 160 °C. TP usually contains a blend of polyester

resin or styrene acrylic copolymers, waxes, and other additives at low concentrations [41]. These small fractions allows it to remain in a state of maximum mobility at the curing temperature, thereby reducing the viscosity and torque of the system. Similar results were reported by Pichaiyut et al. [42] on blends of epoxidized natural rubber (ENR) with thermoplastic polyurethane (TPU). A viscosity reduction of almost half a decade was observed when the ENR/TPU content was varied from 50/50 to 40/60 (i.e., by increasing the thermoplastic phase). Second, the presence of an additive (TP) that does not participate in the formation of crosslinking points with ZnO.

**Table 6.6.** Recipes of the prepared TPV (in phr).

| Ingredient | Unfilled | T5 | T10 | T20 |
|---|---|---|---|---|
| XNBR | 100 | 100 | 100 | 100 |
| Thermoplastic | 11.2 | 11.2 | 11.2 | 11.2 |
| ZnO | 10 | 10 | 10 | 10 |
| Black toner powder (TP) | - | 5 | 10 | 20 |
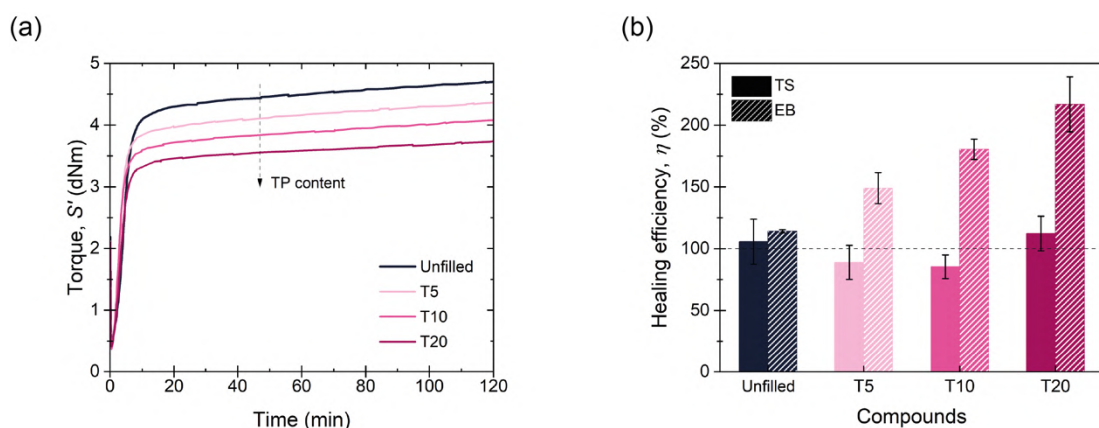


**Figure 6.11.** (a) Curing curves and (b) healing efficiency of the TPV.

**Table 6.7.** Rheometric properties and crosslink density of the TPV.

| Curing parameters | Unfilled | T5 | T10 | T20 |
|---|---|---|---|---|
| Scorch time, ts1 (min) | 3.1 | 1.5 | 1.4 | 1.6 |
| Curing time, t90 (min) | 18.1 | 19.9 | 18.7 | 14.1 |
| Minimun torque, ML (dNm) | 0.5 | 0.4 | 0.4 | 0.4 |
| Maximun torque, MH (dNm) | 4.7 | 4.4 | 4.1 | 3.7 |
| $\Delta M = MH - ML$ (dNm) | 4.2 | 3.9 | 3.7 | 3.3 |
| Cure rate index, CRI $= 100 / (t90 - ts1)$ (min$^{-1}$) | 6.7 | 5.4 | 5.8 | 8.0 |
| Peak cure rate, PCR (dNm min$^{-1}$) | 0.73 | 0.89 | 0.85 | 0.70 |
| Crosslink density, $\nu$ ($\times 10^{-5}$ mol cm$^{-3}$) | $1.6 \pm 0.2$ | $1.7 \pm 0.1$ | $1.23 \pm 0.01$ | $1.54 \pm 0.03$ |

A noticeable change in the t90 at high black toner powder content (20 phr) (a decrease of more than 4 min) was also detected. In addition, ts1 of the filled composites were shorter than those of the unfilled one. This phenomenon may be due to the presence of CB, silica, and iron oxide in the toner, which is more accentuated at higher toner contents, as discussed below. The presence of these additives tends to promote higher heating rates in the sample, thereby increasing the curing degree and decreasing curing time [1]. The mechanical tensile performance, hardness, and crosslink density of the prepared materials were evaluated, and the results are listed in Table 6.8.

It is evident that at higher black toner contents, the modulus at low and medium deformations, hardness, and TS increased. This is because of the typical rubber reinforcing fillers in the powder (such as CB, iron oxide or silica), which improve the mechanical performance of the material [41]. Although the specific composition of the toner powder of this HP product is protected by trade secrets, some studies on other generic brands have shown, for example, that the CB, silica and iron oxide content can vary between 1 % and 40 % [43]. These broad range depend greatly on the quality of the toner and printing capacity. In this way, the reinforcing character of black toner powder in rubber composites at medium and high proportions was demonstrated.

It should be noted that the mechanical properties do not follow a linear trend when the powder content is varied because when 5 phr were added, there was a drop in all mechanical parameters with respect to the unfilled material. These values were increased only by increasing the content to 10 phr and 20 phr. As commented before, TP usually contains a blend of polyester resin or styrene acrylic copolymers, waxes, and other additives at low concentrations [41], which can have a degrading, diluent, or plasticizing effect, with a greater effect at lower concentrations. Nonetheless, this effect can be compensated at higher contents by the presence of CB, silica, and iron oxide.

**Table 6.8.** Mechanical properties and crosslink density of the TPV.

| Parameters | Unfilled | T5 | T10 | T20 |
|---|---|---|---|---|
| Stress at 100 % strain, M100 (MPa) | 0.6 ± 0.3 | 0.8 ± 0.1 | 0.9 ± 0.2 | 1.1 ± 0.4 |
| Stress at 300 % strain, M300 (MPa) | 1.2 ± 0.3 | 0.9 ± 0.1 | 1.2 ± 0.1 | 1.1 ± 0.3 |
| Tensile strength, TS (MPa) | 6.6 ± 0.2 | 3.4 ± 0.1 | 7.7 ± 0.9 | 9.9 ± 0.8 |
| Elongation at break, EB (%) | 1111 ± 57 | 1034 ± 34 | 1251 ± 46 | 1285 ± 41 |
| Hardness (Shore A) | 55 ± 1 | 52 ± 1 | 61±1 | 65 ± 1 |

Regarding the self-healing capacity, all the filled composites exhibited TS and EB healing efficiencies higher than 85 % (Figure 6.11b). The recipe with 20 phr of toner stood out, in which evident mechanical reinforcement was achieved with an increase of 50 % in the TS without affecting the EB and self-healing efficiency, with a value of 112 %. This result is particularly promising because the dichotomy between the repairability and mechanical properties has been again overcome.

The healing capacity of the prepared materials was the result of two combined mechanisms: intrinsic and extrinsic (Figure 6.12). The intrinsic self-healing mechanism is due to the dynamic nature of the ionic clusters. This dynamic character has been demonstrated in previous chapters and extensively discussed in the literature [40,44–46]. When subjected to temperatures above the Ti, these clusters gain mobility and participate in ion-hopping [47,48]. This allows for system-wide rearrangement of ions, which in turn enables damage repair. Simultaneously, an extrinsic repair mechanism was promoted by the incorporation of a thermoplastic into the blend. This process is thermally activated at temperatures around the thermoplastic softening point (120 °C). When exposed to the healing protocol, the thermoplastic diffused within the elastomeric matrix, restoring the damaged areas by creating new molecular entanglements due to the randomization of the polymeric chains.
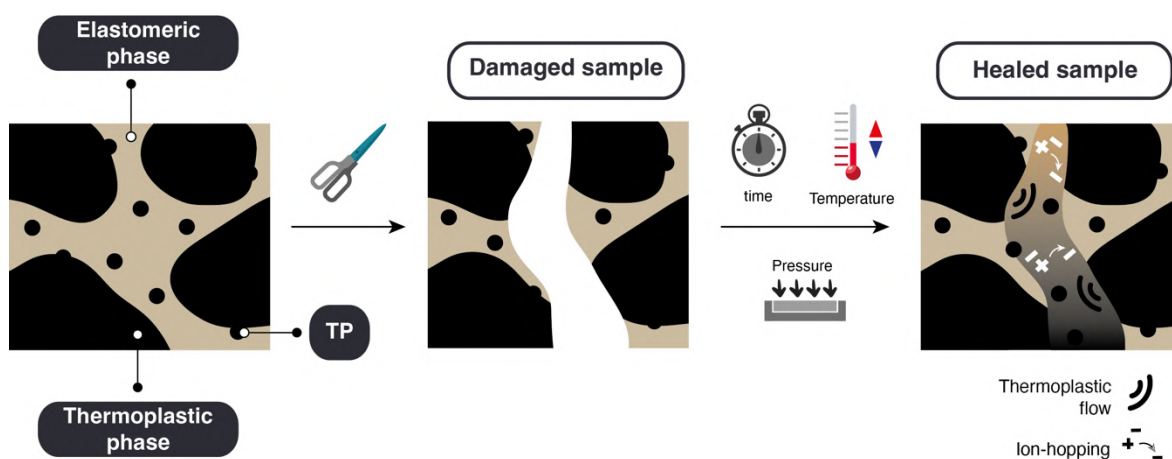


**Figure 6.12.** Self-healing extrinsic and intrinsic mechanisms.

The thermal stability of the composites at high temperatures was also studied. Figure 6.13 shows the thermogravimetric curves, demonstrating that the incorporation of the filler, regardless of its content, did not affect the thermal stability of the developed materials, despite the concentration of thermoplastics, waxes, and other low and medium molecular weight substances in the typical TP composition [43].
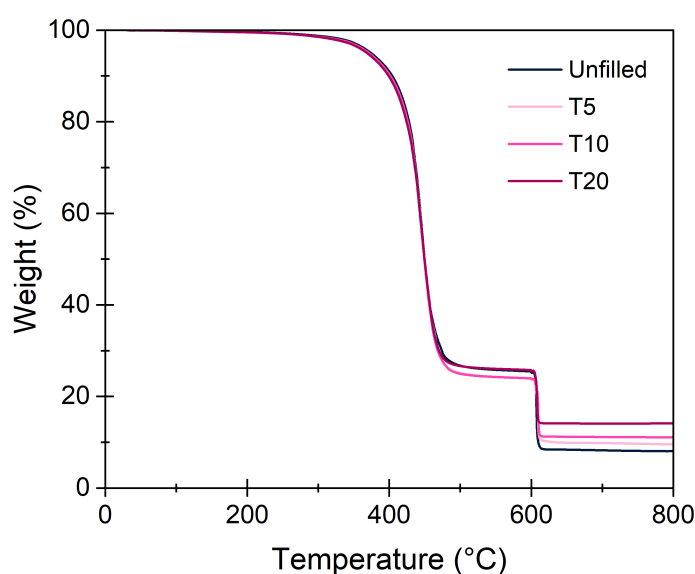


**Figure 6.13.** Thermogravimetric curves of the TPV.

To further extend the reach of this sustainable approach, the study did not limit itself to black toner powder recovery alone but also included the analysis of colored toners, effectively widening the range of waste utilization. In this context, an overall comparison of black and red toners was made at a fixed content of 20 phr. Unlike black toner, which is known for its CB and silica content and acts as an effective reinforcing filler, red toner contains different substances that confer its color [49]. Figure 6.14a and 13b show the results. The impact of red toner (R20) on the mechanical properties was evidenced, yielding a TS of $8.4 \pm 0.4$ MPa and an EB of

$1372 \pm 3$ %. After the thermal protocol, healing efficiencies of 85 % in the TS and 75 % in the EB were determined. The reinforcing capability of the red toner was found to be less effective than that of the black toner (T20) (approximately 27 % increase, compared to + 50 % for black powder). Despite this, the self-healing values attained were positive (>70 %), thus demonstrating that color cartridges could also be effectively used within the same strategy for applications with other mechanically demanding requirements.
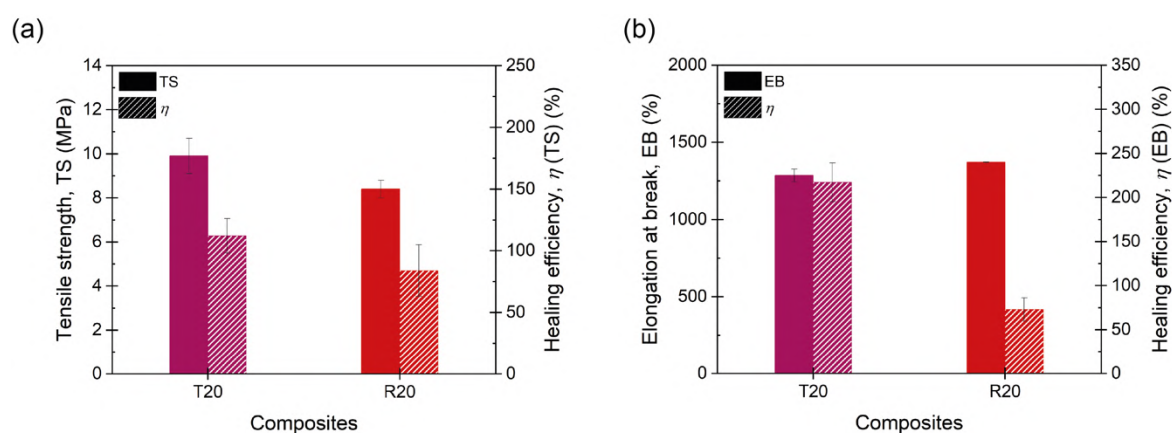


**Figure 6.14.** (a) TS and (b) EB healing efficiency of the *ionic elastomers* filled with black (T20) and red (R20) toner powders.

## 6.3. Summary

Delving into two distinct approaches, this **Chapter 6** first examines a variety of fillers, both conventional and sustainable. The selected fillers demonstrated their reinforcing capacity, notably increasing the mechanical performance of the unfilled *ionic elastomer*. Moreover, the composites demonstrated complete recyclability, preserving their characteristic hyperelastic behavior, as evidenced in the stress-strain curves. The most significant variations emerged in the self-healing capacity, which was notably reduced in the composites with conventional fillers, thus affecting their overall sustainability. However, the integration of sustainable options like cellulose

and GTR led to a favorable balance between repair efficiency, recyclability, and mechanical performance. Notably, the composite with 10 phr of WJ-GTR (10WJ) stood out, showing reinforcement levels on par with conventional composites (10Sil) while simultaneously maintaining 100 % self-healing and recycling efficiencies.

The second approach pivots towards a more unconventional path, exploring the feasibility of utilizing toner cartridge waste as an integral additive in a rubber recipe. The potential of black toner powder, a by-product of cartridge waste, as a reinforcing filler was also confirmed, with an increase of up to 50 % in TS when 20 phr of the powder were incorporated into the sustainable blend, composed of rubber and thermoplastic scrap obtained from the cartridge casing. Additionally, without affecting the outstanding healing performance. The successful incorporation of colored toner powder illustrates the possibility of harnessing the full spectrum of the cartridge waste. This approach introduces a new way of looking at waste management and sustainable materials, not only considering a strategy for the reuse of waste, but also enhancing the mechanical performance of *ionic elastomers* with an upcycling perspective. Figure 6.15 shows a representative schematic summarizing **Chapter 6**.
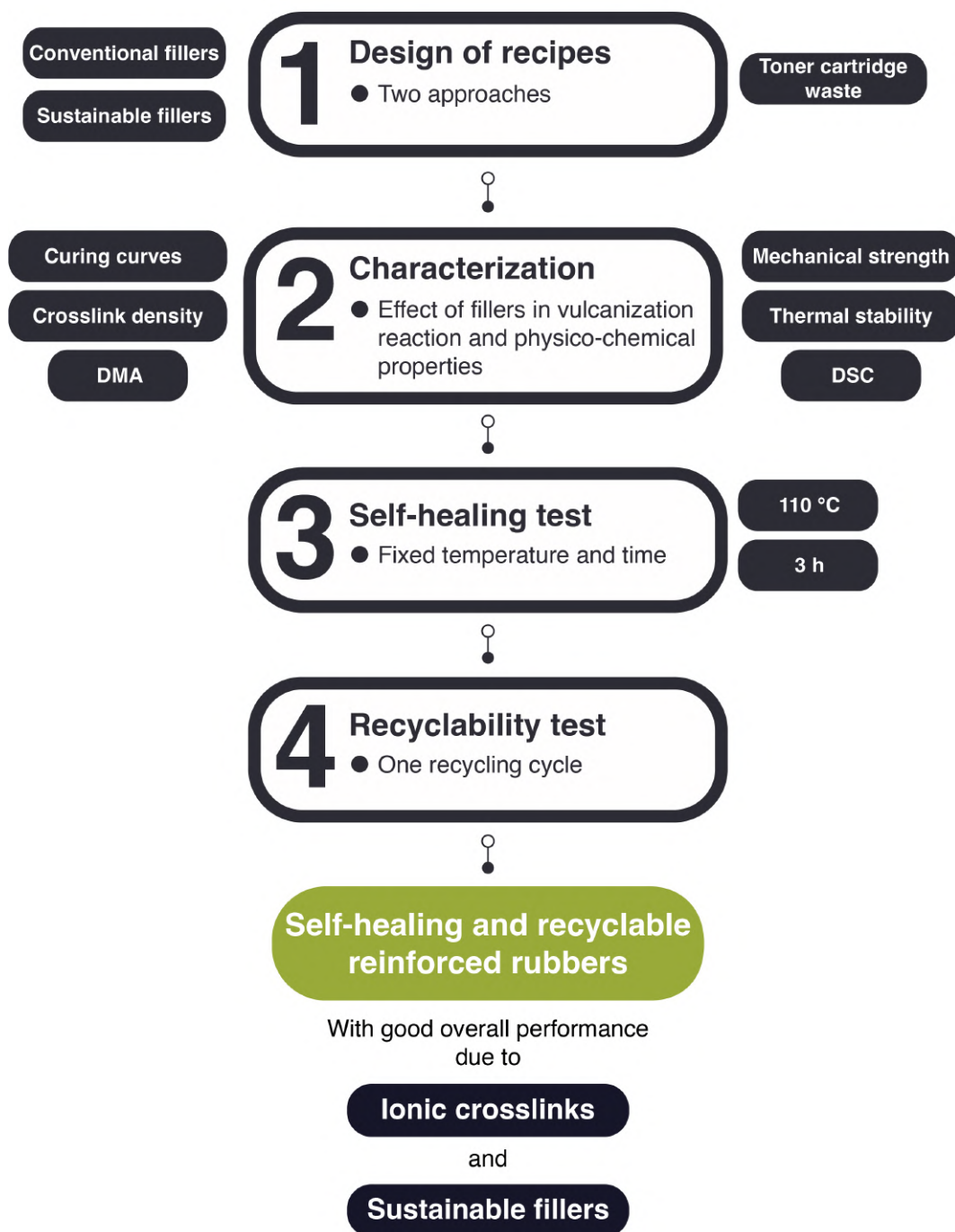
**Figure 6.15.** Schematic representation of **Chapter 6**.

## References

1.    Araujo-Morera, J.; Utrera-Barrios, S.; Olivares, R.D.; Verdugo Manzanares, R.; López-Manchado, M.Á.; Verdejo, R.; Hernández Santana, M. Solving the

Dichotomy between Self-Healing and Mechanical Properties in Rubber Composites by Combining Reinforcing and Sustainable Fillers. *Macromol Mater Eng* **2022**, 2200261, doi:10.1002/mame.202200261.

2. Utrera-Barrios, S.; Verdejo, R.; López-Manchado, M.A.; Hernández Santana, M. Evolution of Self-Healing Elastomers, from Extrinsic to Combined Intrinsic Mechanisms: A Review. *Mater Horiz* **2020**, *7*, 2882–2902, doi:10.1039/d0mh00535e.

3. Hernández Santana, M.; Huete, M.; Lameda, P.; Araujo, J.; Verdejo, R.; López-Manchado, M.A. Design of a New Generation of Sustainable SBR Compounds with Good Trade-off between Mechanical Properties and Self-Healing Ability. *Eur Polym J* **2018**, *106*, 273–283, doi:10.1016/J.EURPOLYMJ.2018.07.040.

4. Yu, H.; Feng, Y.; Gao, L.; Chen, C.; Zhang, Z.; Feng, W. Self-Healing High Strength and Thermal Conductivity of 3D Graphene/PDMS Composites by the Optimization of Multiple Molecular Interactions. *Macromolecules* **2020**, *53*, doi:10.1021/acs.macromol.9b02544.

5. Zhang, L.; Wang, H.; Zhu, Y.; Xiong, H.; Wu, Q.; Gu, S.; Liu, X.; Huang, G.; Wu, J. Electron-Donating Effect Enabled Simultaneous Improvement on the Mechanical and Self-Healing Properties of Bromobutyl Rubber Ionomers. *ACS Appl Mater Interfaces* **2020**, *12*, 53239–53246, doi:10.1021/acsami.0c14901.

6. Faseela, K.P.; Benny, A.P.; Kim, Y.; Baik, S. Highly Conductive Strong Healable Nanocomposites via Diels–Alder Reaction and Filler-Polymer Covalent Bifunctionalization. *Small* **2022**, *18*, 2104764, doi:10.1002/SMLL.202104764.

7. Liu, W.; Xu, C.; Chen, Y. Engineer a Controllable Hierarchical Dynamic Cross-Linked Network. *Compos Sci Technol* **2023**, *234*, 109937, doi:10.1016/J.COMPSCITECH.2023.109937.

8.  Krzemińska, S.M.; Smejda-Krzewicka, A.A.; Leniart, A.; Lipińska, L.; Woluntarski, M. Effects of Curing Agents and Modified Graphene Oxide on the Properties of XNBR Composites. *Polym Test* **2020**, *83*, 106368, doi:10.1016/J.POLYMERTESTING.2020.106368.

9.  Mondal, U.K.; Tripathy, D.K.; De, S.K. Moving Die Rheometry and Dynamic Mechanical Studies on the Effect of Reinforcing Carbon Black Filler on Ionomer Formation during Crosslinking of Carboxylated Nitrile Rubber by Zinc Oxide. *Polymer (Guildf)* **1993**, *34*, 3832–3836, doi:10.1016/0032-3861(93)90507-7.

10. Mousa, A.; Heinrich, G.; Wagenknecht, U. Cure Characteristics and Mechanical Properties of Carboxylated Nitrile Butadiene Rubber (XNBR) Vulcanizate Reinforced by Organic Filler. *Polym Plast Technol Eng* **2011**, *50*, 1388–1392, doi:10.1080/03602559.2011.584242.

11. Laskowska, A.; Marzec, A.; Zaborski, M.; Boiteux, G. Reinforcement of Carboxylated Acrylonitrile-Butadiene Rubber (XNBR) with Graphene Nanoplatelets with Varying Surface Area. *Journal of Polymer Engineering* **2014**, *34*, 883–893, doi:10.1515/POLYENG-2013-0149.

12. A New Circular Paradigm for Reuse and Recycling of Ink Cartridges. *Life Programme* 2021.

13. Huang, J.; Kumar, G.S.; Sun, Y. Evaluation of Workability and Mechanical Properties of Asphalt Binder and Mixture Modified with Waste Toner. *Constr Build Mater* **2021**, *276*, 122230, doi:10.1016/J.CONBUILDMAT.2020.122230.

14. Huang, J.; Li, X.; Kumar, G.S.; Deng, Y.; Gong, M.; Dong, N. Rheological Properties of Bituminous Binder Modified with Recycled Waste Toner. *J Clean Prod* **2021**, *317*, 128415, doi:10.1016/J.JCLEPRO.2021.128415.

15.  Khedaywi, T.S. Study on Utilising Waste Toner in Asphalt Cement. *Road Materials and Pavement Design* **2014**, *15*, 446–454, doi:10.1080/14680629.2013.876925.

16.  Alkurdi, N.M.; Mohammad, F.A.; Klalib, H.A. Mechanical Properties and Direct Tensile Strength of Waste Toner Foamed Concrete. *Journal of Advanced Civil Engineering Practice and Research* **2020**, *11*, 10–20.

17.  Kumar, U.; Gaikwad, V.; Sahajwalla, V. Transformation of Waste Toner to Iron Using E-Waste Plastics as a Carbon Resource. *J Clean Prod* **2018**, *192*, 244–251, doi:10.1016/J.JCLEPRO.2018.05.010.

18.  Li, Y.; Mao, J.; Xie, H.; Li, J. Heat-Treatment Recycling of Waste Toner and Its Applications in Lithium Ion Batteries. *J Mater Cycles Waste Manag* **2018**, *20*, 361–368, doi:10.1007/s10163-017-0599-z.

19.  Kaipannan, S.; Govindarajan, K.; Sundaramoorthy, S.; Marappan, S. Waste Toner-Derived Carbon/Fe3O4 Nanocomposite for High-Performance Supercapacitor. *ACS Omega* **2019**, *4*, 15798–15805, doi:10.1021/acsomega.9b01337.

20.  Balasubramanian, S.; Kanagarathinam, S.; Cingaram, R.; Bakthavachalam, V.; Kulathu Iyer, S.; Rajendran, S.; Natesan Sundaramurthy, K.; Ranganathan, S. Waste Toner-Derived Porous Iron Oxide Pigments with Enhanced Catalytic Degradation Property. *Environ Res* **2023**, *216*, 114695, doi:10.1016/J.ENVRES.2022.114695.

21.  Xu, Q.; Gong, Y.; Zhang, Z.; Miao, Y.; Li, D.; Yan, G. Preparation of Graphene Oxide Quantum Dots from Waste Toner, and Their Application to a Fluorometric DNA Hybridization Assay. *Microchimica Acta* **2019**, *186*, 1–7, doi:10.1007/s00604-019-3539-x.

22.  Ma, D.; Sheng, jie; Hao, Y.; He, J.; Zhong, Y.; Wu, W. Photovoltaic Green Application of Waste Toner Carbon on Fully Printable Mesoscopic Perovskite

Solar Cells. *Solar Energy* **2021**, *228*, 439–446, doi:10.1016/J.SOLENER.2021.09.051.

23. Anandhan, S.; De, P.P.; De, S.K.; Bhowmick, A.K.; Bandyopadhyay, S. Novel Thermoplastic Elastomers Based on Acrylonitrile-Butadiene-Styrene Terpolymer (ABS) from Waste Computer Equipment and Nitrile Rubber. *Rubber Chemistry and Technology* **2003**, *76*, 1145–1163, doi:10.5254/1.3547793.

24. Anandhan, S.; De, P.P.; De, S.K.; Swayajith, S.; Bhowmick, A.K. Thermorheological Studies of Novel Thermoplastic Elastomeric Blends of Nitrile Rubber (NBR) and Scrap Computer Plastics (SCP) Based on Acrylonitrile–Butadiene–Styrene Terpolymer (ABS). *Plastics, Rubber and Composites* **2013**, *32*, 377–384, doi:10.1179/146580103225004144.

25. Araujo-Morera, J.; Verdugo-Manzanares, R.; González, S.; Verdejo, R.; Lopez-Manchado, M.A.; Santana, M.H. On the Use of Mechano-Chemically Modified Ground Tire Rubber (GTR) as Recycled and Sustainable Filler in Styrene-Butadiene Rubber (SBR) Composites. *Journal of Composites Science* **2021**, *5*, 68, doi:10.3390/JCS5030068.

26. Alonso Pastor, L.E.; Núñez Carrero, K.C.; Araujo-Morera, J.; Hernández Santana, M.; Pastor, J.M. Setting Relationships between Structure and Devulcanization of Ground Tire Rubber and Their Effect on Self-Healing Elastomers. *Polymers (Basel)* **2021**, *14*, 11, doi:10.3390/POLYM14010011.

27. Arayapranee, W.; Rempel, G.L. Effects of Polarity on the Filler-Rubber Interaction and Properties of Silica Filled Grafted Natural Rubber Composites. *J Polym* **2013**, *2013*, 279529, doi:10.1155/2013/279529.

28. Ismail, H.; Rusli, A.; Rashid, A.A. Maleated Natural Rubber as a Coupling Agent for Paper Sludge Filled Natural Rubber Composites. *Polym Test* **2005**, *24*, 856–862, doi:10.1016/J.POLYMERTESTING.2005.06.011.

29.     Saowapark, T.; Sombatsompop, N.; Sirisinha, C. Viscoelastic Properties of Fly Ash-Filled Natural Rubber Compounds: Effect of Fly Ash Loading. *J Appl Polym Sci* **2009**, *112*, 2552–2558, doi:10.1002/APP.29700.

30.     Sengloyluan, K.; Sahakaro, K.; Dierkes, W.K.; Noordermeer, J.W.M. Silica-Reinforced Tire Tread Compounds Compatibilized by Using Epoxidized Natural Rubber. *Eur Polym J* **2014**, *51*, 69–79, doi:10.1016/J.EURPOLYMJ.2013.12.010.

31.     Ansarifar, A.; Azhar, A.; Ibrahim, N.; Shiah, S.F.; Lawton, J.M.D. The Use of a Silanised Silica Filler to Reinforce and Crosslink Natural Rubber. *Int J Adhes Adhes* **2005**, *25*, 77–86, doi:10.1016/J.IJADHADH.2004.04.002.

32.     Kaewsakul, W.; Sahakaro, K.; Dierkes, W.K.; Noordermeer, J.W.M. Mechanistic Aspects of Silane Coupling Agents with Different Functionalities on Reinforcement of Silica-Filled Natural Rubber Compounds. *Polym Eng Sci* **2015**, *55*, 836–842, doi:10.1002/PEN.23949.

33.     Salina Sarkawi, S.; Dierkes, W.K.; Noordermeer, J.W.M. Morphology of Silica-Reinforced Natural Rubber: The Effect of Silane Coupling Agent. *Rubber Chemistry and Technology* **2015**, *88*, 359–372, doi:10.5254/RCT.15.86936.

34.     Choi, S.-S. Improvement of Properties of Silica-Filled Styrene-Butadiene Rubber Compounds Using Acrylonitrile-Butadiene Rubber. *J Appl Polym Sci* **2000**, *79*, 959–1149, doi:10.1002/1097-4628.

35.     Das, A.; Debnath, S.C.; De, D.; Basu, D.K. Evaluation of Physical Properties and Curing Characteristics of Silica-Filled Ethylene–Propylene–Diene Terpolymer in the Presence of Chloroprene Rubber. *J Appl Polym Sci* **2004**, *93*, 196–200, doi:10.1002/APP.20452.

36.     Leblanc, J.L. Rubber–Filler Interactions and Rheological Properties in Filled Compounds. *Prog Polym Sci* **2002**, *27*, 627–687, doi:10.1016/S0079-6700(01)00040-5.

37. Thomas, S.K.; Parameswaranpillai, J.; Krishnasamy, S.; Begum, P.M.S.; Nandi, D.; Siengchin, S.; George, J.J.; Hameed, N.; Salim, Nisa.V.; Sienkiewicz, N. A Comprehensive Review on Cellulose, Chitin, and Starch as Fillers in Natural Rubber Biocomposites. *Carbohydrate Polymer Technologies and Applications* **2021**, *2*, 100095, doi:10.1016/j.carpta.2021.100095.

38. Roy, K.; Pongwisuthiruchte, A.; Chandra Debnath, S.; Potiyaraj, P. Application of Cellulose as Green Filler for the Development of Sustainable Rubber Technology. *Current Research in Green and Sustainable Chemistry* **2021**, *4*, 100140, doi:10.1016/j.crgsc.2021.100140.

39. Jiang, G.; Song, S.; Zhai, Y.; Feng, C.; Zhang, Y. Improving the Filler Dispersion of Polychloroprene/Carboxylated Multi-Walled Carbon Nanotubes Composites by Non-Covalent Functionalization of Carboxylated Ionic Liquid. *Compos Sci Technol* **2016**, *123*, 171–178, doi:10.1016/J.COMPSCITECH.2015.12.017.

40. Salaeh, S.; Das, A.; Wießner, S. Design and Fabrication of Thermoplastic Elastomer with Ionic Network: A Strategy for Good Performance and Shape Memory Capability. *Polymer (Guildf)* **2021**, *223*, 123699, doi:10.1016/J.POLYMER.2021.123699.

41. Yordanova, D.; Angelova, S.; Dombalov, I. Utilisation Options for Waste Toner Powder. *J. Environ. Sci* **2014**, *3*, 140–144.

42. Pichaiyut, S.; Nakason, C.; Kummerlöwe, C.; Vennemann, N. Thermoplastic Elastomer Based on Epoxidized Natural Rubber/Thermoplastic Polyurethane Blends: Influence of Blending Technique. *Polym Adv Technol* **2012**, *23*, 1011–1019, doi:10.1002/PAT.2005.

43. Kwan, K.S.-W.; Kan, C.-W. Comparison and Analysis of Colorant in Toner Cartridges: A Material Safety Data Sheet Study. In *Dyes and Pigments* -

*Insights and Applications*; Kumar, Dr.B., Ed.; IntechOpen: Rijeka, 2022 ISBN 978-1-83768-114-3.

44. Basu, D.; Das, A.; Stöckelhuber, K.W.; Jehnichen, D.; Formanek, P.; Sarlin, E.; Vuorinen, J.; Heinrich, G. Evidence for an in Situ Developed Polymer Phase in Ionic Elastomers. *Macromolecules* **2014**, *47*, 3436–3450, doi:10.1021/ma500240v.

45. Xu, C.; Huang, X.; Li, C.; Chen, Y.; Lin, B.; Liang, X. Design of "Zn2+ Salt-Bondings" Cross-Linked Carboxylated Styrene Butadiene Rubber with Reprocessing and Recycling Ability via Rearrangements of Ionic Cross-Linkings. *ACS Sustain Chem Eng* **2016**, *4*, 6981–6990, doi:10.1021/acssuschemeng.6b01897.

46. Chatterjee, T.; Hait, S.; Bhattacharya, A.B.; Das, A.; Wiessner, S.; Naskar, K. Zinc Salts Induced Ionomeric Thermoplastic Elastomers Based on XNBR and PA12. *Polymer-Plastics Technology and Materials* **2019**, *59*, 141–153, doi:10.1080/25740881.2019.1625389.

47. Das, M.; Pal, S.; Naskar, K. A New Route of Cross-Linking of Carboxylated Acrylonitrile-Butadiene Rubber via Zinc Oxide-Amino Acid Network Formation. *J Appl Polym Sci* **2021**, *138*, 49996, doi:10.1002/APP.49996.

48. González-Jiménez, A.; Malmierca, M.A.; Bernal-Ortega, P.; Posadas, P.; Pérez-Aparicio, R.; Marcos-Fernández, Á.; Mather, P.T.; Valentín, J.L. The Shape-Memory Effect in Ionic Elastomers: Fixation through Ionic Interactions. *Soft Matter* **2017**, *13*, 2983–2994, doi:10.1039/C7SM00104E.

49. Muhammed Rankviz Laser Toner Cartridge: What's inside? Available online: https://www.inkjetwholesale.com.au/blog/printer-education/laser-toner-cartridge-whats-inside/ (accessed on 9 June 2023).

# 7 Final Remarks

# Chapter 7.    Final Remarks

## 7.1. Conclusions

In the current context of environmental consciousness, the sustainable use of resources and the adoption of responsible consumption practices are crucial for advancing towards a CE. This doctoral thesis introduced two fundamental concepts that are pivotal to ecological transition: **Repair** and **Recycle**. To achieve this, *ionic elastomers* based on XNBR have been developed, which uniquely combine superior mechanical performance and sustainability. This development successfully addressed the traditional trade-off between these properties, promoting an extended service life, reducing the demand for finite resources, and minimizing rubber waste. The key to this innovation lies in the dynamic nature of the ionic crosslinks, thermally-responsive structures, which facilitate rubber reprocessing. The following conclusions were drawn from this study:

An in-depth comparison between the covalent, ionic, and dual (combined) crosslinked networks was performed. It was demonstrated that *ionic elastomers* not only offer robust mechanical performance, which is essential for demanding applications, but also benefit from an expedited curing process that boosts production efficiency. Although slightly outperformed by dual networks in terms of chemical ($+26\ \%$) and abrasion resistance ($+15\ \%$), ionic networks still provide good performance, making them suitable for situations where minimal liquid effects or surface wear is a concern.

A straightforward and scalable two-step recycling process (cutting and remolding) specifically designed for XNBR was used to study the recyclability of *ionic*

*elastomers.* This recyclability was qualitatively and quantitatively demonstrated for up to three recycling cycles.

A deep dive into the molecular dynamics changes during recycling was provided, revealing a minimal impact on the overall performance during the first two recycling cycles. The most significant changes, essentially observed in mechanical strength after the third cycle, were attributed to changes in molecular entanglements, crosslink densities, and ionic domain structures.

The effects of different metal oxides on the formation of the ionic networks were investigated. These findings revealed that increasing the oxide content enhanced the vulcanization efficiency, leading to a higher cure rate and degree of crosslinking. This results in an improved mechanical performance. A comparative analysis with equal crosslink densities indicated that excess ZnO contributes to the stiffness owing to its role as a semi-reinforcing filler. Conversely, in composites with equal metal oxide content, MgO outperformed ZnO in terms of mechanical properties, which was attributed to the stronger electrostatic attraction of its smaller cations.

BDS was employed to optimize self-healing protocols, a marking a significant shift away from conventional resource-consuming trial-and-error methods was confirmed. By studying the molecular dynamics of compounds with different metal oxides, it was possible to determine the minimum temperature required (110 °C) to ensure the complete mobility of the polymeric chains, which guarantees good self-healing capability and recyclability.

An important milestone in rubber applications was the unlocking of the potential of *ionic elastomers* in the manufacture of soft robotic grippers. These exhibited excellent accuracy and a fast response during actuation by recovering after deformability in just 80 ms (quick-release test).

*Ionic elastomer*-based composites reinforced with sustainable fillers have been developed using two approaches: in the first approach, the reinforcing character of cellulose and GTR as sustainable fillers was evidenced, increasing in both cases the

overall mechanical performance of the unfilled material and obtaining excellent healing efficiencies higher than 80 % after an optimized protocol of 110 °C for 3 h.

The incorporation of 10 phr of GTR as a waste-based filler, allowed the obtention of a material capable of full repair and recycling (100 % efficiency) with mechanical properties close to those of a conventional filler, such as silica (modulus ~2 MPa, TS >17 MPa, and a long deformability >1000 %). An enhanced effect between filler-filler and filler-rubber interactions was key to this result.

In the second approach, a radically different strategy was explored, in which toner cartridge waste was incorporated as an integral additive in the rubber recipe, i.e. as part of the matrix and as part of the reinforcing system. The feasibility of developing a TPV composed of a blend of a thermoplastic phase (based on HIPS from a waste cartridge carcass) and XNBR selectively vulcanized with an ionic system was tested.

A toner-powder-reinforced TPV was successfully developed. The reinforcing character of the toner powder was demonstrated, which increased the mechanical performance of the unfilled material by 50 % without affecting its thermal stability. The composite could repair macroscopic damage with an efficiency of 85 %. This approach introduces a new way of looking at waste management and sustainable materials, not only considering a strategy for the reuse of waste but also enhancing the mechanical performance of *ionic elastomers* from an upcycling perspective.

## 7.2. Outlook and Future Work

This doctoral thesis has presented important advances that unlock the potential of *ionic elastomers* to achieve the long-awaited circularity of crosslinked rubbers. The promising results reported herein have enabled the visualization of self-healing and recyclable nitrile rubber as a pathway to sustainability. However, certain pending issues and challenges must be addressed. The following are five recommended future research lines:

**Exploring the practical applications of reinforced ionic elastomers:** Sustainable filler-reinforced *ionic elastomers*, particularly those incorporating GTR, have shown significant benefits over traditional systems in terms of sustainability. However, their practical application requires further exploration. To fully realize the potential of the composites developed in **Chapter 6**, their application in soft robotics must be examined. Additionally, investigating a broader spectrum of sustainable filler combinations at higher contents could yield more finely tuned composites that would not only possess diverse properties but also embody a robust commitment to sustainability.

**Design and analysis of rubber recipes for specific applications:** The diverse applications of crosslinked elastomers require specific considerations in the formulation of rubber recipes. High-performance applications, such as tires, often require substantial filler contents (> 40 phr), demanding the use of plasticizers as processing aids. Products, such as sporting-goods or toys, may require the addition of colorants or odorants. In cases where rubber interfaces with metals, the addition of rubber-to-metal bonding agents is essential. The range of possibilities is endless. Each additive, as a chemical entity, can interact with rubber in multiple ways. Therefore, assessing the impact of specific ingredients on the self-healing and recyclability properties of *ionic elastomers* is an intriguing avenue for future research.

**Advancing 3D printing technologies with ionic elastomers:** By taking advantage of the dynamic character of ionic crosslinks, temperature-driven additive manufacturing strategies, such as 3D printing, can be explored. This area remains a frontier in Rubber Science and Technology, which can be approached with the proper optimization of the viscosity and printing conditions applied to *ionic elastomers*.

**Evaluation of ionic elastomers as stimuli-responsive materials:** In addition to temperature, a variety of stimuli can be investigated to determine their effects on the reversibility of ionic crosslinks. These stimuli include pH, electric fields, exposure

to light, specific solvents or humidity, magnetic effects, and applied pressure. Furthermore, exploring different environments and atmospheric conditions can enhance our understanding of potential applications of *ionic elastomers*.

**Assessing full sustainability:** The developed materials in this doctoral thesis present an undoubtedly unique combination of improved mechanical performance, self-repair, and recyclability that complies with the CE principles. However, a comprehensive study that considers the processes involved in the production of these materials is lacking. In this context, Life Cycle Assessment (LCA) is a tool that should be applied in future studies. LCA examines the environmental impact of a product throughout its lifetime from cradle-to-grave (preferable from cradle-to-cradle). This includes production, use, and recycling, self-healing, or reuse strategies at the end of their service life. One of the main advantages of LCA is its ability to identify and quantify specific steps and processes that have the greatest environmental impact. This will enable future developments in this area to make informed adjustments to the material selection, repair or recycling conditions, and management strategies. In doing so, the environmental impact is minimized and resource efficiency is improved, which is necessary in a world that must be increasingly aware of its environmental responsibilities.

**Appendices**

# Appendix A. Publications

## A.1. Publications derived from this Doctoral Thesis

IF: impact factor; CA: corresponding author; X/X: author position.

1.  **S. Utrera-Barrios\***, I. Mar-Gines, R. Verdugo Manzanares, R. Verdejo, M. A. López-Manchado, M. Hernández Santana\*. Recyclability and self-healing capability in reinforced ionic elastomers. ***Polymer***, 2023. (Polymer Science - SCIE, 18/86, **Q1**, IF: 4.6). **CA; 1/6.** [Submitted].

2.  **S. Utrera-Barrios\***, N. Steenackers, S. Terryn, P. Ferrentino, R. Verdejo, G. Van Asche, M. A. López-Manchado, J. Brancart, M. Hernández Santana\*. Unlocking the Potential of Self-Healing and Recyclable Ionic Elastomers for Soft Robotics Applications. ***Materials Horizons***, 2024, 10, Advance Article, DOI: 10.1039/D3MH01312J. (Materials Science, Multidisciplinary - SCIE, 29/344, **Q1**, IF: 13.3). **CA; 1/9. Open Access. (Invited article)**

3.  **S. Utrera-Barrios\***, M. F. Martínez, I. Mas-Giner, R. Verdejo, M. A. López-Manchado, M. Hernández Santana\*. New recyclable and self-healing elastomer composites using waste from toner cartridges. ***Composites Science and Technology***, 2023, 244, 110292. (Materials Science, Composites - SCIE, 4/28, **Q1**, IF: 9.1). **CA; 1/6. Open Access.**

4.  **S. Utrera-Barrios**, R. Verdugo Manzanares, A. M. Grande, R. Verdejo, M. A. López-Manchado\*, M. Hernández Santana\*. New Insights into the Molecular Structure and Dynamics of a Recyclable and Ionically Crosslinked Carboxylated Nitrile Rubber (XNBR). ***Materials & Design***, 2023, 233, 112273. (Materials

Science, Multidisciplinary - SCIE, 65/342, **Q1**, IF: 8.4). **1/6.** Total no. of cites: 1. **Open Access.**

5. **S. Utrera-Barrios**, R. Verdejo, M. A. López-Manchado\*, M. Hernández Santana\*. The final frontier of sustainable materials: current developments in self-healing elastomers, *International Journal of Molecular Sciences*, 2022, 23, 9, 4757. (Biochemistry & Molecular Biology - SCIE, 66/285, **Q1**, IF: 5.6). **1/4.** Total no. of cites: 11. **Open Access. (Most Downloaded Articles 2022) (Invited article)**

6. **S. Utrera-Barrios**, R. Verdugo Manzanares, J. Araujo-Morera, S. González, R. Verdejo, M. A. López-Manchado, M. Hernández Santana\*. Understanding the molecular dynamics of dual crosslinked networks by dielectric spectroscopy, *Polymers*, 2021, 13, 9, 3234. (Polymer Science - SCIE, 16/90, **Q1**, IF: 4.967). **1/7.** Total no. of cites: 13. **Open Access. (Most Notable Articles September-December 2021)**

7. **S. Utrera-Barrios**, J. Araujo-Morera, L. Pulido de los Reyes, R. Verdugo Manzanares, R. Verdejo, M. A. López-Manchado, M. Hernández Santana\*. An effective and sustainable approach for achieving self-healing in nitrile rubber, *European Polymer Journal*, 2020, 139, 110032. (Polymer Science - SCIE, 15/90, **Q1**, IF: 4.598). **1/7.** Total no. of cites: 34.

8. **S. Utrera-Barrios**, M. Hernández Santana\*, R. Verdejo, M. A. López-Manchado. Evolution of self-healing elastomers, from extrinsic to combined intrinsic mechanisms – A review, *Materials Horizons*, 2020, 7, 11, 2882-2902. (Chemistry: Multidisciplinary - SCIE, 19/178, **Q1**, IF: 13.266). **1/4.** Total no. of cites: 179. **Open Access. ("Materials Horizons 2020 Paper Awards" as "Outstanding Review") (Top 20 Most Popular Articles 2020) (Top 1 % cited 2021)**

9. **S. Utrera-Barrios**, A. Bascuñán, R. Verdejo, M. López-Manchado, H. Aguilar-Bolados, M. Hernández Santana. (2023). Sustainable Fillers for Elastomeric Composites. In: Avalos Belmontes, F., González, F.J., López-Manchado, M.Á. (eds) Green-Based Nanocomposite Materials and Applications. Engineering Materials. Springer, Cham. DOI: 10.1007/978-3-031-18428-4_3.

## A.2. Publications Related to this Doctoral Thesis

1. **S. Utrera-Barrios\***, O. Pinho Lopes, I. Mas-Giner, R. Verdejo, M. A. López-Manchado, M. Hernández Santana\*. Sustainable composites with self-healing capability: epoxidized natural rubber and cellulose propionate reinforced with cellulose fibers. ***Polymer Composites***. (Polymer Science - SCIE, 13/86, **Q1**, IF: 5.2) **CA; 2/9.** [Submitted]

2. **S. Utrera-Barrios**, R. Verdejo, M. A. López Manchado, M. Hernández Santana\*. Self-healing elastomers: a sustainable solution for automotive applications, ***European Polymer Journal***, 2023, 190, 112023. (Polymer Science - SCIE, 7/86, **Q1**, IF: 6.0). **1/4.** Total no. of cites: 6. **Open Access.**

3. **S. Utrera-Barrios,** O. Ricciardi, S. González, R. Verdejo, M. A. López-Manchado, M. Hernández Santana\*. Development of sustainable, mechanically strong, and self-healing bio-thermoplastic elastomers reinforced with alginates, ***Polymers***, 2022, 14, 21, 4607. (Polymer Science - SCIE, 16/86, **Q1**, IF: 5.0). **1/6.** Total no. of cites: 6. **Open Access.**

4. J. Araujo-Morera, **S. Utrera-Barrios**, R. Doral Olivares, R. Verdugo Manzanares, M. A. López-Manchado, R. Verdejo\*, M. Hernández Santana\*. Solving the dichotomy between self-healing and mechanical properties in rubber composites by combining reinforcing and sustainable fillers, ***Macromolecular Materials and Engineering***, 2022, 307, 10, 2200261. (Polymer Science - SCIE, 27/86, Q2, IF: 3.9). **2/7.** Total no. of cites: 7. **Open Access.**

## A.3. Patents Related to this Doctoral Thesis

1. **European Patent** (EP23382922.5). Method for obtaining a self-repairing natural rubber, material thus obtained and use thereof. ***Inventors:*** M. Hernández, **S. Utrera Barrios**, R. Verdejo, M. A. López Manchado. ***Applicants:*** Spanish National Research Council (CSIC, Spain) and Bridgestone Corporation (Japan). ***Status***: Filed, 23/09/2023.

## A.4. Dissemination Articles

1. **S. Utrera-Barrios,** M. Hernández Santana, M. A. López-Manchado, R. Verdejo. El «Lobezno» de los materiales que podría salvar a nuestro planeta (*The "Wolverine" of materials that could save our planet*). ***The Conversation***. Publication date: August 29, 2023. Available at: https://theconversation.com/el-lobezno-de-los-materiales-que-podria-ayudar-a-salvar-el-planeta-210925.

2. **S. Utrera-Barrios,** O. Pinho Lopes, M. Hernández Santana. Materiales compuestos elastoméricos reforzados con fibras naturales y con capacidad autorreparadora (*Natural fiber-reinforced elastomeric composite materials with self-healing capabilities*). ***Materiales Compuestos*** (Online first). Available at: https://www.scipedia.com/public/Utrera-Barrios_et_al_2023a.

3. M. Hernández Santana & **S. Utrera-Barrios**. Innovación y desafíos en el uso de cauchos autorreparables para el vehículo del futuro (*Innovation and challenges in the use of self-healing rubber for the vehicle of the future*). ***Revista de la Sociedad Latinoamericana de Tecnología del Caucho***, 55, 2023, 8 − 11.

4. M. Hernández Santana & **S. Utrera-Barrios**. Reutilización de desechos de neumáticos en compuestos de caucho autorreparables – Segunda parte (*Reuse of

*waste tires in self-healing rubber compounds - Part Two*). **Revista de la Sociedad Latinoamericana de Tecnología del Caucho**, 51, 2022, 8 – 11.

5. M. Hernández Santana & **S. Utrera-Barrios**. Reutilización de desechos de neumáticos en compuestos de caucho autorreparables (*Reuse of waste tires in self-healing rubber compounds*). **Revista de la Sociedad Latinoamericana de Tecnología del Caucho**, 50, 2022, 4 – 6.

6. M. Hernández Santana, M. A. López-Manchado, **S. Utrera-Barrios**, R. Verdejo. Self-healing Elastomers. **Encyclopedia**, Available at: https://encyclopedia.pub/entry/22776.

7. **S. Utrera-Barrios,** J. Araujo-Morera, O. Ricciardi, R. Verdejo, M. A. López-Manchado, M. Hernández Santana*. Desarrollo de biocompuestos elastoméricos autorreparables como estrategia sostenible – bioHEAL (*Development of self-healing elastomeric biocomposites as a sustainable strategy - bioHEAL*). **Materiales Compuestos**, 6, 1, 2022, 9-17. Available at: https://www.scipedia.com/public/Utrera-Barrios_et_al_2022a.

8. M. Hernández Santana & **S. Utrera-Barrios**. Self-Healing Natural Rubber: A Window of Massive Opportunities for New Applications. **Global Catalyst**, 2021, Available at: https://www.confexhub.com/2021/07/09/special-edition-natural-rubber -2-0/.

9. **S. Utrera-Barrios** & J. Araujo-Morera. Cauchos autorreparables: La nueva frontera en el Desarrollo de elastómeros inteligentes y sostenibles (*Self-healing rubbers: The new frontier in the development of smart and sustainable elastomers*). **Revista de la Sociedad Latinoamericana de Tecnología del Caucho**, 41, 2021, 6-8.

10. **S. Utrera-Barrios**, L. Pulido de los Reyes, R. Verdugo Manzanares, J. Araujo-Morera, R. Verdejo, M. Hernández Santana*. Neumáticos fuera de uso: una carga sostenible para el desarrollo de nuevos elastómeros con capacidad

autorreparadora (*End-of-life tires: a sustainable filler for the development of new elastomers with self-healing capabilities*). **Revista de Plásticos Modernos**, 120, 762, 2020, 22-26.

11. J. Araujo-Morera, **S. Utrera-Barrios**, M. Peñas-Caballero, M. Hernández Santana, R. Verdejo, M. A. López-Manchado. La autorreparación, un aliado efectivo contra el impacto ambiental de los polímeros (*Self-healing, an effective ally against the environmental impact of polymers*). **Revista Ambiente y Medio de la Universidad Nacional Educación a Distancia**, 2020.

## A.5. Conferences

21 contributions (with 7 participations) to scientific conferences.

1. S. Utrera Barrios, I. Mas Giner, R. Verdejo, M. A. López Manchado, <u>M. Hernández Santana</u>. La autorreparación como estrategia para prolongar la vida útil de los elastómeros (*Self-healing as a strategy for extending the service life of elastomers*). XVII Jornadas Latinoamericanas de Tecnología del Caucho (*XVII Latin American Conference on Rubber Technology*), American Society for Rubber Technology (SLTC), Lima, Peru, 2023. **Invited conference.**

2. S. Utrera-Barrios, O. Pinho Lopes, <u>M. Hernández Santana</u>. Materiales compuestos elastoméricos reforzados con fibras naturales y con capacidad autorreparadora (*Natural fiber-reinforced elastomeric composite materials with self-healing capabilities*). MATCOMP 2023, Spanish Composite Materials Association (AEMAC), Gijon, Spain, 2023. **Oral communication**.

3. <u>P. Prosr</u>, D. Háže, Z. Rychlík, P. Kadlec, S. Utrera-Barrios, M. Hernández Santana, R. Polanský. Thermal stability and self-healing capacity of modified carboxylated nitrile rubber. IEEE Conference on Electrical Insulation and Dielectric Phenomena (IEEE CEIDP 2023), East Rutherford, New Jersey, United States of America, 2023. **Oral communication**.

4. <u>S. Utrera-Barrios</u>, O. Ricciardi, R. Verdejo, M. A. López-Manchado, M. Hernández Santana. Self-healable bio-based thermoplastic elastomers reinforced with alginic acid salts. International Elastomer Conference (IEC 2022), Rubber Division, American Chemical Society, Tennesse, United States of America, 2022. **Oral communication**.

5. <u>V. Nikolic</u>, P. Kadlec, R. Polansky, S. Utrera-Barrios, M. Hernández Santana. Dielectric and thermal properties of self-healing carboxylated nitrile rubber ionically crosslinked with zinc oxide. IEEE Electrical Insulation Conference (IEEE EIC 2022), Tennessee, United States of America, 2022. **Poster**.

6. S. Utrera-Barrios, R. Verdugo Manzanares, R. Verdejo, M. A. López-Manchado, <u>M. Hernández Santana</u>. Self-healing and recyclable nitrile rubber: a myriad solution for the automotive industry. International Congress of Self-Healing Materials ICSHM 2022, Milano Polytechnique, Milano, Italy, 2022. **Keynote conference**.

7. S. Utrera-Barrios, J. Araujo-Morera, R. Verdugo-Manzanares, R. Verdejo, M. A. López-Manchado, <u>M. Hernández Santana</u>. Estrategias de autorreparación en compuestos elastoméricos (*Self-healing strategies in elastomeric composites*). MATCOMP 2021, Spanish Composite Materials Association (AEMAC), Sevilla, Spain, 2022. **Oral communication**.

8. <u>S. Utrera-Barrios</u>, R. Verdugo Manzanares, O. Ricciardi, R. Verdejo, M. A. López-Manchado, M. Hernández Santana. Giving another opportunity to trash: a complete study of recyclability in carboxylated nitrile rubber. Spring Technical Meeting, Rubber Division, American Chemical Society, Ohio, United States of America, 2022. **Oral communication**.

9. <u>M. Hernández Santana</u>, J. Araujo-Morera, S. Utrera-Barrios, R. Verdejo, M. López-Manchado. Rubber nano(composites) with self-healing capability, ImagineNano/IC2 Composites 2021, Bilbao, Spain, 2021. **Invited conference**.

10. <u>S. Utrera-Barrios</u>, L. Pulido de los Reyes, R. Verdugo Manzanares, J. Araujo-Morera, R. Verdejo, M. A. López-Manchado, M. Hernández Santana. Polvo de neumáticos fuera de uso: un aliado efectivo para conferir capacidad autorreparadora al caucho nitrilo (*End-of-life tires: an effective ally for imparting self-healing capacity to nitrile rubber*). XVI Jornadas Latinoamericanas de Tecnología del Caucho (*XVII Latin American Conference on Rubber Technology*), Latin American Society for Rubber Technology (SLTC), Buenos Aires, Argentina, 2021. **Oral communication**.

11. <u>J. Araujo-Morera</u>, S. Utrera-Barrios, R. Verdugo Manzanares, M. Hernández Santana, R. Verdejo, M. A. López Manchado. Compuestos elastoméricos autorreparables: estrategia clave en el desarrollo de una economía circular *(Self-healing elastomeric composites: a key strategy in the development of a circular economy*). XVI Jornadas Latinoamericanas de Tecnología del Caucho (*XVII Latin American Conference on Rubber Technology*), Latin American Society for Rubber Technology (SLTC), Buenos Aires, Argentina, 2021. **Oral communication**.

12. <u>R. Verdugo Manzanares</u>, S. Utrera-Barrios, R. Verdejo, M. A. López-Manchado, M. Hernández Santana. Giving another opportunity to trash: a study of recyclability of carboxylated nitrile rubber. 5th Young Polymer Scientist Seminar SEJIPOL 2021, Institute of Polymer Science and Technology (ICTP), CSIC, Madrid, Spain, 2021. **Poster**.

13. <u>O. Ricciardi</u>, S. Utrera-Barrios, R. Verdejo, M. A. López-Manchado, M. Hernández Santana. The last frontier in composites materials: thermoplastic elastomers reinforced with new biofillers. 5th Young Polymer Scientist Seminar SEJIPOL 2021, Institute of Polymer Science and Technology (ICTP), CSIC, Madrid, Spain, 2021. **Poster**.

14. <u>S. Utrera-Barrios</u>. Mecanismos de Autorreparación Intrínseca en Compuestos de Elastómeros (*Intrinsic Self-Healing Mechanisms in Elastomeric Composites*). V

Simposio Annual en Química Avanzada (*5th Annual Symposium on Advanced Chemistry*), Complutense University of Madrid, Madrid, Spain, 2020. **Oral communication**.

15. J. Araujo-Morera, S. Utrera-Barrios, R. Verdejo, M. López-Manchado, <u>M. Hernández Santana</u>. Self-Healing Natural Rubber: A Window of Massive Opportunities for New Applications. Global Rubber Conference, Bangkok, Thailand, 2020. **Invited conference**.

16. <u>S. Utrera-Barrios</u>, J. Araujo-Morera, M. Peñas-Caballero, R. Verdugo Manzanares, P. Tanasi, L. Pulido de los Reyes, R. Verdejo, M. López-Manchado, M. Hernández Santana. Like Human Skin: Self-Healing Smart Materials. LatinXChem, 2020, DOI: 10.26226/morressier.5f6c5f439b74b699bf390b79. **Poster. (Audience Award – Most Popular Poster, sponsored by Royal Society of Chemistry)**.

17. <u>M. Hernández Santana</u>, J. Araujo-Morera, S. Utrera-Barrios, R. Verdejo, M. López-Manchado. Recent Developments in Self-Healing Rubber Composites, Online Meeting on Self-healing Materials / GVCSHM-20, Texas, United States of America, 2020. **Invited conference**.

18. <u>S. Utrera-Barrios</u>, M. Hernández Santana. A new generation of elastomer-based composites with self-healing capability. 4th Young Polymer Scientist Seminar SEJIPOL 2019, Institute of Polymer Science and Technology (ICTP), CSIC, Madrid, Spain, 2019. **Oral communication. (Selected for publication)**.

19. <u>S. Utrera-Barrios</u>, J. Araujo-Morera, M. Peñas-Caballero, M. Hernández-Santana, R. Verdejo, M. A. López-Manchado. The role of chemical element in the self-healing capability of elastomer-based composites. Brainwars, Complutense University of Madrid, Madrid, España, 2019. **Poster**.

20. <u>J. Araujo-Morera</u>, S. Utrera-Barrios, M. Peñas-Caballero, M. Hernández Santana, R. Verdejo, M. A. López-Manchado. Development of sustainable and

self-healing SBR composites. International Rubber Conference (IRC), The Polymer Society of the Institute of Materials, Minerals and Mining, London, United Kingdom, 2019. **Oral communication**.

21. M. Peñas-Caballero, J. Araujo-Morera, S. Utrera, <u>M. Hernández Santana</u>, M. López-Manchado, R. Verdejo. Self-healing polymer composites. 7th International Seminar on Modern Polymeric Materials for Environmental Applications, Krakow University of Technology, Poland, 2019. **Invited conference**.

## A6. Dissemination Activities

1. **Science Week** at CSIC. Workshop on elastomer composite development, 2022.

2. **"4 ESO+Empresa" Days.** Workshop on elastomer composite development, 2020-2022.

3. **Invited speaker** at the Webinars of the Latin American Society of Rubber Technology (SLTC), 2020.

4. **PHOTOPOL** Scientific Outreach Contest. La metamorfosis del neumático (*The metamorphosis of tires*), 2019. **(Accésit)**

## A7. Mentoring Activities

1. Desarrollo de elastómeros autorreparables para aplicaciones biomédicas (*Development of self-healing elastomers for biomedical applications*). Daniel Valdés Blas, International University of Valencia, Valencia, Spain, 2023. **Internship. (Supervisor)**.

2. Closing the loop: development of new multifunctional, self-repairing elastomeric materials reinforced with waste from toner cartridges. María Fernanda Martínez,

Menéndez Pelayo International University, Madrid, Spain, 2023. **Master thesis. (Co-director)**.

3. Self-healing elastomer-based composites reinforced  with natural fillers. Océane Pinho Lopes, Polytechnique University of Madrid, Madrid, Spain, 2023. **Master thesis. (Co-director)**.

4. Development of new self-healing elastomer-based composite materials reinforced with biofillers. María Ornella Ricciardi Camacho, Polytechnique University of Madrid, Madrid, Spain, 2022. **Master thesis. (Co-director)**.

5. Compuestos de caucho natural (NR) con capacidad autorreparadora para el sector neumáticos (*Natural rubber (NR) compounds with self-healing capacity for the tire sector*). María Ornella Ricciardi Camacho, Polytechnique University of Madrid, Madrid, Spain, 2021. **Internship. (Co-director)**.

6. Desarrollo de elastómeros autorreparables por medio de redes de entrecruzamiento duales (*Development of self-healing elastomers by means of dual crosslinking networks*). Reyes Verdugo Manzanares, Menéndez Pelayo International University, Madrid, Spain, 2020. **Master thesis. (Co-director)**.

## A8. Mobility

1. **Research Stay** at the *Vrije Universiteit Brussel* for the development of self-healing and recyclable soft robotic grippers based on ionically crosslinked carboxylated nitrile rubber (XNBR). ***Supervisor:*** Prof. Joost Brancart. September-November 2022.

# Appendix A

# Appendix B.  First Page of Publications

## B.1. First Page of the Publications Derived from this Doctoral Thesis

**Materials Horizons**

ROYAL SOCIETY OF CHEMISTRY

**COMMUNICATION**

View Article Online
View Journal

Check for updates

# Unlocking the potential of self-healing and recyclable ionic elastomers for soft robotics applications†

S. Utrera-Barrios, [ID] *[a] N. Steenackers,[bc] S. Terryn,[bc] P. Ferrentino, [ID] [c] R. Verdejo,[a] G. Van Asche, [ID] [b] M. A. López-Manchado, [ID] [a] J. Brancart [ID] [b] and M. Hernández Santana [ID] *[a]

In the field of soft robotics, current materials face challenges related to their load capacity, durability, and sustainability. Innovative solutions are required to address these problems beyond conventional strategies, which often lack long-term ecological viability. This study aims to overcome these limitations using mechanically robust, self-healing, and recyclable ionic elastomers based on carboxylated nitrile rubber (XNBR). The designed materials exhibited excellent mechanical properties, including tensile strengths (TS) exceeding 19 MPa and remarkable deformability, with maximum elongations (EB) over 650%. Moreover, these materials showed high self-healing capabilities, with 100% recovery efficiency of TS and EB at 110 °C after 3 to 5 h, and full recyclability, preserving their mechanical performance even after three recycling cycles. Furthermore, they were also moldable and readily scalable. Tendon-driven soft robotic grippers were successfully developed out of ionic elastomers, illustrating the potential of self-healing and recyclability in the field of soft robotics to reduce maintenance costs, increase material durability, and improve sustainability.

**New concepts**

This study exploited mechanically robust, self-healing, and recyclable ionic elastomers based on carboxylated nitrile rubber (XNBR), a widely commercially available product, for soft robotic applications. The developed materials combine reprocessability and elasticity, offer superior performance under demanding conditions, and embody a sustainable approach. Zinc oxide (ZnO) and magnesium oxide (MgO) were used as crosslinking agents, semi-reinforcing fillers, and processing aids, thereby streamlining the production process. An exhaustive analysis was conducted on the impact of both oxides on the behavior of the material. The conclusions drawn suggest that the mechanical performance, repairability, and recyclability are influenced by factors such as the nature of the cation ($Zn^{2+}$ or $Mg^{2+}$), concentration, free volume, crosslink density, and binding energy. Broadband dielectric spectroscopy was used for the first time to ascertain the optimal temperature for the healing protocol, which differs from conventional trial-and-error methods. Using an optimized compound, the feasibility of manufacturing tendon-driven soft robotic grippers was demonstrated, thereby unlocking the potential of ionic elastomers for this application. This study sets a precedent for the development of sustainable and efficient materials without intricate synthesis processes, signifying a pivotal step towards the adoption of such rubbers in the field of soft robotics.

## 1. Introduction

The 4th industrial revolution requires a significant increase in the use of robotic automation, with the goal of improving productivity and efficiency. Among robotic automations, soft robots are particularly well-suited for applications that require real and safe human–robot collaboration and manipulation of fragile or sensitive objects.[1] The outstanding compliance of soft robots allows them to flexibly deform and adapt their shapes upon contact with objects, making them ideal candidates for delicate handling tasks such as electronic components and food items. However, the load capacity of soft grippers remains a significant challenge due to the inherent properties of soft materials, characterized by a Young's modulus below 1 GPa.[2] Several approaches have been explored to address this limitation, including the reinforcement of the elastic structure with high-strength fibers[3,4] or using variable stiffness technology, such as particle jamming,[5–7] soft actuator coupling,[8,9] and

[a] Institute of Polymer Science and Technology (ICTP), CSIC, Juan de la Cierva 3, 28006 Madrid, Spain. E-mail: sutrera@ictp.csic.es, marherna@ictp.csic.es
[b] Physical Chemistry and Polymer Science (FYSC), Department of Materials and Chemistry (MACH), Vrije Universiteit Brussel (VUB), Pleinlaan 2, B-1050 Brussels, Belgium
[c] Brubotics, Vrije Universiteit Brussel (VUB) and Imec, Pleinlaan 2, B-1050 Brussels, Belgium

† Electronic supplementary information (ESI) available: (S1) Product data for Krynac X 750 supplied by Arlanxeo; (S2) IR spectra of the ionic elastomers; (S3) DSC and TGA results; (S4) healing efficiency based on M300 values of the ionic elastomers; (S5) stress–strain curves of the ionic elastomers in pristine and healed state (healing protocol: 110 °C, 3 h, rectangular specimens); (S6) storage ($E'$) and Loss moduli ($E''$) by DMA; (S7) evolution of the mechanical properties (M300, TS, and EB) and crosslink density of 10ZnO through three recycling cycles; (S8) video of the actuation. See DOI: https://doi.org/10.1039/d3mh01312j

# New recyclable and self-healing elastomer composites using waste from toner cartridges

S. Utrera-Barrios [**], M.F. Martínez, I. Mas-Giner, R. Verdejo, M.A. López-Manchado, M. Hernández Santana [*]

*Institute of Polymer Science and Technology (ICTP), CSIC, Juan de la Cierva 3, 28006, Madrid, Spain*

ABSTRACT

Product recycling reintroduces what is discarded as waste and minimizes the environmental impact on our society. Among the different types of waste from electrical and electronic equipment, toner recycling often falls short, downcycling plastic components. This study introduces an innovative approach in which waste parts from toner cartridges are valorized to develop (recyclable and) self-healing elastomeric composite materials. The synergy between carboxylated nitrile rubber (XNBR) as the elastomeric phase and high-impact poly (styrene) (HIPS) as the thermoplastic phase derived from toner cartridge waste was explored and optimized. This combination resulted in the creation of a thermoplastic elastomer exhibiting robust mechanical properties and self-healing capabilities with a tensile strength of $6.6 \pm 0.2$ MPa and a temperature-driven mechanical recovery of 100%. Furthermore, the capacity of toner powder, an integral component of waste, to act as a reinforcing filler was confirmed, with a 50% increase in mechanical strength compared with the unfilled composite. Moreover, an increase in toner content (up to 20 phr) resulted in an optimal balance between tensile strength and self-healing capacity, surpassing the traditional antagonism between these properties. As a result, this research opens a new pathway in the field of self-healing composites and suggests a practical and environmentally friendly approach for managing electronic waste, effectively supporting the principles of Circular Economy.

## 1. Introduction

The escalating problem of toner cartridge waste poses challenges for its efficient management, owing to its environmentally hazardous components. To regulate and mitigate the adverse impacts of waste from electrical and electronic equipment (WEEE) on the environment and human health, Directive 2012/19/EU of the European Parliament and the Council of the European Union (EU) was issued on July 4th, 2012 [1]. It aims to promote sustainable production and consumption by preventing WEEE and encouraging techniques such as preparation for reuse [2]. Therefore, it is crucial to develop designs that prolong their lifespan and improve the recovery, reusability, disassembly, and recycling processes.

According to data from the European Commission, the market for ink and toner cartridges sells approximately 370 million inkjet cartridges and 135 million toner cartridges, annually. On average, nearly every resident of the EU-27 purchases, utilizes, and disposes of one cartridge

every year; however, despite the regulations, only approximately 20% of these are recycled or reused [3]. Amid the impetus of the Circular Economy (CE), scientific exploration has commenced into the potential recycling and reuse of these wastes.

In this context, the reuse of WEEE, including waste toner, has been promoted in a wide-range of materials and applications such as asphalt binders [4,5], asphalt cement [6], foamed concrete [7], as a carbon source for the production of ferrous components [8] useful in lithium-ion batteries [9], supercapacitors [10], and pigments [11], as well as other carbon by-products such as graphene oxide quantum dots [12] and carbon electrodes for perovskite solar cells [13]. However, their use is limited in the context of polymeric materials.

Hammani et al. [14] explores the potential of using waste toner powder (TP) as a filler into a polymer blend of low-density poly (ethylene)/high-impact poly (styrene) (LDPE/HIPS). The addition of up to 10 wt % of TP significantly improved the blend's electrical conductivity, reflected in a decreased electrical resistivity to $\sim 2.9 \times 10^7$ Ohm cm. This

# New insights into the molecular structure and dynamics of a recyclable and ionically crosslinked carboxylated nitrile rubber (XNBR)

Saul Utrera-Barrios [a], Reyes Verdugo Manzanares [a], Antonio Mattia Grande [b], Raquel Verdejo [a], Miguel Ángel López-Manchado [a,*], Marianella Hernández Santana [a,*]

[a] Institute of Polymer Science and Technology (ICTP), CSIC, Juan de la Cierva 3, 28006 Madrid, Spain
[b] Department of Aerospace Science and Technology, Politecnico di Milano, Milano, via la Masa 34, 10156 Milano, Italy

A B S T R A C T

Ionic crosslinking offers a route to rubber reprocessability due to ion pairs' dynamism, with recent studies focusing on tensile properties recovery. However, this research aims to provide, for the first time, a comprehensive overview of the recyclability of carboxylated nitrile rubber (XNBR), spotlighting changes in molecular dynamics through multiple recycling cycles beyond tensile tests. A uniquely recyclable XNBR, incorporating ZnO as a multifunctional additive, was designed alongside a simple, scalable, two-step recycling process. Evidence of the delicate balance between crosslink density and molecular entanglements that affects the dynamics of the recycled material was found. Recycling also restricts the molecular dynamics near ionic domains; attributed to a higher crosslink density (from $3.69 \times 10^{-5}$ mol cm$^{-3}$ in the pristine sample to $6.00 \times 10^{-5}$ mol cm$^{-3}$ after the third cycle), caused by a decreased ionic clusters size (aggregation number drops from 12.2 to 6.9). Remarkably, negligible differences ($< 10\%$) in compressive fatigue behavior and an enhanced chemical resistance in different solvents (up to 350% increase in motor oil) were also observed, ensuring suitable performance in conditions closer to service. Overall, this study demonstrates the feasibility of XNBR recycling and provides a broad understanding of this material at the molecular level.

## 1. Introduction

The carboxylation of elastomers is a well-known strategy in the rubber industry [1]. The goal is to impart improved functionalities such as abrasion, tear, and chemical resistance to the rubber chain [2]. One of the most common carboxylated elastomers is carboxylated nitrile rubber (XNBR), a terpolymer obtained from the copolymerization of acrylonitrile, butadiene, and carboxylic acid (mainly acrylic acid or methacrylic acid) [3]. The incorporation of this third monomer allows these materials to react with metal oxides, metal peroxides, salts, and thiolates, among others [4–7], resulting in the formation of carboxylic salts that behave as ionic crosslinks [8]. These carboxylic salts tend to associate as multiplets and clusters following an accepted structure known as the Eisenberg Model [9,10]. Multiplets consist of six to eight dipole ions associated to form larger structures, which disperse in the elastomeric matrix without forming a separate phase [11]. Clusters are considered aggregates formed by such multiplets and trapped chains. This association is caused by electrostatic interactions and is affected by the elastic shrinkage forces of rubber macromolecules. The restricted mobility of elastomer chains in the vicinity of ionic groups results in the formation of a hard phase immersed in a polar matrix [12]. This heterogeneity results in a distinct "ionic domain" with its own "glass/ionic transition". The release of polymer chains during long-range hopping of ions [13] leads to an increase in the molecular motion of the system, which is a reversible process [14].

Unlike the common covalent crosslinks formed during conventional vulcanization with sulfur/accelerant systems or peroxides, ionic crosslinks are dynamic, and cluster formation is responsible for the enhanced physical properties of ionic elastomers even without the addition of fillers [4,14–18]. Their dynamic character allows them to be reprocessable by applying medium to high temperatures, such as a thermoplastic elastomer (TPE) [19,20]. This has resulted in a substantial change from an environmental point of view. It is well known that crosslinked rubbers cannot be reprocessed using non-dynamic covalent systems. Thus, the use of dynamic networks in elastomeric materials is of great scientific, industrial, and environmental importance [21–23].

*Review*

# The Final Frontier of Sustainable Materials: Current Developments in Self-Healing Elastomers

**Saul Utrera-Barrios** [ID], **Raquel Verdejo** [ID], **Miguel Ángel López-Manchado \*** [ID]
**and Marianella Hernández Santana \*** [ID]

Institute of Polymer Science and Technology (ICTP-CSIC), Juan de la Cierva 3, 28006 Madrid, Spain;
sutrera@ictp.csic.es (S.U.-B.); r.verdejo@csic.es (R.V.)
**\*** Correspondence: lmanchado@ictp.csic.es (M.Á.L.-M.); marherna@ictp.csic.es (M.H.S.)

**Abstract:** It is impossible to describe the recent progress of our society without considering the role of polymers; however, for a broad audience, "*polymer*" is usually related to environmental pollution. The poor disposal and management of polymeric waste has led to an important environmental crisis, and, within polymers, plastics have attracted bad press despite being easily reprocessable. Nonetheless, there is a group of polymeric materials that is particularly more complex to reprocess, rubbers. These macromolecules are formed by irreversible crosslinked networks that give them their characteristic elastic behavior, but at the same time avoid their reprocessing. Conferring them a self-healing capacity stands out as a decisive approach for overcoming this limitation. By this mean, rubbers would be able to repair or restore their damage automatically, autonomously, or by applying an external stimulus, increasing their lifetime, and making them compatible with the circular economy model. Spain is a reference country in the implementation of this strategy in rubbery materials, achieving successful self-healable elastomers with high healing efficiency and outstanding mechanical performance. This article presents an exhaustive summary of the developments reported in the previous 10 years, which demonstrates that this property is the last frontier in search of truly sustainable materials.

**Keywords:** self-healing materials; self-healing rubbers; natural rubber; synthetic rubber; dynamic networks; supramolecular chemistry

## 1. Introduction

In the actual environmental context, polymers like rubbers are particularly critical due to their reprocessing difficulties. These macromolecular materials are composed of irreversible crosslinked networks that act as "*anchor points*", preventing the flow of polymeric chains. Consequently, the material cannot be reshaped [1], and a considerable amount of rubber waste could be generated. One of the strategies to solve this issue has been the recovery of end-of-life rubbers for their use as a diluent or reinforcing filler in new composite materials [2–6]. Also, the selective breaking of the crosslinking points, known as devulcanization [7–11], has been extensively studied; however, both strategies are considered insufficient. Thus, the redesign of crosslinked rubbers is mandatory. Most recent redesign strategies point toward building dynamic networks [1,12,13].

The creation of crosslinked polymers with dynamic networks has spawned a new generation of polymers known as DYNAMERS (*DYNAmic polyMERS*) [14,15]. The construction of these networks is based on multiple dynamic bonds and/or supramolecular interactions, like hydrogen bonds [16,17], ionic interactions [18], metal–ligand coordination [19], disulfide exchange [20], and Diels–Alder chemistry [21,22], among other covalent, non-covalent mechanisms and/or combinations between them [23–30]. The reversible nature of these networks can be controlled by an external stimulus, which can be temperature, pressure, electrical current, magnetic field, or further changes in the medium, such as pH [31–35]. In this way, the stimuli-responsive material would be able to release its "*anchor points*",

*polymers*

MDPI

*Article*

# Understanding the Molecular Dynamics of Dual Crosslinked Networks by Dielectric Spectroscopy

**Saul Utrera-Barrios [†]**, **Reyes Verdugo Manzanares [†]**, **Javier Araujo-Morera**, **Sergio González**, **Raquel Verdejo**, **Miguel Ángel López-Manchado** and **Marianella Hernández Santana ***

Institute of Polymer Science and Technology (ICTP-CSIC), Juan de la Cierva 3, 28006 Madrid, Spain; sutrera@ictp.csic.es (S.U.-B.); reyes@ictp.csic.es (R.V.M.); jaraujo@ictp.csic.es (J.A.-M.); sergio@ictp.csic.es (S.G.); r.verdejo@csic.es (R.V.); lmanchado@ictp.csic.es (M.Á.L.-M.)

* Correspondence: marherna@ictp.csic.es
† S.U.-B. and R.V.M. contributed equally to this work.

**Abstract:** The combination of vulcanizing agents is an adequate strategy to develop multiple networks that consolidate the best of different systems. In this research, sulfur (S), and zinc oxide (ZnO) were combined as vulcanizing agents in a matrix of carboxylated nitrile rubber (XNBR). The resulting dual network improved the abrasion resistance of up to ~15% compared to a pure ionically crosslinked network, and up to ~115% compared to a pure sulfur-based covalent network. Additionally, the already good chemical resistance of XNBR in non-polar fluids, such as toluene and gasoline, was further improved with a reduction of up to ~26% of the solvent uptake. A comprehensive study of the molecular dynamics was performed by means of broadband dielectric spectroscopy (BDS) to complete the existing knowledge on dual networks in XNBR. Such analysis showed that the synergistic behavior that prevails over purely ionic vulcanization networks is related to the restricted motions of rubber chain segments, as well as of the trapped chains within the ionic clusters that converts the vulcanizate into a stiffer and less solvent-penetrable material, improving abrasion resistance and chemical resistance, respectively. This combined network strategy will enable the production of elastomeric materials with improved performance and properties on demand.

**Keywords:** nitrile rubber; metal oxides; ionic crosslinks; dual networks; molecular dynamics; dielectric spectroscopy

## 1. Introduction

Elastomers usually undergo a crosslinking process of their polymeric chains (known as vulcanization), which gives them their characteristic elastic behavior. Typically, the vulcanizing agent depends on the elastomer nature, but sulfur is the most widespread used in diene rubbers, forming covalent crosslinks. Sulfur vulcanization allows a precise control over material processing. By varying the proportions of sulfur and of the rest of the ingredients in the vulcanization system (accelerants and activators), networks can be obtained on demand. Peroxide vulcanization is also widely used in rubber matrices for the creation of covalent networks [1].

Special synthetic elastomers such as carboxylated rubbers admit other vulcanization agents like metal oxides (mainly zinc oxide, ZnO, and magnesium oxide, MgO) that generate ionic crosslinks (ion pair) [2]. The rise of carboxylated elastomers as promising elastomeric materials was a consequence of the early work of Brown and Gibbs [3]. In 1955, they presented the first study of properly crosslinked carboxylated elastomers, considering the role of the carboxylic group in the vulcanization. At that time, the carboxylation of elastomers was a novel synthesis proposal that opened the possibility of an alternative crosslinking to that of sulfur. The benefits of the carboxylic group over different properties that were being discovered were adequately collected in multiple reviews of the literature [2,4]. However, it was not until the work of Eisenberg, in which a molecular model (currently in

Contents lists available at ScienceDirect

## European Polymer Journal

# An effective and sustainable approach for achieving self-healing in nitrile rubber

Saul Utrera-Barrios, Javier Araujo-Morera, Laura Pulido de Los Reyes, Reyes Verdugo Manzanares, Raquel Verdejo, Miguel Ángel López-Manchado, Marianella Hernández Santana[*]

*Institute of Polymer Science and Technology (ICTP-CSIC), Juan de la Cierva 3, Madrid 28006, Spain*

## ARTICLE INFO

## ABSTRACT

Nitrile rubber is considered the workhorse of the automotive rubber industry, thanks to its chemical resistance and mechanical performance. However, applications such as hoses, seals or gaskets are prone to damage, limiting their lifetime. In this work, carboxylated nitrile rubber (XNBR) was ionically crosslinked with zinc oxide (ZnO), forming ionic domains grouped into ionic clusters. These clusters have the advantage of being reversible under the application of an external stimulus such as temperature, conferring the material a certain self-healing capability and enabling a lifecycle extension. Ground tire rubber selectively modified by grafting of poly(acrylic acid) (gGTR), was added to XNBR-ZnO compounds with the aim of improving the healing properties of the rubber matrix. The incorporation of acid groups contributed to the formation of additional ionic clusters during the crosslinking process, resulting in a notorious increase in healing efficiency from 15% for the XNBR-ZnO to 70% for the XNBR-ZnO-gGTR compound. Chemical and mechanical resistance were also evaluated, showing that the addition of a waste material like gGTR keeps mechanical strength suitable for many applications; meanwhile, it does not deteriorate its resistance to aliphatic solvents such as motor oil and gasoline. These promising results open the path for developing sustainable rubber products with extended lifetime and applicable within the automotive industry.

## 1. Introduction

Nitrile rubber (NBR) is a random copolymer of acrylonitrile and butadiene. It is commonly considered one of the pillars of the automotive rubber industry because of its good mechanical properties, its resistance to lubricants and greases and its relative low cost. A wide range of choices is also possible as far as the NBR chemical structure is concerned. As an example, carboxylated nitrile rubber (XNBR) contains carboxyl groups as active functional groups, resulting in a rubber more abrasion resistant and more convenient for industrial seal applications.

The different molecular structure and the presence of active functional groups also enable following different crosslinking routes. Several strategies have been put forward for the formation of rubber networks composed of chemical (covalent) and/or physical (noncovalent) crosslinks [1–4]. Under deformation, physical crosslinks usually dissociate before the chemical crosslinks since their bond energies are generally lower. After the deformation is removed, physical crosslinks can form again but the damage caused by the rupture of

chemical crosslinks remains [5].

Ionic elastomers consist of a physically crosslinked network formed by ionic-rich domains due to the formation of a salt as a consequence of the approximation of the $Zn^{2+}$ ion of the oxide with two $COO^-$ of XNBR [1]. These ionic domains gather in higher structures known as multiplets which in turn form clusters that can dissociate and associate with temperature, demonstrating their reversible nature [1,6–9]. The latter are characterized by having high proportions of trapped chains, which restrict mobility and lead to the appearance of a new transition (i.e. the ionic transition) above the glass transition temperature (Tg). This dynamic characteristic enables them to be considered as healing moieties [10,11], understanding self-healing as the ability to repair damages and partially restore the original material properties [12–15]. The strategy of incorporating ionic domains as healing moieties has been used in different elastomers. The most widespread approach is the direct incorporation of zinc dimethacrylate (ZDMA), a complex formed by the combination of one $Zn^{2+}$ with two $-OOC-C(CH_3)=CH_2$ (an ion pair) with a powerful electrostatic interaction that enables the

---

# Materials Horizons

**ROYAL SOCIETY OF CHEMISTRY**

## MINIREVIEW

Check for updates
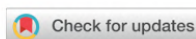
# Evolution of self-healing elastomers, from extrinsic to combined intrinsic mechanisms: a review

Saul Utrera-Barrios, [ID] Raquel Verdejo, [ID] Miguel A. López-Manchado [ID] and Marianella Hernández Santana [ID]*

The evolution of self-healing polymers has resulted in a myriad of healing designs that have given way to complex systems capable of supporting multiple cycles, among other features. This progression enables us to propose the implementation of a timeline that classifies self-healing polymers in generations based on the healing mechanism, and correlated with historical development. The first generation employed the encapsulation of external healing agents; the second one, based on intrinsic mechanisms, applied reversible chemistries; and the third generation was inspired by natural examples such as plants and human skin, in which the healing agent is embedded in vascular networks. Despite great efforts and, with a few exceptions, polymers with high healing efficiency and high mechanical performance are not common. To improve this situation, a combination of different mechanisms is currently emerging, giving birth to the fourth generation of self-healing materials. This article, focused on self-healing elastomers, provides a rigorous overview of this new generation, in which the combination of covalent bonds and non-covalent interactions provides an optimal balance between mechanical performance and repairability. The implementation of this concept leads to materials with real commercial potential in functional applications, such as coatings, sensors, actuators, controlled release of drugs, seals, gaskets, hoses, and even high-performance applications such as tires and railway components.

Institute of Polymer Science and Technology (ICTP-CSIC), Juan de la Cierva, 3, 28006, Madrid, Spain. E-mail: marherna@ictp.csic.es

*Saul Utrera-Barrios (SUB) is a Materials Engineer (Simon Bolivar University, Venezuela) with a MSc in Plastics and Rubber (Menendez Pelayo International University UIMP – Spanish National Research Council CSIC, Spain) and a PhD candidate in Advanced Chemistry (Complutense University of Madrid, Spain). Since 2018, he has developed his experimental work at the Institute of Polymer Science and Technology (ICTP-CSIC) in the area of elastomer-based composite materials with self-healing capability, under the supervision of Dr Marianella Hernández Santana and Prof. Miguel Ángel López Manchado. His scientific main interests include the development, characterization, and production of elastomer-based composite materials and intrinsic self-healing concepts.*

**Saul Utrera-Barrios**

*Raquel Verdejo (RV) is Senior Research Scientist at the Institute of Polymer Science and Technology (ICTP-CSIC). She did her PhD in Metallurgy and Materials at the University of Birmingham (UK) and later joined Imperial College London. She returned to Spain thanks to a Juan de la Cierva and afterwards held a prestigious Ramón y Cajal position, getting tenure in 2010. She is currently the Academic Director of the Master of High Specialization in Plastics and Rubber (UIMP-CSIC). Her main line of research is focused on the development of polymer composites and nanocomposites with special emphasis on polymer foams.*

**Raquel Verdejo**

# Sustainable Fillers for Elastomeric Compounds

**Saul Utrera-Barrios, Allan Bascuñan, Raquel Verdejo, Miguel Ángel López-Manchado, Héctor Aguilar-Bolados, and Marianella Hernández Santana**

**Abstract** The development of sustainable rubber compounds is gaining traction due to the environmental issues caused by the extensive use of polymers and the need to move towards a circular economy. However, the conventional fillers used in elastomer compounds to improve their mechanical performance hinder their degradation. Therefore, materials such as chitin, chitosan, lignin, and cellulose, are being considered as sustainable fillers in elastomeric compounds. This chapter presents a review that addresses the promising biodegradable fillers from vegetable sources, their biosynthesis, chemical properties, applications, reinforcing effect, and the improvements in the performance of composite materials based on natural and synthetic rubber matrices. This review also provides brief information on recently identified bacterial and fungal strains for the degradation of both polymer and fillers.

**Keywords** Elastomers · Rubbers · Sustainable fillers · Sustainable materials · Circular economy

## 1 Introduction

Polymers outstand over other materials, because of their thermal and mechanical properties, lightweight, wide range of applications, and simple chemical composition mostly made up of carbon and hydrogen. Polymers are mainly obtained from fossil sources. They are also cheap, and have excellent processability. However, conventional polymers are difficult to degrade, and current waste management policies have led to an exponential increase of pollution. This fact has become a big concern, which extends to the elastomers and rubbers, a decisive group of elastic

S. Utrera-Barrios · R. Verdejo · M. Á. López-Manchado · M. Hernández Santana (✉)
Institute of Polymer Science and Technology (ICTP), CSIC, Juan de la Cierva 3, 28006 Madrid, Spain
e-mail: marherna@ictp.csic.es

A. Bascuñan · H. Aguilar-Bolados (✉)
Departamento de Polímeros, Facultad de Ciencias Químicas, Universidad de Concepción, Concepción, Chile
e-mail: haguilar@udec.cl

31

# B.2. First Page of the Publications Related to this Doctoral Thesis

Review

## Self-Healing Elastomers: A sustainable solution for automotive applications

Saul Utrera-Barrios, Raquel Verdejo, Miguel Ángel López-Manchado, Marianella Hernández Santana *

Institute of Polymer Science and Technology (ICTP), CSIC, Juan de la Cierva 3, 28006 Madrid, Spain

A B S T R A C T

Among the most fruitful material-industry relationships is that of rubber and the automotive industry. Tires, seals, gaskets, hoses, tubes, soft, and damping parts are common applications in an industry that consumes more than 75 % of world rubber production. However, this relationship faces significant challenges. The difficulty of reprocessing rubbers due to their irreversible crosslinked network that ensures thermal stability, mechanical robustness and chemical resistance, makes them incompatible with the Circular Economy model. Numerous efforts are coordinated daily to overcome the Linear Economy model and achieve more environmentally friendly rubbers. Strategies like devulcanization, recycling, and self-healing are already being considered by several researchers and industries. Thanks to self-healing, a tire will be able to seal damage due to punctures or cracks. Thanks to self-healing, materials will be able to live longer and thus have an extended lifetime. This review delves into the key concepts of self-healing in the most commonly used elastomeric matrices in the automotive industry. While a more application-oriented approach is still necessary, the first steps have been taken towards future scalability in the sector. By analyzing the state-of-the-art taking into consideration the nature of the elastomeric matrix (natural or synthetic), as well as the different healing mechanisms (extrinsic, intrinsic and combinations), the chemistry behind them, and the mechanical performance, this review highlights the potential transformative impact of these concepts to revolutionize the industry and pave the way for a more sustainable future.

## 1. Introduction

Periods of human history have been classified according to the use that has been given to materials to satisfy humans basic needs. The discovery of new materials and the advance in the manipulation of those already known have implied reforms in social structures and have served to understand the evolution of humankind.

In the nineteenth century, cellulose was isolated, Charles Goodyear discovered vulcanization and patented it in the United States of America, while Thomas Hancock did the same in the United Kingdom, and Leo Baekeland invented bakelite, which would undoubtedly be the starting point of an industrial and commercial phenomenon. Despite these developments, the bases of polymers were still not understood, until in 1922 Hermann Staudinger published an article in which he presented the term *Macromolecule* (*Makromolekül*), thanks to the study of the Natural Rubber (NR) structure [1,2]. Later on, in 1950, the advances in the polymerization of polyethylene and polypropylene, allowed polymers to take over the scientific scene and industrial development

[3,4].

Polymers brought with them huge advances to most industrial sectors. In fact, the world, as we know it today, is unimaginable without these materials; but certainly, the most prolific relationship that was consolidated in this period, between a material and a manufacturing sector, has been that between rubbers and the automotive industry.

While rubbers are also used in many other industries such as electronics (in cable sheathing, casings, buttons and keys), construction (in insulation, shock absorbers, flooring and roofing), aerospace (in seals and gaskets), medical (in gloves, syringes and catheters) and food (in conveyor belts), more than 75 % of the world's rubber consumption is dedicated to the automotive industry, and its rise has been essential for understanding the popularity of the automobile as a key transportation system in modern society. However, its use has not been limited only to automobiles, on the contrary, airplanes, short and long-distance trains and ships have also made rubber an essential material [5].

A modern automobile contains hundreds of parts, many of these made from rubber in their different forms (latex, soft rubber, hard

*polymers*

MDPI

*Article*

# Development of Sustainable, Mechanically Strong, and Self-Healing Bio-Thermoplastic Elastomers Reinforced with Alginates
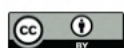
Saul Utrera-Barrios ⓘ, Ornella Ricciardi, Sergio González, Raquel Verdejo ⓘ, Miguel Ángel López-Manchado ⓘ and Marianella Hernández Santana *ⓘ

Institute of Polymer Science and Technology (ICTP), Spanish National Research Council (CSIC), Juan de la Cierva 3, 28006 Madrid, Spain
* Correspondence: marherna@ictp.csic.es

**Abstract:** New bio-thermoplastic elastomer composites with self-healing capacities based on epoxidized natural rubber and polycaprolactone blends reinforced with alginates were developed. This group of salts act as natural reinforcing fillers, increasing the tensile strength of the unfilled rubber from 5.6 MPa to 11.5 MPa without affecting the elongation at break (~1000% strain). In addition, the presence of ionic interactions and hydrogen bonds between the components provides the material with a thermally assisted self-healing capacity, as it is able to restore its catastrophic damages and recover diverse mechanical properties up to ~100%. With the results of this research, an important and definitive step is planned toward the circularity of elastomeric materials.

**Keywords:** epoxidized natural rubber; polycaprolactone; thermoplastic elastomers (TPEs); alginic acid; alginates; self-healing materials

## 1. Introduction

One of the agents that has a notable impact in environmental pollution is the uncontrolled management of polymer waste [1]. However, at the same time, polymers are a key player in achieving the Sustainable Development Goals (SDGs) of the United Nations (UN) [2]. There is no doubt about the importance of polymers for our development and for achieving true environmental sustainability, but not all polymers have the same impact on the ecosystem. Despite the bad press of the different types of polymers, plastics can be environmentally compatible because they can be reprocessed (with proper management). However, elastomers and thermosets cannot be due to their crosslinked chemical structure, which is responsible for their main characteristics as well as their limited flow [3].

Nevertheless, living without elastomers is not an option since their main characteristics are difficult to imitate. In the context of the circular economy [4], numerous strategies have been presented to reduce those consequences. Devulcanization is a widely studied option [5]. Another strategy is the development of thermoplastic elastomers (TPEs), which are formed by two different phases, one thermoplastic and another elastomeric, which means that the material can be melted and, thus, processed again. Other strategies are also framed within the concepts of the 7Rs of the circular economy: recover [6], reuse [7], redesign [8], reduce [9], renew [10], recycle [11], and repair [12].

The concept of self-healing (as a repair strategy) has gained special interest within the scientific community in the last 20 years [13–18]. Self-healing is understood as the ability of materials to repair or restore damage automatically, autonomously, or by applying an external stimulus [19]. In general, there are two approaches to achieve this feature: intrinsic self-healing, which is associated with the use of dynamic chemistry and supramolecular interactions, and extrinsic self-healing, in which an external healing agent is incorporated

**RESEARCH ARTICLE**

# Solving the Dichotomy between Self-Healing and Mechanical Properties in Rubber Composites by Combining Reinforcing and Sustainable Fillers

*Javier Araujo-Morera, Saul Utrera-Barrios, Raúl Doral Olivares, María de los Reyes Verdugo Manzanares, Miguel Ángel López-Manchado, Raquel Verdejo,\* and Marianella Hernández Santana\**

The dichotomy between mechanical performance and repairability is a well-known fact in the self-healing field. One alternative to overcome this trade-off is the inclusion of reinforcing fillers. In this research, hybrid reinforced self-healing styrene-butadiene rubber (SBR) composites are developed by combining mechano-chemically modified ground tire rubber (mGTR) with carbon black (CB). The SBR matrix is systematically analyzed by means of dynamic mechanical analysis and broadband dielectric spectroscopy. The SBR composite reinforced with 20 phr mGTR and 20 phr CB maintains the healing efficiency of the unfilled SBR (80%) and improves its tensile strength by 300%, balancing perfectly well both properties. The healing efficiency is determined at different damage levels. The damage at the microscopic scale is easier to recover and does not depend on the presence of fillers, while the recovery at the macroscopic level clearly relies on the addition of filler, with more demanding healing conditions.

## 1. Introduction

In the past years, the development of self-healing elastomers has shown an exponential growth,[1–9] although the vast majority still exhibit relatively poor mechanical properties compared to traditional elastomers. Adding common reinforcing fillers (i.e., carbon black (CB) and silica (Si)) definitely enhances the mechanical strength, but it usually is accompanied by a decrease in the self-healing capability; showing a trade-off between healing and

mechanical performance.[10,11] The strategies reported so far to overcome this compromise are i) inclusion of nanofillers;[12–15] ii) surface modification of the fillers;[16,17] and iii) combinations of different types of fillers.[18,19] The first two strategies have been widely used, considering different combinations depending on the nature of the filler and/or matrix, their interaction, and final desired properties. As an example, Kuang et al.[12] reported improved mechanical properties without decreasing the healing capability when multi-walled carbon nanotubes (MWCNT) were added to sytrene-butadiene rubber (SBR) using Diels–Alder reactions as healing moiety. Furfuryl modified SBR and furfuryl functionalized MWCNT were reacted with bis-maleimide to form a reversibly cross-linked SBR/MWCNT composite by means of covalent bonds. The nanofiller acted as reinforcing and healing agent, playing a double role. Zhao et al.[13] fabricated polydimethylsiloxane (PDMS)-graphene nanocomposites cross-linked by Diels–Alder bonds which imparted the self-healing ability to the composites. Wang et al.[14] developed a flexible conductive and self-healing composite with electromagnetic interference (EMI) shielding functions. They used dynamically cross-linked polyurethane bearing Diels–Alder bonds as polymer matrix and carbon nanotubes (CNT) as conductive filler. Zhang et al.[15] designed stretchable conductive self-healing PDMS composites filled with amino-functionalized MWCNT based on multiple reversible hydrogen bonds. The elastomer composites showed excellent mechanical properties and self-healing efficiency without external stimuli. Sallat et al.[16] ionically modified bromobutyl rubber (BIIR) with 1-butylimidazole, and added precipitated silica silanized using three different alkoxysilanes (n-propyltriethoxysilane, 1-butyl-3-(trimethoxysilylpropyl) imidazolium bromide, and 3-bromopropyltrimethoxysilane). The ionic imidazolium groups of the rubber were rearranged in reversible ionic clusters, and the Si particles became part of the dynamic network by the interaction of their functional groups with the imidazolium. By this mean, they reported a good mechanical performance without sacrificing the self-healing capability of the rubber. In another investigation, Jia et al.[17]

J. Araujo-Morera, S. Utrera-Barrios, R. Doral Olivares, M. de los Reyes Verdugo Manzanares, M. Á. López-Manchado, R. Verdejo, M. Hernández Santana
Institute of Polymer Science and Technology (ICTP), CSIC
Juan de la Cierva 3, Madrid 28006, Spain
E-mail: r.verdejo@csic.es; marherna@ictp.csic.es

## B.3. First Page of the Dissemination Articles



**THE CONVERSATION**

Rigor académico, oficio periodístico

Ciencia + Tecnología   Cultura   Economía   Educación   Medicina + Salud   Medioambiente + Energía   Política + Sociedad

# El 'Lobezno' de los materiales que podría ayudar a salvar el planeta

Publicado: 29 agosto 2023 20:22 CEST

Aisyaqilumaranas/Shutterstock

Correo
Twitter
Facebook   24
LinkedIn
Imprimir

¿Sabías que Lobezno (*Wolverine*), Deadpool, Piccolo y Terminator comparten la capacidad de sanar al instante sus heridas? Aunque parezca un concepto alejado de lo "natural", lo cierto es que los organismos pluricelulares también tenemos esta capacidad, pero más limitada.

Ahora imagina un mundo en el que objetos cotidianos, como los neumáticos o el envoltorio de tus alimentos, puedan repararse solos cuando se rompen o desgastan. Estaríamos hablando de haber conseguido el "Lobezno" de los materiales.

No es una trama de un cómic, un manga o una película de ciencia ficción, sino más bien un concepto genuino e innovador en el campo de la ciencia de materiales conocido como autorreparación.

Inspirados en la naturaleza, los objetos con la misma capacidad de sanarse que el popular personaje de Marvel podrían ser clave en el contexto ambiental actual que exige un uso más eficiente de

Autoría

**Saul Utrera Barrios**
Investigador en Ciencia y Tecnología del Caucho, Instituto de Ciencia y Tecnología de Polímeros (ICTP - CSIC)

**Marianella Hernandez Santana**
Investigadora Ramón y Cajal, especialista en materiales autorreparables y economía circular, Instituto de Ciencia y Tecnología de Polímeros (ICTP - CSIC)

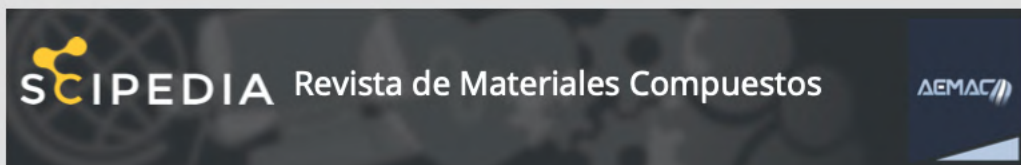**Miguel Angel Lopez Manchado**
Profesor de Investigación de materiales compuestos, Instituto de Ciencia y Tecnología de Polímeros (ICTP - CSIC)

**Raquel Verdejo Márquez**
Investigadora Científica, Consejo Superior de Investigaciones Científicas (CSIC)

**SCIPEDIA** Revista de Materiales Compuestos AEMAC

# Elastomeric composite materials reinforced with natural fibers and with self-healing capacity

Saul Utrera-Barrios[1], Océane Pinho Lopes[1], Marianella Hernandez Santana[1]

1 Instituto de Ciencia y Tecnología de Polímeros (ICTP), CSIC

## Abstract

Elastomeric composite materials are widely used in multiple applications, especially in the automotive industry; however, they have the drawback of being difficult to recycle, generating a significant environmental impact. For this reason, in recent years there has been an increase in research for the development of self-healing and biodegradable materials that minimize this impact by extending their lifetime. In this context, the aim of this work is to design a new generation of self-healing elastomeric composite materials using additives of natural origin. For this, epoxidized natural rubber (ENR) and cellulose propionate (CP) were used as matrix, reinforced with cellulose fibers. Self-healing was achieved by combining the flow of the thermoplastic (CP) phase (extrinsic mechanism) and the formation of hydrogen bonds between the ENR and the CP (intrinsic mechanism). A promising repair efficiency of 95% was obtained, as well as an increase in tensile strength in the presence of cellulose fibers, without affecting the healing capacity of the material. Therefore, this work overcomes the well-known dichotomy between mechanical performance and self-healing and constitutes a new contribution in the field of self-healing elastomeric composites using bio-based additives.
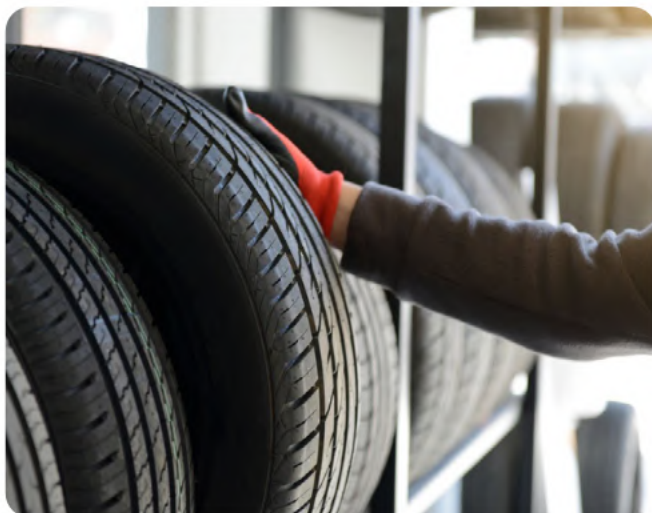
## 1. Introducción

El impacto ambiental de los materiales compuestos de matriz elastomérica requiere acciones inmediatas que permitan asegurar la sostenibilidad de esta familia de polímeros. Una de las principales líneas de actuación para avanzar hacia una economía más circular es la sustitución total o parcial de las cargas reforzantes utilizadas actualmente en los materiales compuestos elastoméricos. Refuerzos como el negro de carbono son extremadamente contaminantes, insostenibles y de gran impacto desde el punto de vista medioambiental, ya que requiere mucha energía para su producción y emite una cantidad significativa de $CO_2$ a la atmósfera [1]. Para solucionar este problema, los científicos han estado buscando aditivos sostenibles que puedan reemplazar las cargas reforzantes de origen no renovable y garantizar un buen rendimiento mecánico en materiales compuestos. Las características de estos aditivos biobasados son prometedoras ya que tienen baja toxicidad, baja densidad y, sobre todo, son biodegradables [2].

Entre las cargas reforzantes biobasadas, las de origen animal o las fibras vegetales han generado un creciente interés para los investigadores; sin embargo, su incorporación en materiales compuestos elastoméricos sigue siendo un desafío. Los cauchos son hidrófobos, mientras que los refuerzos biobasados (como la quitina, la lignina, el almidón y la celulosa) son hidrófilos; en este sentido, son incompatibles. Por lo tanto, es necesario modificar la superficie de las cargas o de la matriz elastomérica antes de mezclarlos para garantizar una buena compatibilidad entre ellos [3,4].

Otra de las líneas de actuación que se debe considerar para avanzar hacia una economía verdaderamente circular es conferirle autorreparación a los materiales compuestos de matriz elastomérica. Gracias a esta capacidad, la vida útil del material se verá prolongada, a la vez que se podrá reducir la cantidad de desechos generados. No obstante, en el campo de la autorreparación, hay un problema común a resolver: el compromiso entre el rendimiento mecánico y la eficiencia de reparación. Estas dos propiedades son antagónicas, por lo que la mejora de una implica el detrimento de la otra [5].

En este trabajo de investigación se presenta el desarrollo de nuevos materiales compuestos autorreparables a partir de mezclas de caucho natural epoxidado (ENR) y propionato de celulosa (CP) reforzados con fibras de celulosa. Hemos desarrollado con éxito un material compuesto en el que la resistencia a la tracción y la eficiencia de reparación aumentan de forma simultánea, resolviendo la principal limitación de los elastómeros autorreparables.

1

Appendix B

8

# Innovación y desafíos en el uso de cauchos autorreparables para el vehículo del futuro

**COLUMNISTA INVITADO**

**Ing. Saúl Utrera Barrios** (ESP)
Instituto de Ciencia y Tecnología de Polímeros (ICTP-CSIC), España.

**COORDINADORA**

**Marianella Hernández Santana** (ESP)
Directora de la Red Internacional de Tecnología del Caucho (RITC).

### INTRODUCCIÓN

Entre las relaciones material-industria más fructíferas, está la del **caucho** y la **industria automotriz**. Neumáticos, sellos, juntas, mangueras, tubos, piezas blandas y amortiguadores son aplicaciones habituales en una **industria que consume más del 75 % de la producción mundial de caucho**.

Sin embargo, esta relación se enfrenta a importantes retos. La dificultad de reprocesar los cauchos debido a su red entrecruzada irreversible, que garantiza su estabilidad térmica, robustez mecánica y resistencia química, los hace incompatibles con el modelo de economía circular.

Cada día se coordinan numerosos esfuerzos para superar el modelo de **economía lineal** y conseguir cauchos más respetuosos con el medio ambiente.

Estrategias como la desvulcanización, la recuperación y el reciclaje, así como la autorreparación, ya están siendo consideradas por varios investigadores e industrias. Empleando la **estrategia de autorreparación**, un neumático podrá sellar los daños debidos a pinchazos o grietas. Los materiales podrán vivir más tiempo y, por tanto, tener una vida útil más larga.

Aunque todavía es necesario un enfoque más orientado a la aplicación, ya se han dado los primeros pasos hacia la futura escalabilidad en el sector. Se pueden citar desarrollos empleando caucho natural (NR) y cauchos sintéticos, como el caucho estireno-butadieno (SBR), caucho butadieno (BR), caucho butilo (IIR), caucho nitrilo (NBR), poliuretanos (PU), caucho de etileno-propileno-dieno (EPDM), cloropreno (CR), siliconas (Q), entre otros.

8

# Reutilización de desechos de neumáticos en compuestos autorreparables- Segunda parte

**COLUMNISTA**

**Marianella Hernández Santana** (ESP)
Directora de la Red Internacional de Tecnología del Caucho (RITC)
ritc@sltcaucho.org

**COLABORADOR INVITADO**

**Saúl Utrera Barrios** (ESP)
Consejo Superior de Investigaciones Científicas (CSIC)

## RESULTADOS Y DISCUSIÓN

Retomando la primera parte de este trabajo, veremos a continuación los resultados del mismo. Desde ya, con respecto a las **propiedades mecánicas**, como se muestra en la **tabla 1**, parece ocurrir una disminución en el rendimiento mecánico, así como en la densidad de entrecruzamientos cuando se incorpora el gGTR (polvo de neumático fuera de uso funcionalizado selectivamente) a compuestos de caucho nitrilo carboxilado (XNBR).

En ese sentido, se puede atribuir tal comportamiento a dos posibles factores: en primer lugar, a la **migración de los componentes del sistema de vulcanización (ZnO) hacia el GTR**, compitiendo con la reacción de vulcanización.

Y, en segundo lugar, a la **incompatibilidad entre la matriz y los cauchos que constituyen al GTR y gGTR**. Esta incompatibilidad se vería mejorada con el injerto de AA (ácido acrílico), lo que explicaría las mejores propiedades del compuesto 6ZnO-6gGTR frente al 6ZnO-6GTR.

Por otro lado, cuando el contenido de gGTR varía, se observan diferentes efectos. Primero, hay un **aumento en la densidad de entrecruzamientos y los módulos.** También se muestra una **ligera disminución de la resistencia a la tracción cuando se pasa de 5 ppc (partes en peso por 100 de caucho) a 6 ppc de gGTR**, mientras que para 8 ppc de gGTR este valor aumenta considerablemente, alcanzando cifras más cercanas a la muestra sin carga.

4

# Reutilización de desechos de neumáticos en compuestos autorreparables

**COLUMNISTA**

**Marianella Hernández Santana** (ESP)
Directora de la Red Internacional de Tecnología del Caucho (RITC)
ritc@sltcaucho.org

**COLABORADOR INVITADO**

**Saúl Utrera Barrios** (ESP)
Consejo Superior de Investigaciones Científicas (CSIC)

En esta entrega compartiré un trabajo publicado por el grupo de Compuestos Poliméricos del Instituto de Ciencia y Tecnología de Polímeros (ICTP-CSIC) de España. **En esta investigación se abarcaron dos frentes: la autorreparación y el uso de polvo de neumáticos fuera de uso (GTR) para lograr dicha reparación.** Para ello, se desarrollaron compuestos de caucho nitrilo carboxilado (XNBR) con GTR funcionalizado selectivamente (gGTR) con grupos promotores de diferentes mecanismos de autorreparación intrínseca. Este nuevo enfoque puede considerarse como una **estrategia de partida para el desarrollo de productos sostenibles con una vida útil prolongada, de valor para la industria automotriz.**

## INTRODUCCIÓN

El **caucho nitrilo (NBR)** es un copolímero de acrilonitrilo y butadieno considerado **uno de los pilares de la industria automotriz** debido a sus buenas propiedades mecánicas, su resistencia a lubricantes y grasas, y su costo relativamente bajo. Gracias a su estructura química, **se pueden llevar a cabo múltiples**

**modificaciones para adaptar dicha estructura a requerimientos bajo demanda.**

El caucho nitrilo carboxilado (XNBR), una de las modificaciones más conocidas del NBR, contiene unidades carboxílicas como grupos funcionales activos, las cuales dan como resultado un caucho **más resistente a la abrasión y más conveniente para aplicaciones industriales** como sellos y juntas, entre otras aplicaciones avanzadas. [1][2][3]

Las diferentes estructuras moleculares y la presencia de grupos funcionales activos en los cauchos permiten seguir diferentes rutas de vulcanización, entre las cuales se destaca la construcción de redes elastoméricas dinámicas capaces de reaccionar ante un estímulo externo, dando paso a **una nueva generación de materiales reciclables, e incluso con capacidad autorreparadora. Los elastómeros iónicos se encuentran dentro de esta generación** y consisten en una **red entrecruzada formada por dominios iónicos** (gracias a la asociación de pares de iones)

# Self-Healing Elastomers

It is impossible to describe the recent progress of our society without considering the role of polymers; however, for a broad audience, "*polymer*" is usually related to environmental pollution. The poor disposal and management of polymeric waste has led to an important environmental crisis, and, within polymers, plastics have attracted bad press despite being easily reprocessable. Nonetheless, there is a group of polymeric materials that is particularly more complex to reprocess, rubbers. These macromolecules are formed by irreversible crosslinked networks that give them their characteristic elastic behavior, but at the same time avoid their reprocessing. Conferring them a self-healing capacity stands out as a decisive approach for overcoming this limitation. By this mean, rubbers would be able to repair or restore their damage automatically, autonomously, or by applying an external stimulus, increasing their lifetime, and making them compatible with the circular economy model.

## 1. Introduction

In the actual environmental context, polymers like rubbers are particularly critical due to their reprocessing difficulties. These macromolecular materials are composed of irreversible crosslinked networks that act as "*anchor points*", preventing the flow of polymeric chains. Consequently, the material cannot be reshaped [1], and a considerable amount of rubber waste could be generated. One of the strategies to solve this issue has been the recovery of end-of-life rubbers for their use as a diluent or reinforcing filler in new composite materials [2][3][4][5][6]. Also, the selective breaking of the crosslinking points, known as devulcanization [7][8][9][10][11], has been extensively studied; however, both strategies are considered insufficient. Thus, the redesign of crosslinked rubbers is mandatory. Most recent redesign strategies point toward building dynamic networks [1][12][13].

The creation of crosslinked polymers with dynamic networks has spawned a new generation of polymers known as DYNAMERS (*DYNAmic polyMERS*) [14][15]. The construction of these networks is based on multiple dynamic bonds and/or supramolecular interactions, like hydrogen bonds [16][17], ionic interactions [18], metal–ligand coordination [19], disulfide exchange [20], and Diels–Alder chemistry [21][22], among other covalent, non-covalent mechanisms and/or combinations between them [23][24][25][26][27][28][29][30]. The reversible nature of these networks can be controlled by an external stimulus, which can be temperature, pressure, electrical current, magnetic field, or further changes in the medium, such as pH [31][32][33][34][35]. In this way, the stimuli-responsive material would be able to release its "*anchor points*", allowing the flow of its chains until it reforms and/or repairs. In fact, the use of dynamic networks is the most widespread self-healing strategy used in rubbers [1].

## 2. To Boldly Go Where No Material Has Gone before: Self-Healing Concepts

Self-healing is the ability to repair or restore damages [36][37][38][39]. To scientifically understand healing as a physical process, four key concepts must be considered in rubbers: (1) Mechanism, (2) Mobility, (3) Localization and (4) Temporality [40]. In elastomers, the success of the self-healing process goes hand in hand with the adequate selection of a mechanism that guarantees the necessary molecular mobility of the polymeric chains, as well as enough time for the restoration of the damage according to its location (on a macroscopic or microscopic scale) [41].

The first concept is the *mechanism*. Self-healing can occur extrinsically or intrinsically [42][43]. Extrinsic mechanisms are based on an external healing agent that is incorporated into the matrix in an encapsulated form, in vascular networks or freely dispersed. When damage occurs, these agents are released and/or flow through the damage area, sealing it. Despite being the first mechanisms used, according to the historical development, their use in rubbers is very limited due

# SELF-HEALING STRATEGIES IN RUBBER COMPOSITES

Saul Utrera-Barrios[1], Javier Araujo-Morera[1], Reyes Verdugo Manzanares[1], Raquel Verdejo[1], Miguel A. López-Manchado[1], Marianella Hernandez Santana[1]

1 Institute of Polymer Science and Technology (ICTP), CSIC, Juan de la Cierva 3, 28006 Madrid, Spain

## Abstract

Inspired by some of the mechanisms that occur in nature, self-healing materials are characterized by the ability to recover, partially or totally, their initial properties after suffering damage. These materials constitute an efficient alternative for extending the lifecycle of products, as well as for reducing the amount of waste generated. At the same time, they reduce maintenance and repair costs. In this work, examples of recent developments in the field of elastomeric composite materials are presented, studying different matrices, natural rubber (NR), epoxidized natural rubber (ENR), styrene-butadiene rubber (SBR) and nitrile rubber (NBR), and using diverse repair strategies, hydrogen bonds, disulfide exchange reactions, Diels-Alder chemistry and ionic interactions. The effect of adding carbon-derived reinforcing fillers (graphene oxide) and sustainable alternative fillers (ground tire rubber) is also analyzed. It is studied how the presence and type of filler influences the healing capacity of elastomeric matrices, reaching repair efficiencies of up to ~80%, without detriment to their mechanical performance.

## 1. INTRODUCCIÓN

Los materiales autorreparables representan la vanguardia de los desarrollos recientes en la química e ingeniería de materiales. Debido a su capacidad inherente para reparar daños físicos, pueden prevenir daños catastróficos de manera efectiva y extender la vida útil del material. Existen dos estrategias bien establecidas para desarrollar polímeros autorreparables [1-4]. El primero, el llamado concepto extrínseco, se basa en la integración de contenedores discretos (cápsulas, fibras o redes vasculares) cargados con componentes activos en el material matriz (polímero). Cuando se produce un daño, los contenedores se rompen y liberan el agente reparador que contienen, reaccionando en presencia de otros componentes y, reparando el daño. El sistema tiene un gran potencial para reparar microfisuras internas; sin embargo, la naturaleza irreversible del mecanismo de reparación es una limitación. El segundo enfoque se relaciona con el desarrollo de los llamados materiales intrínsecamente autorreparables, es decir, materiales que contienen enlaces dinámicos (químicos o físicos) que pueden restaurarse después del daño, bajo la influencia de un estímulo externo. A manera de ejemplo de estos enlaces dinámicos se pueden citar los basados en reacciones Diels-Alder (DA) y retro-Diels-Alder (retro-DA); enlaces de hidrógeno en redes supramoleculares; complejos de coordinación; enlaces disulfuros; interacciones iónicas, entre otros. Debido a su carácter reversible, en teoría, pueden conducir a una cantidad infinita de ciclos de reparación.

En el campo de los elastómeros, el trabajo pionero de Leibler y col. aportó una motivación decisiva para el desarrollo de nuevos materiales con capacidad autorreparadora [5]. Los elastómeros derivan sus excelentes propiedades mecánicas de la creación de una red molecular tridimensional estable unida, mayormente, de forma covalente. Esta red reticulada irreversible no suele permitir ni la autorreparación ni el reprocesado. La autorreparación requiere movilidad de las cadenas poliméricas y, por lo tanto, parece estar en contradicción directa con la fijación necesaria para formar una red permanente. Por lo tanto, obtener una red entrecruzada con enlaces covalentes que pueda inferir capacidades de reparación al caucho, así como buenas propiedades mecánicas, se presenta como un desafío. En los últimos años, han surgido diversas estrategias como respuesta a este reto. Una de ellas ha sido el desarrollo de materiales compuestos elastoméricos, donde la carga cumpla una doble función: reforzante y como agente reparador [6-8]. Otra estrategia que despierta gran interés es la combinación de diferentes mecanismos de reparación, creando redes duales entrecruzadas donde se combinan interacciones no-covalentes, enlaces covalentes, o ambos [3,9-13]. Los sistemas no-covalentes se caracterizan por tener una baja energía de enlace en comparación con los sistemas

# SELF-HEALING NATURAL RUBBER:
# A WINDOW OF MASSIVE OPPORTUNITIES FOR NEW APPLICATIONS

## CONTRIBUTOR

**Dr. Marianella Hernández Santana**

*Self-healing Materials Head
Polymer Composite Group
Spanish National Research
Council CSIC*

## CONTRIBUTOR

**Mr. Saul Utrera-Barrios**

*Self-healing Rubber Researcher
Polymer Composite Group
Spanish National Research
Council CSIC*

In the context of the circular economy, the development of new materials with smart properties, that allow them to extend their lifetime, is a key factor in the evolution towards a sustainable society. Inspired by nature, self-healing materials are capable of repairing a damage automatically, autonomously or through the application of an external stimuli, prolonging their useful life and recovering initial functionalities and/or properties.

Self-healing ability can be found in living organisms such as starfish, mollusks, insects, and even in the human skin. In the current environmental context, the waste of some materials, especially polymers, is presented as an environmental threat. Thus, the development of new materials with this ability is a groundbreaking strategy that will give rise to unprecedented generations of materials.

Up to now, four generations of self-healing materials can be distinguished depending on the healing mechanism and its evolution with time: the first involves the use of an encapsulated external healing agent (an extrinsic mechanism). When damage occurs, the propagation of the crack causes the breakage of the capsules with the subsequent release of the healing agent, sealing the damage. The second generation emerged to overcome the limitations of the first one, achieving self-healing materials that would withstand more than one healing cycle (ideal situation).

For this, the chemistry of dynamic bonds and supramolecular interactions (intrinsic mechanisms) was used. Following the occurrence of a damage, these bonds and interactions are broken, but thanks to their reversible nature, they can be restored under the action of an external stimulus (pressure, temperature, and light, among others). In the particular case of elastomers, this has been the generation mostly explored. The third generation replaced the encapsulation of the healing agent in spherical capsules with vascular networks (another extrinsic mechanism), taking inspiration from the bloodstream. The extrinsic mechanisms of the first and third generations have had little development in elastomeric matrices. Finally, the fourth generation, currently under full development, seeks the combination of different healing mechanisms to achieve a win-win situation between the mechanical performance of the material and its self-healing capacity, typically antagonistic properties.
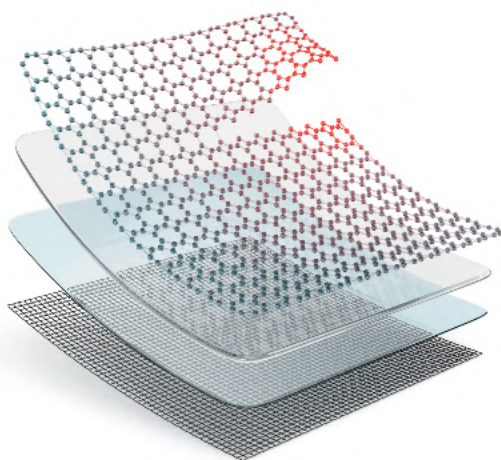
# Cauchos autorreparables: La nueva frontera en el desarrollo de elastómeros inteligentes y sostenibles



**COLUMNISTAS INVITADOS**

**MSc-Ing. Saúl Utrera-Barrios** (ESP)
sutrera@ictp.csic.es

**MSc-Ing. Javier Araujo-Morera** (ESP)
jaraujo@ictp.csic.es

**COORDINADOR**

**Dr. Mariano Escobar** (ARG)
Dpto. Diseño de Materiales, INTI - CONICET.
ritc@sltcaucho.org

Desde el inicio de la Ciencia y Tecnología de Polímeros, hace cien años, la búsqueda de nuevos y mejores materiales ha seguido un enfoque tradicional, es decir, el desarrollo de materiales cada vez más resistentes (en términos de desempeño mecánico) con tiempos de vida útil diversos.

Este enfoque ha estado asociado al modelo de **economía lineal**, modelo basado en el principio de extraer, fabricar, consumir y desechar, por el cual un material al finalizar su vida útil se convierte en un desecho, con consecuencias ambientales cada vez más evidentes.

En este contexto, se han buscado alternativas que permitan contrarrestar los efectos negativos de la economía lineal, y apareció un nuevo enfoque en la Ciencia de Materiales basado en el modelo de **economía circular**.

El modelo de economía circular reemplaza el principio de desechar por restaurar, para alcanzar un uso racional y eficiente de los recursos y prolongar los tiempos de vida útil de los materiales. **La búsqueda de estrategias que permitan el desarrollo de nuevos materiales con propiedades inteligentes que alarguen esos tiempos, es un factor clave** en la evolución hacia una sociedad sostenible; y en este proceso, la naturaleza ha servido como modelo de inspiración.

**Uno de los ejemplos más prometedores de materiales bioinspirados son los materiales autorreparables** (Figura 1). **Estos son capaces de repararse o restaurar sus propiedades de forma automática, autónoma o al aplicar un estímulo externo, prolongando su vida útil, ahorrando energía, materias primas y reduciendo la generación de residuos.**

La capacidad autorreparadora se puede encontrar en la naturaleza, específicamente en estrellas de mar, moluscos, insectos e incluso en nuestra piel. El desarrollo de materiales con esta capacidad

# Neumáticos fuera de uso: una carga sostenible para el desarrollo de nuevos elastómeros con capacidad autorreparadora

**Autores:** Saul Utrera-Barrios; Laura Pulido de los Reyes; Reyes Verdugo Manzanares; Javier Araujo-Morera; Raquel Verdejo; Marianella Hernández Santana*

Instituto de Ciencia y Tecnología de Polímeros (ICTP-CSIC), Juan de la Cierva 3, 28006, Madrid, España.

* marherna@ictp.csic.es
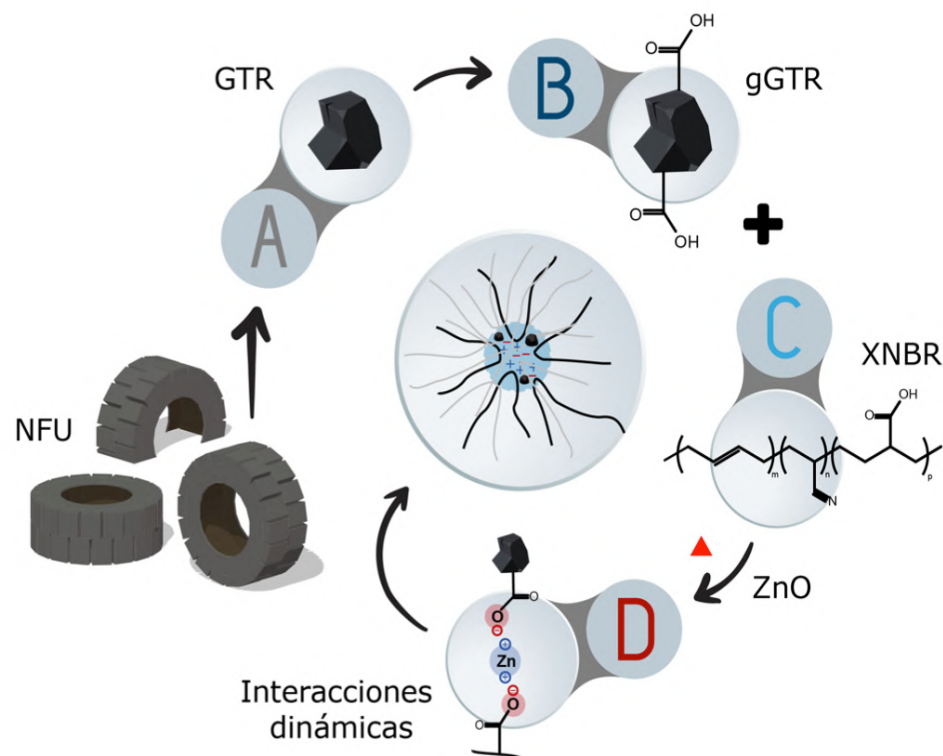
## Resumen

La revalorización de los residuos plásticos, y en concreto de los residuos de neumáticos, supone generar un nuevo ciclo de vida útil a estos materiales reduciendo así la generación de desechos. Dicha revalorización ha supuesto, generalmente, el desarrollo de materiales de bajo valor añadido y poco atractivos comercialmente. En este trabajo, por el contrario, se busca aportar un alto valor añadido a dichos residuos mediante su empleo en elastómeros inteligentes con capacidad autorreparadora. La funcionalización e incorporación de polvo de neumático fuera de uso (GTR) ha permitido aumentar la capacidad de reparación de un caucho nitrilo carboxilado de un 20 a un 70% mediante la formación de entrecruzamientos iónicos reversibles.

**Palabras clave**: caucho nitrilo carboxilado, neumáticos fuera de uso, materiales autorreparables, entrecruzamientos iónicos, propiedades mecánicas.

## Abstract

The revalorization of plastic waste, and specifically of tire waste, means generating a new useful life cycle for these materials, thus reducing the generation of rubbish. This revalorization has generally led to the development of low benefit and commercially unattractive materials. In this work, on the contrary, it is sought to provide a high added value to that waste through its use in smart elastomers with self-healing capacity. The functionalization and incorporation of end-of-life tire powder (GTR) have made it possible to increase the repairability of a carboxylated nitrile rubber from 20 to 70% through the formation of reversible ionic crosslinks.

**Keywords**: carboxylated nitrile rubber, ground tire rubber, self-healing materials, ionic crosslinks, mechanical properties.

# LA AUTORREPARACIÓN, UN ALIADO EFECTIVO CONTRA EL IMPACTO MEDIOAMBIENTAL DE LOS POLÍMEROS

**J Araujo-Morera; S Utrera-Barrios; M Peñas-Caballero;**
**M Hernández Santana; R Verdejo ✉; MA López-Manchado**
*Instituto de Ciencia y Tecnología de Polímeros (ICTP-CSIC), Juan de la Cierva, 3, 28006 Madrid, España*
✉ r.verdejo@csic.es

## Resumen

La mala disposición y manejo de los desechos de polímeros representa uno de los problemas más graves para el medioambiente y, dentro de los polímeros, los termoestables y elastómeros se encuentran en desventaja frente a los termoplásticos, porque no se pueden reprocesar fácilmente debido a su estructura entrecruzada. Una alternativa para solucionar este problema es el desarrollo de una nueva generación de materiales autorreparables, capaces de recuperar o restaurar daños de forma automática y autónoma. Esta nueva generación de materiales se presenta como un elemento indispensable en el contexto ambiental actual, ya que mejoran la eficiencia en el uso de recursos y extienden su ciclo de vida, por lo que suponen una contribución importante a la reducción del impacto medioambiental de los polímeros.

Palabras clave: Autorreparación; Materiales Poliméricos; Materiales Compuestos; Enlaces: Reversibilidad.

## 1. Introducción

Los polímeros, generalizados como "plásticos", son considerados los materiales del siglo XXI. Esto se debe a su relativo bajo costo, facilidad de transformación, bajo peso, durabilidad y a la versatilidad de características y propiedades que presentan [1]. Estas ventajas convierten a los plásticos en materiales de uso habitual en una amplia gama de aplicaciones, entre las que se encuentran las pertenecientes al sector automotriz, construcción, aeroespacial, farmacéutico, entre otros [2].

Actualmente, la mala gestión de desechos y el uso irracional de materias primas, se han convertido en uno de los problemas de mayor relevancia para el medioambiente, empeorando progresivamente como consecuencia del desarrollo y crecimiento económico de la Sociedad [1]. La masiva fabricación de productos plásticos y la mala disposición al final de su ciclo de vida útil, que generalmente termina siendo en vertederos o en el ambiente, ha derivado en un grave impacto medioambiental que representa uno de los retos y desafíos tecnológicos y económicos más significativos de nuestros tiempos [3, 4].

*'Working hard is important.*

*But there's something that matters even more.*

*Believing in yourself.'* —Harry Potter

Harry Potter and the Order of the Phoenix

(David Yates, 2007)

by **Michael Goldenberg & J. K. Rowling**